Protein changes associated with embryonic stem cell differentiation to vascular smooth muscle cells

Yin, Xiaoke

PROTEIN CHANGES ASSOCIATED WITH EMBRYONIC STEM CELL DIFFERENTIATION TO VASCULAR SMOOTH MUSCLE CELLS

Thesis submitted to the

University of London

For the degree of

Doctor of Philosophy

By

Mr. Xiaoke YIN

Division of Medical Engineering

Department of Engineering

Queen Mary, University of London

August 2006

Dedicated to my mother

ABSTRACT

Embryonic stem (ES) cells can differentiate into many different cell lines, including vascular smooth muscle cells (SMCs). The aim of this project is to characterize protein changes during this differentiation process. Mouse ES cells are pre-differentiated by withdrawal of the leukemia inhibitory factor-1 from the culture medium. Subsequently, stem cell antigen-1 positive (Sca-1^+) cells are sorted by magnetic labelling cell sorting with anti-Sca-1 microbeads and cultured in differentiation medium with or without platelet-derived growth factor (PDGF). Protein extracts of ES cells and Sca-1^+ cells are separated by two-dimensional electrophoresis. About 300 protein species of each cell lines are analyzed by mass spectrometry. Proteome maps are available online (http://www.vascular-proteomics.com). After stimulation with PDGF for 5 passages, Sca-1^+ cells differentiate into SMCs (esSMCs) with 95% staining positive for SMC markers such as smooth muscle α-actin, calponin, and smooth muscle myosin heavy chain. Protein profiles of esSMCs and mouse aortic SMCs are compared using the difference gel electrophoresis approach. esSMCs display decreased expression of myofilaments but increased oxidation of redox-sensitive proteins due to higher levels of reactive oxgen species (ROS). While immunoblotting reveals an upregulation of numerous antioxidants in esSMCs, enzymatic assays demonstrate lower glutathione concentrations compared to aortic SMCs despite a 3-fold increase in glutathione reductase activity. Mitochondrial superoxide measurement revealed the mitochondria-derived superoxide is the main source of ROS in esSMCs

and inhibition of electron transport chain complex III by antimycin A showed remarkable increase of ROS in esSMCs. Moreover, depletion of glutathione by diethyl maleate or inhibition of glutathione reductase by carmustine (BCNU) results in a remarkable loss of cell viability in esSMCs compared to aortic SMCs while adding 2-mercaptoethanol increased esSMCs survival. These results indicate that esSMCs require additional antioxidant protection for survival and consequently, treatment with anti-oxidants could be beneficial for tissue repair from ES cells.

TABLE OF CONTENTS

DECLARATION

I have been involved in the design and conduct of all experiments, analysis of data and writing of the thesis.

This includes sample preparation for proteomic and metabolomic analysis, protein separation by 2-D gel electrophoresis, computer-assisted analysis of protein patterns, protein identification by MALDI-MS and tandem MS, bioinformatics, cell culture, standard biochemical methods and statistical analysis.

The following aspects of the study required expert assistance. I worked in collaboration with following colleagues:

1. Dr. Qingzhong Xiao (Department of Cardiology at King's College, University of London) performed the mouse embryonic stem cell differentiation to smooth muscle cells.
2. Dr. Yanhua Hu (Department of Cardiology at King's College, University of London) performed isolation of vascular SMCs from mouse aortic root advantitia.
3. Dr. Yuen-Li Chung (Department of Basic Medical Sciences at St. George's, University of London) recorded and analyzed the NMR spectra.
4. Dr. Robin Wait (Kennedy Institute of Rheumatology Division, Imperial College London) performed part of the protein identifications using Q-ToF mass spectrometer.

ACKNOWLEDGEMENTS

There are many people without whom the studies performed in this thesis would not be possible:

I would like to thank Professor Wen Wang and Professor Qingbo Xu for giving me the opportunity to undertake this research with funding from the Oak Foundation and British Heart Foundation. I am particularly grateful to Dr. Manuel Mayr for his guidance and technical assistance during planning and conducting the research and his critical reading of all the manuscript and valuable discussion.

I am grateful to Dr. Qingzhong Xiao and Dr. Yanhua Hu for culturing the Sca-1$^+$ cells and differentiating them into esSMCs. I would like to thank Dr. Ursula Mayr for teaching me the fundamental experiment skills. I would like to thank Miss Anissa Sidibe and Dr. Lingfang Zeng for the critical reading of my thesis. And I also would like to thank all other staffs in our lab who give me plenty of help during my experiments.

The use of facilities and the helps of the faculties of the Medical Biomics Centre at St. George's, University of London are gratefully acknowledged. Many thanks to Dr. Yuen-Li Chung for kindly performing the NMR spectroscopy.

I would like to thank my father Mr. Guangrong Yin, without whose encouragement I would not dedicate myself to life sciences research. I want to thank my brother Mr. Xiaojian Yin for concerning my studies and caring about my life. I wish to thank my girl friend Miss Qiuru Xing, who constantly supports me, encourages me and pushes me during the writing days.

INDEX OF TABLES

INDEX OF FIGURES

LIST OF ABBREVIATIONS

2-DE	two-dimensional electrophoresis
2-ME	2-mercaptoethanol
ApoE	apolipoprotein E
ATP	adenosine 5'-triphosphate
BCNU	carmustine / 1,3-bis(2-chloroethyl)-1-nitrosourea
bFGF	basic fibroblast growth factor
BMP	bone morphogenetic protein
BSA	bovine serum albumin
CD31/PECAM1	platelet endothelial cell adhesion molecule 1
cDNA	complimentary DNA
cGMP	cyclic guanosine monophosphate
CHAPS	3-[(3-cholamidopropyl)-dimethylammonio]-1-propanesulphonate
CO	carbon monoxide
ddH_2O	double distilled water
DEM	diethyl maleate
DIGE	difference gel electrophoresis
DM	differentiation medium
DMEM	dulbecco's modified eagle's medium
DNA	deoxyribonucleic acid

dNTPs	deoxyribonucleotide triphosphates
DTT	dithiothreitol
EC	endothelial cell
EDRF	endothelium-derived relaxing factor
EDTA	ethylene diamine tetraacetic acid
eNOS	endothelial nitric oxide synthase
EPC	endothelial progenitor cell
ERK	extracellular signal-regulated kinase
ES cell	embryonic stem cell
FACS	fluorescence activated cell sorting
FBS	fetal bovine serum
FCS	fetal calf serum
FITC	fluorescein isothiocyanate
FGF	fibroblast growth factor
Flk-1/VEGFR2	fetal liver kinase 1 / VEGF receptor 2
Flt-1/VEGFR1	fms-like tyrosine kinase 1 / VEGF receptor 1
GAPDH	glyceraldehyde-3-phosphate dehydrogenase
GSH	glutathione
H&E	hematoxylin and eosin
HBSS	Hank's balanced salt solution
HDL	high density lipoprotein
HO	heme oxygenase

HSC	hematopoietic stem cell
HSP	heat shock protein
HUVEC	human umbilical vein endothelial cell
LC	liquid chromatography
LDL	low density lipoprotein
LIF	leukemia inhibitory factor
iNOS	inducible nitric oxide synthase
JNK	c-Jun N-terminal kinase
MALDI-ToF	matrix-assisted laser desorption/ionization time-of-flight
MAPK	mitogen-activated protein kinase
MEM	minimal essential medium
MHC	myosin heavy chain
MM	molecular mass
Mr	molecular weight, relative molecular mass
mRNA	messenger ribonucleic acid
MS	mass spectrometry
MS/MS	tandem mass spectrometry
NADPH	nicotinamide adenine dinucleotide phosphate
NMR	nuclear magnetic resonance
NO	nitric oxide
OD	optical density
PAGE	polyacrylamide gel electrophoresis

PBS	phosphate buffered saline
PCR	polymerase chain reaction
PDGF	platelet-derived growth factor
pI	isoelectric point
Q-ToF	hybrid quadrupole orthogonal acceleration time-of-flight
RNA	ribonucleic acid
ROS	reactive oxygen species
RT-PCR	reverse transcription polymerase chain reaction
Sca-1	stem cell antigen-1
SDS	sodium dodecyl sulphate
SE	standard error of mean
SMC	smooth muscle cell
SSEA-1	stage specific embryonic antigen-1
TGF	transforming growth factor
TNF	tumor necrosis factor
ToF	time of flight
UV	ultra violet light
V	volt
VCAM	vascular cellular adhesion molecule
VE-cadherin	vascular endothelial cadherin
VEGF	vascular endothelial growth factor
W	watt

1 INTRODUCTION

1.1 Vascular Biology

Vascular biology successfully brought together basic scientists and clinical investigators. It stimulated interactions and collaborations among researchers from multiple disciplines and developed new training opportunities. From these activities emerged the discipline of vascular medicine (Dzau, Gibbons et al. 1993). Vascular biology has grown and matured over the past 50 years to emerge as a major area of research with many potential therapeutic applications.

1.1.1 Vasculature

The vessel wall is an integrated functional component of the circulatory system which continually remodels in response to hemodynamic or biomechanical stress (Xu 2000). Vessels are primarily divided into arteries and veins. Arteries are subdivided into large (elastic) arteries (such as aorta) and medium-sized (muscular, distributing) arteries. In general, veins are exposed to a lower blood pressure than arteries. Thus their wall structures are different from each other but both contain three layers: intima, media, and adventitia (Figure 1).

Figure 1. Structure of vessel wall

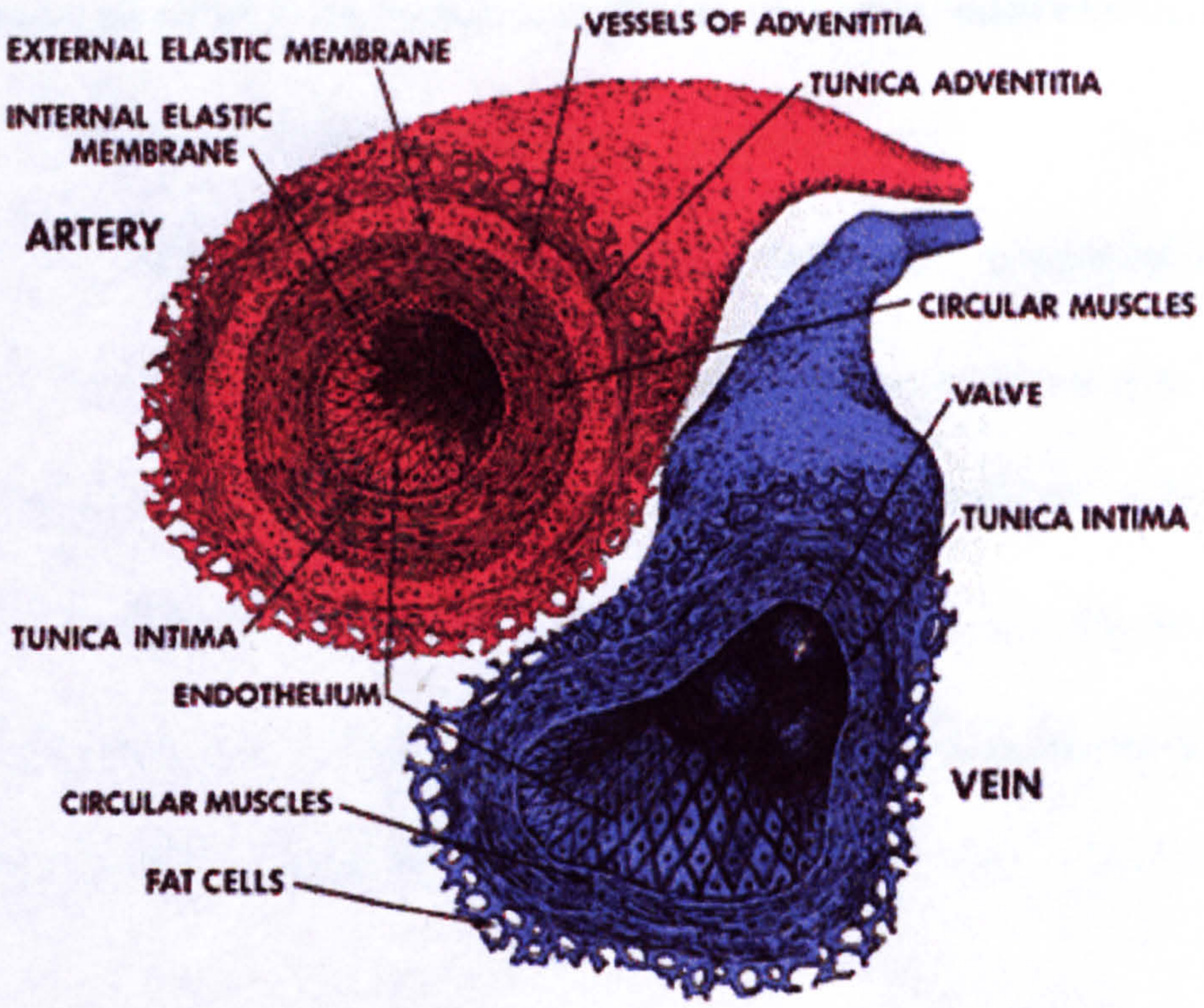

Figure 1. The arterial vessel wall has three layers: the intima with a lining of endothelial cells, the media, consisting of circular muscles between the internal and external elastic membrane, and the adventitia, embedded with *vasa vasorum* (supply vessels within the adventitia). The venous vessel wall is thinner and also has three layers: the intima, the media with less muscle cells, which lacks an elastic component, and the out layer, consists of fat cells. Large veins have valves to prevent blood flowing back under low blood pressure conditions.
(http://accessexcellence.org/AE/AEC/CC/images/vessel.gif)

The term SMC is used within the vasculature to include any connective tissue cell that forms a coating around the endothelial tube (Mahoney and Schwartz 2005). In addition to contractile function, vascular SMCs have been shown to be a pleiotropic cell capable of phenotypic changes associated with the synthesis of many biologically active molecules that mediate cell growth, death, migration, matrix modulation and inflammation. These actions of vascular SMCs play important roles in physiological vascular functions (such as vascular remodelling) and pathological disorders (such as atherosclerosis). A cadre of endogenous biological mediators regulating smooth muscle

phenotype and function have been identified, including growth factors, pro-apoptotic factors, matrix glycoproteins, metalloproteinases, cytokines, chemokines, and adhesion molecules (Alexander and Dzau 2000).

Moreover, SMCs in different parts of the vascular tree developed from different germ layers. For example, the descending aorta and most muscular arteries including the coronary arteries contain SMCs derived from the mesoderm, while the SMC compartment within the pulmonary trunc, the aortic arch and the ascending aorta originates from neuronal crest (ectoderm). Hence, a great variation has been observed among different SMC populations (Frid, Moiseeva et al. 1994; Frid, Dempsey et al. 1997).

The endothelium lines the inner surface of all blood vessels covering an area of approximately 1000 m^2 and amounts to a total weight of 1 kg in humans. The quiescent endothelium forms not only a selective barrier between blood and tissue, but also provides an antithrombotic surface, inhibits leukocyte adhesion and SMC proliferation and regulates the vascular tone via synthesis of nitric oxide (NO). However, injury causes endothelial activation and leads to the loss of its antithrombotic and anti-inflammatory properties. Dysfunctional endothelium expresses adhesion molecules (Cybulsky and Gimbrone 1991) and coagulation factors (Libby and Simon 2001) and produces reactive oxygen species (ROS), resulting in a decreased bioavailability of the vasodilator causing paradoxical vasoconstriction (Cai and Harrison 2000).

Robert Furchgott won the Nobel Prize for demonstrating endothelium-dependent vasodilatation (Furchgott and Zawadzki 1980). Endothelial cells have an obligatory role

in the relaxation of arteries by acetylcholine (ACh) and related muscarinic agonists by releasing a very labile (half-life 3~50 seconds) diffusible factor, endothelium-derived relaxing factor (EDRF), which acts on the adjacent smooth muscle cells to cause their relaxation. The chemical nature of EDRF was identified in 1986, when it was proposed that EDRF is nitric oxide (NO).

Figure 2. Current scheme for endothelium-dependent relaxation

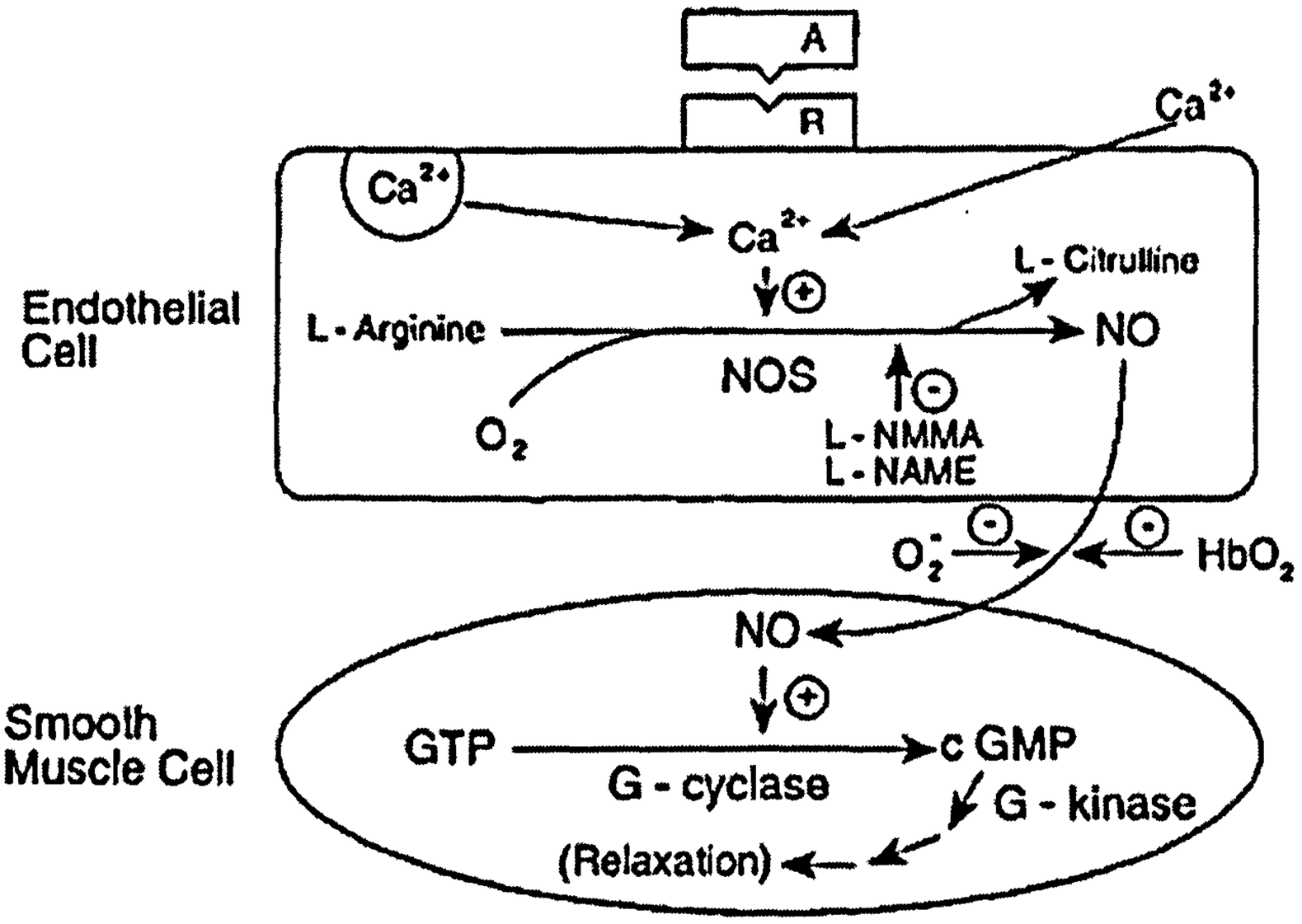

Figure 2. Agent A and receptor (R) of EC interaction activates Ca^{2+} influx. Increased intracellular Ca^{2+} activates NOS, generating NO from L-arginine. NO diffuses to adjacent SMCs where it activates G-cyclase, resulting increase in cGMP, which initiates processes leading to relaxation. L-NMMA and L-NAME are arginine derivatives, which inhibit NOS, and $O_2^{\bullet-}$ and HbO_2 are potent scavengers of NO. (**GTP**, guanosine triphosphate; **G-cyclase**, guanylyl cyclase; **cGMP**, cyclic guanosine monophosphate; **L-NMMA**, N^G-monomethyl-L-arginine; **L-NAME**, N_ω-Nitro-L-arginine methyl ester; **HbO_2**, oxygenated hemoglobin) (http://www.downstate.edu/pharmacology/furch.htm)

Most vasoactive stimuli such as shear stress mediate EC activities through the nitric oxide synthase (NOS)-derived NO. Three NOS enzymes are responsible for the production of NO, neuronal NOS (NOS1, nNOS), inducible NOS (NOS2, iNOS), and endothelial NOS (NOS3, eNOS), with eNOS to be important in the regulation of vascular compliance. eNOS is essential for neovasularization by enhance the

mobilization of stem and progenitor cells, so that contributs to impaired regeneration processes (Aicher, Heeschen et al. 2003). Massive generation of endogenous NO derived from iNOS overexpression leads to a marked apoptosis in vascular SMCs, suggesting an important role of NO as a proapoptotic factor for vascular SMCs in the process of vascular remodelling (Iwashina, Shichiri et al. 1998).

NO relaxes vascular smooth muscle and inhibits platelet aggregation and adhesion via the elevation of cGMP levels. NO is destroyed only by oxygen and superoxide anions ($O_2^{\bullet-}$). Its action both on vascular strips and on platelets is inhibited by hemoglobin and some redox compounds. Hemoglobin may have a complex action involving binding of NO, inhibition of guanylate cyclase and generation of $O_2^{\bullet-}$ during auto-oxidation (Moncada, Radomski et al. 1988).

In the vascular SMCs, the most predominant binding site for NO in the target tissues is heme group or iron-sulfur compound (Hobbs and Ignarro 1996). Heme plays a central role in eukaryotic metabolic pathways, as the prosthetic moiety of hemoproteins is involved in cell respiration and oxidative biotransformations, including hemoglobin and myoglobin, cytochrome P450, NOS and soluble G-cyclase. Heme oxygenase (HO) degrades heme to CO and biliverdin, which is further reduced to bilirubin. Two principal isozymes of HO have been identified, a constitutive isoform HO-2 and an inducible isoform HO-1, which is expressed at a low basal level in vascular ECs and SMCs and is induced by heavy metals, oxidative stress, inflammatory mediators and oxidized LDL. HO degrades heme to regulate hemoprotein levels and protect cells from the deleterious effects of free heme.

The vasodilator function ascribed to the heme-HO system relies on CO and biliverdin acting in a coordinated manner, with biliverdin/bilirubin as antioxidants. Importantly, biliverdin and bilirubin negate the pro-oxidant action of CO and thus enable the gas to effects vasodilation. The mechanism by which CO activates soluble guanylyl cyclase is similar to that of NO, and involves binding and dislocation of its heme-iron to induce a conformational change and activation of the catalytic site of guanylyl cyclase, resulting in elevated intracellular cGMP levels and leading to smooth muscle relaxation (Maines 1997). The heme moiety binds NO to form a 5-coordinate complex or bind CO to form a 6-coordinate complex. Although NO and CO modulate intracellular cGMP levels, platelet aggregation and smooth muscle relaxation, CO has a much lower affinity for soluble G-cyclase than NO (Stone and Marletta 1994). Decreased production or sensitivity to NO in atherosclerosis may be compensated for by an induction of HO-1, with bilirubin acting as a cellular antioxidant and CO as a vasodilator. CO and NO can also be generated in SMCs in response to atherogenic stimuli or pro-inflammatory cytokines, respectively. The metabolic and functional links between CO and NO suggest that vasodilator actions of CO may become important in atherogenesis, where endothelium-derived NO production is inhibited (Siow, Sato et al. 1999). As the heme moiety of NOS and soluble G-cyclase can serve as alternate substrates for HO, their activity may under certain conditions be downregulated. In addition, CO is able to bind to the heme moiety of NOS and thereby inhibit NO production (Maines 1997). (Figure 3)

Figure 3. Network of NOS-NO system and HO-CO system

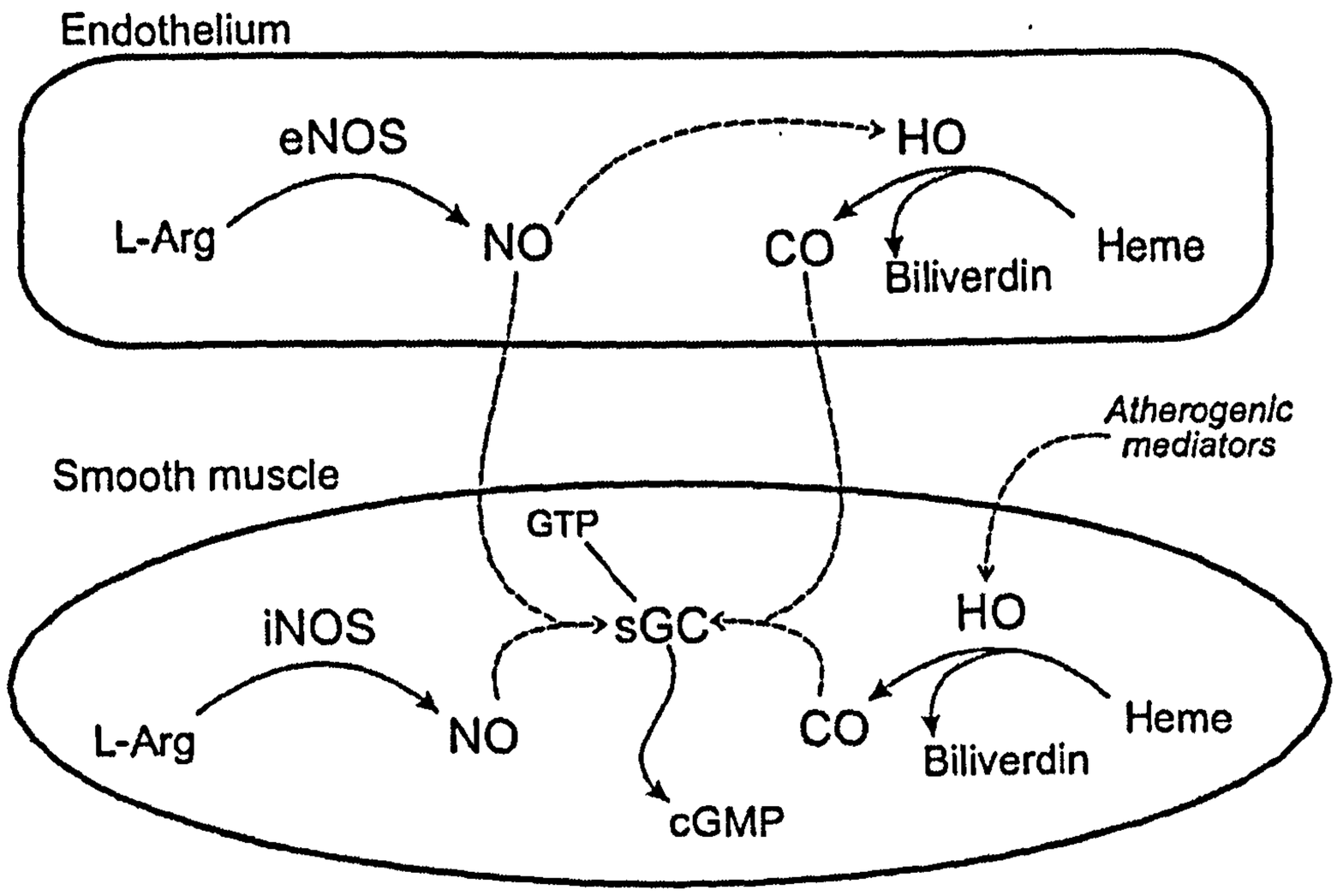

Figure 3. HO metabolizes heme to generate the antioxidant biliverdin and CO, which is similar to NO, stimulates sGC resulting in increased intracellular cGMP. Atherogenic and pro-inflammatory mediators decrease eNOS activity while induce HO-1 and iNOS in SMCs. Diminished production or activity of NO by the endothelium in atherogenesis could be compensated for by induction of HO-derived CO, which can sustain blood flow. At the same time catabolism of heme and generation of biliverdin would attenuate cellular oxidative stress in atherogenesis. (**L-Arg**, L-arginine; **eNOS**, endothelial nitric oxide synthase; **iNOS**, inducible nitric oxide synthase; **HO**, heme oxygenase; **sGC**,soluble guanylyl cyclase) (Siow, Sato et al. 1999).

It is well know that platelets play an important role in thrombosis and haemostasis, and in the maintenance of normal cardiovascular functions. Platelets express both iNOS and eNOS (Mehta, Chen et al. 1995). During platelets adhesion and aggregation, NOS is activated and generates NO. NO regulates platelets activation by inhibiting adhesion and aggregation. The L-arginine transport is rate-limiting for the NO production in uraemic platelets (Brunini, Yaqoob et al. 2003). NOS inhibitor N^G-monomethyl-L-arginine (L-NMMA) and N^G-nitro-L-arginine methylester (L-NAME) inhibits NO production of platelets so that increased their activation and adhesion (Brunini, Mendes-Ribeiro et al. 2006). Platelets-derived NO may play a

significant role in the maintenance of vascular tone and blood flow (Zhou, Hellermann et al. 1995).

NO inhibit the synthesis of platelet-activating factor by neutrophils, monocytes and ECs (Mariano, Bussolati et al. 2003). Increased transport of L-arginine is necessary to sustain NO synthesis in monocytes exposed to increased levels of circulating cytokines (Brunini, Roberts et al. 2002).

1.1.2 Development of vascular system

The embryo develops in the absence of vascularization at the earlies stages. When the embryo grows, the diffusion cannot provide sufficient nutrition for its development. The embryo rapidly transforms into a highly vascular organism, survival being dependent on a functional, complex network of capillary plexuses and blood vessels.

The initial event in vascular growth is vasculogenesis, a process whereby vessels are formed *de novo* from EC precursors (angioblasts). During vasculogenesis, angioblasts migrate to discrete locations, differentiate *in situ* and assemble into solid endothelial cords, later forming a plexus with endocardial tubes, also known as the primary capillary plexus. The subsequent growth, expansion and remodeling of these primitive vessels into a mature vascular network is angiogenesis, characterized by a combination of sprouting of new vessels from the sides and ends of pre-existing ones or by longitudinal branching of existing vessels with periendothelial cells. Angiogenesis is important in the embryo to promote the primary vascular tree as well as an adequate vasculature from developing organs (Conway, Collen et al. 2001).

Both vasculogenesis and angiogenesis have been extensively studied in embryonic stem cells of mouse (Vittet, Prandini et al. 1996; Feraud and Vittet 2003) and human origin (Levenberg, Golub et al. 2002).

1.1.3 Hemodynamics

In vivo, there are two main hemodynamic forces acting on vascular cells: shear stress, the dragging frictional force on ECs created by blood flow, and mechanical stretch, or tension, a cyclic strain stress created by blood pressure (Davies, Polacek et al. 1999). Shear stress is mainly sensed by ECs while all vascular cell types are exposed to stretch stress.

Fluid shear stress represent an essential survival signal for ECs and potently inhibits EC apoptosis via phosphorylation of the serine/threonine kinase Akt (Dimmeler, Assmus et al. 1998), which subsequently mediates the activation of endothelial nitric oxide synthase (eNOS) leading to increased NO production and vessel relaxation (Dimmeler, Fleming et al. 1999). Fluid shear stress also modulates EC structure and function including the organization of F-actin microfilaments, the expression of adhesion molecules, and the attraction, activation and adhesion of leukocytes. Transcription and expression of a variety of genes encoding for growth factors, transforming growth factor, vasodilators, vasoconstrictors, and adhesion molecules appear to be regulated on shear stress stimulation (Lehoux and Tedgui 1998).

Cyclic strain stress influences both ECs and SMCs. The maximum stretch of large diameter vessels (aorta, femoral and pulmonary arteries) in human is 9-12% under

normotensive conditions. A certain level of mechanical stretch is necessary to develop and maintain a differentiated and contractile phenotype of vascular SMCs (Lehoux and Tedgui 1998). Increased tension promotes the generation of vasoconstrictors and mitogenic factors such as endothelium-dependant contracting factors and platelet-derived growth factor (PDGF). If the cyclic strain stress is persistent and chronically elevated, SMCs may change structure supervention, beginning with hypertrophy (mainly seen in small vessels), hyperplasia (in large vessels) and cell migration, leading to gradual thickening of arterial walls, and subsequent hypertension and arteriosclerosis.

The endothelium acts as a mechanotransducer that senses blood flow stress and converts these extracellular mechanical stimuli to biochemical signals (Davies 1995; Resnick and Gimbrone 1995; Davies, Barbee et al. 1997), which is important for both acute vascular regulation and chronic vascular remodelling. *In vitro*, fluid mechanical shear stress elicits acute endothelial responses that include activation of ion channels (Olesen, Clapham et al. 1988) and G proteins (Berthiaume and Frangos 1992; Gudi, Clark et al. 1996; Gudi, Nolan et al. 1998), mobilization of intracellular calcium (Shen, Luscinskas et al. 1992; Ando, Ohtsuka et al. 1993), and induction of protein kinase pathways (Tseng, Peterson et al. 1995). Subsequent transcription factor activation (Lan, Mercurius et al. 1994) and binding to shear stress response-related sequences of several flow-responsive genes (Resnick and Gimbrone 1995) results in important functional and structural changes in the cells including extensive topographic and cytoskeletal reorganization, cellular elongation, and alignment in the direction of shear stress

(Dewey, Bussolari et al. 1981; Remuzzi, Dewey et al. 1984; Barbee, Davies et al. 1994). Physical forces initiate signal pathways, especially mitogen-activated protein kinases (MAPKs), leading to vascular cell death and inflammatory response followed by SMC proliferation. Thus, mechanical stress, similar to cytokines or growth factors, can effectively activate signal transduction pathways, which can result in apoptosis and cell proliferation so that contribute to the development of arteriosclerosis (Mayr, Li et al. 2000; Xu 2000; Mayr, Hu et al. 2002).

1.1.4 Vascular remodelling

Different physical forces lead to a different vessel remodelling. Blood vessels regress when not constantly perfused, they enlarge when chronically exposed to high flows, and their walls become thicker with high pressures (Heil and Schaper 2004). The adaptation and accommodation abilities of the blood vessel to long- and short-term hemodynamic condition changes are critical functions in cardiovascular homeostasis (Figure 4) (Gibbons and Dzau 1994).

Figure 4. The spectrum of structural alterations of blood vessels

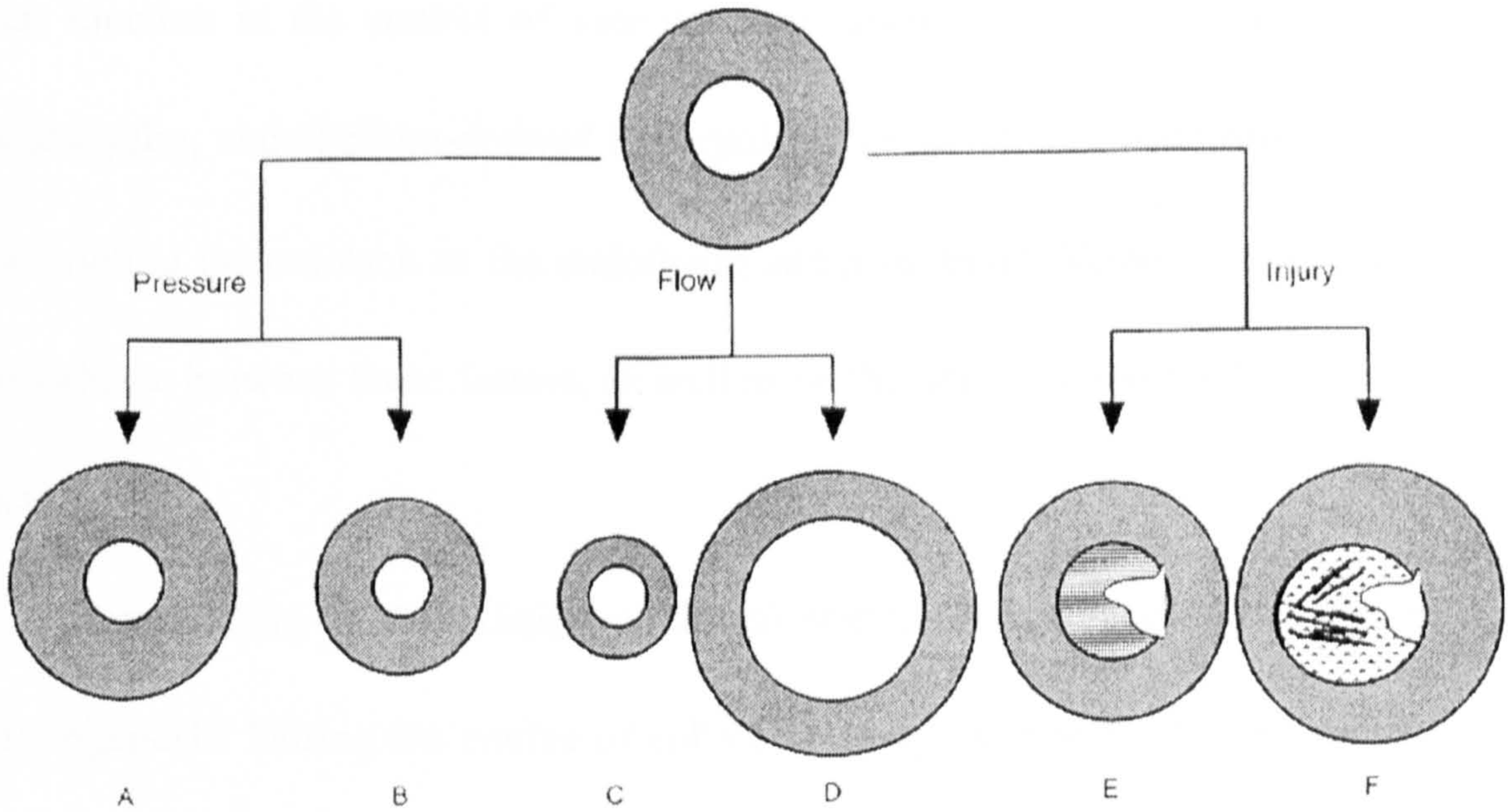

Figure 4. In response to increased arterial pressure, the ratio of the width of the vessel wall to the width of the lumen is elevated by either an increase in muscle mass (A) or rearrangement of cellular and noncellular elements (B). Vascular stenosis increases shear stress and thereby induces an increase in the vessel radius to maintain a constant predetermined level of shear stress (D), such as arteriovenous fistula and aneurysm formation. Conversely, a long-term reduction in blood flow results in vascular mass and calibre reduction (C). The architecture of the vessel wall is also markedly altered in response to vascular injury, such as neointimal hyperplasia (E) and atherosclerosis (F). (Gibbons and Dzau 1994)

Vascular remodelling involves cell growth, migration, apoptosis, extracellular matrix expansion or contraction, and activation or inhibition of specific proteolytic enzymes or glycosidases. It is dependent on a dynamic interaction between locally generated growth factors, vasoactive substances, and hemodynamic stimuli. The remodelling response is usually a long-term adaptive process occurring in response to chronic changes in hemodynamic conditions, but it may subsequently contribute to the pathophysiology of vascular diseases and circulatory disorders, such as atherosclerosis (Gibbons and Dzau 1994).

Although all the vascular cells may participate in the remodelling process, the

endothelium is particularly suited to play a prominent part. The endothelium serves as dual function in the control of vascular tone, secreting relaxing factors such as NO, prostacyclin, endothelium-derived hyperpolarizing factor, and adenosine, in addition to constricting factors such as the endothelin and prostanoid. Vessel tone is dependent on the balance between these factors, as well as on the ability of the SMC to respond to the factors.

Remodelling of pre-existing collateral arteriolar anastomoses is involved during arteriogenesis. During the course of collateral artery development, the collateral vessel wall is exposed to increased fluid shear stress, which initiates the interaction between monocytes and vascular endothelium. After that, growth factors are released from the matrix and monocytes, which not only activate mitosis but also influence the transcription of secondary growth factors, inactivation of the matrix-metalloproteinases (MMPs) inhibitor and down-regulation of elastin. SMCs are transformed from the contractile into the proliferative/synthetic phenotype. Monocytes/macrophages produce MMPs so that they can migrate from the intraluminal side of the collateral arteriole toward deeper vessel wall regions. The invasion of monocytes and proliferation of SMCs transform an arteriole with only 1-2 layers of SMCs into an artery of up to 20-fold larger in diameter and 50-fold larger in tissue mass by SMCs proliferation. The increase of collateral vessel diameter reduces fluid shear stress, which is the signal for maturation and terminates the SMC proliferation. The arteriogenesis, which transform a small microvascular resistance vessel into a large conductance artery, is completed (Heil and Schaper 2004).

1.1.5 Vascular disease

Cardiovascular disease is the principal death reason in western society and much of Asia. Alterations of hemodynamic forces have significant impact on the development of cardiovascular diseases. Excessive accumulation of SMCs has a key role in the pathogenesis of vascular diseases (Sata, Saiura et al. 2002) such as arteriosclerosis, atherosclerosis and graft arterial disease.

1.1.5.1 Risk factors for atherosclerosis

Several important environmental and genetic risk factors are associated with atherosclerosis (Table 1).

Table 1. Risk factors for atherosclerosis

Modifiable risk factors	
Hypertension	Mechanical stress exerts the main influence on atherosclerosis as this disease only occures in arteries but not in veins. Atherosclerotic lesion favours areas of disturbed flow such as bifurcations, branch ostia and curves. These sites are often associated with structural modifications (intimal thickening, cellular rearrangement, SMCs proliferation and extracellular matrix deposition (Gibbons and Dzau 1994).
Hyperlipidaemia	Plasma lipid disorders are associated with an increased risk of atherosclerosis related disease, particularly coronary artery disease (CAD). Lipids are transported in the plasma as lipoproteins. There are three main categories of lipoproteins: high density lipoprotein (HDL), low density lipoprotein (LDL), and very low density lipoprotein (VLDL). LDL is the major carrier of cholesterol in the plasma and LDL-derived cholesterol is important in maintaining overall cholesterol homeostasis within cells. As cellular cholesterol increases, cellular cholesterol synthesis and synthesis of new LDL receptors are inhibited while scavenger receptors of macrophages and SMCs are not down-regulated, leading to foam cell formation in atherosclerotic lesions. Apolipoprotein E (ApoE) deficiency mouse provides an appropriate animal model for hypercholesterolaemia and shows

spontaneous atherosclerosis (Zhang, Reddick et al. 1992). Besides cholesterol, high plasma triglycerides are also associated with premature CAD, probably because they inhibit natural tissue plasminogen activator.

Smoking

There is a direct link between CAD and the number of cigarettes smoked. This risk declines to normal levels within 5 years of giving up smoking. Smoking increases free radical production and therefore oxidized-LDL. Carcinogens in the cigarette smoke cause DNA damage (Izzotti, De Flora et al. 1995; De Flora, Izzotti et al. 1997) therefore smoking contributes to endothelial injury as an early event in atherogenesis.

Diabetes mellitus

Complications of diabetes mellitus can be broadly considered as macro- and microvascular. Macrovascular complications (such as myocardial infarction, stroke and peripheral vascular diseases) are more common in patients with diabetes and improved glycaemic control cannot *per se* reduce the risk of them. Microvascular complications (such as retino-, nephro- and neuropathy) are hallmarks of diabetes mellitus. An attractive hypothesis suggests that elevated blood glucose levels cause glycosylation of various proteins, including lipoproteins. These products accumulate in atherosclerotic lesions and mediate cytotoxic effects on ECs. Improved glycaemic control minimizes and delays microvascular complications.

Hemostatic factors

Increased plasma levels of hemostatic factors (factor VII, factor VIIIC and fibrinogen) are associated with an increased risk of atherosclerosis. It is not known whether a reduction in these factors lowers incidence of angina and myocardial infarction.

Weakly associated factors

There is no clear evidence that the weakly associated factors can cause atherosclerosis. Physical activity may be beneficial on the circulation, or merely indicate a healthy constitution in those who make exercise. Persons with type A personality (aggressive, restless, ambitious people who are constantly anxious about deadlines) have more atherosclerosis than others. This may be due to an increased level of circulating catecholamines. The more alcohol the higher the risk, but no alcohol is also thought to lead to a higher risk. Alcohol intake below 50g per day seems to be protective for atherosclerosis (Kiechl and Willeit 1999).

Virus

Several reports showed a correlation between the incidence of atherosclerosis and the presence of infectious microorganisms, such as herpesviruses and *C. pneumoniae*. They are identified in atheromatous

lesions in coronary arteries and other organs but no direct evidence shows they can cause the lesions of atherosclerosis (Ross 1999).

Non-modifiable risk factors

Aging	Although early lesions can be identified in young people, the incidence of atherosclerosis rises with age. Besides its intima- media thickening effects, aging predicts marked dilation of the vessel because of loss of elastic fibres, which is independent of elevated wall thickness and other determinants of vessel. Notably, structural aging is not an obligatory phenomenon but usually occurs once enhanced intima-media thickening indicates incipient wall pathology (Strong, Oalmann et al. 1984; Wissler 1992).
Sex	Atherosclerosis is more common in men than in women (Strong, Malcom et al. 1992; Strong 1995). After the menopause the incidence in women increases to approach that of men at the same age. The relative protection of women is attributed to female sex hormones. 17β-estradiol inhibits apoptosis in ECs (Alvarez, Gips et al. 1997). Additionally, women show a lower LDL levels and higher HDL levels than men.
Genetics	Premature vascular disease undoubtedly runs in families, but there is no established pattern. In the absence of other risk factors, a history of myocardial infarction increases the risk of ischaemic heart disease in offspring by 20-30%. Inherited metabolic disorders (such as lipopathy and homocystinemia) are associated with increased risk for atherosclerosis.

1.1.5.2 Atherogenesis

Atherogenesis is a slowly progressive process (Stary 1989). Depending on their size and composition, lesions are divided into fatty streaks, early stages of lesions, and advanced stages of atherosclerosis called plaques. Intima-media thickening of the vessel wall commonly precedes definite atherosclerosis. Such precursor lesions of atherosclerosis may occur as early as adolescence, but the frequency of definite atherosclerotic lesions remains low until age 40 in men and onset of menopause in

women.

Pre-existing atherosclerotic lesions may experience one of two different types of disease progression (Kiechl and Willeit 1999). The first main type of plaque growth is described as nonstenotic atherosclerosis. It is characterized by slow and continuous plaque extension, which usually affects several plaques simultaneously and rarely causes lumen obstruction >40%. Nonstenotic atherosclerosis relies on a cumulative exposure to well-established risk factors. It is mediated by a variety of complex biological step-by-step phenomena such as lipid-induced atherogenesis or SMC proliferation. Diffuse dilative atherosclerosis may be assumed as a final stage of this type of disease progression. Compensatory enlargement of the artery at the site of active atherosclerosis effectively preserves a near normal lumen or is even over-compensatory in the early course of disease. Vascular remodelling in response to atherogenesis restores normal blood flow and delays the onset of clinical symptoms. The second main type of plaque growth is a focal disease, which usually develops at sites of high hemodynamic stress. Rapid plaque expansion and insufficient or lacking vascular remodelling act synergistically in producing a significant lumen compromise. Atherothrombosis seems to be the main underlying pathomechanism. Consistent with the concept of underlying plaque thrombosis, stenotic atherosclerosis is a domain of a procoagulant state without a significant age trend. The risk profile consists of clinical conditions known to interfere with coagulation and markers of enhanced thrombotic activity. Actually, both types of atherogenesis develop and proceed independently from each other. Similarly, the degree of arterial stenosis does not predict the likelihood of

myocardial infarction. Plaque fissuring which results in infarction mostly occurs in relatively minor atherosclerotic plaques.

Atherosclerotic plaques contain three major cellular components: the SMCs, which dominate the fibrous cap, the macrophages, which are the most abundant cell type in the lipid-rich core region, and the lymphocytes, which have been mainly ascribed to the fibrous cap (Ross 1999). Vascular SMC migration, proliferation, and matrix synthesis within the intima of medium-sized and large vessels is though to play a major role in atherosclerosis development in adult human subjects (Ross 1993).

The most popular model (Ross 1999) summarized atherogenesis as following four steps: (a) EC damage leads to endothelium dysfunction (increased permeability and endothelial adhesion molecules), allows leukocytes migration into the artery wall. (b) Fatty streaks initiate with lipid-laden monocytes, macrophages (foam cells) and T lymphocytes and further increase by SMCs migration and proliferation, T-cell activation, foam cell formation, and platelet adherence and aggregation. (c) As fatty streaks progress to intermediate and advanced lesions, a fibrous cap is formed to shield the lesion from the lumen. The fibrous cap covers a mixture of leukocytes, lipid, and debris, which may form a necrotic core. (d) Unstable fibrous plaques rupture from a thinning fibrous cap can rapidly lead to thrombosis. (Figure 5)

Figure 5. Atherogenesis model

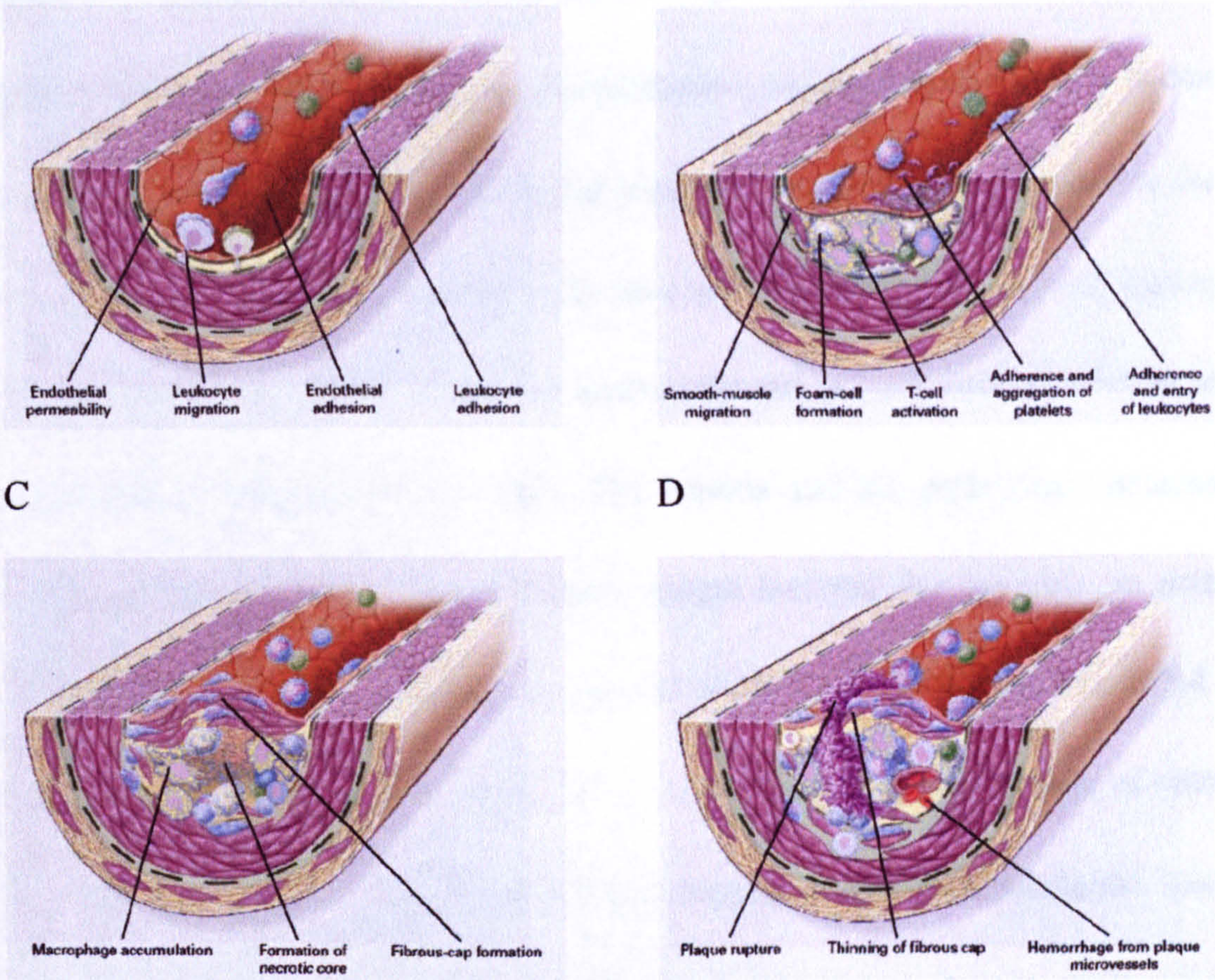

Figure 5. (A) Endothelial dysfunction as an initial step of atherosclerosis. (B) Fatty-streak formation. (C) Formation of an advanced, complicated lesion. (D) Unstable plaques are generated. (Ross 1999)

1.1.5.3 Arteriosclerosis

The arteriosclerotic lesion is characterized by SMC hyperplasia or hypertrophy and matrix protein accumulations in the intima and/or media with or without lipid deposition, resulting in thickening and stiffness of the arterial wall (Schwartz 1999). Biomechanical stress effects on the vessel wall during the development of all types of arteriosclerosis (Zou, Hu et al. 1998).

Abnormal or pathological remodelling in conditions such as hypertensive vascular hypertrophy, atherosclerosis, bypass graft disease, restenosis, and transplant

vasculopathy involves inappropriate cellular and extracellular changes leading to narrowing or occlusion of the lumen. Autologous vein grafts are the only surgical alternative for many types of vascular reconstruction, but occlusion of grafts is common after bypass operations. Three pathological processes are primarily responsible for vein graft occlusion: (a) thrombosis as an early postoperative event; (b) intimal hyperplasia after a few months to a few years; (c) arteriosclerosis occurs usually after at least 3 years (Bourassa, Campeau et al. 1982). The lesions and the pathogenic processes of graft-induced arteriosclerosis appear to have unique features. For instance, an extensive loss of ECs in the intima and a significant loss of SMCs in the media of grafted veins were observed (Kockx, Cambier et al. 1994). In addition, the development of vein graft arteriosclerosis is rather rapid compared to arteries. Hypercholesterolemia has been shown to be a significant risk factor for the development of vein graft atheroma. Evidence indicates that the rates of obstructive atheroma in grafted veins were highly correlated to preoperative serum cholesterol levels, and that lesion development was predicted by higher levels of plasma VLDL and LDL. Accordingly, patients with familiar hypercholesterolemia exhibit a high incidence of late vein graft occlusion after bypass surgery. However, the molecular mechanism, by which hypercholesterolemia initiates, promotes or perpetuates vein graft atherosclerosis, is largely unknown.

1.2 Stem cells

Stem cells represent one of the most promising areas in biological and medical research. All stem cells are defined as having two basic properties: prolonged

self-renewal and the potential to differentiate *in vitro*, via "progenitor cells", into differentiated somatic cells of many tissue types. Stem cells include two broad categories: embryonic stem cells (ES cells) and adult (somatic) stem cells (Gepstein 2002).

1.2.1 Embryonic stem cells

1.2.1.1 Mouse ES cells

The term "embryonic stem cells" originated from the isolation of pluripotent stem cell cultures from early mouse blastocyst by Evans and Kaufman (Evans and Kaufman 1981) and Martin (Martin 1981) independently. ES cells are characterized by their capacity for prolonged undifferentiated proliferation in culture while maintaining the potential to differentiate into every cell type of all three germ layers, including germ cells (Bradley, Evans et al. 1984).

Figure 6. Scheme of early mouse embryonic development

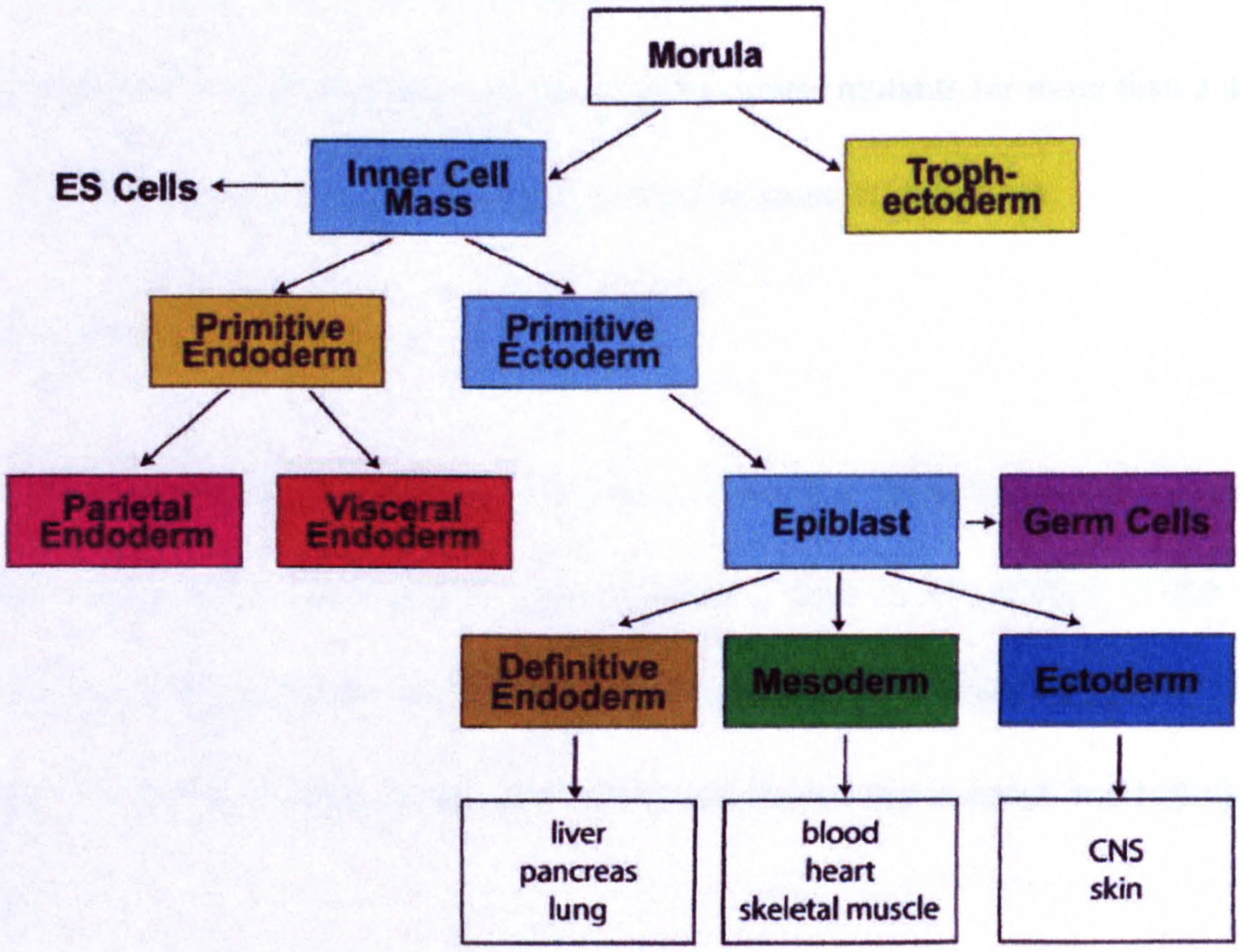

Figure 6. Scheme of early mouse development depicting the contribution of early cell populations such as ES cells to the development of the three germ layers. (Keller 2005)

When co-cultured on confluent feeder layers (Evans and Kaufman 1981; Martin 1981) or cultured in medium containing leukemia inhibitory factor (LIF) (Smith, Heath et al. 1988; Williams, Hilton et al. 1988), mouse ES cells can be maintained in the undifferentiated state, otherwise they will spontaneously differentiate into embryonic structures. Recent development allows mouse ES cells culture with defined factors, such as LIF and bone morphogenetic protein 4 (BMP4) in the absence of serum or feeder cells (Ying, Nichols et al. 2003).

The ability to derive multiple lineages from ES cells opens exciting new opportunities to model embryonic development *in vitro* for studying the events regulating the earliest stages of lineage induction and specification. In addition, ES cell

differentiation system is considered as a novel and unlimited source of cells and tissues for transplantation for the treatment of a broad spectrum of diseases (Keller 2005). The ES cells have been used extensively for creating mouse mutants for more than a decade, but their application in cell replacement therapy remains in its infancy.

1.2.1.2 Human ES cells

The human ES cell lines were first derived from the "inner cell mass" of blastocyst stage embryos that developed in culture within 5 days of fertilization of the oocyte (Thomson, Itskovitz-Eldor et al. 1998). The human ES cells dramatically elevated the interest in the cell therapy aspect of ES cells and moved this concept one step closer to reality.

The regulation of human ES cell growth is less well understood and differs from that of the mouse in that LIF and STAT3 (signal transducer and activator of transcription 3) appears to play no role in their self-renewal. The use of inactivated fetal mouse fibroblast feeder cells is essential to inhibit the spontaneous differentiation of human ES cells *in vitro* and removing the feeder cells markedly enhanced their differentiation (Thomson, Itskovitz-Eldor et al. 1998; Reubinoff, Pera et al. 2000; Daheron, Opitz et al. 2004). With current protocols, human ES cells can be maintained on feeder cells in serum-free medium supplemented with basic fibroblast growth factor (bFGF) (Amit, Carpenter et al. 2000). human ES cells can also be grown in the absence of feeder cells if cultured on matrigel- or laminin-coated plates in medium supplemented with mouse embryonic fibroblast conditioned medium (Xu, Inokuma et al. 2001), which is a

relatively easy maintenance of human ES cells. Further studies are needed to clarify the molecular mechanism that regulates human ES cell self-renewal (Keller 2005).

1.2.2 Embryonic stem cell differentiation

ES cells can differentiate into specialized somatic cells *in vitro* and have shown many early embryonic development processes (Gepstein 2002). It has been reported that ES cells display a remarkable capacity to form differentiated cell types in culture (Keller 1995; Smith 2001), e.g. cardiomyocytes (Doetschman, Eistetter et al. 1985), hematopoietic progenitor cells (Doetschman, Eistetter et al. 1985), ECs (Risau, Sariola et al. 1988; Hristov, Erl et al. 2003), skeletal muscle cells and SMCs (Rohwedel, Maltsev et al. 1994; Drab, Haller et al. 1997; Itskovitz-Eldor, Schuldiner et al. 2000), neuronal and glial cells (Bain, Kitchens et al. 1995; Brustle, Jones et al. 1999), pancreatic islet cells (Soria, Roche et al. 2000), yolk sac (Doetschman, Eistetter et al. 1985), adipocytes (Dani, Smith et al. 1997), chondrocytes (Poliard, Nifuji et al. 1995), melanocytes (Yamane, Hayashi et al. 1999), primitive endoderm (Abe, Niwa et al. 1996), and several other tissue types (Keller 1995). These highlighted totipotency and self-renewal make ES cells a promising source for regeneration medicine (Yurugi-Kobayashi, Itoh et al. 2003).

When removed from the factors that maintain them as stem cells, ES cells will differentiate and, under appropriate conditions, generate progeny consisting of derivatives of the three embryonic germ layers: mesoderm, endoderm, and ectoderm (Keller 1995; Smith 2001). Three general approaches are used to initiate ES cell

differentiation. All of these approaches are effective and have specific advantages and disadvantages and have been used to generate a broad spectrum of cell types from ES cells (Table 2).

Table 2. Three methods of initating ES cells differentiation

Methods	Advantage	Disadvantage
Cells differentiated as embryoid bodies (Doetschman, Eistetter et al. 1985; Keller 1995)	Enhanced cell-cell interactions may be important for certain developmental programs.	Spontaneous differentiation is relatively inefficient and only a small fraction of ES cells differentiate into lineage of interest. Too complicated for interpretating signalling pathway
Cells differentiated on stromal cells (Nakano, Kodama et al. 1994)	Benefit from the growth promoting effects of the particular supportive cell line used.	Undefined factors produced by these supportive cells It is difficult to separate desired cells from the stromal cells
Cells differentiated on extracellular matrix proteins (Nishikawa, Nishikawa et al. 1998)	Culturing with defined proteins minimizes the influence of neighbouring cells and supportive stromal cells, achieve controlled differentiation of stem cells into well-defined lineages *in vitro*.	Different proteins may influence the generation and survival of the developing cell types

1.2.2.1 Mesoderm-derived lineages

Mesoderm-derived lineages, including the hematopoietic, vascular and cardiac are among the easiest to generate from ES cells and have been studied in considerable detail. Besides, the ES cell system also can differentiate to the skeletal muscle (Rohwedel, Maltsev et al. 1994), the osteogenic (Buttery, Bourne et al. 2001; zur Nieden, Kempka et al. 2003), the chrondrogenic (Kramer, Hegert et al. 2000), and adipogenic (Dani, Smith et al. 1997) lineages. All these *in vitro* development recapitulated its development *in vivo*, indicating that these populations progressed through normal differentiation progress.

1.2.2.1.1 Hematopoietic differentiation

There are many studies focus on the hematopoietic differentiation using the ES cells (Burkert, von Ruden et al. 1991; Schmitt, Bruyns et al. 1991; Keller, Kennedy et al. 1993; Nakano, Kodama et al. 1994) since the discovery of the hemoglobinized cells in embryoid bodies 20 years ago (Doetschman, Eistetter et al. 1985). To date, methods have been established for selectively expanding multipotential cell populations, neutrophils, megakaryocytes, master cells, eosinophils, dendritic cells, and definitive erythroid cells from ES cells in culture (Keller 2005).

In optimized culture conditions following serum induction, ES cells will undergo hematopoietic differentiation in a highly reproducible and efficient way, which can be easily monitored by gene expression patterns, the appearance of specific cell surface markers, and the development of clonable progenitor cells, so that investigation of the regulation of hematopoietic commitment become possible.

The progenitor derived from ES cells known as blast colony-forming cell (BL-CFC) gives rise to hematopoietic and vascular progenitors in methylcellulose culture in the presence of VEGF (Kennedy, Firpo et al. 1997; Choi, Kennedy et al. 1998), proved the hypothesis that the hematopoietic and endothelial lineages develop from a common progenitor, the hemangioblast. However, the BL-CFC does not express hematopoietic and vascular markers, such as CD31, VE-cadherin, CD34, or c-kit (Fehling, Lacaud et al. 2003), indicating this progenitor is in the earliest stage of hematopoietic commitment. Also the ES cell-derived hematopoietic cells express EC markers (Flk-1, VE-cadherin and CD41) before the hematopoietic-specific marker (CD45) which presents on most fetal liver and adult bone marrow cells. BMP4 together with VEGF can support hematopoietic differentiation of ES cells in serum-free conditions (Nakayama, Lee et al. 2000; Park, Afrikanova et al. 2004). The development of the BL-CFC and hematopoietic progenitors is positively regulated by bFGF (Faloon, Arentson et al. 2000), VEGF (Nakayama, Lee et al. 2000; Park, Afrikanova et al. 2004) and serum-derived factors.

Several studies have documented hematopoietic development in human ES cell cultures either through co-culture with stromal cells (Kaufman, Hanson et al. 2001) or the generation of EBs (Chadwick, Wang et al. 2003; Cerdan, Rouleau et al. 2004). While differentiation was serum-induced, hematopoietic development was augmented in the EBs by the addition to the cultures of BMP4, VEGF, and a mixture of hematopoietic cytokines (stem cell factor, Flt-3 ligand, interleukin-3, interleukin-6 and granulocyte colony-stimulating factor) (Cerdan, Rouleau et al. 2004). Under this

condition, hematopoietic induction is slower than observed in mouse ES cell differentiation cultures. Only the hemoglobin pattern changes were detected within the ES cell-derived erythroid lineages but no distinct primitive or definitive erythroid population was identified. Similarly, human hematopoietic development also expresses EC markers (Flk-1, VE-cadherin, CD31) before their maturation to $CD45^+$ cells (Wang, Li et al. 2004). The findings from this limited number of studies indicate that it is possible to generate hematopoietic cells from human ES cells in culture and that the sequence of developmental events may reflect the onset of hematopoisis in the early embryo (Keller 2005).

1.2.2.1.2 Vascular differentiation

It has been discussed that the vasculogenic potential of ES cells could be specifically of use in tissue engineering for the induction of tissue vascularization (Levenberg, Golub et al. 2002). Endothelial development can also be detected in early yolk sac blood islands of the embryo (Haar and Ackerman 1971) and ES cell-derived BL-CFC, suggesting that development of the endothelial lineage *in vitro* recapitulates its development *in vivo*. ES cells differentiate *in vitro* to ECs through successive maturation steps with sequential expression of cell lineage-specific markers: Flk-1, platelet endothelial cell adhesion molecule (PECAM) and tie-2, tie-1 and VE-cadherin, and EC specific antigens MECA32 (Hallmann, Mayer et al. 1995) and CD34/MEC-14.7 (Vittet, Prandini et al. 1996). A similar pattern was also observed when isolated $Flk\text{-}1^+$ progenitors were re-cultured on type IV collagen-coated dishes or on OP9 stromal cells (Hirashima, Kataoka et al. 1999).

The Flk-1^{+} cells derived from ES cells can differentiate into both endothelial and mural cells in response to VEGF and PDGF-BB selection respectively, so that to suffice a vascular progenitor cells (VPCs) (Yamashita, Itoh et al. 2000). VEGF is a major growth factor for developing ECs and lack of VEGF will result in embryo death during embryonic vascular development. Several growth factors have been implicated in SMC differentiation, including transforming growth factors (TGF) β1, β3, and PDGF-BB, (Nakajima, Mironov et al. 1997; Hirschi, Rohovsky et al. 1998; Hellstrom, Kalen et al. 1999; Chen and Lechleider 2004). The combinatorial effects of Flk-1 and transcription factor T-cell acute lymphocytic leukemia 1 (Tal-1) regulate cell fate choice in early development into hematopoietic, endothelial and smooth muscle lineage (Ema, Faloon et al. 2003). Flk-1$^{-/-}$ mouse embryo cannot form both hematopoietic and endothelial cells, suggesting they share a common progenitor. Although Tal-1 is dispensable for initial endothelial development, it is required for later vascular remodeling. In the absence of Tal-1, ES cells favour the vascular smooth muscle development pathway and are unable to generate endothelial and hematopoietic progeny, while when expressed, they differentiate to endothelial and smooth muscle cells. Interestingly, in the absence of Tal-1, cell-to-cell interactions play an important role in the generation and maintenance of ECs in vitro (Table 3) (D'Souza, Elefanty et al. 2005).

Table 3. Flk-1^{+} cell fate under different condition

	Cell types	Adherent	Aggregate
Tal-1$^{+/+}$	ECs (CD31^{+},Flk-1^{+},VEcad^{+})	~30%	~60%
	SMCs (SMA^{+})	~50%	~5%
	HSC (Gata-1^{+})	-	+
Tal-1$^{-/-}$	ECs (CD31^{+},Flk-1^{+},VEcad^{+})	0.5%	~27%
	SMCs (SMA^{+})	~70%	~18%
	HSC (Gata-1^{+})	-	-

The functional capacity of the ES cell-derived VPCs has been evaluated both in culture (Doetschman, Eistetter et al. 1985; Bautch, Stanford et al. 1996; Yamashita, Itoh et al. 2000) and in animal models following transplantation. They can organize into vessel-like structures or incorporated into newly formed vessel *in vitro* and *in vivo*, thus participate in neovascularization (Marchetti, Gimond et al. 2002; Yurugi-Kobayashi, Itoh et al. 2003).

Endothelial differentiation has also been demonstrated in human ES cell differentiation cultures. The cells that develop in these cultures express endothelial markers, form tube-like structures in matrigel *in vitro*, and generate capillary structures when transplanted into severe combined immunodeficient mice (Levenberg, Golub et al. 2002).

1.2.2.1.3 Cardiac differentiation

Development of the cardiomyocytes lineage progresses in ES cell differentiation is similar to development of the lineage *in vivo*. The presence of cardiomyocytes can be easily detected by the appearance of contracting cells, expression of cardiac genes, and electrophysiological measurements (Maltsev, Rohwedel et al. 1993; Hescheler, Fleischmann et al. 1997; Boheler, Czyz et al. 2002; Banach, Halbach et al. 2003). Because few antibodies are available for the isolation of cardiac progenitors, ES cells were genetically modified to express either drug-resistance (Klug, Soonpaa et al. 1996; Zandstra, Bauwens et al. 2003) or fluorescent genes (Kolossov, Fleischmann et al. 1998; Muller, Fleischmann et al. 2000; Hidaka, Lee et al. 2003) under the control of stage-specific gene promoters of cardiac development to enable specific cell selection

within the lineage.

ES cell-derived cardiomyocytes selected for α-cardiac MHC expression could incorporate and survive in the hearts of dystrophic mice after direct transplantation (Klug, Soonpaa et al. 1996), providing the source of transplantable cells for the treatment of cardiovascular disease. Expression of VEGF in the cardiomyocytes prior to transplantation into hearts of mice with myocardial infarction shows increased cell survival and enhanced neovascularization and improved cardiac function (Yang, Min et al. 2002). Cardiomyocytes differentiation and maturation have also been demonstrated in human ES cell differentiation cultures, which are similar to that reported *in vivo* (Nir, David et al. 2003). Although the human ES cell-derived cardiomyocytes do not undergo maturation to the stage of adult cardiomyocytes, cells with electrical properties of nodal, atril, and ventricular cells have been identified (He, Ma et al. 2003). Recently, human ES cell-derived cardiomyocytes have been used in xenogeneic transplantation as "biologic pacemakers" for the treatment of bradycardia (Kehat, Khimovich et al. 2004), but the arrhythmia effect should be concerned.

1.2.2.2 Endoderm-derived lineages

The generation of endoderm derivatives, in particular pancreatic β-cells and hepatocytes, has become the focus of many investigators in the filed of ES cell biology. The interest of their development derives from their clinical potential for the treatment of Type I diabetes and liver diseases, etc. ES cells have been successfully induced into pancreatic islets, hepatocytes, thyrocytes, lung, and intestinal cells but several obstacles

still impair the progress of generating endoderm-derived cell types, such as very low frequency of differentiated cells, markers specifity, and lack of specific inducers. Only when large numbers of highly enriched progenitors are available, can these ES cell-derived endoderm cells be used in clinical applications (Keller 2005)

1.2.2.3 Ectoderm differentiation

Most of ectoderm differentiation studies focus on neuroectoderm commitment and neural differentiation. Each of the relatively pure populations of three major neural cell types (neurons, astrocytes, and oligodendrocytes) of the central nervous system can be generated when cultured under appropriate conditions (Okabe, Forsberg-Nilsson et al. 1996; Barberi, Klivenyi et al. 2003). The ability to generate different types of neurons from ES cells has dramatically raised the interest in repair of nervous system disorders by cell replacement therapy, one of which is Parkinson's.

In addition to somatic tissues, several studies have documented the development of germ cells from differentiated ES cells (Lawson, Dunn et al. 1999; Hubner, Fuhrmann et al. 2003; Clark, Bodnar et al. 2004). Before the models can be widely used, it will be important to define the regulators that induce germ cell development.

1.2.2.4 Modelling embryonic development with ES cell

The studies of earliest stages of lineage development in ES cell differentiation highlight the importance of understanding these early events, as the inducing molecules used in the differentiation cultures dramatically influence the cell populations that

ultimately develop and different cell fate needs different set of conditions. When ES cells were cultured without LIF, they will spontaneously differentiate to primitive ectoderm. The brachyury-expressing cells are shown as a hypothetical primitive streak consisting of both posterior and anterior populations. BMP4 is shown to induce posterior mesoderm and skin. Low concentrations of activin/nodal induce more posterior populations and high concentrations induce endoderm (derived from anterior primitive streak). FGF is shown to play a role in neural induction, whereas Wnt, BMP, and activin are all implicated as inhibitors of the early stages of this pathway (Figure 7) (Keller 2005).

Figure 7. ES cell differentiation fate

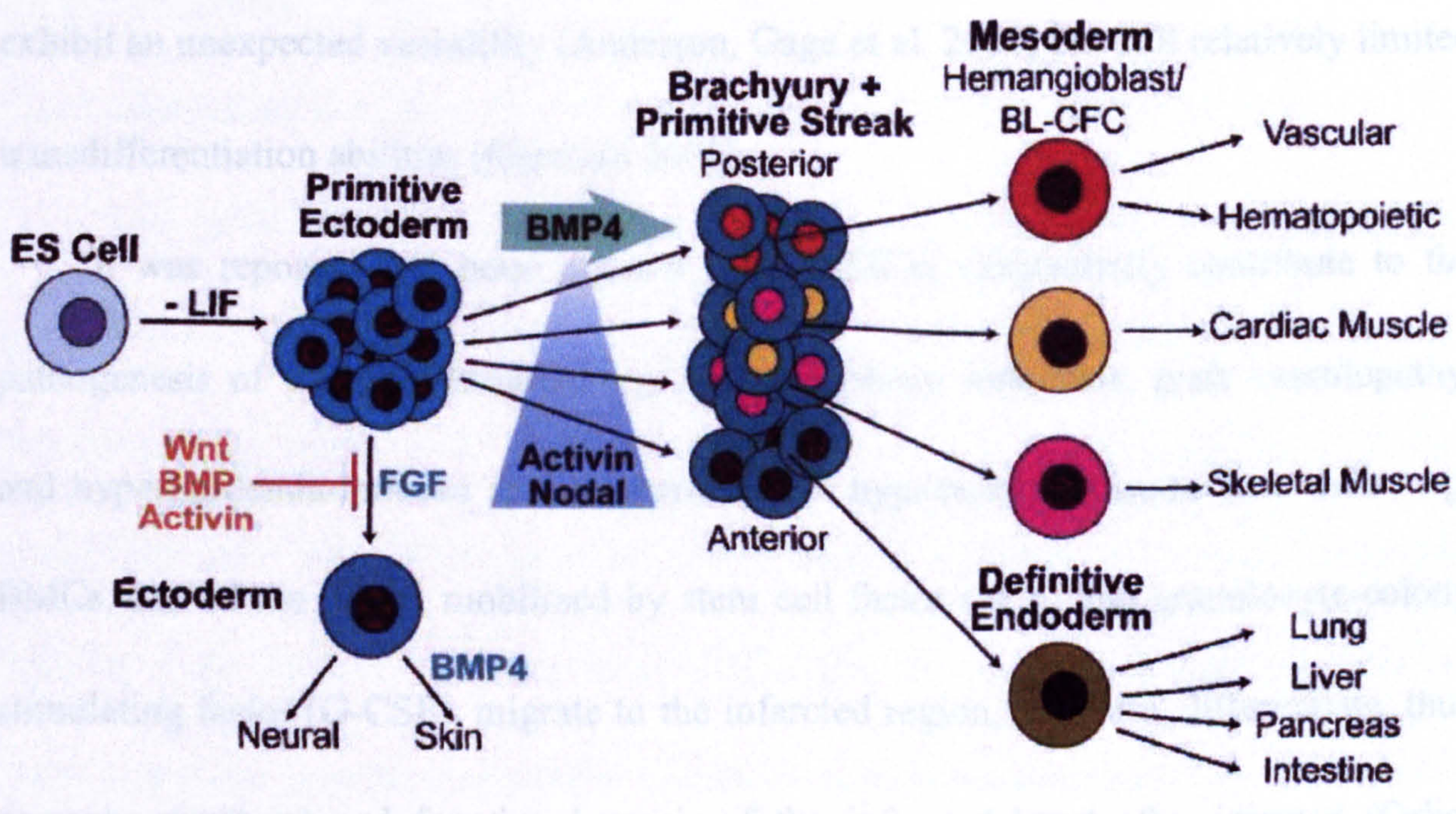

Figure 7. After the withdrawal of LIF, the ES cells will spontaneously differentiate into primitive ectoderm. With BMP4 or FGF stimulation, it will differentiate to primitive streak or ectoderm, respectively. The primitive streak will give the rise to mesoderm lineages or definitive endoderm when high concentration of Activin/Nodal is present. (Keller 2005)

1.2.3 Adult stem cells

Many adult tissues have also been found to harbour adult stem cell populations in recent years, including brain (Bjornson, Rietze et al. 1999; Clarke, Johansson et al. 2000; Galli, Borello et al. 2000), heart (Matsuura, Nagai et al. 2004), skeletal muscle (Jackson, Mi et al. 1999), bone marrow (Ferrari, Cusella-De Angelis et al. 1998; Petersen, Bowen et al. 1999; Pittenger, Mackay et al. 1999; Brazelton, Rossi et al. 2000; Lagasse, Connors et al. 2000; Mezey, Chandross et al. 2000; Sanchez-Ramos, Song et al. 2000; Jackson, Majka et al. 2001; Orlic, Kajstura et al. 2001), and umbilical cord blood. These adult stem cells have generally been regarded as having the capacity to form only the cell types of the organ in which they are found. Recently they have been shown to exhibit an unexpected versatility (Anderson, Gage et al. 2001) but still relatively limited transdifferentiation abilities (Gepstein 2002).

It was reported that bone marrow cells (BMCs) substantially contribute to the pathogenesis of vascular diseases, e.g. postangioplasty restenosis, graft vasculopathy, and hyperlipidemia-induced atherosclerosis. One hypothesis is distant stem cells, e.g. BMCs, sensed the injury, mobilized by stem cell factor (SCF) and granulocyte-colony stimulating factor (G-CSF), migrate to the infarcted region, replicate, differentiate, thus promote structural and functional repair of the infarcted heart after injected (Orlic, Kajstura et al. 2001). One article demonstrated side population cells ($CD34^{-}$/low, $c\text{-}kit^{+}$, $Sca\text{-}1^{+}$) of HSCs in bone marrow have the cardiomyogenic potential and could contribute to the formation of functional tissue so that benefit patients with myocardial infarction (Jackson, Majka et al. 2001). But another study shows the HSCs do not

transdifferentiate into cardiac myocytes in myocardial infarcts (Murry, Soonpaa et al. 2004). Intravenous injection of HSCs or muscle-derived stem cells into irradiated animals results in the reconstitution of the hematopoietic compartment of the transplanted recipients, the incorporation of donor-derived nuclei into muscle, and the partial restoration of dystrophin expression. Transplantation of different stem cell populations using the procedures of bone marrow transplantation might provide an avenue for treating diseases where the systemic delivery of therapeutic cells throughout the body is critical (Gussoni, Soneoka et al. 1999).

In contrast to HSCs, Sca-1^+ cells in the adult murine heart do differentiate into spontaneous beating cardiomyocytes and may contribute to the regeneration of injured hearts (Matsuura, Nagai et al. 2004). This represents an alternative source of functionally intact cardiomyocytes for the treatment of cardiovascular diseases.

Most published papers use the term *progenitor* cells to describe circulating and bone marrow-derived cells (Szmitko, Fedak et al. 2003). Accumulating data indicate that circulating "endothelial" progenitor cells and bone marrow progenitor cells can transdifferentiate into other types of cells (Quaini, Urbanek et al. 2002; Badorff, Brandes et al. 2003; Yeh, Zhang et al. 2003). Because the term progenitor cells are heavily used at present, most paper use both stem/progenitor cells to describe this population of cells rather than use more accurate term stem cells.

1.2.4 Vascular progenitor cells (VPCs)

A number of studies demonstrated that VPCs, including endothelial and smooth

muscle progenitors, which are present in circulating blood and BMCs, have the capacity to proliferate, migrate, and differentiate into mature SMCs and ECs (Asahara, Murohara et al. 1997; Rafii 2000; Simper, Stalboerger et al. 2002; Hill, Zalos et al. 2003; Sata 2003; Szmitko, Fedak et al. 2003), thereby contributing to vascular repair, remodelling, and atherosclerotic lesion formation (Vasa, Fichtlscherer et al. 2001; Assmus, Schachinger et al. 2002; Hill, Zalos et al. 2003; Rauscher, Goldschmidt-Clermont et al. 2003).

Abundant progenitor cells (Sca-1^+ cells) in the adventitia can differentiate into SMCs that participate in lesion formation in vein grafts (Hu, Zhang et al. 2004). These progenitor cells could be a source of SMCs in neointima and might contribute to circulating smooth muscle progenitor cells. Several studies of animal models suggested that both vascular and blood progenitor cells may contribute to the vascular diseases (Han, Campbell et al. 2001; Hillebrands, Klatter et al. 2001; Li, Han et al. 2001; Saiura, Sata et al. 2001; Shimizu, Sugiyama et al. 2001; Hu, Davison et al. 2002; Sata, Saiura et al. 2002).

The numbers of VPCs in blood negatively correlated with risk factors of cardiovascular diseases(Vasa, Fichtlscherer et al. 2001; Hill, Zalos et al. 2003; Rauscher, Goldschmidt-Clermont et al. 2003), highlighting the potential role of these cells in cardiovascular diseases (Assmus, Schachinger et al. 2002). Recently, Xu's group has provided evidence that both ECs and SMCs in atherosclerotic lesions and neointima in mice are derived from stem/progenitor cells presented in blood or the vessel wall, which can differentiate into vascular cells and thus contribute to pathophysiology of vessel

wall as well as generation of microvascular structures in adult neoangiogenesis (Hu, Davison et al. 2002; Hu, Davison et al. 2003; Xu, Zhang et al. 2003). These findings are crucial for understanding the pathogenesis and establishing new therapeutic strategies for vascular diseases, *i.e.* stem cell-based therapy.

1.2.5 Stem cells contribution in atherogenesis

During last 20 years, lots of studies demonstrated the SMC phenotype difference between media and atherosclerotic lesions. Traditionally, it was believed that SMCs can migrate from the media into intima after a transition in their phenotype (Campbell and Campbell 1994) in response to PDGF released by injured ECs and aggregated platelets (Ross, Glomset et al. 1977). However, the investigation of the role of SMC phenotypic switching has met a number of difficulties and deficiencies, such as lack of differentiation markers and regulation factors. Although the phenotypic modulation of SMCs in atherogenesis and vascular repair was widely accepted, no obvious evidence shows the essential role of such phenotypic modulation for atherogenesis.

Recent studies demonstrated that stem/progenitor cells from blood (Saiura, Sata et al. 2001; Hu, Davison et al. 2002), bone marrow(Han, Campbell et al. 2001; Hillebrands, Klatter et al. 2001; Shimizu, Sugiyama et al. 2001), and the vessel wall (Hu, Mayr et al. 2002; Hu, Zhang et al. 2004) may be responsible, at least in part, for endothelial repair and SMCs accumulation in lesions, suggesting that SMCs in lesions may result from differentiation of stem cells. A new theory of atherosclerosis pathogenesis point out the importance of progenitor cells during this process (Figure 8) (Xu 2006). First, ECs on

the arterial wall were damaged in specific areas and regeneration is carried on by endothelial progenitor cells (EPCs). The differentiation of neoendothelial cells into mature state takes several days. During this period, LDL deposits in the intima and blood mononuclear cells adhere to neoendothelial cells and migrate into the subendothelial space. Progenitor cells are also the source of smooth-muscle accumulation in atherosclerotic lesions. Circulating or adventitial progenitor cells migrate into the intima and differentiate into neo-SMCs. All known risk factors for atherosclerosis can also exert their effects on the vessel wall partially via increase in endothelial turnover, inhibition of differentiation and promotion of SMC and macrophage accumulation. Thus, the progenitor cells comprise the main cell source responsible for the formation of atherosclerotic lesions.

Figure 8. Stem cell theory of atherosclerosis

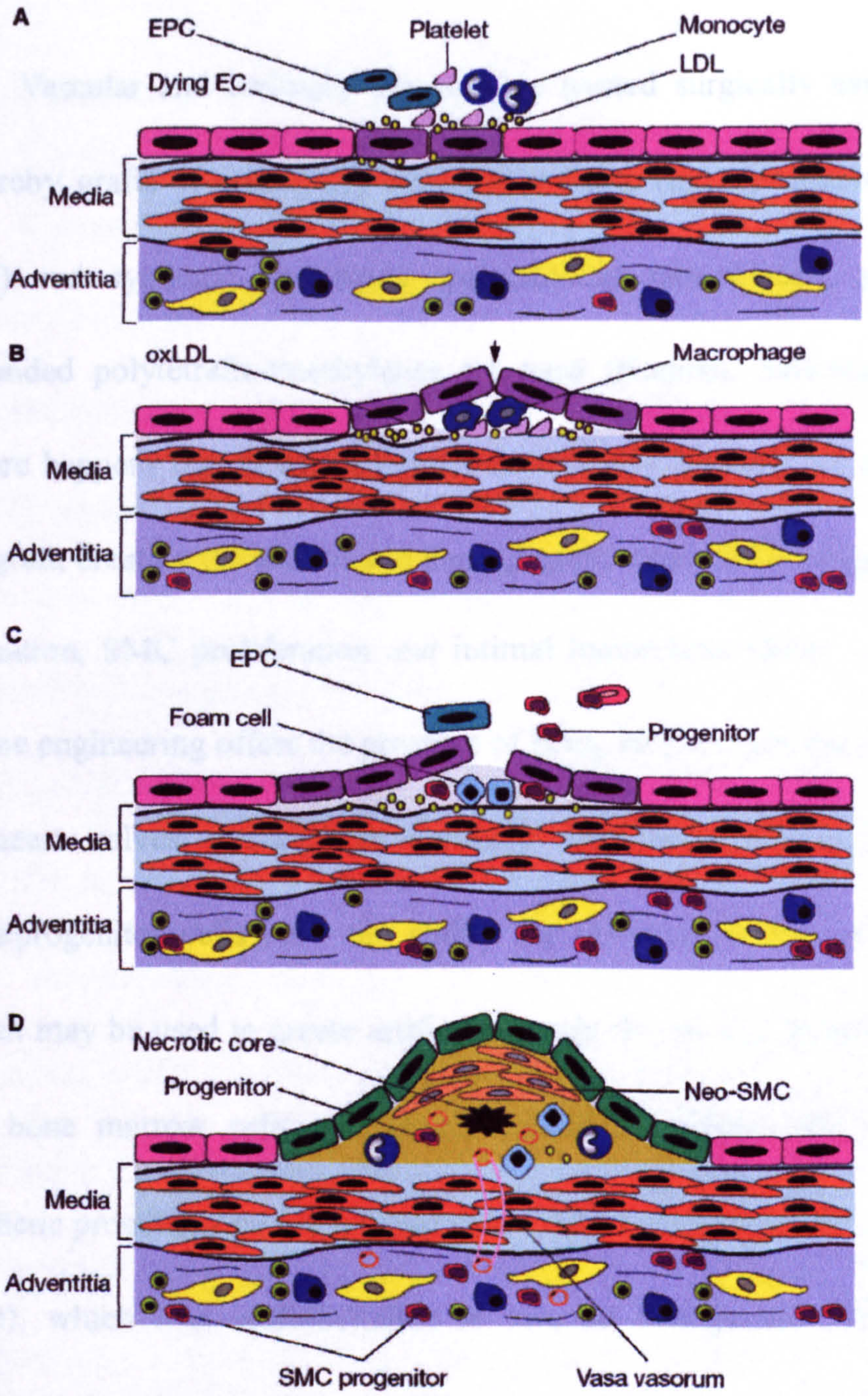

Figure 8. (A) Dead ECs are replaced by EPCs allowing increased endothelium permeability for monocytes and platelets (B) Monocytes migrate into subendothelial area and differentiate into macrophages to take up oxidized LDL, forming foam cells. (C) Progenitor cell-derived ECs have a shortened lifespan due to locally generated cytokines, free radicals, and risk factors. Endothelial cell death results in loss of endothelium in certain areas and vascular progenitor cells might migrate into the fatty streak. (D) Angiogenesis within atherosclerotic lesions occurs. The microvessels transport vascular stem or progenitor cells from the adventitia into the lesion. They differentiate into neo-smooth muscle cells within atherosclerotic lesions, which differ from medial smooth muscle cells and further develop into atheroma. (**EC**, endothelial cell; **EPC**, endothelial progenitor cell; **oxLDL**, oxidized LDL; **neo-SMC**, neo-smooth muscle cell; **SMC**, smooth muscle cell) (Xu 2006)

1.2.6 Tissue engineering

Vascular and coronary diseases are treated surgically using bypass procedures, whereby grafts of principally autogenous tissue (internal mammary artery, saphenous vein) and synthetic prostheses (polyethylene tetraphthlate, polytetrafluoroethylene, expanded polytetrafluoroethylene) are used (Kannan, Salacinski et al. 2005). Graft failure happens due to the difference in elasticity between the native blood vessel and the graft, creating turbulence and damaging the endothelial lining, resulting in thrombus formation, SMC proliferation and intimal hyperplasia (Sales, Salacinski et al. 2005). Tissue engineering offers the prospect of being able to meet the demand for replacement of heart valves, vessels for coronary and lower limb bypass surgery. Human stem/progenitor cells have the ability for self-renewal and potential to differentiate, which may be used to create artificial vessels for the bypass surgery. Circulating EPCs and bone marrow cells have been applied for single- and two-stage seeding into synthetic prostheses before implantation (Tiwari, Salacinski et al. 2001; Shirota, He et al. 2003), which may endothelialize *in vivo* so that prevent thrombus formation and significantly improve patency. Mesenchymal stem cells (MSCs) are also used for orthopaedic therapeutic applications, especially bone formation and cartilage tissue repairing (Tuan, Boland et al. 2003). Difficulties are associated with finding suitable numbers of cells with high quality and purity, especially under emergency circumstances. For these reasons, the study on stem cell differentiation is urgent for the basic medical researchers.

1.3 Proteomics

1.3.1 Definition of Proteomics

Because the genomic sequence or the transcriptional profile cannot be directly correlated with actual protein levels or protein function (Humphery-Smith, Cordwell et al. 1997) and cellular processes are largely attributed to posttranslational modifications (PTM) (Hart 1992; Faux and Scott 1996), measuring protein levels has become imperative. Proteomics, defined as "the entire PROTEin complement expressed by the genOME" of an organism at a given time-point (Wilkins, Pasquali et al. 1996), was thus developed to study cell functions at protein level (Wilkins, Sanchez et al. 1996).

The dynamic range of protein expression and modification makes the proteomics more complex than genomics. The appearance of entire genomes of a number of organisms, unified protein sequence database, and more powerful computers, make proteomics one of the fastest developed research area in the past few years. Proteomic techniques are ideal for clarifying quantitative protein changes in physiological and diseased conditions (Lopez and Melov 2002; Huber, Pfaller et al. 2003; Loscalzo 2003; McGregor and Dunn 2003) but additional experiments are still needed to clarify the functional consequence of the changes in the proteome.

A typical proteomic analysis includes experimental design, sample preparation, separation, identification and quantification of many proteins simultaneously from a mixture. To date, two-dimensional electrophoresis (2-DE) is the most preferred method to resolve proteins mixture from cellular lysate (Banks, Dunn et al. 2000; Dunn 2000).

Supported by high throughput mass spectrometry (MS) techniques, which allow rapid identification and characterization of very small quantities of peptides, 2-DE allows analyzing thousands of protein species at the same time.

1.3.2 Sample preparation

Efficient and reproducible sample preparation methods are key to successful 2-DE (Rabilloud 1999; Molloy 2000). An effective sample preparation should reproducibly solubilize proteins of all classes including hydrophobic proteins, prevent protein aggregation and loss of solubility during focusing, prevent post-extraction chemical modification, remove or thoroughly digest nucleic acids and other interfering molecules, yield proteins of interest at detectable levels.

Because of the significant mask effect of the most predominantly expressed proteins (enzymes, cytoskeletal proteins, albumin and immunoglobulin G) to the lower abundant but more important co-migrating proteins (such as signalling proteins) in the whole cell lysate, some reduction in the complexity of samples is needed to display the majority of protein species on 2-DE gels. Sample pre-fractionation techniques aim to reduce the diversity and complexity of protein mixtures, thus increase the concentration of distinct subsets of proteins that can be resolved. Different pre-fractionation methods based on different protein properties are developed, such as differential extraction (relative solubility, hydrophobicity), subcellular fractionation (co-localization within the cell), chromatography (affinity), preparative isoelectric focusing (net charge), etc. In general, pre-fractionation methods should be kept as simple as possible, target different

molecular properties and employ downstream compatible solutions to minimize sample loss and the chance of degradation and artifactual protein modifications.

1.3.3 Two-dimensional electrophoresis (2-DE)

2-DE is a powerful and widely used method for the analysis of complex biological samples. It was first introduced in 1975 (Klose 1975; O'Farrell 1975) and has a renaissance in the past decade. 2-DE separates proteins according to two independent properties in two step: the first-dimension, isoelectric focusing, separates proteins according to their isoelectric point (pI) in pH gradient gels; the second-dimension, SDS-polyacrylamide gel electrophoresis (SDS-PAGE), separates proteins according to their molecular weight (Mr) (Patton, Pluskal et al. 1990) (Figure 9).

Figure 9. Principles of 2-DE

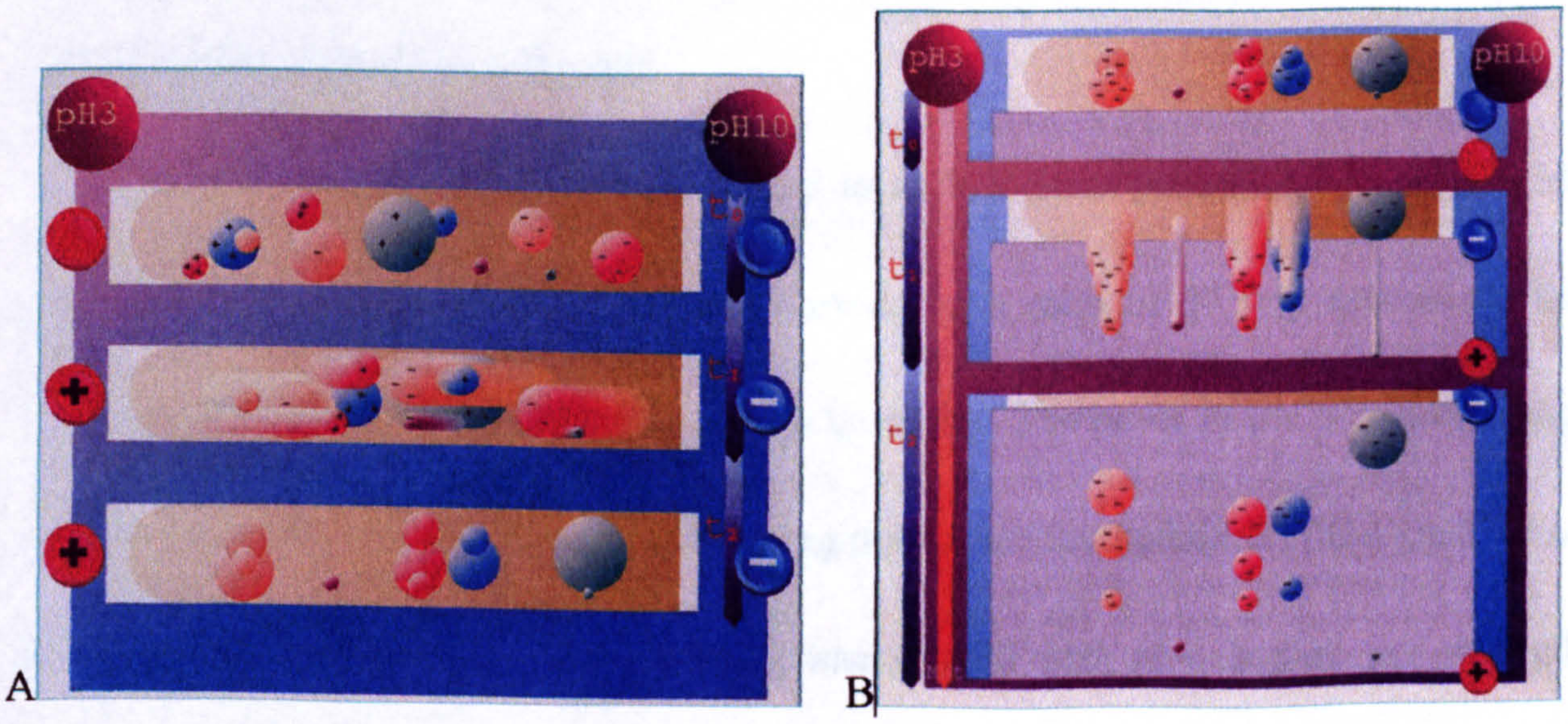

Figure 9. (A) First dimention, proteins are separated by isoelectric point under electric field in pH gradient gels, called isoelectric focusing. (B) Second dimention, proteins are separated by molecular weight in polyacrylamide gels.

pH gradients for IPG strips are created with sets of acrylamide buffers, CH_2=CH-CO-NH-**R**, where the **R** contains either a carboxyl [-COOH] or a tertiary

amino group [e.g., -$N(CH_3)_2$]. These acrylamide derivatives are covalently incorporated into polyacrylamide gels at the time of casting and can form almost any conceivable pH gradient (Righetti 1990). According to both theory and experiment, the difference in pI between two adjacent isoelectric focusing-resolved protein bands is directly proportional to the square root of the pH gradient and inversely proportional to the square root of the voltage gradient at the position of the bands. Thus, narrow pH ranges and high applied voltages yield high resolution in isoelectric focusing.

A default current limit of 50μA per strip is intended to minimize protein carbamylation reactions in urea sample buffers. If different strips are run at the same time, the electrical conditions experienced by individual strips will be different, perhaps exposing some strips to more current than desired. Thus, strip length, pH range and protein amount should be the same to get similar electronic resistant so that to produce similar protein pattern in 2-DE gels.

The percentage of acrylamide referred to as %T (total percentage of acrylamide plus corsslinker, N, N-methylene- bisacrylamide, at a ratio of 37.5:1) determines the pore size of a gel. Higher %T means smaller pore size. The pores of the polyacrylamide gel sieve proteins according to the size. Using piperazine diacrylamide (PDA) instead of bisacrylamide can reduce silver staining background and give higher gel strength (Wiersma, Bos et al. 1994). Polymerization is typically accomplished using a chemical reaction with ammonium persulfate (APS) and N,N,N',N'-tetramethylethylenediamine (TEMED), which are the initiator and the catalyst respectively (Figure 10).

Figure 10. Chemical basis of the polymerization of polyacrylamide gel

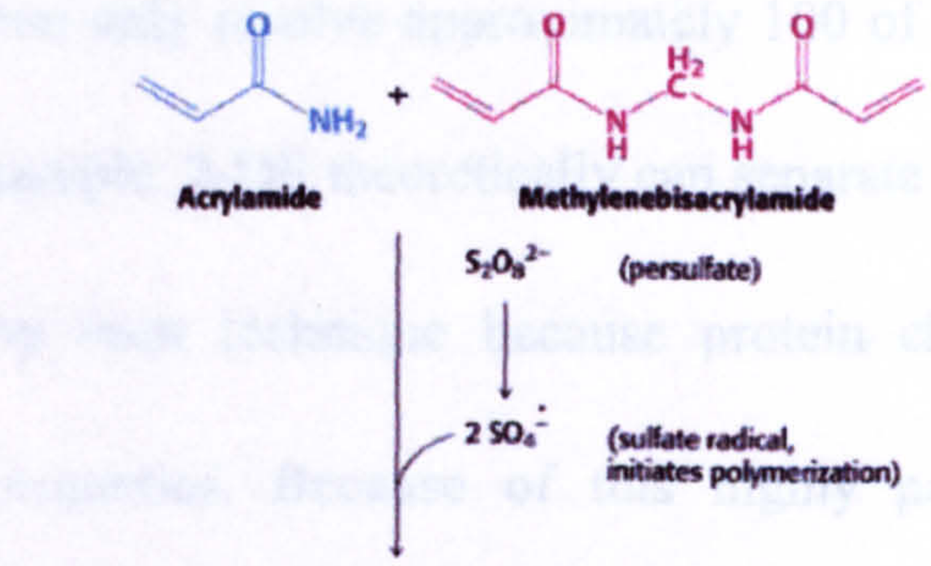

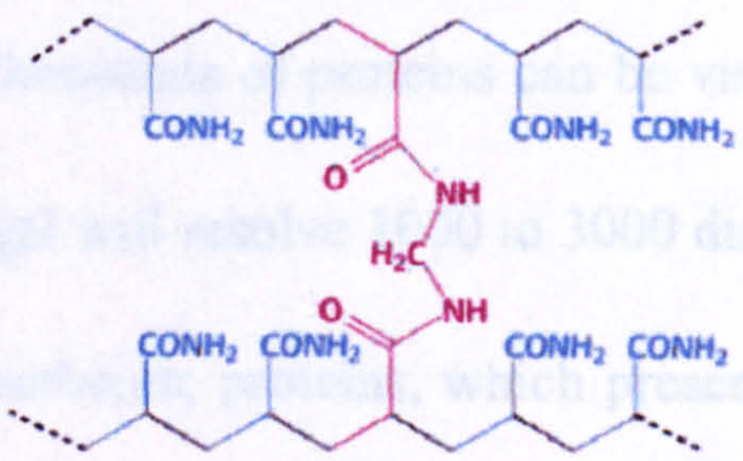

Figure 10. Acrylamide and bisacrylamdie are polymerized with the catalysis of aminum persulfate (http://oregonstate.edu/instruction/bb450/stryer/ch04/Slide10.jpg).

Homogeneous (single-percentage acrylamide) gels generally give excellent resolution of sample proteins with a narrow Mr range. Gradient gels are cast with acrylamide concentrations that increase from top to bottom so that allow proteins with a wide range of Mr to be analyzed simultaneously and sharpen the spots. However, gradient gel cannot obtain the same resolution as single-percentage gels optimized for a narrow Mr range. A proteomics experiment might start out with an 8-16%T gradient for global comparison. After interesting regions of the 2-D array have been identified, a new set of single-percentage gels may be run to study a particular size range of proteins. In single-percentage gel, the migration rate of polypeptides in SDS-PAGE is inversely proportional to the logarithm of its Mr. In gradient gels, log(migration distance) is inversely proportional to log(Mr).

It is highly recommended casting and running 2-DE gels in batches to ensure minimum gel-to-gel variation within one experiment.

2-DE gels are high-resolution protein arrays suitable for the separation of complex

protein mixtures. Conventional one-dimensional IEF and one-dimensional SDS-PAGE can only resolve approximately 100 of the most abundant proteins in a heterogeneous sample. 2-DE theoretically can separate the product of the number of proteins separated by each technique because protein charge and molecular weight are independent properties. Because of this highly parallel nature of the technique, hundreds to thousands of proteins can be visualized simultaneously, *i.e.* a single large-format 2-DE gel will resolve 1000 to 3000 different polypeptide spots. A 2-DE gel is also an array of authentic proteins, which preserves protein charge, molecular weight, and PTMs (such as phosphorylation, glycosylation, and oxidation) during electrophoresis. This allows direct analysis of protein isoforms that may be involved in particular metabolic or disease processes. 2-DE gels present different PTM of one protein because the different PTM forms have slightly different molecular weight and/or pI. The glycosylation normally resulted in a series of spot chain in the 2-DE gels, which are easily recognized while the phosphorylation and oxidation only present horizontal shifting of spots with almost the same Mr but huge difference in pI. In addition, the quantitative differences between proteins in mixtures can be determined from the intensity of spots on 2-DE gel images by statistic analysis so that the differences of protein expression levels can be directly detected.

A simple method to view more protein spots is using a series of complementary narrow pH-range immobilized pH gradient strips. Commercially available narrow-range and micro-range pH immobilized pH gradient strips can resolve proteins in 1 pH unit, most focus on acidic area.

Another way to get the information of low abundant proteins is to develop more sensitive detection method. The sensitivity that is achievable in staining is determined by the amount of stain that binds to the proteins, the intensity of the colouration, and the difference in colouration between stained proteins and the background (signal-to-noise ratio). Currently, there are no stains that can span the approximately 7 or 8 orders of magnitude dynamic range of cellular proteins. However, improved methods of protein detection by using fluorescent dyes offer a broader dynamic range and linear quantitative range of detection than silver staining. For example, SYPRO Ruby (Molecular Probes), a ruthenium-based fluorescent dye that binds non-covalently to proteins in gels, provides sensitive (1-10ng) and linear (over 3 orders of magnitude) stain with high signal-to-noise ratio, and compatible with MS and Edman sequencing (Patton 2000). It also allows detection of glycoproteins, lipoproteins, low Mr proteins and metalloproteins that are not stained well by other stains. The linear dynamic range of fluorescent dye, which covers the ranges of both Coomassie blue and silver stains, potentially increases accuracy of quantitative comparisons. Because all stains interact differently with different proteins (Carroll, Ray et al. 2000), replicate gels should be stained with at least two different stains for critical analysis. Normally the gels should be stained by Coomassie blue or a fluorescent stain prior to silver stain.

Unfortunately, standard 2-DE gels do not reflect a true representation of hydrophobic, highly insoluble, very basic (pI >9.5), very small (<10kDa) and very large (>100kDa), as well as very low abundance proteins. Very high molecular weight proteins do not easily enter the gels and should be separated using one-dimensional

SDS-PAGE, preferably following sample pre-fractionation to enrich the targeted proteins. Improved second-dimensional separation of very low molecular weight proteins can be achieved if the Tris-glycine buffer is substituted by the Tris-tricine-SDS buffer system in combination with high percentage gradient gels. Also more sensitive mass spectrometers are needed for identifying small proteins. The process of solubilization and subsequent separation of hydrophobic proteins in immobilized pH gradient strips have been improved by combining more effective reducing agents such as the uncharged agent tributyl phosphine with more powerful chaotropes such as thiourea and surfactants such as linear sulfobetaine-type zwitterionic detergents containing a carboxyamido group to improve urea tolerance. The development of basic immobilized pH gradients up to pH 12 will facilitate easy, reproducible analysis of alkaline proteins as soon as the problem of reverse electroendosmotic flow (anode-directed water flow) is fully solved.

1.3.4 Difference gel electrophoresis (DIGE)

Traditional 2-DE is a well-established technique and a relatively simple visual method for mapping differences in protein expression. There are certain limitations to the universal use of this technology, such as irreproducible between gels and has significant system variability, low detection sensitivity and linearity. It is hard to get highly confident result of protein expression changes by using traditional 2-DE. Recently, the difference gel electrophoresis (DIGE) (Unlu, Morgan et al. 1997) is invented and widely used in proteomics studies. With this technology, samples are

labelled with one of three fluorescent dyes (Cy2, Cy3 or Cy5) and run in a single 2-DE gel. DIGE displays two or more complex protein mixtures labelled with different fluorescent dyes in a single 2-DE gel, offers the opportunity of direct comparison of different samples, thus eliminating gel-to-gel variations inherent to comparative gel analysis. Fluorescent labelling also renders 2-D DIGE much more quantitative than colorimetric methods. It has a linear dynamic range of 4 or 5 orders of magnitude, by contrast with the approximately 1 or 2 order range of Coomassie and silver stains. As regards sensitivity, 1ng of standard protein is detected with Cy3/Cy5 fluorescent labelling. The use of a pooled internal standard labelled with Cy2 will further improve the accuracy of quantitative comparisons in differential display experiments by normalizing quantitative expression data across multiple samples run on several 2-DE gels.

The CyDye DIGE Fluor minimal dyes have an N-hydroxysuccinimide (NHS)-ester reactive group and covalently attach to the epsilon amino group of protein lysine residues via an amide linkage. When coupled to a lysine residue, the dye will replace the positive charge of lysine with its own positive charge so that does not significantly alter the pI of the protein. Their size and charge match properties insure that same labelled protein from different samples have the same relative mobility regardless of the dye used to tag them. Their fluorescent signals are relatively stable during the labelling, separation, and scanning. The excitation and emission wavelengths of these dyes are resolvable, which contributes to the accuracy of DIGE. (Table 4) (CyDye DIGE fluor Data File, 18-1164-84, GE healthcare)

Table 4. CyDye DIGE Fluor minimal dyes characteristics

Fluor	Fluorescence colour	Max. absorption wavelength (nm)	Max. fluorescence wavelength (nm)	Added molecular weight (Mr)
Cy2	Green	491	509	434
Cy3	Orange	553	569	466
Cy5	Red	645	664	464

The workflow of three-dye DIGE system is as simple as traditional 2-DE. Samples are washed and lysed in special DIGE lysis buffer without primary amino reagent, which may interfere with DIGE labelling. After adjust the pH of protein extracts to 8.5 (optimal pH for DIGE labelling), one of three fluorescent dyes is added to samples in a dye/protein ratio at 400pmol dye/50μg protein. In this condition, only 3% of total amount of each protein is tagged. Normally the same amount of two different protein extracts are labelled with Cy3 and Cy5 and also a randomized crisscross experimental design is used in which two extracts are each tagged with Cy3 or Cy5 to eleminate differences between dyes. The pooled internal standard, which contains equal amounts of each protein extract, is labelled with Cy2, and is included in all gels to normalize protein abundance measurements across multiple gel experiments. After labelling, protein extracts and the pooled internal standard are mixed together and resolved in a single 2-DE gel. Protein spot patterns are visualized by alternately illuminating the gel with the excitation wavelengths for each of the three fluorescent dyes by fluorescence scanner. The 2-D images are analyzed by specific software, such as DeCyder. The intensity of protein spots on the 2-D images of different protein extracts are compared with the pooled internal standard, which reduces variation between gels and enables automated and accurate spot quantitation, gel-to-gel matching and statistical analysis

(Figure 11). In order to maximize the amount of protein available for MS, the total protein should by visualized using a post-staining method (silver staining or SYPRO ruby) (Monteoliva and Albar 2004).

Figure 11. Workflow of three-dye DIGE system

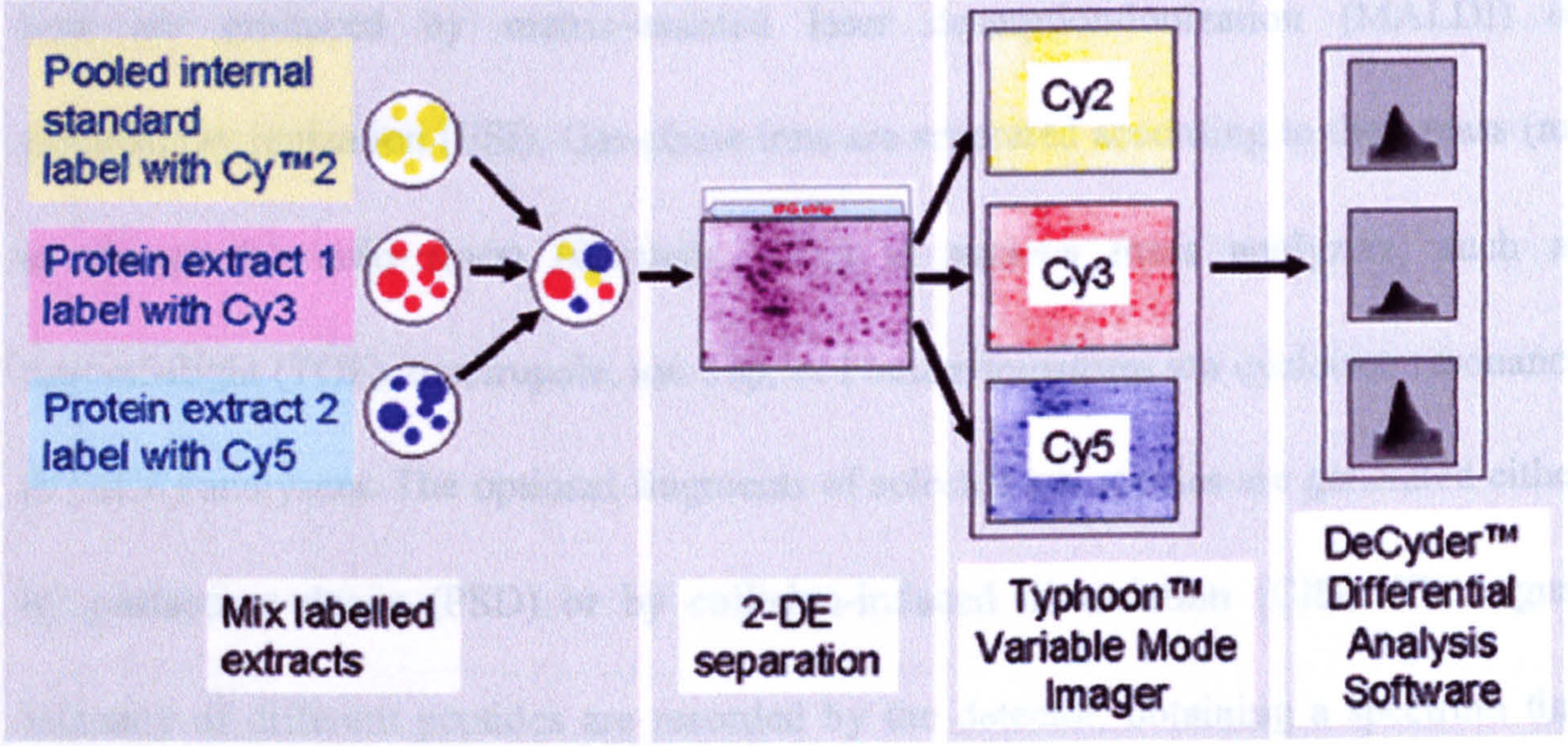

Figure 11. Two samples are labelled with Cy3 or Cy5. Pooled internal standard is labelled with Cy2. Mixtures are co-separated by 2-DE and separate images are acquired for each dye by a fluorescence scanner. Quantitative analysis is carried out by DeCyder software.
(http://www5.amershambiosciences.com/aptrix/upp00919.nsf/Content/Proteomics+DIGE~Proteomics+DIGE+Applications)

1.3.5 Biological mass spectrometry

Before biological mass spectrometry was invented, protein characterization was mainly undertaken by Edman degradation. However, this approach fails in the analysis of subpicomole (10^{-12} M) quantities or N-terminally blocked proteins (which are very common in eukaryotes). By contrast, biological mass spectrometry can provide an analytical sensitivity down to the subfemtomole (10^{-15} M) level and is not restricted by terminal modifications.

In the basic workflow for protein identification, mass spectrometric analysis is preceded by site-specific proteolysis (Shevchenko, Wilm et al. 1996). Trypsin normally is the best enzyme for unknown substrate, which can generate peptides between 1000 to 2000 Da in mass (most convenient mass range for biological MS). Next, the peptide ions are produced by matrix-assisted laser desorption/ionization (MALDI) or electrospray ionization (ESI). Gas-phase ions are separated according to their mass (m) to charge (z) ratio (m/z) (Corthals 2000) in various mass analyzers, such as time-of-flight (TOF), quadrupole, ion trap, or Fourier-transform ion cyclotron resonance (FT-ICR) analyzers. The optional fragments of selected ion species are generated either by postsource decay (PSD) or by collision-induced dissociation (CID). The signal intensity of different peptides are recorded by the detector, obtaining a spectrum that displays ion intensity versus m/z values (Roepstorff 1997; Mann, Hendrickson et al. 2001). Experimentally obtained peptide masses from the MS spectrum are subjected to database searches. There are several websites for database searching with mass spectrometric data (such as http://www.matrixscience.com, http://www.expasy.ch/tools). The common aspect of all search engines is the generation of a protein ranking based on peptide mass matching probabilities using various computer algorithms, such as PROFOUND, MASCOT, MOWSE and SEQUEST.

In MALDI-ToF MS, the laser ionizes predominantly singly charged peptides within a mixture of sample and matrix. Because in an electric field the time a peptide takes to hit the detector is proportional to its ratio of mass to charge (m/z), peptides with different mass spend different time to reach the detector. The ion signal intensity *versus*

its m/z (measured as time of flight) was ploted (Figure 12). The spectra were analyzed and the prominent intensity peaks were labelled and searched against protein databases. i.e. using the MASCOT program (http://www.matrixscience.com) (Perkins, Pappin et al. 1999). One specific protein has one set of defined peptide masses after tryptic digestion, so called peptide mass fingerprint (PMF). By comparing the observed PMF with the calculated PMF, the probability (P) of the proteins that the observed match is a random event can be calculated and shown as protein score, which is -10*Log(P). A higher score means lower possibility that the observed match is a random event. Scores > 59 are considered significant ($p<0.05$).

Figure 12. A representative MALDI-ToF MS spectrum

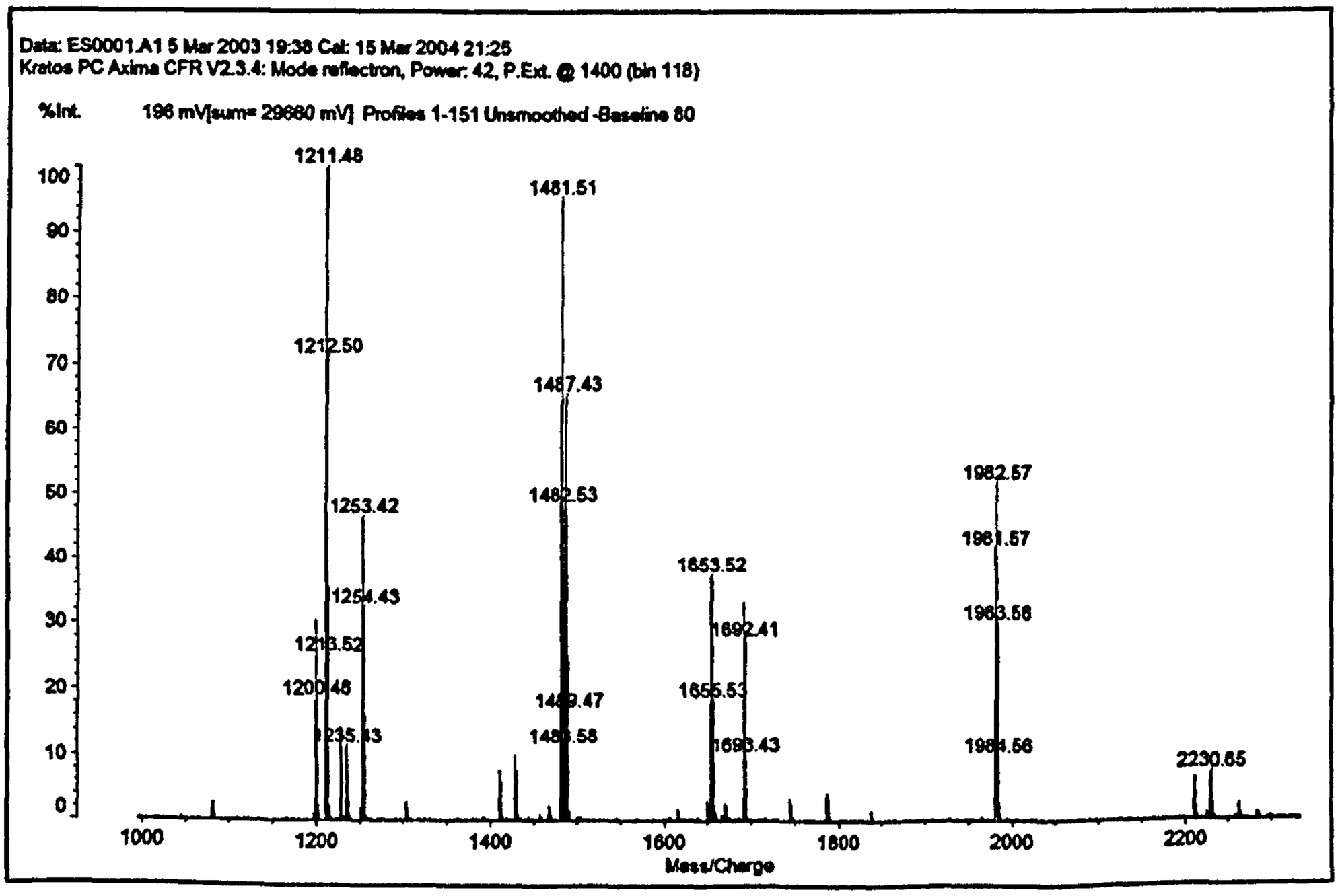

Figure 12. Spectrum was recorded by Kratos Axima CFR MALDI-ToF MS and ploted as relative intensity versus m/z. The m/z values of predominant peaks were labelled and subjected to database search.

Recently, tandem mass spectrometry (MS/MS) is commonly used to get partial peptides sequence information so that obtain highly confident protein identifications. A

peptide isolated in the gas phase of the first mass scanning stage is further dissociated by PSD or CID. The peptide will be broken at where the peptide bonds formed and B ions and Y ions are generated (Figure 13). The masses of the peptide fragments are determined in the second mass stage with the resulting data used for sequence analysis and database searching (Yates, Eng et al. 1995). MS/MS instruments include combination of MALDI-MS with PSD or ESI-MS coupled to triple-quadrupole MS or ion-trap MS. The latter is commonly regarded to be superior to MALDI-PSD MS/MS because of its greater sensitivity and less complex fragment ion spectra. Notably, MALDI MS is more tolerant to sample contamination and less time consuming than MS/MS.

Figure 13. A representative LCQ MS/MS spectrum

(A)

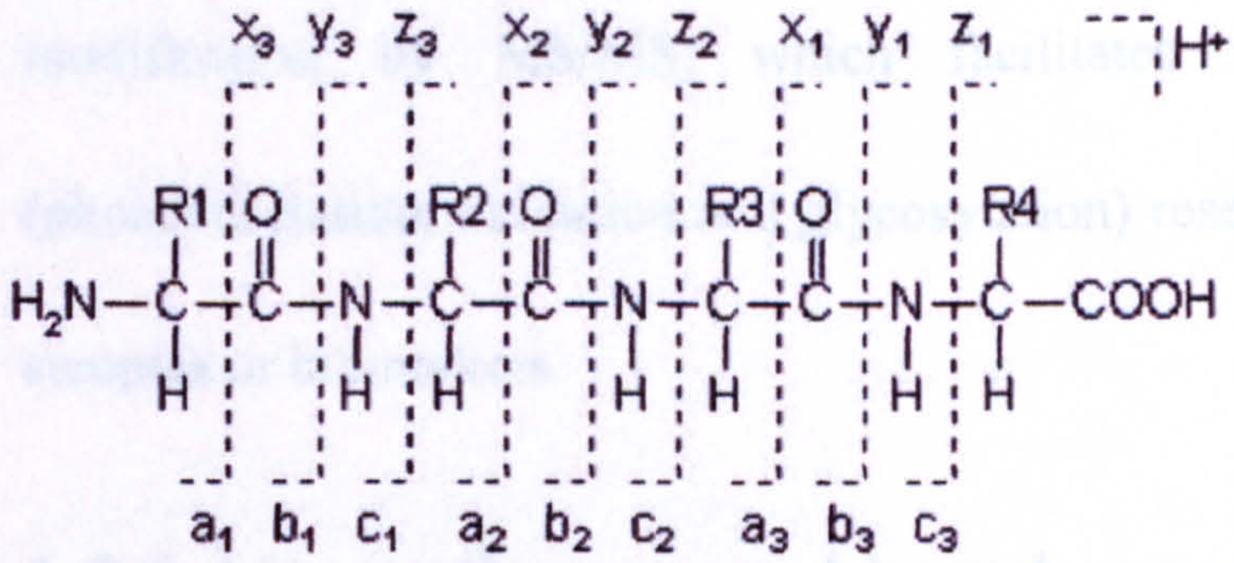

(B)

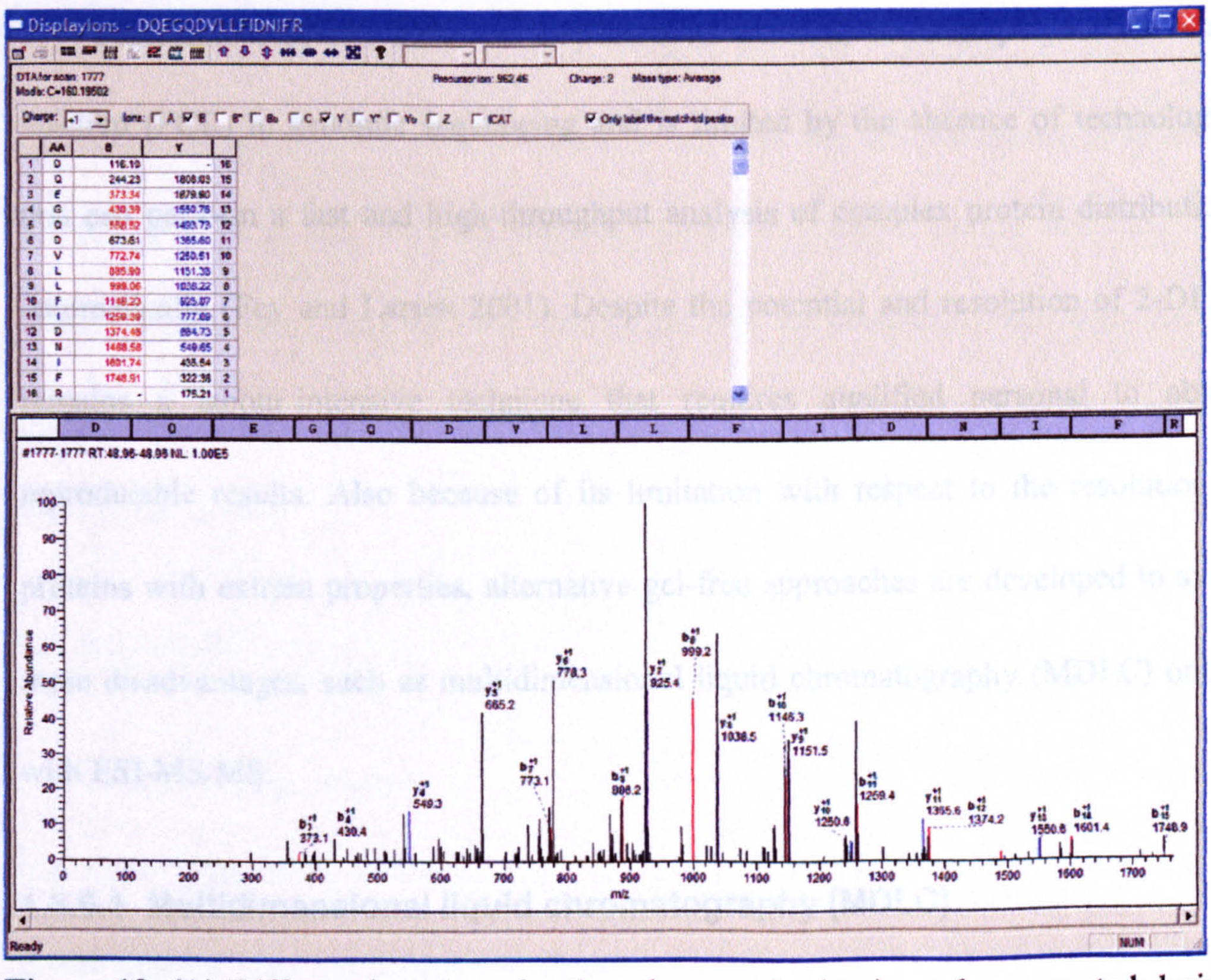

Figure 13. (A) Different ions (a and x, b and y, c and z ions) can be generated during the MS/MS. (B) Peptide ion spectrum obtained by LCQ Deca XP Plus MS/MS (Thermo). B ions and Y ions were recognized and labelled with red and blue colour, respectively.

With rapid development during these years, mass spectrometers have emerged as a core technology for peptide and protein structural analysis, forensic analysis, metabolomics, and pharmaceutical drug discovery. Newly developed orbitrap (Hu, Noll

et al. 2005) and electron transfer dissociation (ETD) (Syka, Coon et al. 2004) provides the abilities of obtaining high mass accuracy and analysing posttranslational modification by MS/MS, which facilitates us in the protein modification (phosphorylation, oxidation and glycosylation) research and analysis of complex blood samples or biomarkers.

1.3.6 Alternative non-gel based approaches

Proteomic research lacks an amplification method, such as polymerase chain reaction (PCR) in genomic sequencing and is limited by the absence of technologies that can perform a fast and high-throughput analysis of complex protein distributions automatically (Fey and Larsen 2001). Despite the potential and resolution of 2-DE, it remains a labour-intensive technique that requires qualified personal to obtain reproducible results. Also because of its limitation with respect to the resolution of proteins with extrem properties, alternative gel-free approaches are developed to avoid these disadvantages, such as multidimensional liquid chromatography (MDLC) online with ESI-MS/MS.

1.3.6.1 Multidimensional liquid chromatography (MDLC)

As an alternative to 2-DE approach, initial efforts have focused on MDLC to decrease sample complexity coupled with MS for protein identification (Lopez and Melov 2002). In LC/MS-based approaches, complex protein mixtures are digested in solution and fractionated by one or several steps of capillary chromatography and

analysed in a data-dependent manner by MS/MS.

A clear advantage is that most of these methods are very automation-friendly. However, exhaustive analysis of the sequence data obtained demands powerful computing facilities. The MDLC can minimize the bias toward larger proteins with more numerous peptides but it is not quantitative and the purified peptides are not all ionized, leading to underrepresentation of these proteins.

Major limitation of LC/MS-based methods is the difficulty in performing differential display analysis. To date, several different chemical, metabolic and enzymatic labelling techniques are used to perform non-gel MS-based quantatitive proteomics, such as stable isotope labelling with amino acides in culture media (SILAC), isotope-coded affinity tags (ICAT), iTRAQ, etc. For the comparison between different experiments or for the absolute quantification, reference peptides need to be introduced into MDLC system.

1.3.6.2 SILAC

SILAC (Ong, Blagoev et al. 2002) is a simple and accurate approach for MS-based quantitative proteomic methods. Two groups of cells are grown in culture media that are identical except one contains the light form (labelled with ^{1}H, ^{12}C and ^{14}N) and the other contains the heavy form (labelled with ^{2}H, ^{13}C and ^{15}N) of a particular essential amino acid (e.g. L-leucine or arginine). After several times of cell doubling, the cell population replaces the original form of the amino acid with the given light or heavy form of the amino acid. In this way, the same proteins from two different

samples will show the same chemical behaviour but with a difference in mass detectable by MS. Peptide peak intensities can be used for relative quantification of these proteins (Figure 14A).

Figure 14. Scheme of SILAC

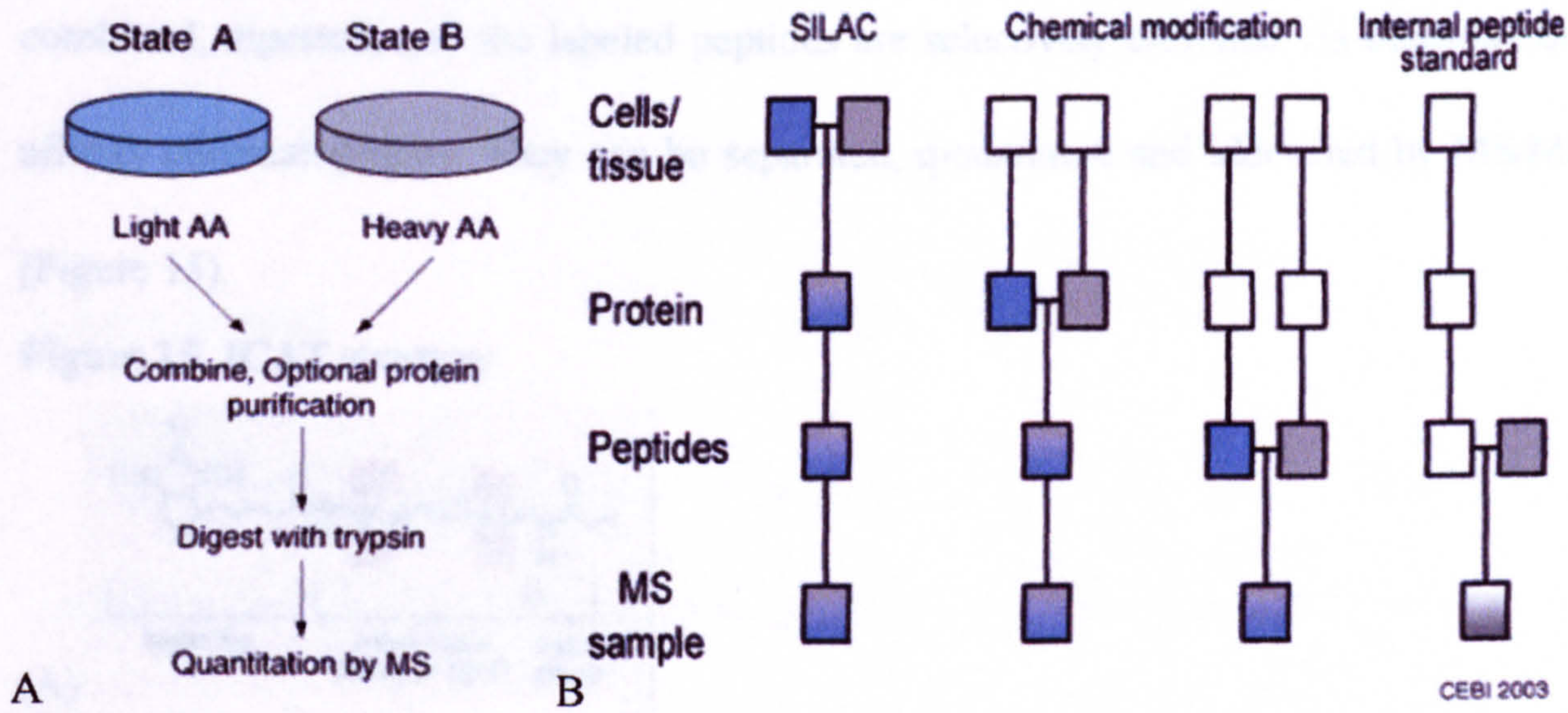

Figure 14. (A) Worke flow of SILAC. Different samples are cultured in medium contain light or heavy amino acid. Cell lysates are combined, digested and quantified by MS. (B) Comparison between different labelling methods. SILAC labels samples at the cell level, which has high efficiency and minimum artificial error.

The advantages of SILAC are that it incorporates with nearly 100% efficiency and does not require multiple chemical processing and purification steps, thus ensures the two different samples have been subjected to same conditions throughout the experiment and allows using any method of protein or peptide purification without introducing error into the final quantitative analysis.

1.3.6.3 ICAT

Isotope-coded affinity tags (ICAT) represented the first labeling strategy for protein expression analysis using LC/MS approaches that facilitated high throughput proteomics and enabled relative quantitation between two samples for proteins that

contain the amino acid cysteine (Gygi, Rist et al. 1999).

In this elegant and straightforward approach, two samples are labelled with structurally identical tags that differ in isotopic composition and contain a thiol-reactive group, which covalently links to cysteine residues, and a biotin moiety. The samples are combined, digested, and the labeled peptides are selectively enriched via biotin-avidin affinity chromatography. They can be separated, quantitated and identified by MS/MS (Figure 15).

Figure 15. ICAT strategy

(A)

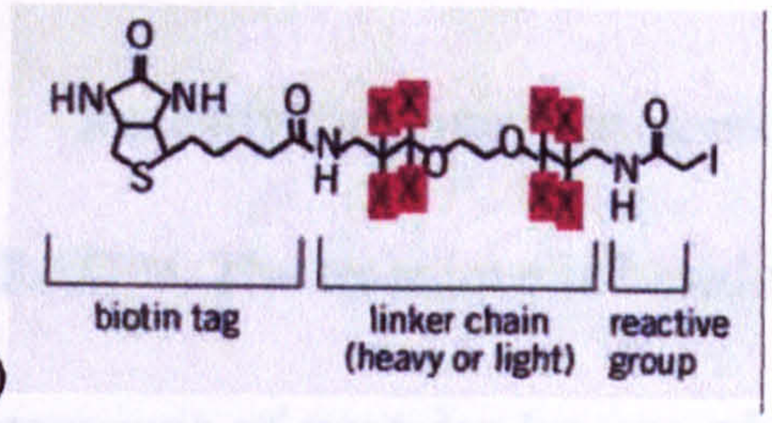

(B)

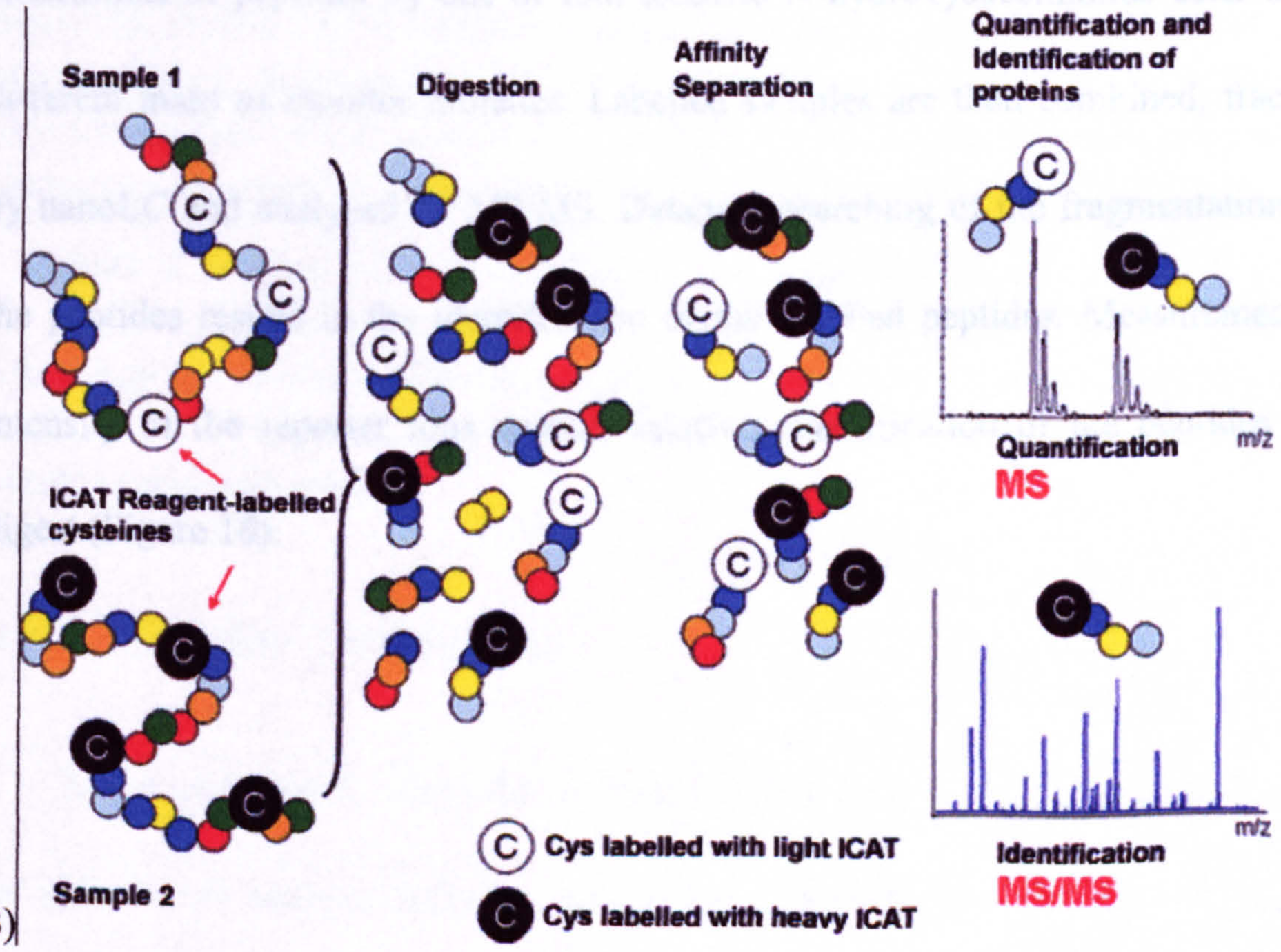

Figure 15. Proteins from different samples are labelled with different ICAT tags and then combined, digested, affinity separated and analyzed by MS/MS. Relative intensity of the peptides from different samples indicates the relative abundance of the original proteins. Protein identifications are obtained by the sequence analysis of the peptide. (http://www.cnic.es/proteomica/img/ICAT.gif)

One of the main advantages of ICAT is that it selects for peptides that contain relatively rare cysteine residues, which significantly reduces the complexity of the sample and its resulting mass spectrum. At the same time, this is also one of its drawbacks because many important proteins, including those with PTMs, do not contain cysteine. As a result, several groups have described alternative labeling strategies that target lysine and tryptophan residues or peptide N- or C- termini.

1.3.6.4 iTRAQ

Recently, an improved approach analogous to ICAT has been developed called iTRAQ™. The technique is based upon chemically tagging the lysine sidechain and the N-terminus of peptides by one of four isobaric N-hydroxysuccinimide ester tags with different mass of reporter moieties. Labelled samples are then combined, fractionated by nanoLC and analyzed by MS/MS. Database searching of the fragmentation data of the peptides results in the identification of the labelled peptides. Measurement of the intensity of the reporter ions enables relative quantification of the peptides in each digest (Figure 16).

Figure 16. iTRAQ principles

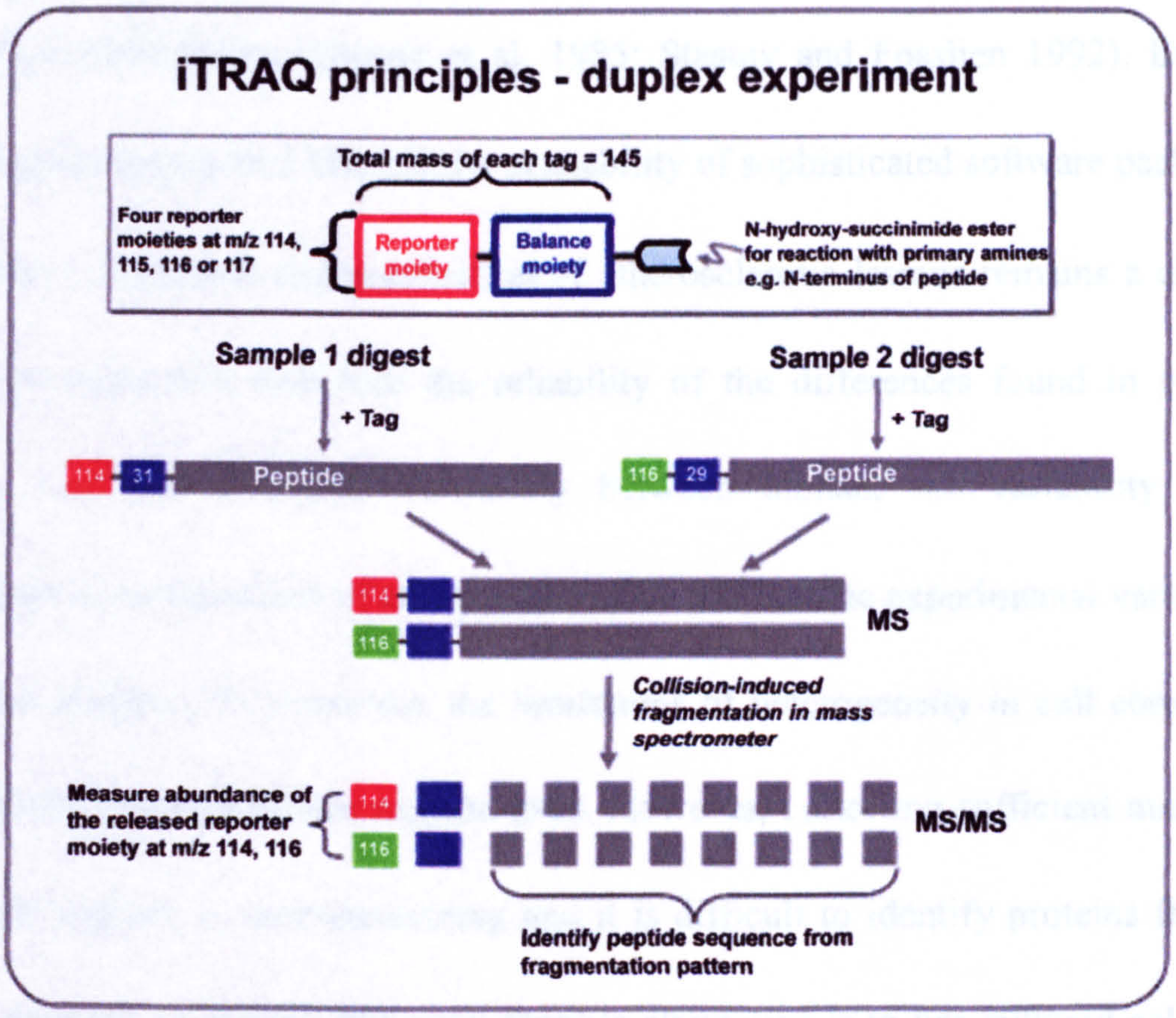

Figure 16. Peptides from different samples are labelled with different iTRAQ tags and then combined, fractionated and analyzed by MS/MS. Protein is identified by the sequence analysis of the peptide and their relative abundance derived from the relative intensity of the reporter moiety. (http://www.proteome.soton.ac.uk/iTRAQ.htm)

Both ICAT and iTRAQ techniques require proteins to be chemically modified before they are mixed so that these techniques have the potential to introduce artifical sample preparation biases.

1.3.7 Vascular Proteomics

In the early times, when the absence of immobilized pH gradients and powerful computer-based analysis software limited the reproducibility and accuracy of 2-DE, only the most obvious changes were detected, *i.e.* albumin, fibrinogen, immunoglobulin G, alpha-1 antitrypsin, transferrin, haptoglobin, ApoA-I and ApoA-II, which were originated from the plasma and accumulated in diseased vessels (Stastny, Fosslien et al.

1986). Later studies reflect the compromised endothelial barrier function of diseased and aged vessels (Song, Stastny et al. 1985; Stastny and Fosslien 1992). Even with recent improvements in 2-DE and the availability of sophisticated software packages for gel analysis, proteomic characterization of atherosclerotic lesions remains a challenge. Many variations will influence the reliability of the differences found in proteomic analysis, e.g. the biological variability between human, the variability between heterogeneous composition of atherosclerotic lesions and the experimental variability of proteomic analysis. To overcome the limitations of heterogeneity in cell composition, laser capture microdissection may be used. However, collecting sufficient material for proteomic analysis is time-consuming and it is difficult to identify proteins from very limited amounts of tissues. The most feasible alternative is to use cultured cells and to study proteomic changes in response to cardiovascular risk factors, such as high levels of glucose, cholesterol, and mechanical stress.

An interesting alternative approach to study atherosclerotic plaques with proteomic techniques was performed recently (Duran, Mas et al. 2003). Normal arteries and carotid endarterectomy samples were cultured in protein-free medium and the supernatant was analyzed by 2-DE. Proteins involved in reverse cholesterol transport, apoptosis, protein degradation and antioxidants were found to be released from plaques, which fits well in the pathophysiological context of atherosclerosis. However, it remains to be clarified whether these proteins are really secreted by plaques or just because of the diffusion difference between plaques and normal arteries.

Several SMCs proteome maps have been published recently (McGregor, Kempster

et al. 2001; Dupont, Corseaux et al. 2005; Mayr, Mayr et al. 2005). Proteomic changes in venous SMCs exposed to hemodynamic stress were observed for proteins of the gelsolin family and actin filament remodelling. These indicate that mechanical stress-induced protein changes favour the generation of contractile stress fibbers (McGregor, Kempster et al. 2004). Proteomic techniques are applied to several functional studies on arterial SMCs, such as SMC hypertrophy and hyperplasia (Holycross, Peach et al. 1993; Patton, Erdjument-Bromage et al. 1995), aging-associated effect on SMC differentiation (Cremona, Muda et al. 1995), SMC apoptosis and proliferation (Guevara, Kim et al. 1999; Taurin, Seyrantepe et al. 2002) and vascular SMC response to oxidative stress (Liao, Jin et al. 2000). In a recent study combined proteomics and metabolomics to investigate the mechanism of the neointima formation in vein graft of protein kinase C delta (PKCδ)-deficient mice (Mayr, Siow et al. 2004).

Similarly, annotated 2-DE map of proteins expressed in human umbilical vein endothelial cells (HUVECs) has been published (Bruneel, Labas et al. 2003; Bruneel, Labas et al. 2005) and is available on the web at http://www.huvec.com. Data were accumulated from separations conducted on 3-10, 4-7 and 4-6.5 pH gradients and displayed more than 1,000 protein species and more than 200 have been identified, providing a representative overview about the most abundant proteins in this important cellular model.

1.4 Oxidative Stress

Oxidative stress is the disturbance in the prooxidant-antioxidant balance in favour of the former (Sies and Cadenas 1985). It induces cellular redox imbalance and leads to potential tissue damage (or altered cell responses) (Sies 1991). Cellular prooxidants include reactive oxygen species (ROS), reactive nitrogen species (RNS), lipid hydroperoxides (ROOH), paraquat, adriamycin, etc. There are two kinds of antioxidants: enzyme systems (SODs, catalase, glutathione peroxidase, peroxiredoxins) and radical scavengers (ascorbic acid, α-tocopherol, GSH, thioredoxin, selenium, etc). Also there are mainly two kinds of redox pairs: thiol redox (GSH/GSSG, protein sulphydryls), and pyridine nucleotide redox (NADPH / $NADP^+$, NADH / NAD^+).

1.4.1 Source of ROS

ROS come from both endogenous and exogenous sources, including mitochondria, cytochrome P450 metabolism, peroxisomes, and inflammatory cell (neutrophils, eosinophils and macrophages) activation (Inoue, Sato et al. 2003). The oxygen free radical is the ultimate source of many ROS, which is mainly generated by the mitochondria. The electron transport chain leakage (ubiquinone and several iron-sulphur clusters transfer electron directly to oxygen instead of to the next electron carrier, shown in Figure 17) will generate superoxide anion radical ($O_2^{\bullet-}$), which form hydrogen peroxide (H_2O_2) and hydroxyl radical ($HO^{\bullet}$). SOD-2 and glutathione peroxidase (GPx) is the main scavenger of $O_2^{\bullet-}$ and H_2O_2 in mitochondria, respectively. Thus mitochondria represent the main source of the intracellular oxygen radicals ($O_2^{\bullet-}$ and

H_2O_2) in mammalian organs.

Figure 17. Mitochondrial electron transport chain and ROS generation

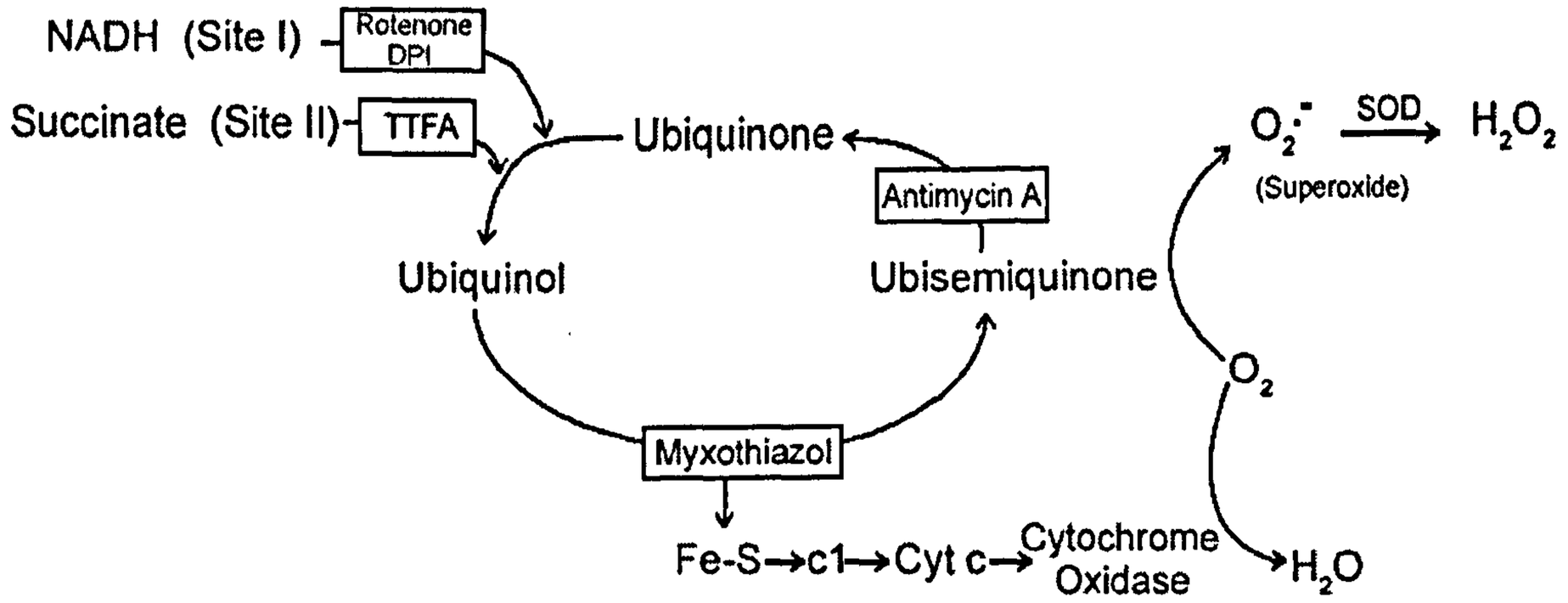

Figure 17. Mitochondrial complex I and II transfer electrons from NADH and succinate, respectively, to ubiquinone. The reduced ubiquinol will pass electrons to complex III and becomes ubisemiquinone. Antimycin A inhibits the recycle of ubisemiquione back to ubiquinone. Accumulation of ubisemiquinone will generate superoxide. Site of inhibition are indicated with boxes. **DPI**, diphenylene iodonium; **SOD**, superoxide dismutase; **TTFA**, thenoyl trifluoracetone. (Chandel, Maltepe et al. 1998)

NAD(P)H oxidase is considered as major source of ROS in vasculature and SMCs. In neutrophils, high levels of ROS generated by NAD(P)H oxidase are used to kill invading microorganisms, while nonphagocytic cells only produce low levels of ROS. NAD(P)H oxidase comprises several subunits, $p22^{phox}$, $gp91^{phox}$, $p47^{phox}$, $p40^{phox}$, $p67^{phox}$, and Rac. When cells are stimulated with cytokines, growth factors, and hormones (Sauer and Wartenberg 2005) (such as interleukin, TNF-α, PDGF, TGF-β1, VEGF), the cytosolic subunits (p47, p40, and p67) will translocate to the membrane subunits (p22 and gp91), resulting in NAD(P)H oxidase activation and the oxidative burst.

Besides the above main source of ROS generation, there are several other endogenous or exogenous sources of cellular oxidants, shown in Table 5 (Klaunig and Kamendulis 2004).

Table 5. ROS and reactive nitrogen species generation in the cell

Cellular oxidants	Source	Oxidative species
Endogenous	Mitochondria	$O_2^{\bullet-}$, H_2O_2, $HO^{\bullet}$
	Cytochrome P450	$O_2^{\bullet-}$, H_2O_2
	Macrophage/inflammatory cells	$O_2^{\bullet-}$, $NO^{\bullet}$, H_2O_2, OCl^-
	Peroxisomes	H_2O_2
Exogenous	Redox cycling compounds	$O_2^{\bullet-}$
	Metals (Fenton reaction)	$HO^{\bullet}$
	Radiation	$HO^{\bullet}$

1.4.2 Oxidative effects

All macromolecules can be damaged by ROS and lead to various diseases: (a) nucleic acid damage cause mutation and carcinogenesis (Nakabeppu, Sakumi et al. 2006); (b) membrane damage by lipid peroxidation (Girotti 1998); (c) protein damage, deactive enzymes, receptors and transporters (Davies 2005); (d) polysaccharide damage, hyaluronic acid degradation caused arthritis (Jahn, Baynes et al. 1999).

Glutathione (GSH, L-γ-glutamyl-L-cysteinylglycine), first discovered in 1920s, is present in millimolar concentrations within most eukaryotic cells and involves in various biologic phenomena. Cellular GSH comes from glutathione synthesis, reduction of oxidized glutathione (GSSG), and luminal and plasma GSH transportation. It is an important protective antioxidant against free radicals and other oxidants by oxidation of the thiol (-SH) group of its cysteine residue. The functions of different GSH-related enzymes (GSSG reductase, thioredoxin-thioredoxin reductase system, thiol transferase, and protein-disulphide isomerase) demonstrate GSH's capability of catalysing protein thiol-disulphide interchange for defence against oxidative stress. Hence, GSH plays an important role in enzyme activation and regulation of complex biochemical processes.

The ratio of GSH to GSSG (GSH/GSSG) is crucial in cells (Cotgreave and Gerdes 1998). GSH depletion and altered GSH/GSSG ratios can signal the development of oxidant-mediated tissue injury (White, Mimmack et al. 1986; De Vecchi, Lubatti et al. 1998) and malformations during embryogenesis (Trocino, Akazawa et al. 1995). Sustained low level of GSH/GSSG can cause cell death.

Thiol antioxidant 2-mercaptoethanol (2-ME) has been reported to support lymphopoiesis and to maintain a variety of other cell lines *in vitro*, including enhancing leukaemia and lymphoma cells proliferation, stimulation of the proliferation of murine spleen cells by enhancing the transport of L-cysteine into the TCA-insoluble pool, and benefit for the optimal maintenance of colony formation, cell proliferation and differentiation of marrow osteoprogenitor cells in primary human bone marrow fibroblast cultures (Inui, Oreffo et al. 1997). The uptake of the essential amino acid cysteine and consequently the maintenance of intracellular glutathione levels are enhanced by 2-ME. Furthermore, 2-ME causes lymphocytes to release thiols into the culture medium, which may protect the cells from oxidative damage (Neumann, Zierke et al. 1998)

Many proteins have been shown to be sensitive to thiol disulphide interchange reactions, including enzymes involved in central and peripheral metabolism, signal transduction, protein catabolism, and anti-oxidative enzymes (Cotgreave and Gerdes 1998). The activation of many proteins is related with the modifications induced on thiols by redox changes while some proteins lose their function after these modifications.

The peroxiredoxin (PRX) family represents a special type of peroxidases, as the protein is the reducing substrate itself. According to the number of cysteine in the active site and the reaction procedure, they can be classified into typical 2-Cys peroxiredoxin (PRX-1, -2, -3, -4), atypical 2-Cys peroxiredoxin (PRX-5) and 1-Cys peroxiredoxin (PRX-6). Upon oxidative stress, the cysteine in the active site is either oxidized to cysteine sulfenic acid or overoxidized to cysteine sulfinic acid (Manevich, Sweitzer et al. 2002; Wood, Schroder et al. 2003) (Figure 18). While the first modification is DTT sensitive and therefore undetectable in 2-DE gels, the latter modification is DTT resistant and results in a charge shift towards a more acidic pI (Wagner, Luche et al. 2002). Peroxiredoxin 6 only has one cysteine in the active site and is more easily oxidized than other peroxiredoxins so that it can be used as an indicator for high level of ROS in cells.

Figure 18. Redox modification of reactive cysteine in proteins

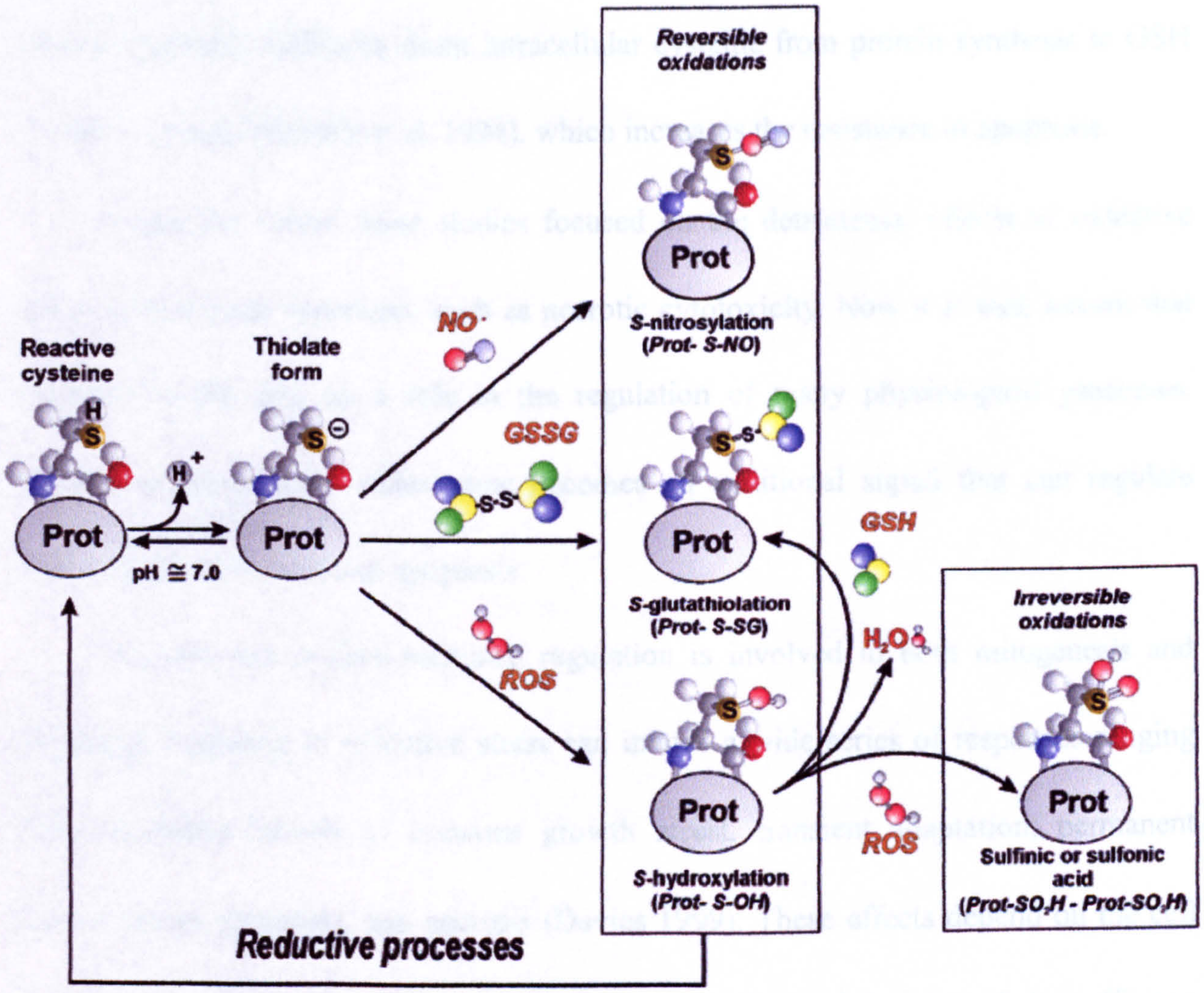

Figure 18. The main target of proteins under oxidative attack is the cysteine residue of the protein. Under physiological pH, a reactive cysteine can exist as thiolate anion, which more easily undergoes reversible oxidation either by the reaction with ROS (S-hydroxylation), NO radical (S-nitrosylation), or GSSG (S-glutathiolation). The reaction products are Prot-SOH, Prot-S-NO, or Prot-S-SG, respectively. Prot-S-OH can be transformed into Prot-S-SG when GSH exists to protect the protein from further oxidation into sulfinic acid (Prot-SO_2H) or sulfonic acid (Prot-SO_3H), which are irreversible modifications of cysteine. (Filomeni, Rotilio et al. 2005)

Oxidized proteins are recognized by proteases and completely degraded to amino acids in mitochondria. In cytoplasm, nucleus and endoplasmic reticulum of eukaryotic cells, these biological reactions occurre in the proteasome complex. When exposed to high oxidative stress or in the presence of declined proteolytic capacity (aging or certain disease states), the oxidized proteins will accumulated and cross-link with one another

or form extensive hydrophobic bonds and further impair the normal cell functions. Protein synthesis inhibitors shunt intracellular cysteine from protein synthesis to GSH synthesis (Ratan, Murphy et al. 1994), which increases the resistance to apoptosis.

During the 1980s, most studies focused on the detrimental effects of oxidative stress in biological processes, such as necrotic cytotoxicity. Now it is well known that oxidative stress take up a role in the regulation of many physiological processes. Change of intracellular redox state becomes an additional signal that can regulate proliferation, cell cycle and apoptosis.

Oxidants and oxidant-mediated regulation is involved in both mitogenesis and apoptosis. Exposure to oxidative stress can induce a wide series of responses ranging from increased mitosis to transient growth arrest, transient adaptation, permanent growth arrest, apoptosis, and necrosis (Davies 1999). These effects depend on the cell type, source, species, intracellular oxidants concentration and duration of stress (Figure 19).

Figure 19. Cellular responses to oxidative stress

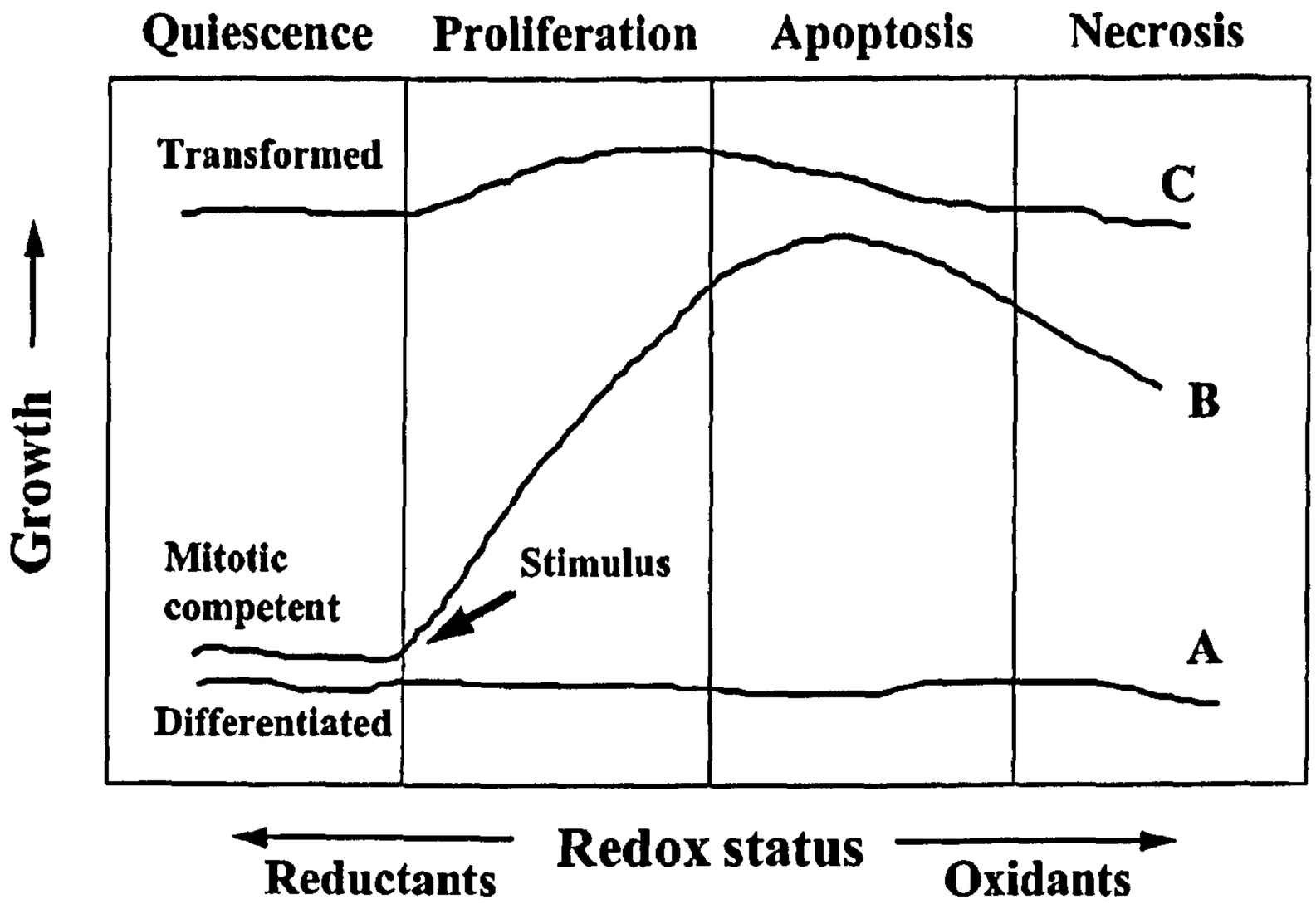

Figure 19. For terminally differentiated cells (A), highly proliferative tumour or transformed cells (C), oxidative stress can induce apoptosis or necrosis. For mitotically competent cells, lower level of oxidative stress can stimulate cell proliferation, but at higher oxidative stress, cells will die by apoptosis or necrosis (B). (Aw 1999)

1.4.3 Apoptosis

Apoptosis is a common mechanism of cell replacement, tissue remodelling, and removal of damaged cells (Chandra, Samali et al. 2000). The most prominent protease families implicated in apoptosis are caspases. About 100 proteins are potential caspase substrates and caspase-mediated proteolysis is the essential step of most apoptosis events. Caspases are cysteine-containing, aspartate-specific proteases which exist as zymogens in cytoplasm, mitochondrial intermembrane space, and nuclear matrix of virtually all cells. The activity of caspases is optimal under reducing environments.

There are three proposed models for caspase activation. First, apoptosis can be induced by ligation of cell surface receptors, causes assembly of death-inducing signalling complex (DISC) and activates caspase-8, caspase-3 and other caspases,

ultimately cleaves various substrates. Second, cytochrome *c* released from mitochondrial forms apoptosome with apoptotic protease activating factor 1 (Apaf-1) and activates caspase-9, caspase-3 and caspase-7 (Figure 20). The third pathway is initiated by cytotoxic cells, which release perforin to attack the target cells. Perforin permeabalizes target cells, allowing granzyme into the cytosol, where it activates caspas-3 and induces apoptosis in tumour cells and infected cells (Chandra, Samali et al. 2000).

Figure 20. Intracellular ROS-mediated apoptotic pathways

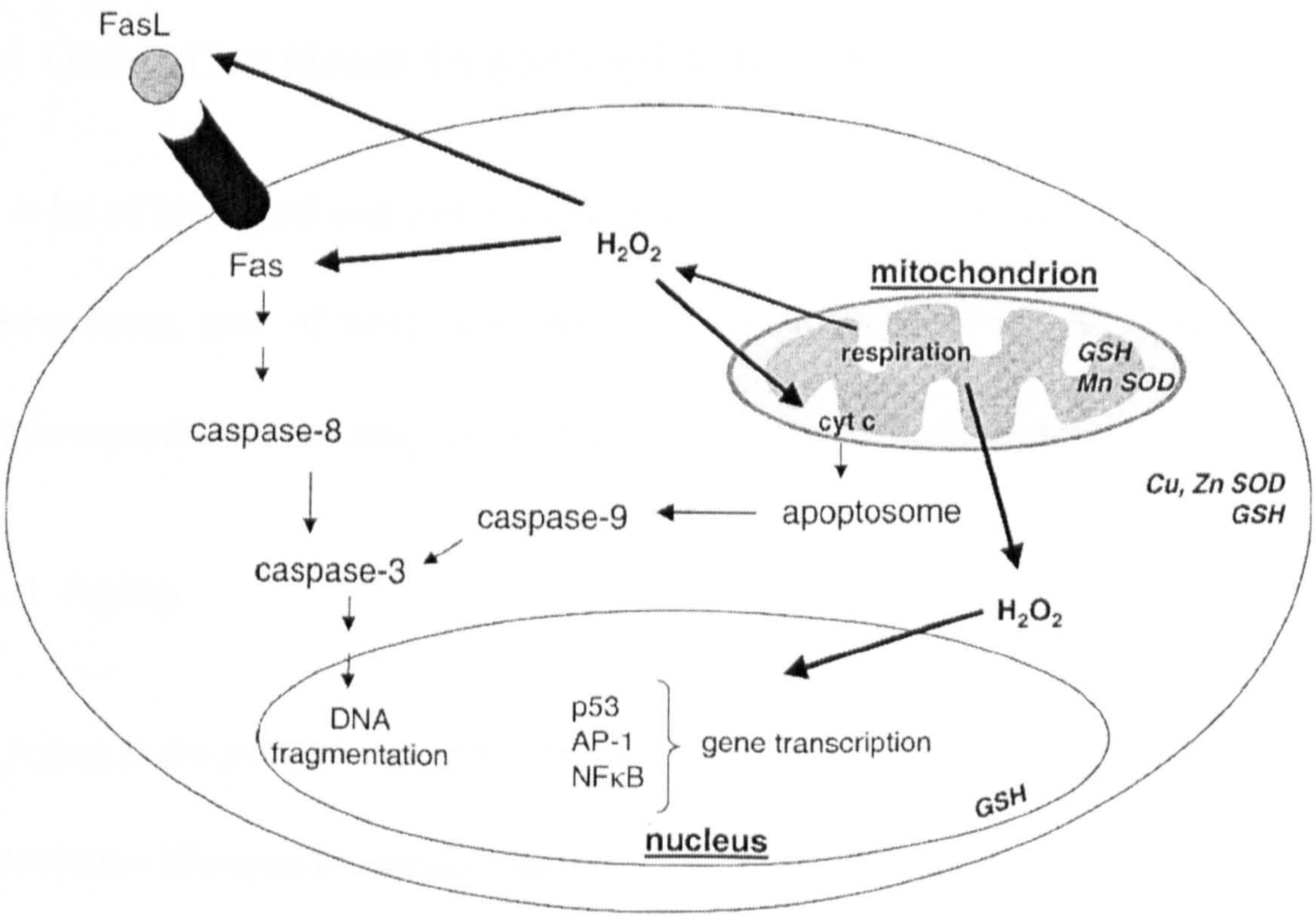

Figure 20. Apoptosis can be induced by H_2O_2-induced upregulation of Fas-FacL system, leading to activation of caspase-8 and downstream caspases, and ultimately cleaves various substrates. Another pathway focuses on H_2O_2-caused release of cytochrome *c* from mitochondria into the cytosol, which forms apoptosome and activates caspase-9 and caspase-3. H_2O_2 also activates nuclear transcription factors and induced cell death. GSH and SODs are the main cellular defenses against ROS. (Chandra, Samali et al. 2000)

A role for oxidative stress in apoptosis has been elucidated by several independent observations. Apoptotic cell death can be switched to necrosis during oxidative stress by

oxidation of active site thiol group of caspases and oxidative-induced mitochondrial energy production failure. Oxidative stress can inhibit caspases activity directly by modifying cysteines of the active site or indirectly by activating caspase inhibitors (Chandra, Samali et al. 2000). During the oxidant-induced apoptosis, oxidative stress causes a mitochondrial calcium influx, which activates mitochondrial nuclease to degrade all mitochondrial polynucleotides. It is possible that partially digested mitochondrial polynucleotides play a similar role as released cytochrome *c* in activating pro-apoptotic enzymes (Cadenas and Davies 2000).

1.4.4 Oxidative stress in pathophysiology

A lot of biological and pathological processes and various diseases are caused by oxidative stress, most of which are linked with apoptosis, such as aging, inflammation, ischemia-reperfusion, carcinogenesis, AIDS, Parkinson's (Chandra, Samali et al. 2000).

1.4.4.1 Aging

Aging is progressive and endogenous. This ultimately determines the rate of aging and maximum life-span potentials (MLSPs) of different animal species. (Barja 2002).

Many recent studies support that free radicals, especially those of mitochondrial origin, are related to the basic aging process (Weindruch and Sohal 1997; Beckman and Ames 1998; Barja 1999). Most investigations showed that endogenous antioxidants are negatively correlated with maximum longevity without normalization by metabolic rate (Perez-Campo, Lopez-Torres et al. 1998), suggesting that the rate of oxygen radical

generation in tissues *in vivo* at normal conditions must be lower in long-lived than in short-lived species. Overexpression of GSH reductase in *Drosophila melanogaster* did not prolong their MLSP (Mockett, Sohal et al. 1999) and aging rate does not seem to change in SOD- or GPx-knockout mice (Barja 2002), indicated that antioxidants do not slow the intrinsic aging process. However, antioxidants can non-specifically protect against many causes of early death, normally exogenous oxidative stress, so that increase animal survival, especially under suboptimum conditions. These can be very important to prevent early death in human populations living in suboptimum environment.

Various studies point to two parameters that can elucidate the connection between aging and oxidative stress. One parameter is the rate of generation of ROS by mitochondria, which correlates better than the metabolic rate with maximum longevity. Long-live animals have a lower ROS generation rate and lower antioxidants level correspondingly. On the other hand, the higher oxidative stress caused more damage in the mitochondrial DNA (measured as 8-OHdG) of short-lived than in that of long-lived animals, which will be accumulated during aging and result in mitochondrial malfunction (Cadenas and Davies 2000). The other parameter is the degree of fatty acid unsaturation of tissue cellular membranes, measured as the total number of fatty acid double bonds (double bond index, DBI). DBI is negatively correlated with body size in mammals, which is due to the endogenous desaturase activities in different species. Thus, the low DBI of long-lived animals would protect them against lipid peroxidation (Barja 2002).

1.4.4.2 Cardiovascular disease

Cardiovascular diseases are associated with increased oxidative stress in blood vessels. ROS are regarded as one of the risk factors for the pathogenesis of various cardiovascular diseases, including hypertension, atherosclerosis, restenosis, cardiac hypertrophy, and heart failure.

ROS generated from NAD(P)H oxidases expressed in ECs and SMCs have been demonstrated to be involved in artherosclerosis, hypertension, heart failure, and diabetic vasculopathy (Sauer and Wartenberg 2005). Vascular SMCs contain potent oxidant-generating systems, acting as major superoxide source in the normal vessel wall (Griendling, Minieri et al. 1994). NADPH-derived superoxide and H_2O_2 are intimately involved in SMC growth and apoptosis. In ECs, laminar shear results in a transient activation of NADPH oxidase, whereas oscillatory shear causes a sustained increase in their activity. Superoxide in the vessel wall will react with NO and form peroxynitrite, thereby impairing endothelium-dependent vasodilatation, oxidize LDL, increase adhesion molecule expression in ECs, and activate matrix metalloproteinases (Griendling, Sorescu et al. 2000). oxLDL has been shown to produce multiple functional alterations that are potentially involved in atherosclerosis (Steinberg, Parthasarathy et al. 1989). Low concentration of oxLDL stimulates SMC proliferation, while higher doses can induce apoptosis (Dietrich, Hu et al. 2000). Although ROS serve as short-term second messenger in vascular cells, the long-term effect of ROS induces cellular damage and lesion formation. Notably, over-expression of the uncoupling protein 1 promotes atherosclerosis by triggering mitochondrial dysfunction, depleting

energy stores and increasing superoxide production (Bernal-Mizrachi, Gates et al. 2005), which is in agreement with our observations (Mayr, Chung et al. 2005). Thus, there is a growing body of evidence that mitochondrial energy metabolism and oxidative stress are intertwined in cardiovascular disease.

1.4.5 Antioxidant therapy

The antioxidant therapeutic interventions, which reduce the generation of ROS, include vitamin E-like antioxidant, native SOD, SOD mimic, and $ONOO^-$ decomposition catalyst.

Protective and beneficial roles of SOD have been demonstrated in broad range of diseases. SOD effectively attenuates both acute and chronic inflammatory responses in animal models of human diseases. Bovine erythrocyte SOD-1 attenuated the inflammatory injury of the colons and showed promising therapeutic efficacy with rheumatoid arthritis, osteoarthritis, and side effects associated with chemotherapy and radiation therapy. However, they have several disadvantages: (a) $HO^{\bullet}$ formation from SOD product H_2O_2; (b) short circulating half-time, antigenicity, bell-shaped dose response curves, high susceptibility to proteolytic digestion; and (c) they cannot penetrate cells or cross the blood-brain barrier (Cuzzocrea, Riley et al. 2001).

A series of low molecular weight SOD mimics, such as manganese-based metalloporphyrin complexes, have been developed to overcome some limitations of the native enzymes. An important and unique property of these SOD mimics is that they are stable to dissociation and oxidation in the Mn(II) oxidation state. In addition, they are

not deactivated by $ONOO^-$ or H_2O_2 but possess catalase activity, scavenge $ONOO^-$ and inhibit lipid peroxidation. Mn(II)-based SOD mimics shows cardio-protective effects in isolated heart preparations and in the *in vivo* models of myocardial ischemia/reperfusion injury (Cuzzocrea, Riley et al. 2001). The most profound effects of metalloporphyrin are depressing the neutrophil influx and reducing nitrotyrosine formation. Although they are very effective compounds in a wide range of oxidative stress paradigms, its potency and efficacy can be quite variable. One general limitation is their poor blood-brain permeability that complicates their use in neurodegenerative diseases (Cuzzocrea, Riley et al. 2001).

Peroxynitrite decomposition catalysts also have anti-inflammatory function. Fe(III)-porphyrin complexes show a peroxynitrite isomerase activity, which measurably reduces the lifetime of peroxynitrite under physiologically relevant conditions. It is likely that peroxidase enzymes might function additionally as endogenous peroxynitrite isomerase, such as mammalian heme haloperoxidases. An active drug will duplicate peroxidase reactivity at critical sites where these enzymes are not present in optimal quantities (Cuzzocrea, Riley et al. 2001).

It is well established that ROS formation plays a critical role in the development of atherosclerosis (Griendling and FitzGerald 2003; Griendling and FitzGerald 2003). Oxidative stress has been implicated in development of potentially proatherogenic actions on SMC proliferation, inflammatory cell recruitment, and redox-sensitive gene expression. Results of antioxidant trials, however, were disappointing (Touyz 2004). Several explanations have been put forward including the fact that many oxidation

pathways are not effectively inhibited by certain antioxidants, that under certain conditions both vitamin E and C can exhibit pro-oxidant rather than anti-oxidant actions (Hazell and Stocker 1997; Podmore, Griffiths et al. 1998) and that doses of antioxidants that are effective in reducing systemic oxidative markers may not cause a significant reduction in oxidative injury in the site of interest (Touyz 2004).

RATIONALE

SMCs are the key player involved in vascular modelling and vascular disease pathogenesis. Initially, it was thought that SMCs from the media migrated, dedifferentiation into the neointima thereby contributing to lesion development. There are now compelling data to suggest that smooth muscle progenitor/stem cells participate in atherogenesis. With regards to this novel hypothesis, the true contribution of stem/progenitor cells may be wholly established by understanding the mechanisms of vessel wall integration, specific recruitment signals, homing, differentiation and adhesion properties of these precursor cells. In addition, these mechanisms may provide new insight into therapeutic strategies such as vascular tissue engineering.

Protocols to differentiate stem cells, more specifically ES cells into vascular SMCs have already been established by many labs. Using proteomics in conjunction with these protocols, we believe immense knowledge on stem cell differention may be obtained. First, by analyzing protein profiles including expression changes occurring at various stages during ES cell differentiation into SMCs, key proteins involved in molecular pathways governing this process may be highlighted. Second, the end stage proteomic profile may be used to confirm that a fully functional vascular SMCs similar to that present in native tissue can be successfully acquired by *in vitro* differentiation.

Hence, within the field of stem cell vascular biology, proteomics can provide insight into the new atherogenesis hypothesis, and give new perspectives into therapeutic strategies for controlling this process *in vivo*. In addition, proteomics such as

that described here may be a potential tool to validify SMCs derived *in vitro* and subsequently used for vascular tissue engineering strategies.

AIMS AND OBJECTIVES

As we now know, the ES cells have potential to differentiate into many kinds of other cell lines and replenish different tissue types. The two main ES cell lines currently available are human ES cells and mouse ES cells. Thorough studies of the mouse ES cells' functions and differentiation mechanisms will be fundamental for any future medical applications of human ES cells. Although ES cells and differentiated progenitor cells are already applied in medical therapy, the mechanism of ES cell differentiation toward a specific lineage and the protein expression changes involved are still not fully elucidated yet.

In the present thesis, I will utilize proteomic techniques to study the ES cell differentiation and try to find some important protein changes and investigate their function in detail.

Aim 1: There are no reliable ES cell proteome maps before I started my PhD, which is the fundamental reference if we want to compare the protein changes during their differentiation. Mouse ES cell were cultured and maintained in an undifferentiation state by using LIF-1 in the culture medium. The whole ES cell lysate were separated on a large format 2-DE gels and the proteins were identified by MS. Thus a reliable mouse ES cell proteome map was obtained.

Aim 2: Mouse ES cells were induced to differentiate into SMC-like cells via the Sca-1^+ progenitor cells. ES cells were predifferentiated by withdrawal of LIF-1 and Sca-1^+ progenitor cells were then isolated by magnetic beads. Further culturing Sca-1^+

progenitor cells in differentiation medium supplemented with PDGF-BB will induce their differentiation into ES cell-derived SMCs (esSMCs), which express SMC markers and their purity was verified by FACS. The proteome map of Sca-1^+ progenitor cells was also generated using the same protocols as the ES cell proteome map.

Aim 3: Differences in protein expression of esSMCs and aortic SMC were directly compared by using DIGE approach. The majority of protein changes between these two cell lines were identified by tandem MS and verified by immunoblotting. Further comparison using enzymatic assay, cell viability experiment and treatment by a panel of inhibitors were carried on to find out some part of the mechanisms involved in ES cell differentiation.

2 MATERIALS AND METHODS

2.1 Cell culture and differentiation

2.1.1 Mouse ES Cells Culture

The clonal mouse ES cell line ES-D3 (CRL-1934, ATCC) was derived from blastocysts of a 129S2/SvPas mouse. ES cells were maintained as described previously (Vittet, Prandini et al. 1996). Briefly, ES cells were cultured in complete stem cell medium (see Appendix) in a humidified incubator with 95% air/5% CO_2 at 37°C. The medium is buffered with 1.5 g/L sodium bicarbonate, which requires 5% CO_2 to maintain the medium in the optimal pH range for cells ($CO_2 + H_2O \rightarrow H_2CO_3 \leftrightarrow H^+ + HCO_3^-$). Undifferentiated ES cells were passaged into flasks coated with 0.04% gelatine (G1393, Sigma) at a ratio of 1:6 to 1:10 every 2 days to maintain an undifferentiated state. The addition of 2-mercaptoethanol provides an alternative source of -SH groups to regulates the redox level and protect cells from oxidative stress.

2.1.2 ES cells differentiation to esSMCs

To induce differentiation, ES cells were cultured on type IV mouse collagen (Trevigen) coated flasks for 3-4 days in basic differentiation medium (DM) (see Appendix) as described before (Hirashima, Kataoka et al. 1999). Sca-1^+ cells were sorted from the cell culture by magnetic labelling cell sorting (MACS) with anti-Sca-1 magnetic microbeads (Miltenyi Biotec) as described in our previous studies (Hu, Zhang et al. 2004). Briefly, cells were detached with 0.05% trypsin/0.02% EDTA solution (Invitrogen) from flasks and incubated with the antibody-conjugated/coated microbeads.

With occasional agitation for 15min at 4°C, the bead-bound cells were selected with magnetic cell separator (Miltenyi Biotec) and cultivated in collagen type IV-coated 24-well plate. After cultured with DM for 4 days, these cells were subcultured into collagen type IV-coated 6-well plate with DM. These cells were called Sca-1$^+$ cells, passage 0. After 2-3 days, Sca-1$^+$ cells were subcultured and expanded in gelatin-coated flasks with DM and passaged every 2 days and change medium every day (Xiao, Zeng et al. 2006) Sca-1$^+$ cells, passage 15, were harvested for proteomic analysis.

Sca-1$^+$ cells, passage 5-7, were stimulated with DM contains 10ng/mL PDGF-BB (P4056, Sigma) in gelatin-coated flasks. These cells will express SMC markers after 5 passages, so called ES-derived SMCs (esSMCs), passage 0. esSMCs were continuously passaged every 2 days in DM at ratio of 1:2 to 1:3 and change medium every day (Xiao, Zeng et al. 2006). esSMCs, passage 5~12, were harvested for proteomic analysis and immunoblotting. (Figure 21)

Figure 21. Schematic illustration of ES cell differentiation procedure

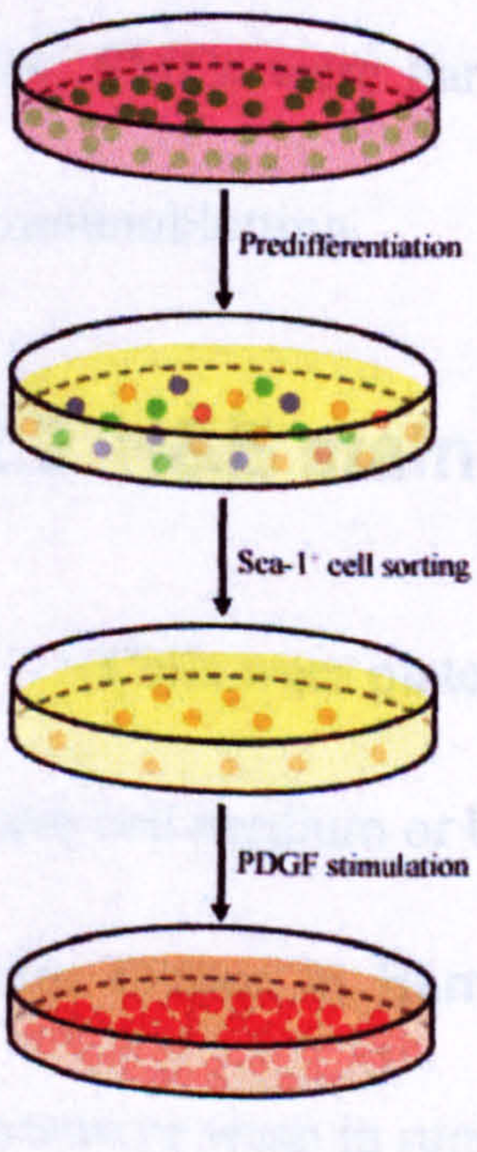

Figure 21. Dissociated mouse ES cells were predifferentiated in collagen IV-coated dishes in basic differentiation medium (DM) without LIF-1. Sca-1$^+$ cells were isolated with Sca-1 magnetic beads. When stimulated by 10ng/mL PDGF-BB for 5 passages, more than 95% of these cells express smooth muscle cell markers, and were termed ES cell-derived SMCs (esSMCs).

2.1.3 SMCs culture

Mouse mature vascular SMCs of C57BL/6J mice (Charles River, Sulzfeld, Germany) were cultivated from their aortas as described previously (Hu, Zou et al. 1999). Briefly, mouse thoracic aortas were removed and washed with RPMI 1640 (Invitrogen) medium. The intima and inner two thirds of the media were carefully dissected from the vessel under an anatomic microscope, cut into pieces and planted onto a gelatine (0.02%) coated plastic bottle. The bottle was incubated upside down at 37°C in a humidified atmosphere of 95% air/5% CO_2 for 3 hours, and then primary culture medium (see Appendix) was slowly addes. Cells were incubated at 37°C for 7 to 10 days and passaged by treatment with 0.05% trypsin/0.02% EDTA solution. The ECs will not survive during following cultures and no contamination was detected previously. Then these cells were cultured in the exactly same condition as the esSMCs. SMCs were cultured in 0.04% gelatine-coated flasks with DM in a humidity incubator with 5% CO_2 at 37°C, passaged every 2 days at ratio of 1:2 to 1:3 with medium changes every day. SMCs were harvested at the same time as esSMCs for proteomic analysis and immunoblotting.

2.2 H&E staining

Cells were plated in 8-well chamber slides (Nalge Nunc) and cultured in complete stem cell medium or basic DM for 3 days then fixed and stained with H&E. Briefly, cell were stained in Harris' haematoxylin for 5min and in Eosin for 3min, followed by extensive wash in running water, then mounted with coverslip and left to dry.

2.3 Flow cytometry analysis

The procedure was similar as described previously (Hu, Zhang et al. 2004). Briefly, cultured cells were incubated with dissociation buffer (Invitrogen) for 3min and blocked with diluted serum (the species of serum is the same as the secondary antibody) for 20min on ice. The single-cell suspension was aliquoted and incubated with either isotype control or SSEA-1 (MAB4301, Chemicon), Sca-1 (553333, BD Biosciences), smooth muscle α-actin (C6198, Sigma), calponin (C2687, Sigma), and SMMHC (M7786, Sigma) antibodies for 30min on ice and incubated with rabbit anti-mouse or anti-rat immunoglobulin conjugated with FITC (DAKO). Cell suspensions were analyzed with FACS scan flow cytometer (Becton Dickinson Immunocytometry Systems). Data analysis was carried out using CellQuest software (Becton Dickinson).

2.4 Immunofluorescence staining

The procedure was similar as described previously (Hu, Zhang et al. 2004). Briefly, cultured cells were labelled with mouse monoclonal antibodies to stage-specific embryonic antigen-1 (SSEA-1; clone MC-480; Chemicon) and Sca-1 (clone E-13-161.7; BD biosciences), and visualized with rabbit anti-mouse immunoglobulin conjugated with fluorescein isothiocyanate (FITC; DAKO Cytomation) or phycoerythrin (PE; DAKO). 4', 6-diamidino-2-phenylindole (DAPI; Sigma) was used as counterstaining. Cells were mounted in Floromount-G (DAKO) and examined under fluorescence microscope (ZEISS).

2.5 Molecular biology methods

2.5.1 RNA isolation

The RNA extraction was performed according to the RNeasy Mini Kit (Qiagen, Valencia, CA, USA) protocol for isolation of total RNA from animal cells. All steps of the RNeasy protocol were performed at room temperature. The cells were washed and scraped off in PBS and centrifuged at 13.2krpm for 1min. Cell pellet was disrupted by RLT Buffer (350μL for small flask, 600 μL for medium flask) and mixed by pipetting to make sure no cell clumps are visible. The lysate was transferred directly onto a QIAshredder spin column placed in a 2 mL collection tube, and centrifuged for 2min at 13.2krpm. Same volume of 70% ethanol was added to the homogenized lysate and mixed well by pipetting. 700 μL of the sample were applied to an RNeasy mini column placed in a 2 mL collection tube and centrifuged for 15 seconds at 13.2krpm. The flow-through was discarded and another 700 μL of sample were applied if there was any. 700μL of RW1 buffer was added to the RNeasy column and centrifuged for 15sec at 13.2krpm to wash the column. 500μL RPE buffer was pipetted onto the RNeasy column and centrifuged for 15 seconds at 13.2krpm to wash the column and another 500 μL RPE buffer was added to the column and centrifugation for 2min at 13.2krpm was taken place to dry the RNeasy silica-gel membrane. The flow-through and the collection tube were discarded. Finally, the RNeasy column was transferred to a clean 1.5 mL collection tube. 50 μl RNase-free water was pipetted directly onto the RNeasy column, following by centrifugation for 1min at 13.2krpm to elute the RNA. The RNA

concentration was determined by measuring the absorbance at 260nm in a spectrophotometer and diluted with RNase-free water and ethanol to make a final mRNA concentration of 0.25μg/μL in 75% ethanol.

2.5.2 Reverse transcription PCR (RT-PCR)

RT-PCR was performed using Improm-II™ RT kit (Promega, Madison, WI, USA) with RNase inhibitor (Rnasin, Promega) and random primers (Promega). Control RT reactions were performed without reverse transcriptase. Total RNA was used as a template for cDNA synthesis.

RT reaction system was set up by drying 10μL mRNA (0.25μg/μL) at 70°C and mixing with 0.2μL random primer (0.5μg/μL) and 9.8μL distilled water. The sample was incubated at 70°C for 5min and cooled down on ice for 5min. 10μL of 5× RT Buffer, 6μL of 25mM $MgCl_2$, 2μL of 25mM dNTPs, 1μL of Rnasin (40U/μL) and 2μL of reverse transcriptase (200U/μL) were added to make a final volume 50μL. The RT-PCR was carried on in thermal cycler (TC-312 or TC-412, TECHNE) with following program: preheat lid at 105°C, initial denaturation at 25°C for 5min, elongation at 42°C for 1.5 hours and final extension at 72°C for 15min.

2.5.3 Polymerase chain reaction (PCR)

The expressions of cell markers were detected by PCR using cDNA from RT-PCR as templete. Oligonucleotide primer sequences were as follows (Table 6) (Hu, Zhang et al. 2004):

Table 6. PCR primers for SMC markers

Gene Name	Primer	Cycles
h1-calponin		30
	forward 5'-GAT ACG AAT TCA GAG GGT GCA GAC GGA GGC TC-3'	
	reverse 5'-GAT ACA AGC TTT CAA TCC ACT CTC TCA GCT CC-3'	
glyceraldehyde-3-phosphate dehydrogenase (GAPDH)		25
	forward 5'-GAT ACA AGC TTT CAA TCC ACT CTC TCA GCT CC-3'	
	reverse 5'-CGG AGT CAA CGG ATT TGG TCG TAT-3'	
smooth muscle α-actin (SMA)		30
	forward 5'-ACG GCC GCC TCC TCT TCC TC-3'	
	reverse 5'-GCC CAG CTT CGT CGT ATT CC-3'	
smooth muscle protein 22 (SM22)		25-30
	forward 5'-GCA GTC CAA AAT TGA GAA GA-3'	
	reverse 5'-CTG TTG CTG CCC ATT TGA AG-3'	
smooth muscle myosin heavy chain (SMMHC)		35-40
	forward 5'-GAC AAC TCC TCT CGC TTT GG-3'	
	reverse 5'-GCT CTC CAA AAG CAG GTC AC-3'	

Glyseraldehyde-3-phosphate dehydrogenase (GAPDH) is a catalytic enzyme involved in glycolysis. The GAPDH gene is constitutively expressed in almost all tissues at high levels and has been widely used as an internal control in conventional RT-PCR to normalize the expression of a target gene.

PCR was performed using PCR kit (Invitrogen) following the manufacturer's

instructions and reaction system was prepared on ice as follows: 0.50μL DNA template, 1.25μL dNTP (2mM), 1.25μL 10× buffer, 1.00μL primer, 1.00μL $MgCl_2$ (50mM), 0.10μL Taq Polymerase, and 7.40μL distilled water. The total volume is 12.50μL for each reaction. After prepared the reaction system, tubes were put into thermal cycler (Model TC-312 or TC-412, TECHNE) and the following programs were used: preheat lid at 105°C, initial denaturation at 94°C for 4min, then 25-40 cycles of denaturing at 94°C, annealing at 55°C and elongation at 72°C, each step for 50 seconds. The final extension step is at 72°C for 5min and then PCR products can be stored at 4°C.

2.5.4 Agarose gel electrophoresis

Agarose gels (2%) were prepared by dissolving 3g agarose with 150mL TAE buffer (40mM Tris-acetate, 2mM Na_2EDTA, pH 8.3) diluted from 50× TAE stock (EC-872, National Diagnostics) by heating in a microwave oven. Then, the gel was cooled and 7.5μL ethidium bromide (10 mg/mL) was added to the clear gel solution to a final concentration of 0.5μg/mL. After mixing, the gel was poured into a plastic mould with casting combs in place and allowed to solidify for 20-30min. The tape and the gel casting combs were removed and the gel was placed in a horizontal gel electrophoresis apparatus (GIBCO BRL, Horizon® 11.14, Catalogue No. 11068-012). TAE electrophoresis buffer was added to the reservoirs until the buffer covered the agarose gel. PCR products were mixed with 6× loading buffer (30% Glycerol or 15% ficoll 400, 0.25% Bromophenol blue, 0.25% Xylene cyanole) and loaded into the wells together with 1kb DNA ladder. Agarose gel electrophoresis was performed for 45-60min with

constant current of 130mA. Finally, the target fragments were visualized on a transilluminator UV light box (254 nm) and pictures were taken.

2.6 Protein concentration measurement

The protein concentration was determined using the Bradford method (Bradford 1976). For lysates in urea buffer, 2.8μL of samples was mixed with 2.8μL of 0.1M HCl, 22.4μL of distilled water, and 972 μL of diluted Protein Assay Reagent (1:5 dilution, Bio-Rad) was added and mixed well. For samples without urea, 2μL of samples was mixed with 998μL of diluted Protein Assay Reagent. Absorbance at 595nm was measured by SmartSpec™ 3000 spectrophotometer (Bio-Rad) and protein concentration was calculated based on the BSA standard curve.

2.7 Proteomic techniques

Figure 22. Proteomics workflow

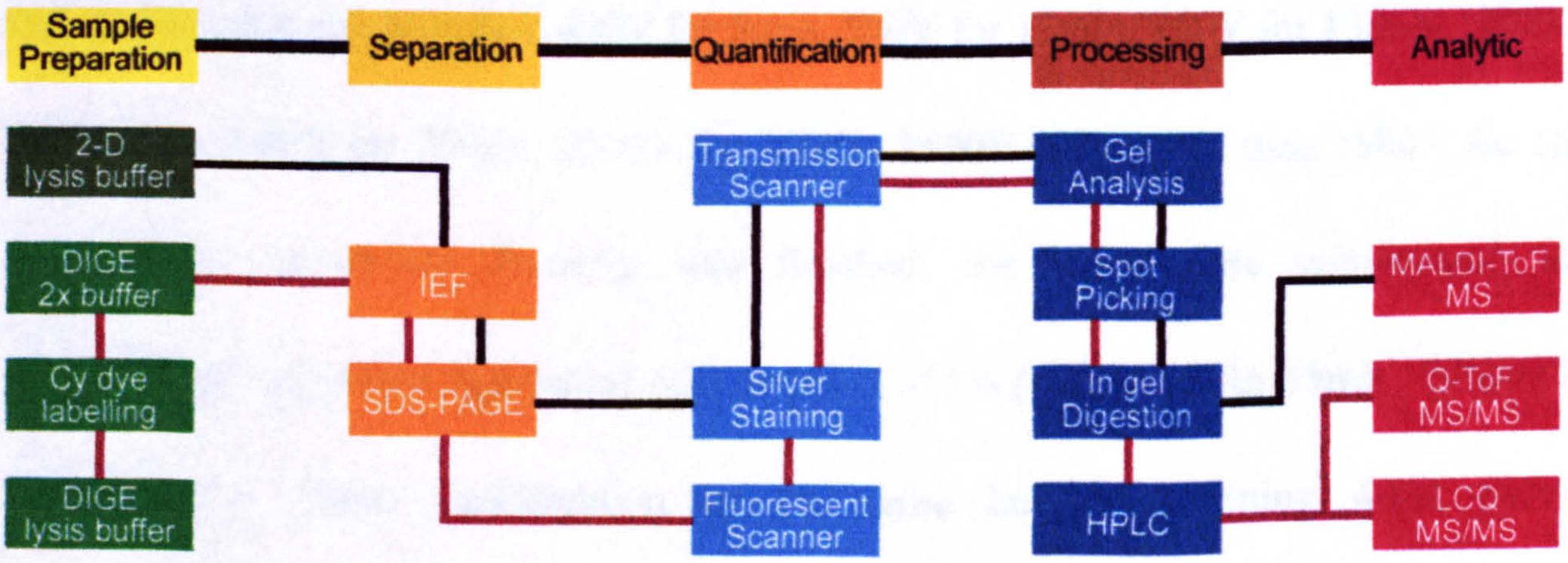

Figure 22. The brief workflow of proteomics used in this thesis. Black line indicates normal 2-DE, silver staining and MALDI-ToF MS process. Red line denotes DIGE and MS/MS procedure.

2.7.1 2-DE

The protocol used for proteomics analysis is similar to that described previously (Dunn 1997; McGregor, Kempster et al. 2001). Cells were washed by 2-DE wash buffer (see Appendix) then scraped and centrifuged at 4°C, 13.2krpm, for 1min. Cell pellets were lysed in 2-DE lysis buffer (see Appendix) for 30min and centrifuge at 13.2krpm at 20°C for 20min. Supernatant was divided into aliquots and protein concentration was determined, then stored at -80°C. Extracts were diluted with rehydration solution (see Appendix) or subject to an additional clean-up procedure by using 2-D PrepReady CleanUp Kit (Bio-Rad) to remove contaminants interfering with isoelectric focusing. Protein samples were loaded on 18cm nonlinear immobilized pH gradient strips, pH 3-10 (Immobiline DryStrips, GE healthcare). One hundred micrograms total proteins were used for analytical gels and 400μg for preparative gels. After 24 hours rehydration, strips were focused in Multiphor™ II isoelectric focusing System (GE healthcare) at 20°C with following protocol: 400V for 5min, 500V for 15min, 750V for 15min, 1250V for 30min, 2000V for 20min, 2500V for 15min, 3500V for 15min, then 3500V for 18 hours. Once isoelectric focusing was finished, the strips were equilibrated in equilibration buffer (see Appendix) with addition of 1% (w/v) DTT for 15min, followed by a further 15min equilibration in the same buffer containing 4.8% (w/v) iodoacetamide in place of DTT. SDS-PAGE was performed using 12%T (total acrylamide concentration), 2.6% C (degree of cross-linking) separating polyacrylamide gels without a stacking gel, running with Ettan™ DALTsix vertical electrophoresis system (GE healthcare). The second dimension was carried out at 10°C with the

following protocol: for 6 gels, 600V, 400mA, 12W for 15min, 15W for 30min, 100W for 4.5 hours, using 2× running buffer in the upper chamber and 1× running buffer in the lower chamber, until the Bromphenol Blue dye front had migrated off the lower end to the gels. The lower power step at the beginning allows all proteins in the IPG strip enter the polyacrylamide gel before separation by the following high power step.

2.7.2 DIGE

The design of a DIGE experiment is shown as Table 7. esSMCs and aortic SMC were labelled with Cy3 and Cy5 and crisscross experimental design was used to eleminate differences between dyes

Table 7. DIGE experiment design

Strip No.	Cy Dye	Sample
20372	Cy3	esSMC-X2 p6
	Cy5	EDSMC8 p6
20373	Cy3	Aortic SMC p13
	Cy5	SM 1
20374	Cy3	esSMC-R1 p5
	Cy5	Aortic SMC p15
20375	Cy3	ApoE p21
	Cy5	esMC-X5.2 p11
20377	Cy3	St III
	Cy5	esSMC-X5.1 p10
20378	Cy3	ESC p16
	Cy5	esSMC-X1 p6
20379	Cy3	Sca1 p12
	Cy5	esSMC-R2 p5

Aortic SMCs and esSMCs were washed with DIGE wash buffer (see Appendix) and lysed in DIGE lysis buffer (see Appendix). After centrifugation at 13.2k rpm for 20min, the supernatant containing soluble proteins was harvested and protein concentration was determined. The fluorescence dye labelling reaction was carried out at a dye/protein ratio of 200pmol/50μg. After incubation on ice for 30min, the labelling reaction was stopped by scavenging non-bound dyes with 10mM lysine (L8662, Sigma) for 15min. Fifty micrograms whole cell extracts of each sample were labelled with fluorescent dyes (Cy3 or Cy5) and mixed with internal pool standard (labelled with Cy2). Samples were mixed with 2× buffer (see Appendix) and loaded on immobilized pH gradient strips (18cm, pH 3-10, nonlinear). As in traditional 2-DE, after rehydration overnight, samples were separated using the same protocols. Fluorescence images were acquired using the Typhoon variable mode imager 9400 (GE healthcare), visualized by silver staining and scanned in transmission scan mode using a calibrated scanner (GS-800, Bio-Rad) for documentation. Detailed protocols can be downloaded from our website (http://www.vascular-proteomics.com).

2.7.3 Silver Staining

Protein profiles of 2-DE gels were visualized by silver staining using the PlusOne™ Silver Staining Kit, Protein (GE healthcare) with slight modifications, i.e. only formaldehyde was used in developing solution but no glutardialdehyde or formaldehyde in other solutions (Yan, Wait et al. 2000), which is compatible with mass spectrometry. 250mL of solutions are needed per large format gel. All steps should be

performed with gentle shaking of the glass dish and all solutions are made in double distilled water.

Gels were taken out from the glass plates carefully and fixed in fixation solution (see Appendix) overnight. On the next day, gels were sensitized for 30min in sensitizing solution (see Appendix) followed by silver reaction for 20min in 0.25% w/v $AgNO_3$ with 3×5min washing between these two steps. After brief washing for 2 times, the developing solution (see Appendix) was added and the gels were shaken until protein spots are observed and before background becomes over-developed. The developing solution was replaced by the stopping solutions (see Appendix). After shaking for 10min, the gels were washed 3×5min, sealed in bag and kept in 4°C.

2.7.4 Analysis of 2-DE gels

Three different software have been used for 2-DE gel analysis, PDQuest (version 7.0 for Mac, Bio-Rad), ProteomWeaver (version 2.1, Definiens) and DeCyder (version 6.5, GE healthcare).

PDQuest is used for generating Mr/pI grid image. After identification of the proteins, Mr/pI Grid was made according to most confident Mr/pI pairs. The observed Mr and pI of proteins were derived from this Mr/pI Grid.

ProteomWeaver detects spots on each gel and make a match matrix to compare these gels in a short time. After the matching process, an overlay picture of two gel images can be obtained, orange colour for bottom gel and blue colour for top gel. One image is distorted to make the matched spot exactly on the top of another image. When

the matched spots in two images are nearly the same size and intensity, the spot on overlay picture will appear black. Using this strategy, the difference between two gels can be easily found.

DeCyder is the dedicated software for DIGE gels. It automatically detects spots using the standard gel image among the three images of one gel and does not allow artificial modifications on spots boundary. One DIGE gel has unique spots boundaries on three CyDye images, which can present the different protein expressions on the same gel directly. By matching and normalising the internal standard from different DIGE gels, samples from different DIGE gels using same standard can be matched and compared, and statistical analysis can be carried on. Average ratio of the intensity of each protein spots and *p* values between two groups were calculated. Spots showing a statistically significant difference (2 fold increase or decrease, $p<0.05$) in intensity were excised for in-gel tryptic digestion.

2.7.5 In-gel tryptic digestion

At the beginning, we used manual digestion according to a published protocol (Shevchenko, Wilm et al. 1996). Silver-stained spots were picked and washed with 50μL 100mM ammonium bicarbonate (ABC, A6141, Sigma) followed by 200μL acetonitrile (ACN, 27071-7, Aldrich) twice. After dried in Speed Vac for 5min, gel pieces were soaked in 50μL 10mM DTT (D9779, Sigma) in 100mM ABC for 30min at 56°C followed by 50μL 50mM iodoacetamide (I1149, Sigma) in 100mM ABC for 30min at room temperature to reduce disulfide bond and alkylate cystaine residues.

After washed with 100μL 100mM ABC, 200μL ACN, 100μL 100mM ABC, 200μL ACN twice sequentially and dried in Speed Vac for 5min, gel pieces were treated overnight at 37°C with 50μL trypsin (20μg/mL in 50mM ABC, V5111, Promega). Peptide fragments were recovered by sequential extractions with 100mM ABC and extraction solution (see Appendix) twice, each for 20min. Extracts were combined together, lyophilized, and resuspended in 10μl 0.1% (v/v) trifluoroacetic acid (T0274, Sigma). The peptides solution was desalted with μC-18 ZipTip (Millipore) according to the manufacturer's instruction and spoted on MALDI plate (Kratos, Manchester, UK).

Now the in-gel digestion was performed with an Investigator ProGest (Genomic Solutions) robotic digestion system according to published methods (Shevchenko, Wilm et al. 1996; Wilm, Shevchenko et al. 1996; Perkins, Pappin et al. 1999; Yan, Wait et al. 2000). Briefly, silver stained gel slices were destained with 50μL of destaining solution (see Appendix) for 15min then washed with 100μL ddH_2O 2×10min then with 100μL 25mM ABC for 10min. All solutions were purged by N_2 and gels were dehydrated in 50μL ACN and neutralized with ABC then shrinked with another 100μL of ACN. The gels were reduced in 30μL DTT (10mM in 50mM ABC) at 60°C for 10min and cooling for 20min then alkylated in 30μL iodoacetamide (50mM in 50mM ABC) for 15min. After washed with 40μL of 50mM ABC for 10min and shrinked with 50μL ACN for 2×15min, trypsin solution was prepared (see Appendix) and 15μL of trypsin solution was added to each well and digestion was carried on at 37°C for 7.5 hours, 10μL of ddH_2O was added after 1.5 hours of digestion to cover the gels. After the reaction, 10μL of 25mM ABC, 20μL of ACN and 20μL of 10% formic acid were consequently added

and each incubation were 10min. after final extraction by 20μL ACN for 15min and 30μL of ACN for 15min, all the solution were purged into collection plate and the digestion is finished. The plate was lyophilized and digestion products were resuspended in 15μL of 0.1% formic acid and ready for MS.

2.7.6 MALDI-ToF MS

MALDI-MS was performed using an Axima CFR spectrometer (Kratos). The instrument was operated in the positive ion reflectron mode. 1μl of sample and 1μL of matrix (see Appendix) were applied to MALDI plate. The spectra were recorded and analyzed by Kompact software (version 2.3.4, Kratos) and the prominent intensity peaks were labelled and internally calibrated using trypsin autolysis products (monoisotopic masses at *m/z* = 842.51, *m/z* = 1045.56, and *m/z* = 2211.10). Their peptide masses were searched against SwissProt databases using the MASCOT program (http://www.matrixscience.com) (Perkins, Pappin et al. 1999). One missed cleavage per peptide was allowed and carbamidomethylation of cysteine as well as partial oxidation of methionine were assumed. Protein scores greater than 59 were considerd significant ($p<0.05$).

2.7.7 Q-ToF MS/MS

Mass spectra were recorded using a Q-ToF mass spectrometer (Micromass) interfaced to a Micromass CapLC capillary chromatograph. Samples were dissolved in 0.1% formic acid, injected onto a 300μm × 5mm Pepmap C18 column (LC Packings),

and eluted with an acetonitrile/0.1% formic acid gradient. The capillary voltage was set to 3500V, and data-dependent MS/MS acquisitions were performed on precursors with charge states of 2, 3, or 4 over a survey mass to charge range of 540~1000. The collision gas was argon, and the collision voltage was varied between 18V and 45V depending on the charge-state and mass of the precursor. Initial protein identifications were made by correlation of uninterpreted tandem mass spectra to entries in SWISS-PROT and TREMBL, using ProteinLynx Global Server (V 1.1, Micromass).

2.7.8 LCQ ion-trap MS/MS

Following enzymatic degradation, peptides were separated by capillary liquid chromatography on a reverse-phase column (BioBasic-18, 100mm × 0.18mm, particle size 5μm, Thermo Electron Corporation) and applied to a LCQ ion-trap mass spectrometer (Finnigan LCQ Deca XP Plus, Thermo Electron Corporation) interfaced with a Finnigan Surveyor autosampler (Thermo Electron Corporation). The peptides were eluted using an acetonitrile/0.1% formic acid gradient. Acetonitrile concentration was increased gradually from 5% to 80%. Spectra were collected from the ion-trap mass analyzer using full ion scan mode over the mass to charge range 300-1800. MS-MS scans were performed on each ion using dynamic exclusion. Database search was performed using TurboSEQUEST program (BioWorks Browser v3.2, Thermo Electron Corporation) against UniProt database. Protein probabilities were calculated in the comparison of esSMCs and aortic SMCs. Following filter was applied: for charge state 1, $X_{Corr} > 1.50$; for charge state 2, $X_{Corr} > 2.00$; for charge state 3, $X_{Corr} > 2.50$.

2.8 Immunoblotting

Immunoblotting was performed as described previously (Li, Hu et al. 1999; Li, Hu et al. 2000). Cells were washed with cold PBS and scraped on ice. After lysis in RIPA lysis buffer (see Appendix) for 30min at 4°C and centrifuged at 13.2krpm at 4°C for 20min, supernatant was collected and the protein concentration was determined using Bradford method. Samples were stored at -20°C. Cell extracts were mixed with 1/4 volume of 5× Laemmli buffer (see Appendix), denatured at 96°C for 5min and a quick spin was following. 50μg protein samples were loaded on each lane of Novex Tris-Glycine Gel (4-20%, 1.0mm × 10 wells, Invitrogen) and electrophoresed at 125V constant voltage for 2.5 hours. When the Bromphenol Blue dye front reaches the end of the gel, electrophoresis was terminated and proteins were electrotransferred from gel to nitrocellulose membrane at 25V constant voltage for 2.5 hours in transfer buffer (see Appendix). The membranes were labelled as appropriate and blocked with 5% PBS-milk for 1 hour at room temperature or overnight at 4°C. Specific primary (Table 8) and corresponding secondary antibody (both in 5% PBS-milk) were applied to the membrane in turn and incubated at room temperature with gentle agitation for 1 hour, wash with PBS for 3×5min between two incubations. After washing with 0.05% Tween in PBS for 3×5min, ECL Western Blotting Detection Reagents (RPN2209, GE healthcare) were applied for 1min. The membranes were drained from excess ECL solution and sealed in sample bags. Hyper film was exposed by membranes and developed in developing solution (Kodak GBX developer/replenisher, P7042, Sigma) and fixation solution (Kodak GBX fixer/replenisher, P7167, Sigma).

Table 8. Antibodies used in immunoblotting.

Antibody	Company	Cat No	Dilution
Actin	Santa Cruz	sc-1616	1:1000
Catalase	Abcam	ab1877	1:3000
Crystallin α/β (HSP20)	Abcam	ab13497	1:1000
Heat shock protein 27 (HSP27)	Santa Cruz	sc-1049	1:1000
Heat shock protein 60 (HSP60)	Stressgen	SPA-807	1:400
Heat shock protein 70 (HSP70)	Stressgen	SPA-810	1:100
Heat shock protein 90 (HSP90)	Santa Cruz	sc-7947	1:300
Heme oxygenase 1 (HO-1)	Santa Cruz	sc-10789	1:200
Heme oxygenase 2 (HO-2)	Santa Cruz	sc-11361	1:1000
Myosin light chain-1 (MLC-1)	Abcam	ab680	1:1000
Peroxiredoxin 1 (PRX-1)	Lab Frontier	LF-PA0001	1:2000
Peroxiredoxin 2 (PRX-2)	Lab Frontier	LF-PA0007	1:2000
Peroxiredoxin 3 (PRX-3)	Lab Frontier	LF-PA0030	1:2000
Peroxiredoxin 6 (PRX-6)	Abcam	ab16824	1:1000
Peroxiredoxin-SO_3 (PRX-SO_3)	Lab Frontier	LF-PA0004	1:2000
Peroxiredoxin 6-SO_3 (PRX6-SO_3)	Lab Frontier	LF-PA0005	1:2000
Superoxide dismutase [CuZn] (SOD-1)	Santa Cruz	sc-11407	1:100
Superoxide dismutase [Mn] (SOD-2)	Upstate	06-984	1:500
α-Tubulin	Abcam	ab7750	1:100

2.9 Total reactive oxygen species (ROS) measurement

The oxidative fluorescent dyes dihydrorhodamine 123 (DHR123, D632, Molecular Probes) were used to evaluate in situ production of ROS by use of a method described previously (Miller, Gutterman et al. 1998). DHR123 are freely permeable to cells and are oxidized to hydrorhodamine in the presence of ROS and labels proteins in cytoplasm with green fluorescence. Cells were incubated with 10μM DHR123 for 1 hour, washed with PBS and lysed in lysis buffer (see Appendix). The cell lysates were sonicated for 15 seconds then 30 seconds and centrifuged at 13.2krpm for 20min at 4°C. The supernatant were analyzed at excitation and emission wavelengths of 502 and 523nm, respectively, by Fusion™ universal microplate analyzer (Packard). Protein concentration was determined by the Bradford method. The fluorescence intensity was expressed as relative fluorescence units (RFU) per μg protein.

2.10 Mitochondrial superoxide and ROS measurement

MitoSOX™ Red mitochondrial superoxide indicator (M36008, Molecular Probes) is live-cell permeant and is rapidly and selectively targeted to the mitochondria. Once in the mitochondria, it is oxidized by superoxide but not by other ROS- or reactive nitrogen species (RNS)-generating system and exhibits red fluorescence. Hence it can be used for highly selective detection of superoxide in the mitochondria of live cells (http://probes.invitrogen.com/media/pis/mp36008.pdf). Cells were cultured in 24-well plates, change medium after 24 hours. After 48 hours, cells were pretreated with normal medium, 20μg/mL antimycin A or 10μM rotenone for 3 hours and incubated with

2.5μM MitoSOX™ Red mitochondrial superoxide indicator and 10μM DHR123 in HBSS (14025-092, Invitrogen) for 30min. After washed with HBSS, plates were scanned on a fluorescence scanner (Typhoon 9400, GE healthcare), excitation/emission wavelengths 532nm/580nm for MitoSOX and 488nm/520nm for DHR123. Fluorescence intensity was quantified using the ImageQuant software (Molecular Dynamics) and normalized with aortic SMC control.

2.11 ATP concentration measurement

ATP concentration was determined by using a bioluminescence assay as described previously (Jenner, Ruiz et al. 2002). The ATP assay uses luciferase extract of firefly tails and depends on the detection of the bioluminescence produced by it in the presence of ATP. ATP levels in samples can be calculated because the amount of light produced is proportional to the amount of ATP. Cells were cultured on 6-well plate (2.5×10^5 cells/well for SMC and 5×10^5 cells/well for esSMC), change medium after 24 hours. After 48 hours, cells were washed briefly with cold PBS twice. Cold trichloroacetic acid (TCA, 6.5% w/v) was added to each well (1mL/well) and incubated on ice for 10min. TCA extracts were transferred into eppendorf tubes. 10μL sample or acid ATP standard was added to 140μL of reaction buffer (see Appendix) and mixed with 50μL of firefly lantern extract solution (1mg/mL, F3641, Sigma). Bioluminescence was measured by luminescence plate reader (Fusion™ universal microplate analyzer, Packard). Adherent cell protein was solublized by adding 1mL of 0.5M NaOH and incubating for 1 hour on ice. Protein concentrations were determined using Bradford method. ATP concentration

was adjusted for protein concentration and expressed as μmol per gram protein.

2.12 GSH concentration measurement

The fluorometric method for determination of GSH is described previously (Hissin and Hilf 1976; Jenner, Ruiz et al. 2002). The sample harvest procedure was the same as ATP measurement. 7.5μL of acid sample extract or acid GSH standard was added to reaction buffer (see Appendix) followed by 15μL of 0.1% (w/v) o-phthalaldehyde in methanol. After 25min, fluorescence was measured on a Fusion™ universal microplate analyzer (Packard) by using excitation and emission wavelengths of 350nm and 420nm, respectively. GSH concentration was adjusted for protein concentration and expressed as μmol per gram protein.

2.13 Glutathione reductase activity

Glutathione reductase catalyzes the reduction of glutathione (GSSG) in the presence of NADPH, which is oxidized to $NADP^+$. The decrease in absorbance at 340nm is measured to determine the glutathione reductase activity. Cells were cultured on 6-well plates, medium was changed after 24 hours. After 48 hours, cells were washed briefly with PBS twice and lysed in lysis buffer (see Appendix). Cell lysates were sonicated for 30 seconds and centrifuged at 13.2krpm for 20min at 4°C. The supernatant were analyzed for glutathione reductase activities by using glutathione reductase kit (GR2368, Randox Laboratories Ltd) on Cobas Mira chemistry analyzer (Roche) according to the manufacturer's instruction. The glutathione reductase activities were

adjusted for protein concentration and expressed as IU per gram of cell proteins.

2.14 Cell viability assay

To investigate the GSH's influence on cell viability, GSH depletion reagent diethyl maleate (DEM) and GSH reductase inhibitor 1,3-Bis(2-chloroethyl)-1-nitrosourea, (carmustine, or BCNU) were administered. DEM is a commonly used electrophiles which leads to more rapid and more extensive depletion effect than that obtained with γ-GCS inhibitors (Griffith 1999). It is relatively non-toxic and conjugates directly with GSH in a reaction catalyzed by the glutathione S-transferase system (16,17) (Weber, Duncan et al. 1990). The antitumor agent carmustine (BCNU) is unstable in aqueous solution, and will spontaneously degrade to reactive alkylating, 2-chloroethyl diazohydroxide, and carbamoylating intermediate, 2-chloroethyl isocyanate. The alkylating component is responsible for the antitumor effects, whereas the carbamoylating species inhibit carbamoylation of Cys-58 in glutathione reductase and carbamoylate glutathione (Becker and Schirmer 1995).

Cells were cultured on 96-well plates (2.5×10^3 cells/well for SMCs, 5×10^3 cells/well for esSMCs), medium was changed after 24 hours. After 48 hours, cells were incubated with different concentrations of diethyl maleate (DEM, D97703, Sigma) or 2-mercaptoethanol for 24 hours, or with 100μM carmustine (BCNU, C0400, Sigma) for different time. After removal of medium, CellTiter 96® AQ_{ueous} One Solution (Cell Proliferation Assay, Promega) was added with dilution ratio of 1:6 in DMEM (Invitrogen). After 3 hours incubation, the optical density at 490nm was recorded by

photometer (Mayr, Mayr et al. 2002). The reagent concentration used was optimized in preliminary experiments.

2.15 JC-1 staining

A high mitochondrial membrane potential ($\Delta\Psi$) guarantees the normal function of mitochondria. The fall in $\Delta\Psi$ is one of the early events during the apoptosis. 5,5',6,6'-tetrachloro-1,1',3,3'-tetraethyl-benzimidazolylcarbocyanine iodide (JC-1) is a lipophilic cationic dyes that exhibit potential-dependent accumulation in mitochondria, indicated by a fluorescence emission shift from green (~525nm) to red (~590nm) (Cossarizza, Baccarani-Contri et al. 1993). Consequently, mitochondrial depolarization is indicated by a decrease in the red/green fluorescence intensity ratio, which only depends on the $\Delta\Psi$ and not on other factors (size, shape, density) (Salvioli, Ardizzoni et al. 1997).

Cells were diassociated in PBS and treated with 5μM of JC-1 (T3168, Molecular Probes) with or without 50μM of carbonyl cyanide 3-chlorophenylhydrazone (CCCP, C2759, Sigma) for 30min at 37°C. Cell suspensions were analyzed by FACS scan flow cytometer (Becton Dickinson Immunocytometry Systems). Signals of FL-1 (green, 525nm) and FL-2 (red, 590nm) channel were recoded and data analysis was carried out by CellQuest software (Becton Dickinson).

2.16 Metabolites measurement

To evaluate the metabolites changes, a set of metabolites concentration in esSMCs

and aortic SMCs were measured by nuclear magnetic resonance (NMR) spectroscopy. Cells were cultured in big flasks (culture surface is 175cm^2) for 48 hours, with medium change after 24 hours. Cells were washed by cold sodium chloride for 2 times after decanting the medium. Water-soluble metabolites were extracted in 6% perchloric acid (380083, Sigma). Adherent cells were scraped and transferred to ice cold centrifuge tubes. After centrifuged at 4000 rpm for 15min at 4°C, the supernatant was transferred to new tubes. The pellet was solubilized by adding 2mL of 0.5M NaOH and protein concentration was determined by the Bradford method. The supernatant was neutralized to pH 7 with 10M KOH and centrifuged at 4000 rpm for 15min at 4°C. The supernatant was collected, lyophilized and reconstituted in deuterium oxide (D_2O). Immediately before the NMR analysis, the pH was readjusted to 7 with perchloric acid or KOH. 500µl of the extracts were placed in 5mm NMR tubes. ^{1}H NMR spectra were obtained using a Bruker 600MHz spectrometer. The water resonance was suppressed by using gated irradiation centred on the water frequency. Sodium 3-trimethylsilyl-2,2,3,3-tetradeuteropropionate (TSP) was added to the samples for chemical shift calibration and qualification.

2.17 Glucose concentration measurement

D-glucose can be oxidized to gluconic acid by glucose oxidase releasing H_2O_2. In the presence of peroxidase, H_2O_2 reacts with o-dianisidine (colourless) to form a brown coloured product. Oxidized o-dianisidine reacts with sulphuric acid to form a more stable pink coloured product. The intensity of the pink colour measured at 540nm is

proportional to the original glucose concentration.

Cells were cultured in 6-well plates. Medium from different time points was collected and gluocose concentration were measured by using Glucose (GO) Assay Kit (GAGO-20, Sigma). According to the manufacture's instruction, samples and glucose standard were added into 96-well ELISA plates. After addition of 100μl of the mixture of glucose oxidase/peroxidase/o-Dianisidine, the solution showed brown colour. After incubation in 37°C for 30min, the reaction was stopped by adding 100μl 12N sulphuric acid. The intensities of each well at 540nm were measured and glucose concentrations were calculated.

2.18 Statistical analysis

Statistical analysis was performed using Student's *t*-test. Results were given as means ± SE. Mean = $\sum x/n$. Standard error of the mean (SE) = $(\sum(x-x_{mean})^2/(n\cdot(n-1)))^{1/2}$. *p* value of less than 0.05 was considered significant. Number of different samples (*n*) used for different experiments were stated in each section of Results Chapter where applicable.

3 RESULTS

3.1 ES cells differentiation

Mouse ES cells were pre-differentiated in collagen-IV coated flasks by withdrawal of LIF. Subsequently, Sca-1$^+$ cells were isolated by magnetic labelling cell sorting (MACS) with anti-Sca-1 microbeads. Stimulation by PDGF-BB for 5 passages induces Sca-1$^+$ cells to differentiate to ES-derived SMCs (esSMCs). At least 3 Sca-1$^+$ cell cultures and 6 esSMC cultures were generated using this protocol and studied in this project. Aortic SMCs isolated from 2 C57BL/6J mice were used as control. Their phenotype was verified by using H&E staining, RT-PCR, FACS, and immunofluorescence staining.

Sca-1$^+$ progenitors and esSMCs displayed a monolayer in culture, while ES cells showed clusters in an undifferentiated status for more than 35 passages. Comparison of H&E staining pictures between mature and differentiated SMCs showed a morphological similarity (Figure 23).

mRNA levels of SMC markers, e.g. smooth muscle α-actin, smooth muscle protein 22, calponin, and smooth muscle myosin heavy chain, were very low in Sca-1$^+$ cells. After stimulation with PDGF-BB for 5 passages, they were strongly expressed in esSMCs but slightly weaker than those in aortic SMCs (Figure 24).

Figure 23. H&E staining of ES cells, Sca-1$^+$ cells, esSMCs and SMCs

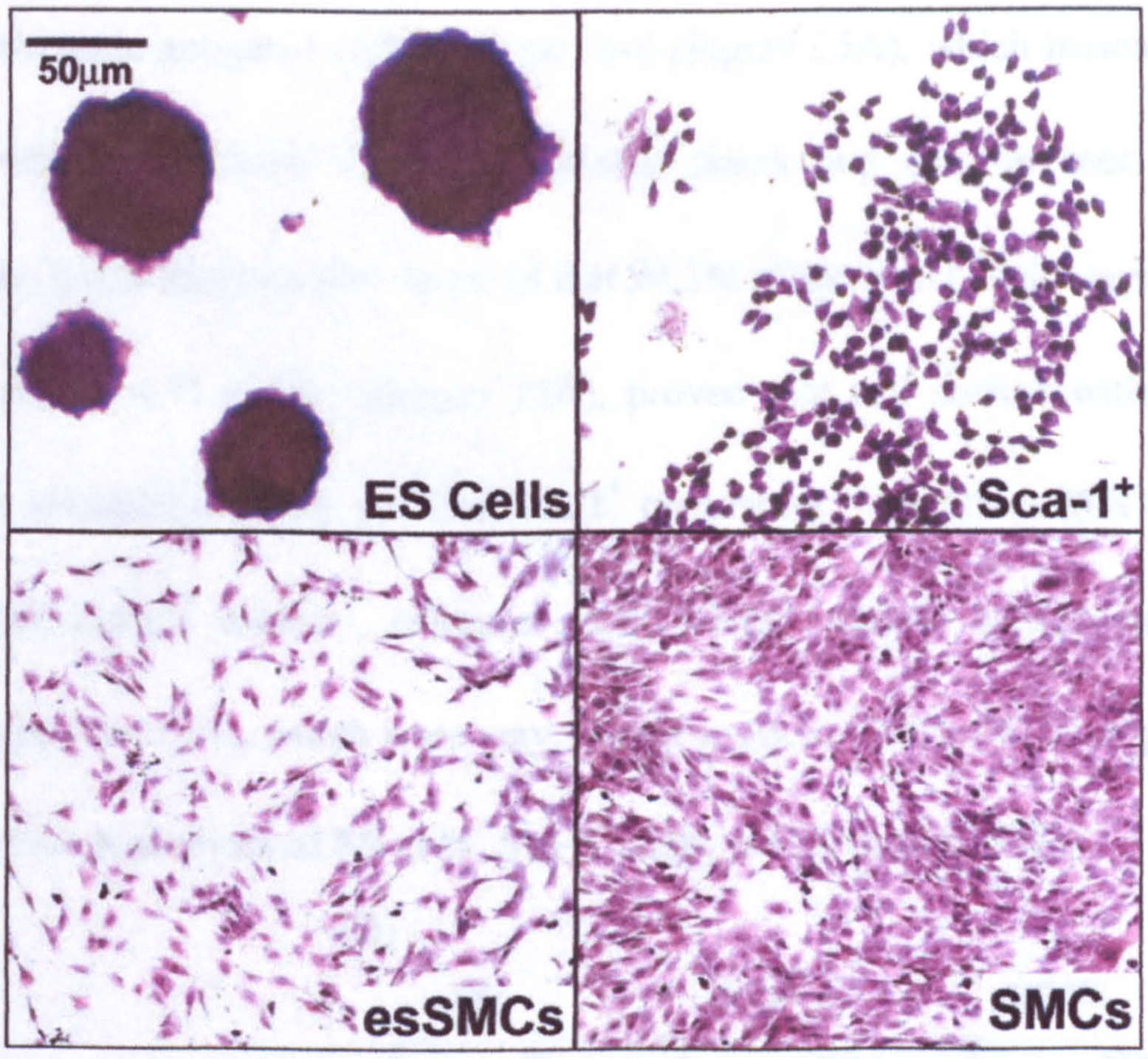

Figure 23. ES cells, Sca-1$^+$ cells, esSMCs and SMCs were cultured in chamber slides and stained with H&E staining. The ES cells showed clusters while other three cell lines displayed a monolayer. These four pictures were shown with same scale. Black bar indicates 50μm.

Figure 24. RT-PCR results of ES cells, Sca-1$^+$ cells, esSMCs and SMCs

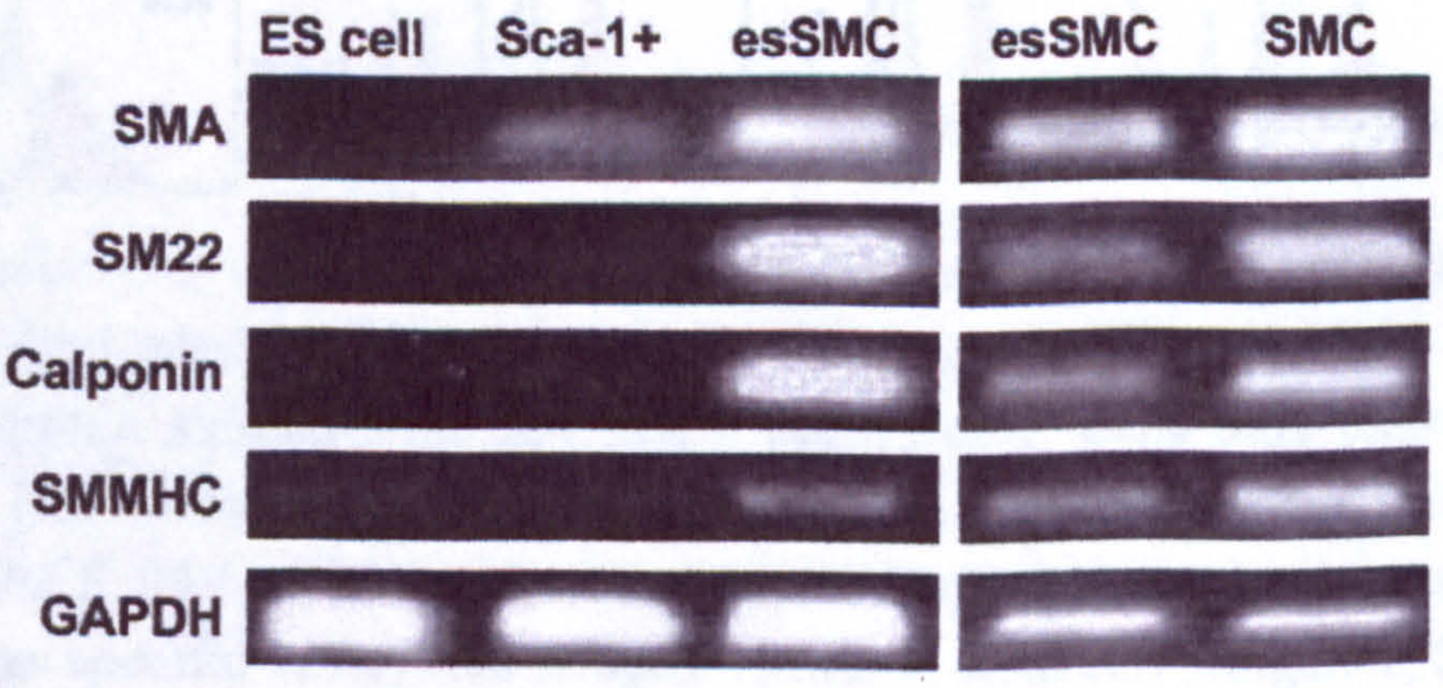

Figure 24. mRNA of ES cells, Sca-1$^+$ cells, esSMCs and SMCs were harvested and RT-PCR was utilized to detect the mRNA level of smooth muscle cell markers. The SMA, SM22, caponin and SMMHC were highly expressed in esSMCs compared to ES cells and Sca-1$^+$ cells but slightly less than in aortic SMCs. GAPDH was included as loading control. (**SMA**, smooth muscle α-actin; **SM22**, smooth muscle protein 22; **SMMHC**, smooth muscle myosin heavy chain; **GAPDH**, glyceraldehyde- 3-phosphate dehydrogenase)

The flow cytometric analysis demonstrated that 96.5% of ES cells were stage specific embryonic antigen-1 (SSEA-1) positive (Figure 25A), which indicates that the ES cells were maintained in undifferentiated status and can be used in further experiments. FACS analysis also revealed that 94.3% of the Sca-1$^+$ cells expressed stem cell antigen-1 (Sca-1) marker (Figure 25A), proved that cell sorting with anti-Sca-1 microbeads obtained a highly purified Sca-1$^+$ population. More than 95% of esSMCs were smooth muscle α-actin-, calponin-, and smooth muscle myosin heavy chain (SMMHC)-positive cells, which were very similar as aortic SMCs (99%) (Figure 25B).

Figure 25. FACS analysis of ES cells, Sca-1$^+$ cells, esSMCs and SMCs

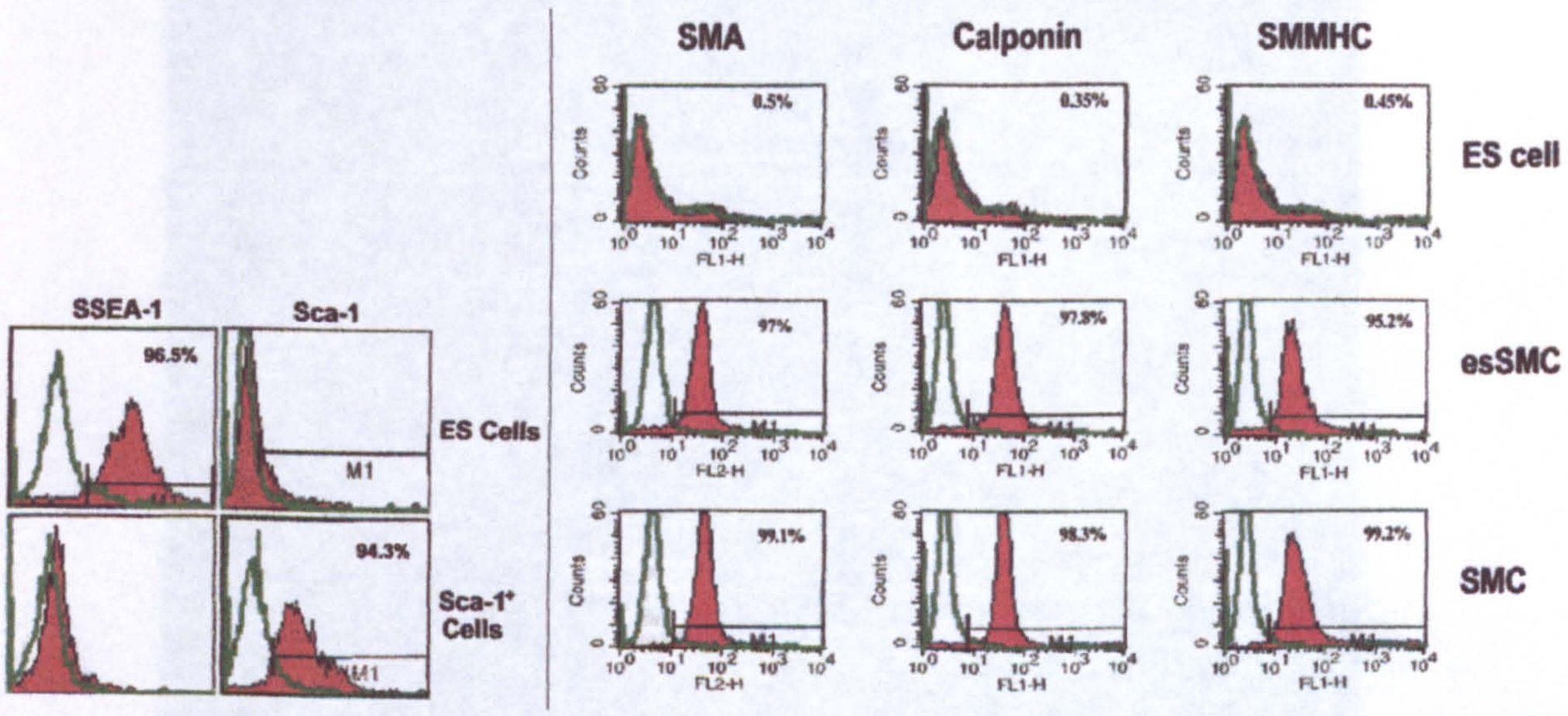

Figure 25. Cells were dissociated and incubated with either isotype control (green line) or antibodies (red area) and analyzed by FACS. (A) ES cells specificly express stage specific embryonic antigen-1 but not Sca-1 while Sca-1$^+$ cells only express Sca-1 but not SSEA-1. (B) Smooth muscle cell markers of ES cells, esSMCs and SMCs were detected by FACS. The esSMCs showed similar cell marker expressions as aortic SMCs. (**SSEA-1**, stage specific embryonic antigen-1; **Sca-1**, stem cell antigen-1; **SMA**, smooth muscle α-actin; **SMMHC**, smooth muscle myosin heavy chain)

Immunofluorescent staining of SSEA-1 and Sca-1 also showed that ES cells and Sca-1$^+$ cells expressed SSEA-1 and Sca-1, respectively (Figure 26A). The immunofluorescent staining also confirmed that the esSMCs expressed SMA, calponin

and SMMHC (Figure 26B).

Figure 26. Immunofluorescent staining of ES cells, Sca-1$^+$ cells, and esSMCs.

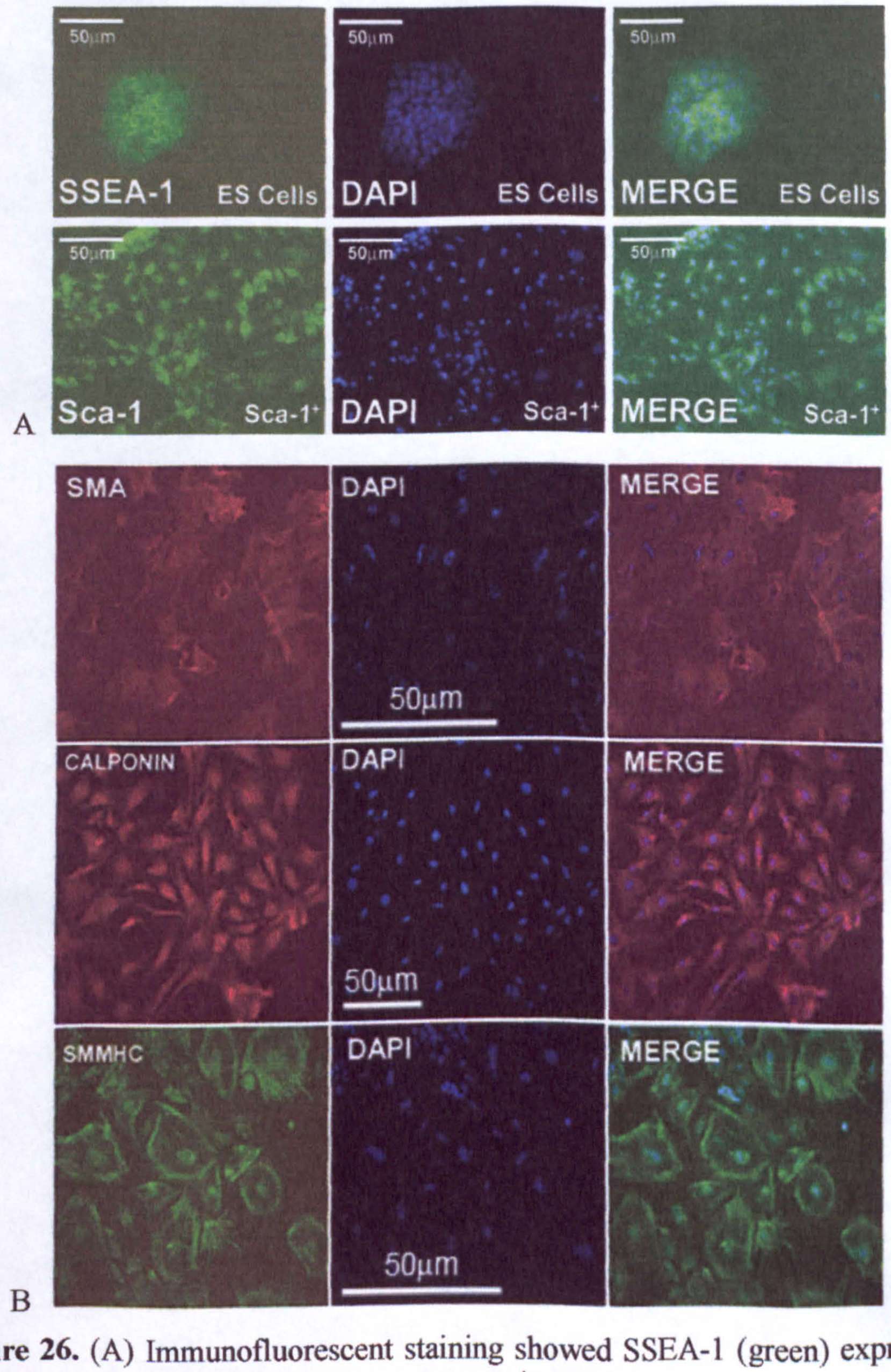

Figure 26. (A) Immunofluorescent staining showed SSEA-1 (green) expression in ES cells and Sca-1 (green) expression in Sca-1$^+$ cells. Nuclei were counter-stained with DAPI (blue). White bar indicates 50μm. (B) Smooth muscle cell marker expressions of esSMCs were detected by immunofluorescent staining, including smooth muscle α-actin (red), calponin (red) and smooth muscle myosin heavy chain (green). Nuclei were counter-stained with DAPI (blue). White bar indicates 50μm. (**SMA**, smooth muscle α-actin; **SMMHC**, smooth muscle myosin heavy chain)

All these results confirmed the undifferentiated stage of ES cells, high

homogeneity of the Sca-1^{+} progenitor cells, and SMC marker expressions of esSMCs after PDGF-BB stimulation.

3.2 Proteome map of ES cells

3.2.1 ES cell proteome map

The proteome of ES cells was separated by 2-DE. On a large format 2-DE gel, there are about 2000 spots visible by silver staining. Comparison of different gels (n=6) by ProteomWeaver showed high consistency of the protein pattern between different ES cell cultures. A representative overlay picture is shown as Figure 27. Nearly 300 proteins were picked and identified (Figure 28) by mass spectrometry, in a MM range from 10kDa to 130kDa, and a pI range from 4 to 9. The proteins were labelled and listed in Table 13 (see Appendix). The Mr/pI Grid map was generated by PDQuest software with internal calibration (Figure 29).

Figure 27. Overlay picture of two 2-DE gels of ES cells

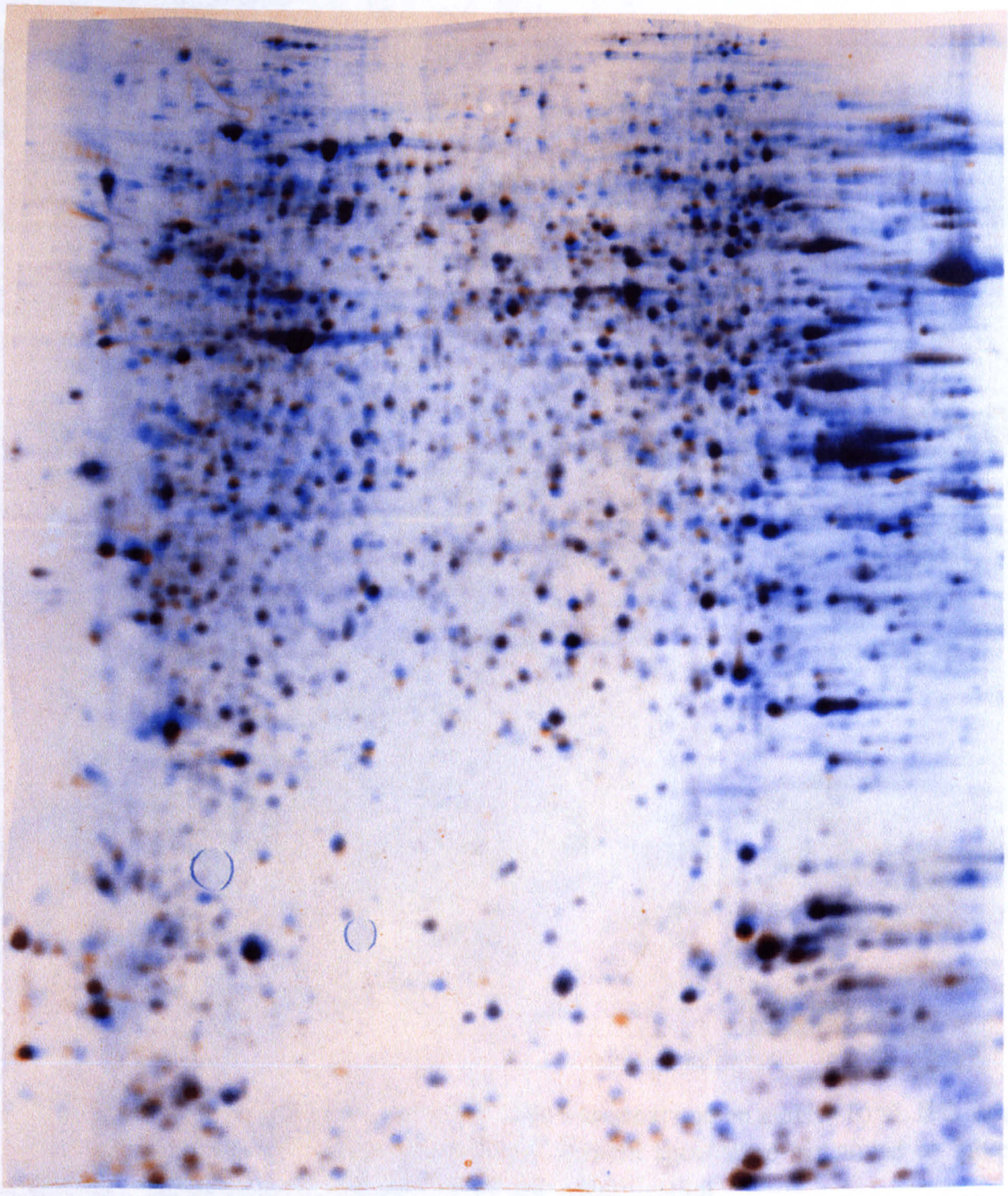

Figure 27. Overlay of two 2-DE gels from different ES cell cultures were generated by ProteomWeaver software. The orange colour and blue colour indicate protein spots on different gels. Matched proteins with similar expression are shown in black colour.

Figure 28. Proteome map of ES cells

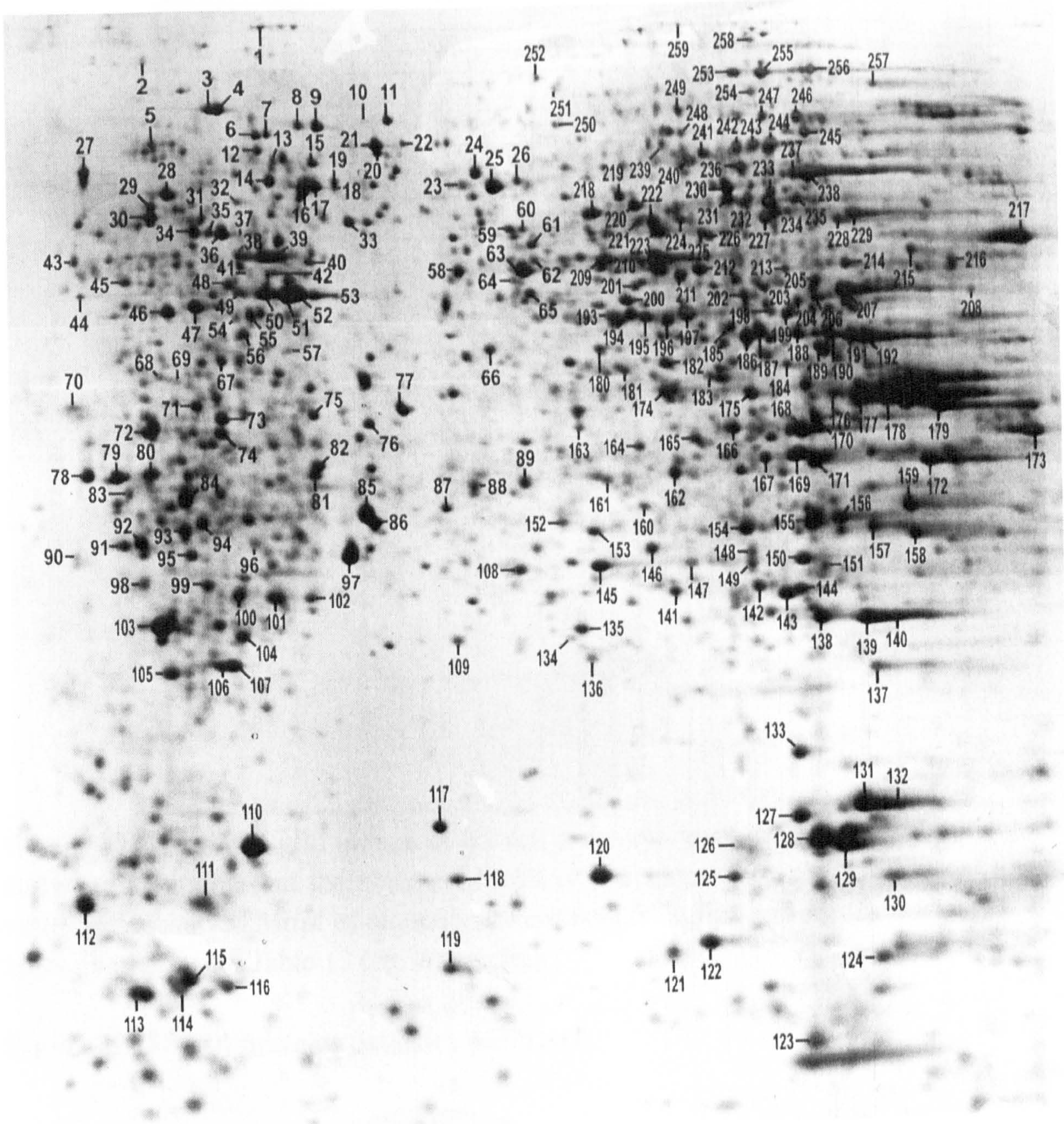

Figure 28. 100μg of protein extract of ES cells was separated on a pH 3-10NL IPG strip, followed by a 12% SDS polyacrylamide gel. Protein spots were visualized by silver staining. Labelled spots were picked for protein identification.

Figure 29. Mr/pI grid picture of ES cell proteome map

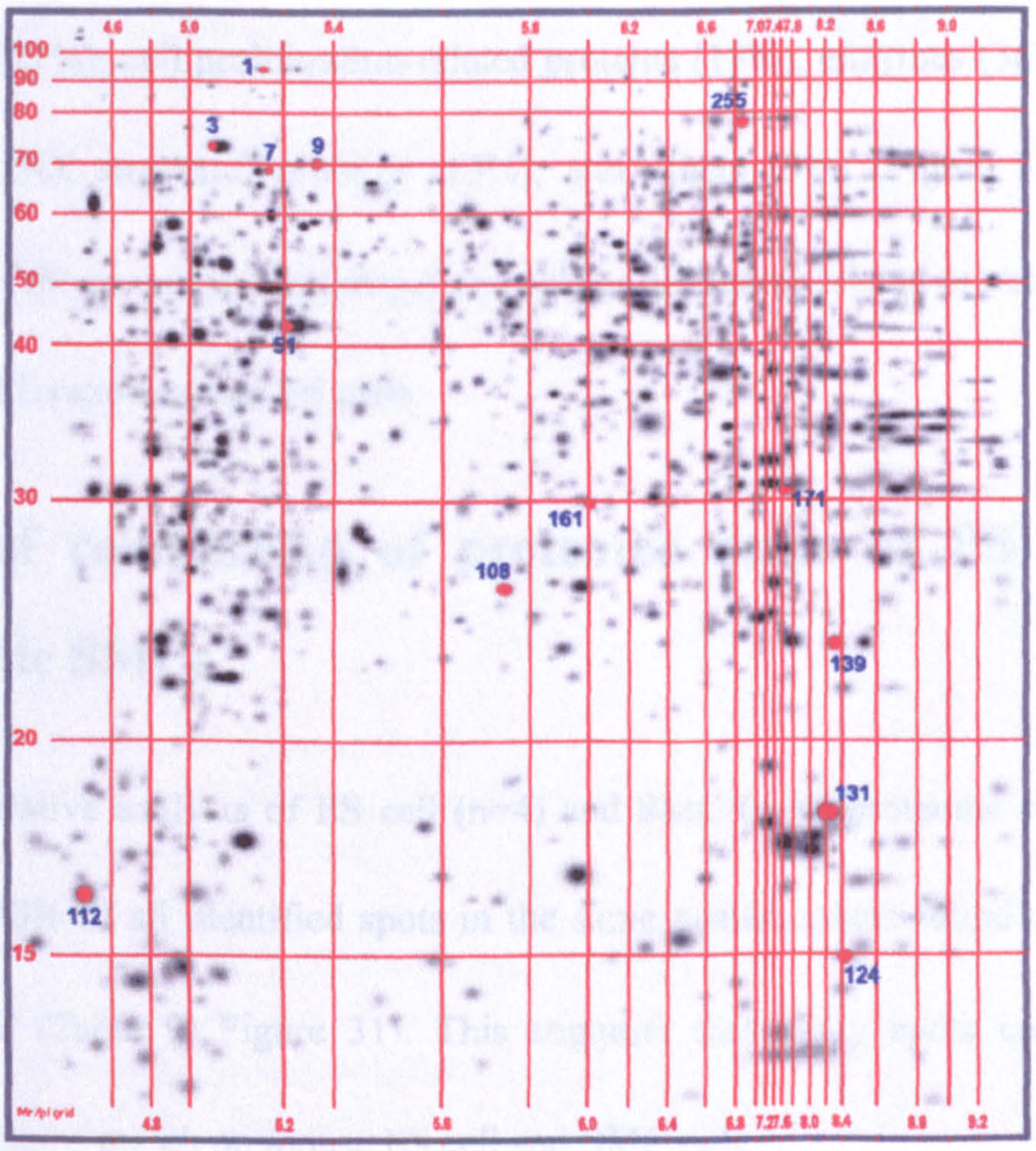

Figure 29. The Mr/pI grid picture of ES cell proteome map was generated by PDQuest software, assuming that the observed Mr/pI of red spots were equal to the calculated value. The observed Mr/pI of other spots were read from this grid. Blue numbers are the spots numbers as in Table 13 (see Appendix).

Figure 30. ES cell proteins category pie chart

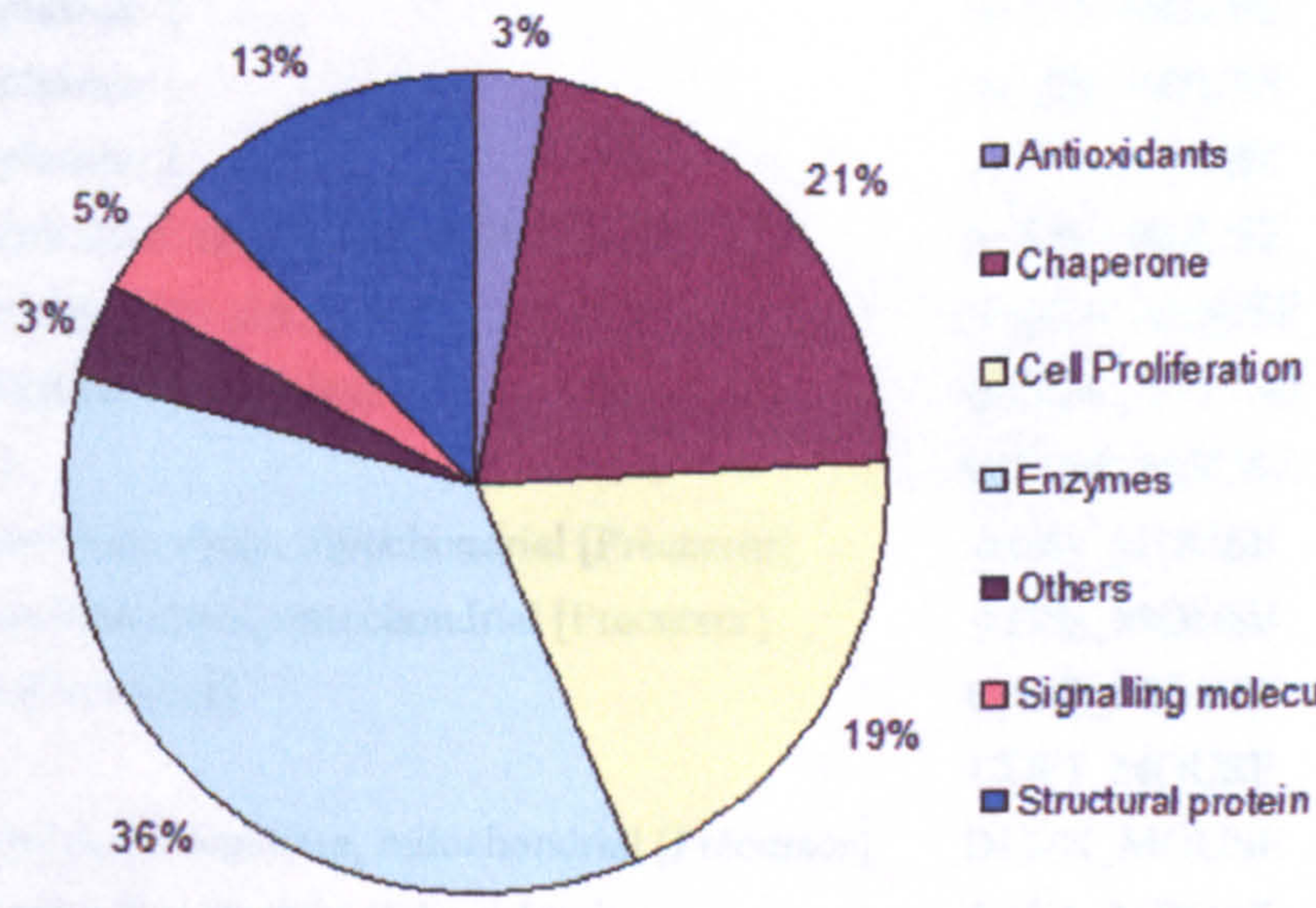

Figure 30. Proteins category pie chart showed that enzymes, chaperones and cell proliferation-related proteins are most abundant proteins species in ES cells.

All 231 identified proteins were classified into 7 categories, antioxidants (3%), chaperones (21%), cell proliferation-related proteins (19%), enzymes (36%), signalling molecules (5%), structural proteins (13%), and others (3%) (Figure 30). The large proportion of the enzymes, chaperones and cell proliferation-related proteins may due to the high proliferation rate of ES cells.

3.2.2 Brief comparison of proteome maps of ES cells and aortic SMCs

Comparative analysis of ES cell (n=4) and SMC (n=4) proteome map were also performed. 30% of all identified spots in the same position were found containing the same protein (Table 9, Figure 31). This suggests that many spots containing high abundant proteins match on mouse ES cell and SMC gels.

Table 9. Co-localization of proteins between ES cell and SMC maps

No	Protein Name	UniProt Entry Name	* SMC map No.	ES cell map No.
A1	Actin, cytoplasmic 2	ACTG_MOUSE	50	50
A2	Actin, cytoplasmic 1	ACTB_MOUSE	48	55
A3	Actin, cytoplasmic 1	ACTB_MOUSE	83	97
A4	Actin, cytoplasmic 2	ACTG_MOUSE	50	52
A5	Aconitate hydratase, mitochondrial [Precursor]	ACON_MOUSE	199	256
A6	Fructose-bisphosphate aldolase A	ALDOA_MOUSE	187	191
A7	Fructose-bisphosphate aldolase A	ALDOA_MOUSE	188	192
A8	Annexin A2	ANXA2_MOUSE	165	176
A9	ATP synthase alpha chain, mitochondrial [Precursor]	ATPA_MOUSE	197	229
A10	ATP synthase beta chain, mitochondrial [Precursor]	ATPB_MOUSE	32	36
C1	Calreticulin [Precursor]	CALR_MOUSE	17	27
C2	Cofilin-1	COF1_MOUSE	124	131
D	Dihydrolipoyl dehydrogenase, mitochondrial [Precursor]	DLDH_MOUSE	229	230
E1	Electron transfer flavoprotein alpha-subunit, mitochondrial [Precursor]	ETFA_MOUSE	168	169
E2	Endoplasmin [Precursor]	ENPL_MOUSE	3	2

E3	Alpha-enolase	ENOA_MOUSE	249	210
F1	Far upstream element binding protein 1	FUBP1_MOUSE	204	246
F2	Far upstream element binding protein 2	FUBP2_RAT	200	255
G1	78 kDa glucose-regulated protein [Precursor]	GRP78_MOUSE	5	4
G2	Glutamate dehydrogenase, mitochondrial [Precursor]	DHE3_MOUSE	240	227
G3	Glyceraldehyde 3-phosphate dehydrogenase	G3P_MOUSE	164	177
G4	Glyceraldehyde 3-phosphate dehydrogenase	G3P_MOUSE	163	178
G5	Guanine nucleotide-binding protein subunit beta2-like 1	GBLP_HUMAN	169	171
H1	Heat shock cognate 71 kDa protein	HSP7C_MOUSE	45	47
H2	Heat shock cognate 71 kDa protein	HSP7C_MOUSE	7	9
H3	Heat shock cognate 71 kDa protein	HSP7C_MOUSE	11	21
H4	Heat shock cognate 71 kDa protein	HSP7C_MOUSE	153	156
H5	47 kDa heat shock protein [Precursor]	HSP47_MOUSE	192	216
H6	60 kDa heat shock protein, mitochondrial [Precursor]	CH60_MOUSE	219	63
H7	Heat-shock protein beta-1	HSPB1_MOUSE	144	145
H8	Heterogeneous nuclear ribonucleoprotein L	HNRPL_MOUSE	231	244
H9	Heterogeneous nuclear ribonucleoproteins A2/B1	ROA2_MOUSE	160	179
I	Inosine-5'-monophosphate dehydrogenase 2	IMDH2_MOUSE	237	234
L	LIM and SH3 domain protein 1	LASP1_MOUSE	183	183
N1	NASCENT polypeptide associated complex alpha subunit	NACA_MOUSE	68	70
N2	Nucleoside diphosphate kinase B	NDKB_MOUSE	127	127
O	Ornithine aminotransferase, mitochondrial [Precursor]	OAT_MOUSE	220	64
P1	Peptidyl-prolyl cis-trans isomerase A	PPIA_MOUSE	122	129
P2	Peptidyl-prolyl cis-trans isomerase A	PPIA_MOUSE	125	128
P3	40 kDa peptidyl-prolyl cis-trans isomerase	PPID_MOUSE	256	188
P4	Peroxiredoxin 1	PRDX1_MOUSE	136	139
P5	3-phosphoglycerate dehydrogenase	Q8C603_MOUSE	215	219
P6	Phosphoglycerate kinase 1	PGK1_MOUSE	190	207
P7	Phosphoglycerate mutase 1	PGAM1_MOUSE	151	154
P8	Poly(rC)-binding protein 1	PCBP1_MOUSE	259	186
P9	Profilin I	PROF1_MOUSE	120	124
P10	Prohibitin	PHB_MOUSE	85	86
P11	26S protease regulatory subunit 8	PRS8_MOUSE	253	213
P12	Pyruvate kinase, M2 isozyme	KPYM_MOUSE	235	237
S1	Stress-70 protein, mitochondrial [Precursor]	GRP75_MOUSE	9	11
S2	Superoxide dismutase [Cu-Zn]	SODC_MOUSE	114	120
S3	Superoxide dismutase [Mn], mitochondrial [Precursor]	SODM_MOUSE	138	138
T1	T-complex protein 1 subunit beta	TCPB_MOUSE	217	218
T2	Transgelin 2	TAGL2_MOUSE	133	137
T3	Transketolase	TKT_MOUSE	233	245
T4	Translationally controlled tumour protein	TCTP_MOUSE	102	103
T5	Triosephosphate isomerase	TPIS_MOUSE	140	150
V	Voltage-dependent anion-selective channel protein 1	VDAC1_MOUSE	158	172

* The SMC No. come from the mouse arterial SMC map (Mayr, Mayr et al. 2005).

Figure 31. Overlay of SMC and ES cell 2-DE average gels

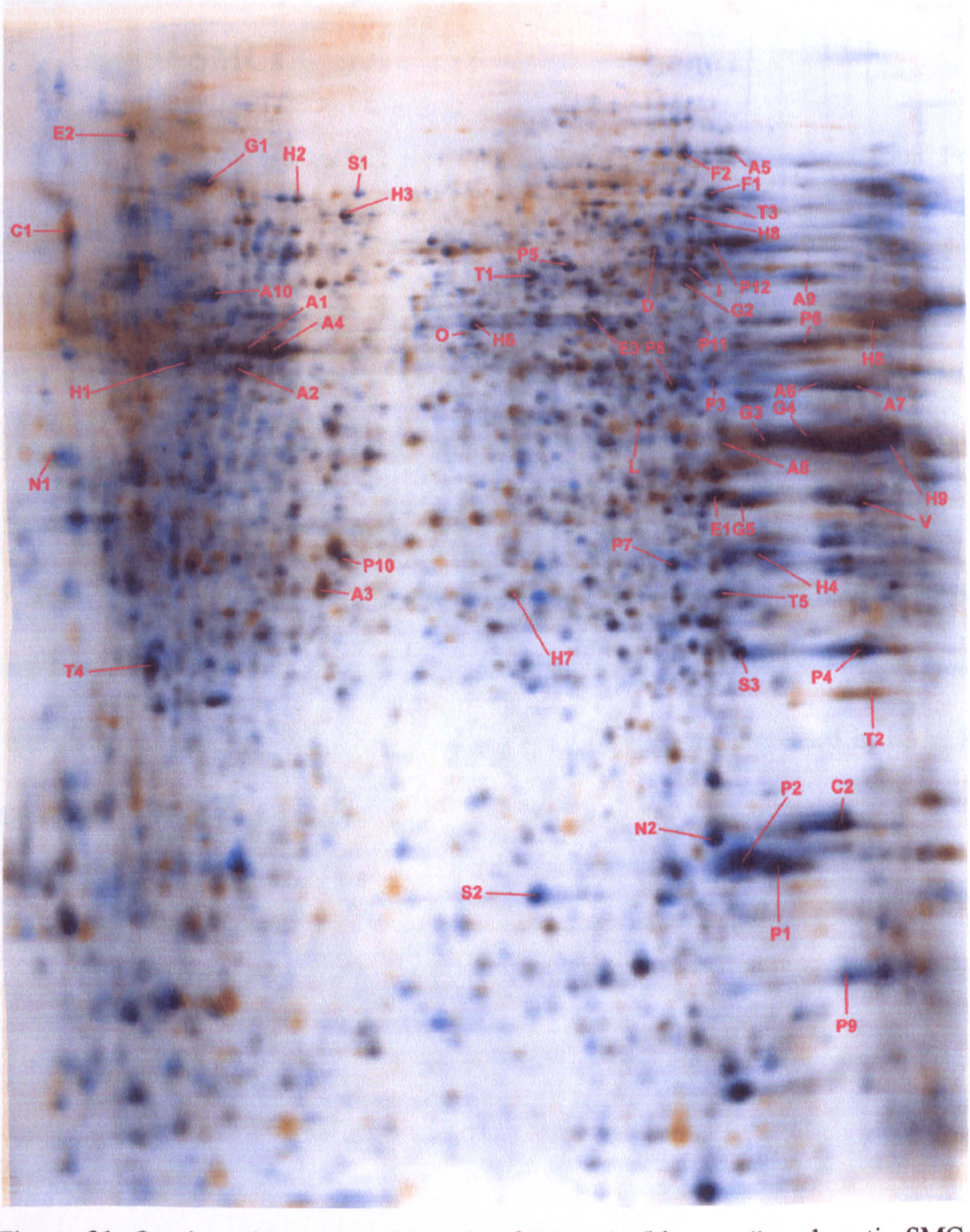

Figure 31. Overlay of average 2-DE gels of ES cells (blue, n=4) and aortic SMCs (orange, n=4) were generated by ProteomWeaver software. Matched proteins with similar expression are shown in black colour. Labelled spots were identified and revealed identical proteins in both cell lines, listed in Table 9, indicating the consistency of these proteins.

3.2.3 Differentially expressed proteins between ES cells and aortic SMCs

Immunoblotting was carried out to verify differences in protein expression. For each protein, at least 2~3 Western blots were run with different cell lysates for comparison of protein expression between ES cells and aortic SMCs. Results showed that most heat shock proteins were more abundant in ES cells, e.g. HSP27, HSP60, and HSP90. However, crystallin α/β (HSP20), which is known to regulate actin polymerization, was expressed at higher levels in SMCs (Figure 32). Another significant difference between these two cells is the antioxidants. The main oxidants such as catalase, peroxiredoxin 1 (PRX-1) and Cu-Zn superoxide dismutase (SOD-1) were all upregulated in ES cells while heme oxygenase 1 (HO-1) was decreased in ES cells compared to aortic SMCs (Figure 32).

Figure 32. Western blot comparison of protein expressions between ES cells and SMCs.

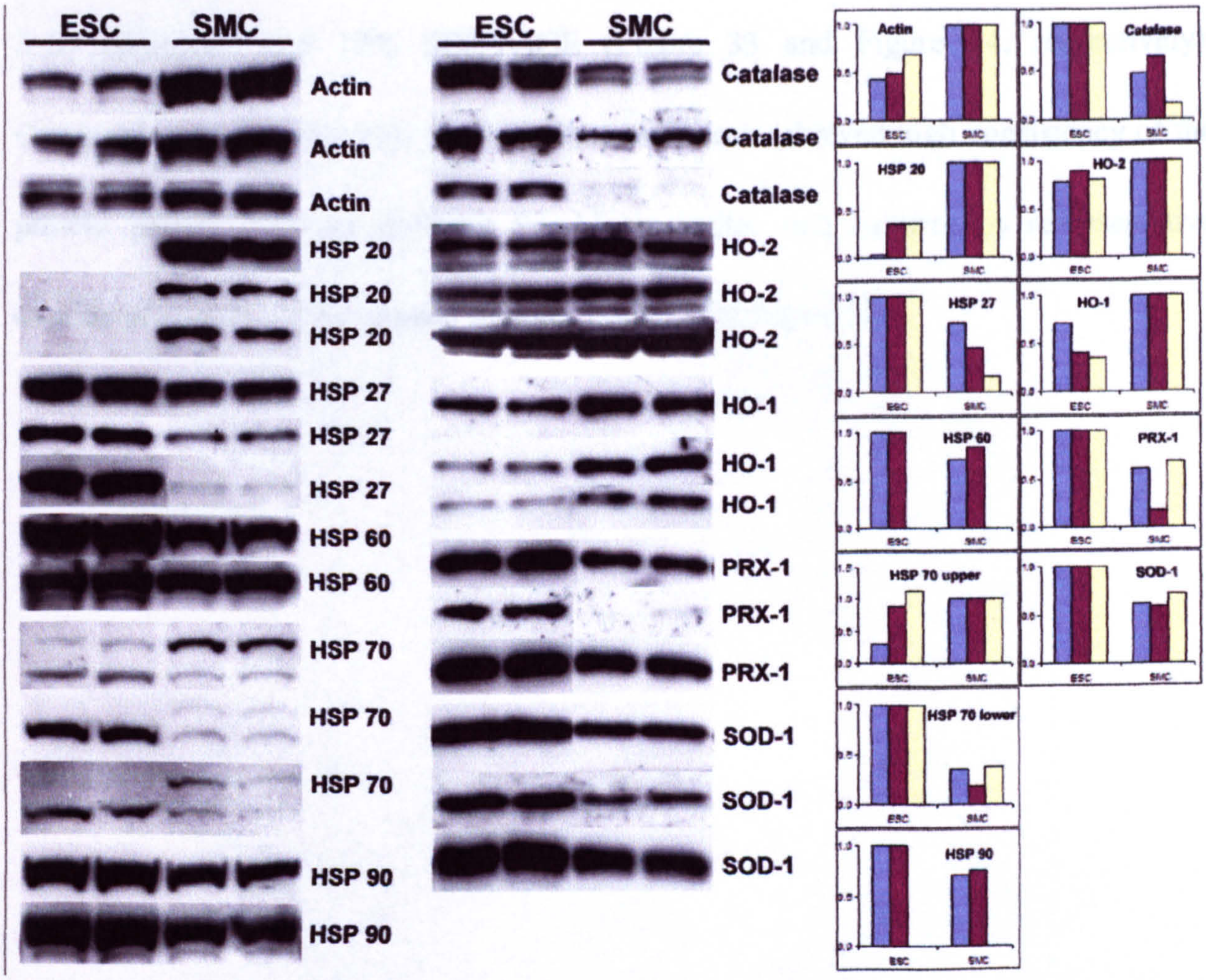

Figure 32. (A) Most heat shock proteins were upregulated in ES cells. However, crystallin α/β (HSP20) is expressed at higher levels in SMCs because of the regulation role in actin polymerization. Higher expressions of antioxidants (catalase, peroxiredoxin 1 and SOD-1) were observed in ES cells, indicating altered oxidative stress in ES cells. (B) Bar graph show clear differences of the protein expressions between the two cells. The relative average intensity (Y-axis) of each sample in each blot was calculated by normalizing with the average of the stronger sample band of all blots. (**HSP**, heat shock protein; **HO**, heme oxygenase; **PRX**, peroxiredoxin; **SOD**, superoxide dismutase)

3.3 Proteome map of Sca-1$^+$ cells

3.3.1 Sca-1$^+$ cell proteome map

After isolation from primitive differentiation culture by magnetic labelling cell sorting, Sca-1$^+$ progenitor cells were cultured in gelatine-coated flasks for 15 passages

and harvested for 2-DE. Protein samples were separated before and after using a clean-up kit (Bio-Rad) and separated by isoelectric focusing on 18cm dry strips (pH 3-10 nonlinear) and 12% SDS-PAGE (Figure 33 and Figure 34, respectively). Comparison of different gels (n=4) by ProteomWeaver showed high consistency of the protein pattern between different Sca-1$^+$ progenitor cell cultures. A representative overlay picture of unprecipitated samples is shown as Figure 35.

Figure 33. Proteome map of Sca-1^{+} progenitor cells

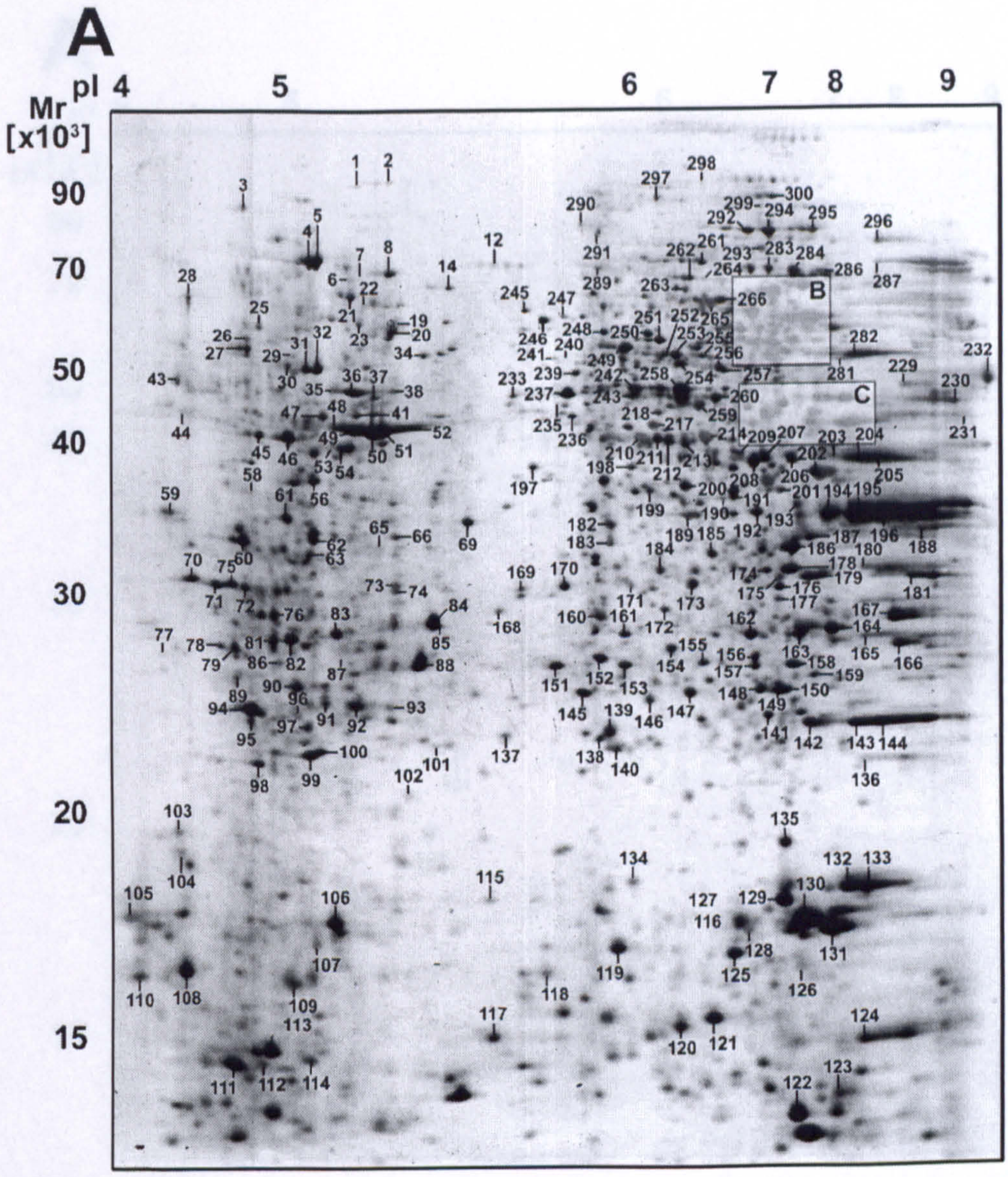

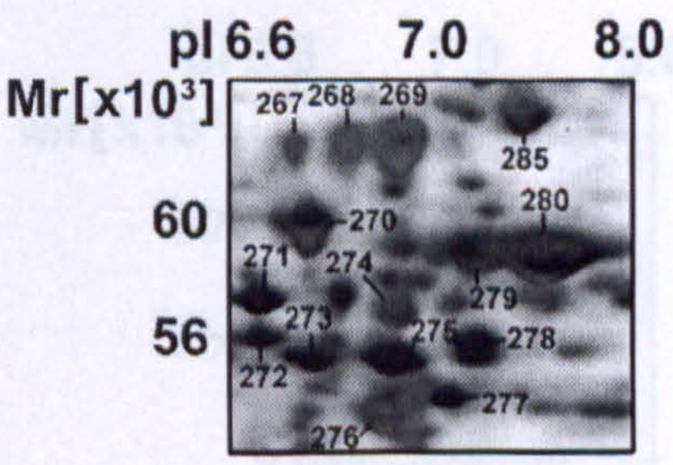

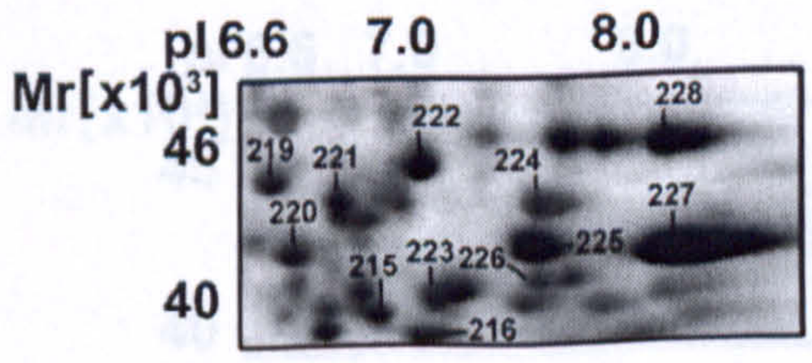

Figure 33. 400 μg of protein extract was separated on a pH 3-10NL IPG strip, followed by a 12% SDS polyacrylamide gel. Protein spots were visualized by silver staining. Labelled spots were picked for protein identification (A). The highlighted areas are enlarged in inset B and C.

Figure 34. Proteome map of Sca-1^{+} progenitor cells after using clean-up kit

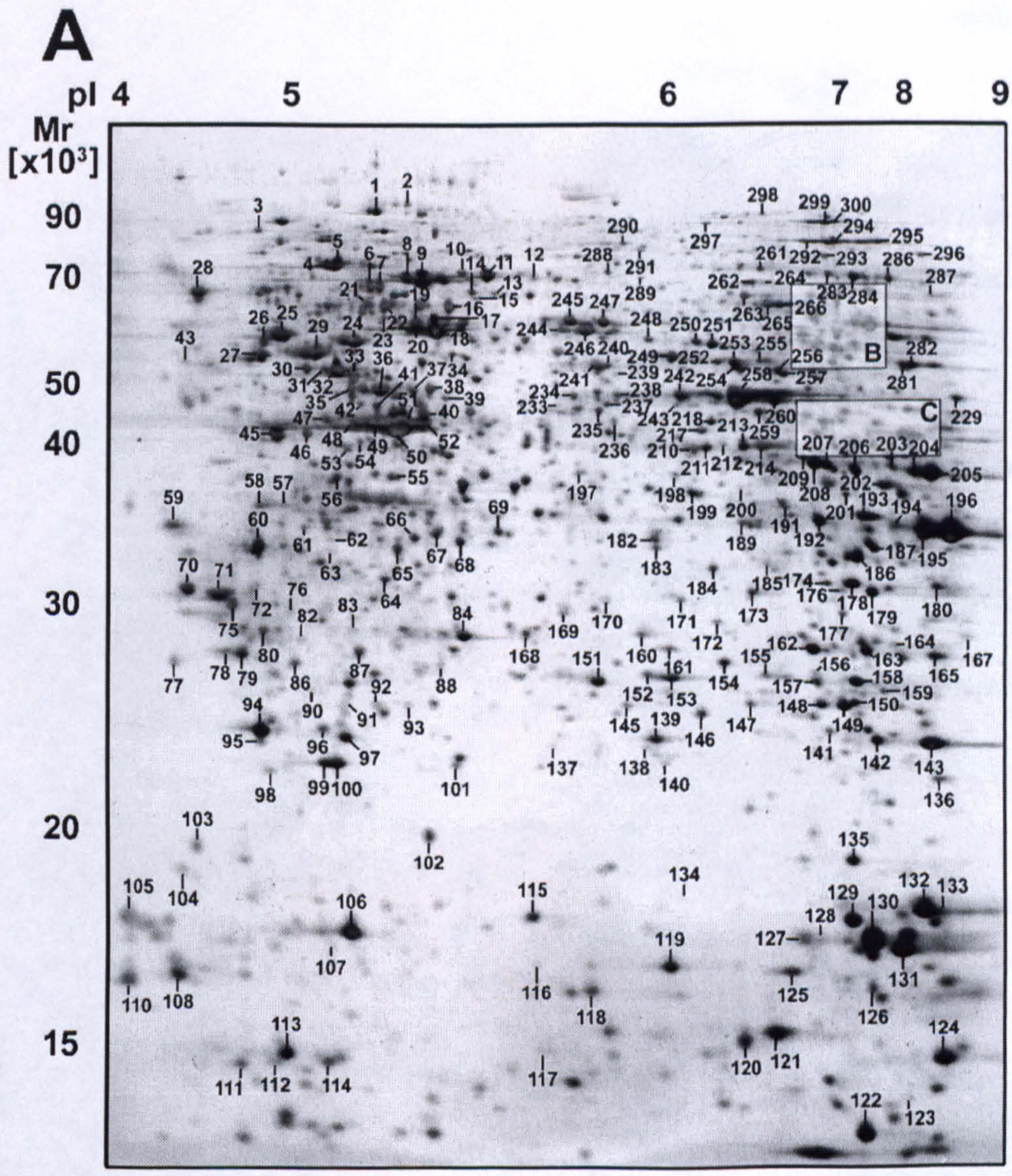

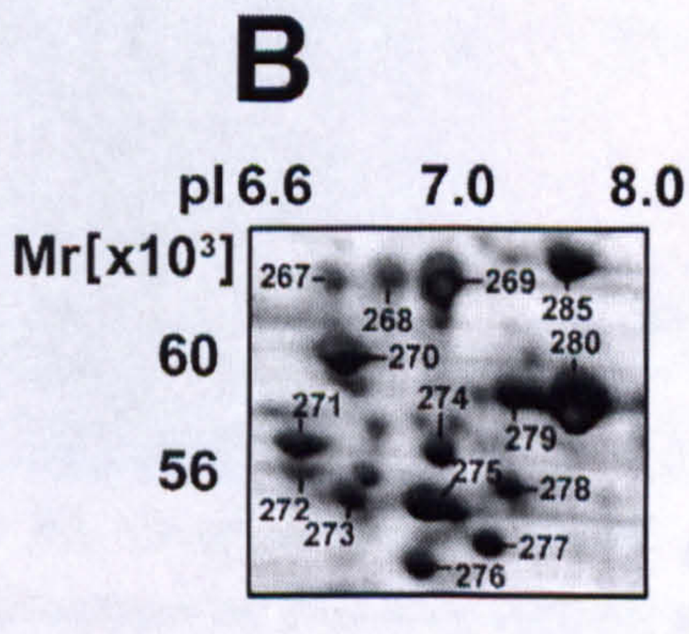

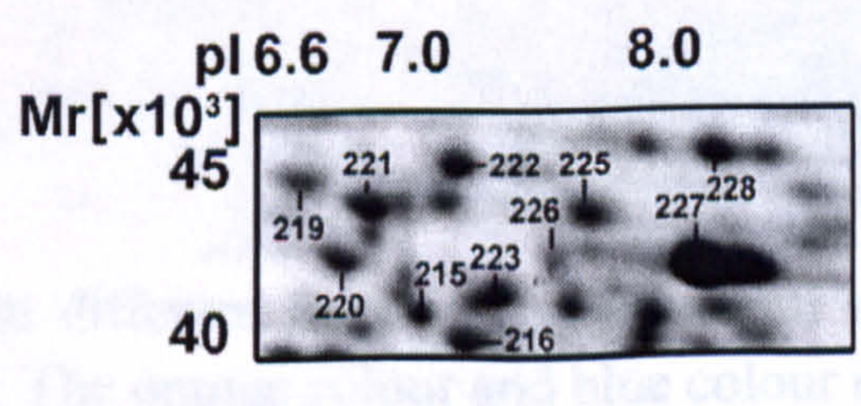

Figure 34. 400 µg of protein extract was treated with clean-up kit (Bio-Rad) and separated on a pH 3-10NL IPG strip, followed by a 12% SDS polyacrylamide gel. Protein spots were visualized by silver staining. Labelled spots were picked for protein identification (A). The highlighted areas are enlarged in inset B and C.

Figure 35. Overlay picture of two 2-DE gels of Sca-1$^+$ progenitor cells

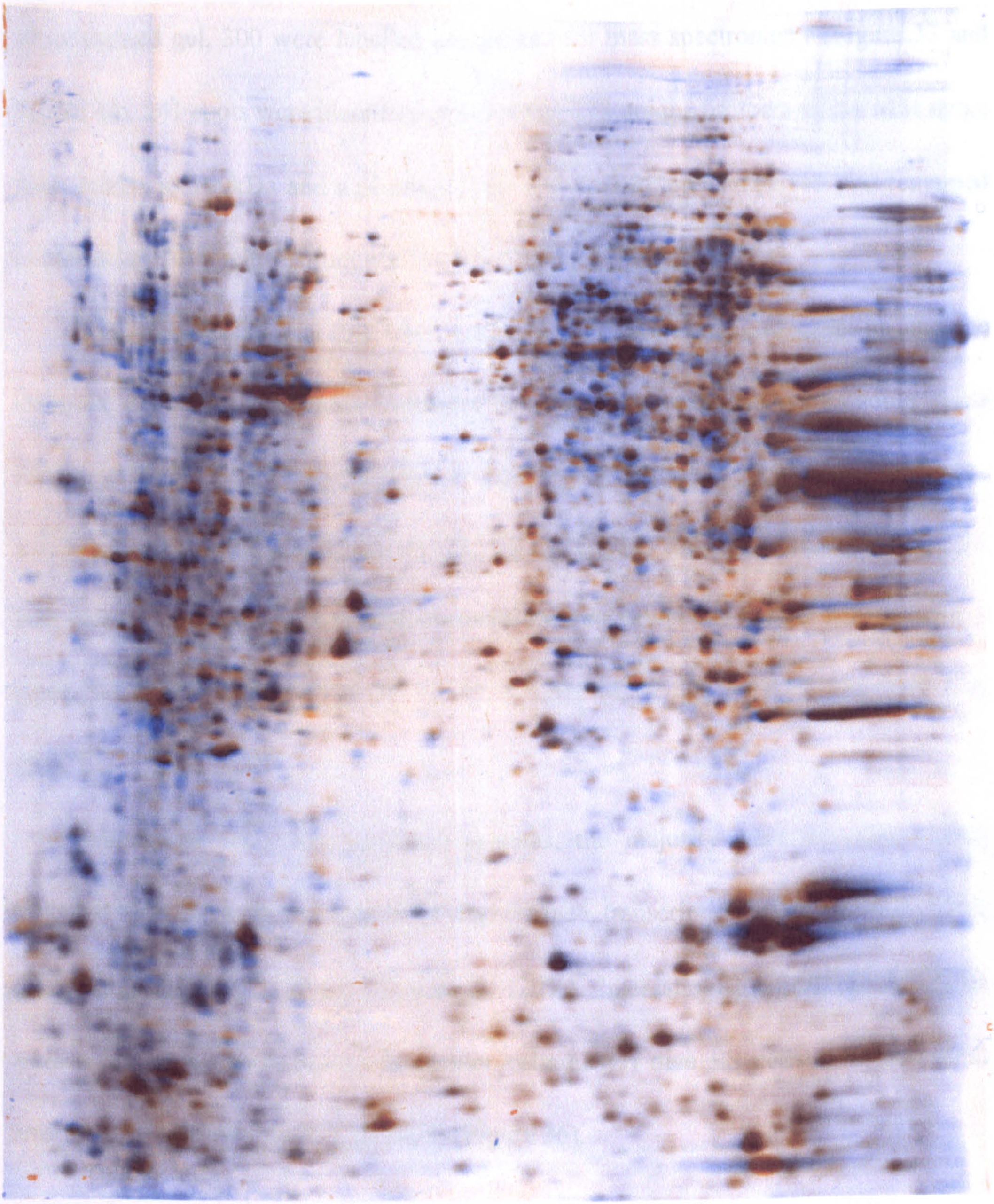

Figure 35. Overlay of two 2-DE gels from different Sca-1$^+$ progenitor cell samples were generated by ProteomWeaver software. The orange colour and blue colour indicate protein spots on different gels. Matched proteins with similar expression are shown in black colour.

From approximately 2000 spots that were resolved on a single large format silver-stained gel, 300 were labelled and picked for mass spectrometry (Figure 33 and Figure 34). 241 spots were identified representing 173 unique proteins with a MM range from 10kDa to 100kDa and a pI range from 4 to 9. Fifty-nine spots (19.7%) remained unidentified. All identifications are listed in Table 14 (see Appendix).

Overall, the spot patterns were very similar before and after clean-up and the clean-up procedure prevented streaking in the basic area. However, some spots disappeared after using the clean-up kit, mainly in the basic region (pI >8) and in the lower left corner of the gel (spots 44, 73, 74, 81, 85, 89, 109, 144, 166, 175, 181, 188, 190, 224, 230-232), while additional spots became detectable in the treated sample (spots 9-11, 13, 15-18, 24, 33, 39, 40, 42, 55, 57, 64, 67, 68, 80, 116, 234, 238, 244, 288).

Among the total 241 identified proteins, the majority were enzymes (33%), followed by proteins involved in DNA maintenance, transcription and translation (18%), structural proteins (13%) and chaperones (20%). Interestingly, signalling molecules were more abundant in Sca-1^+ progenitor cells (10%) than ES cells (5%) and adult arterial SMCs (Mayr, Mayr et al. 2005) (Figure 36).

Figure 36. Sca-1$^+$ cell proteins category pie chart

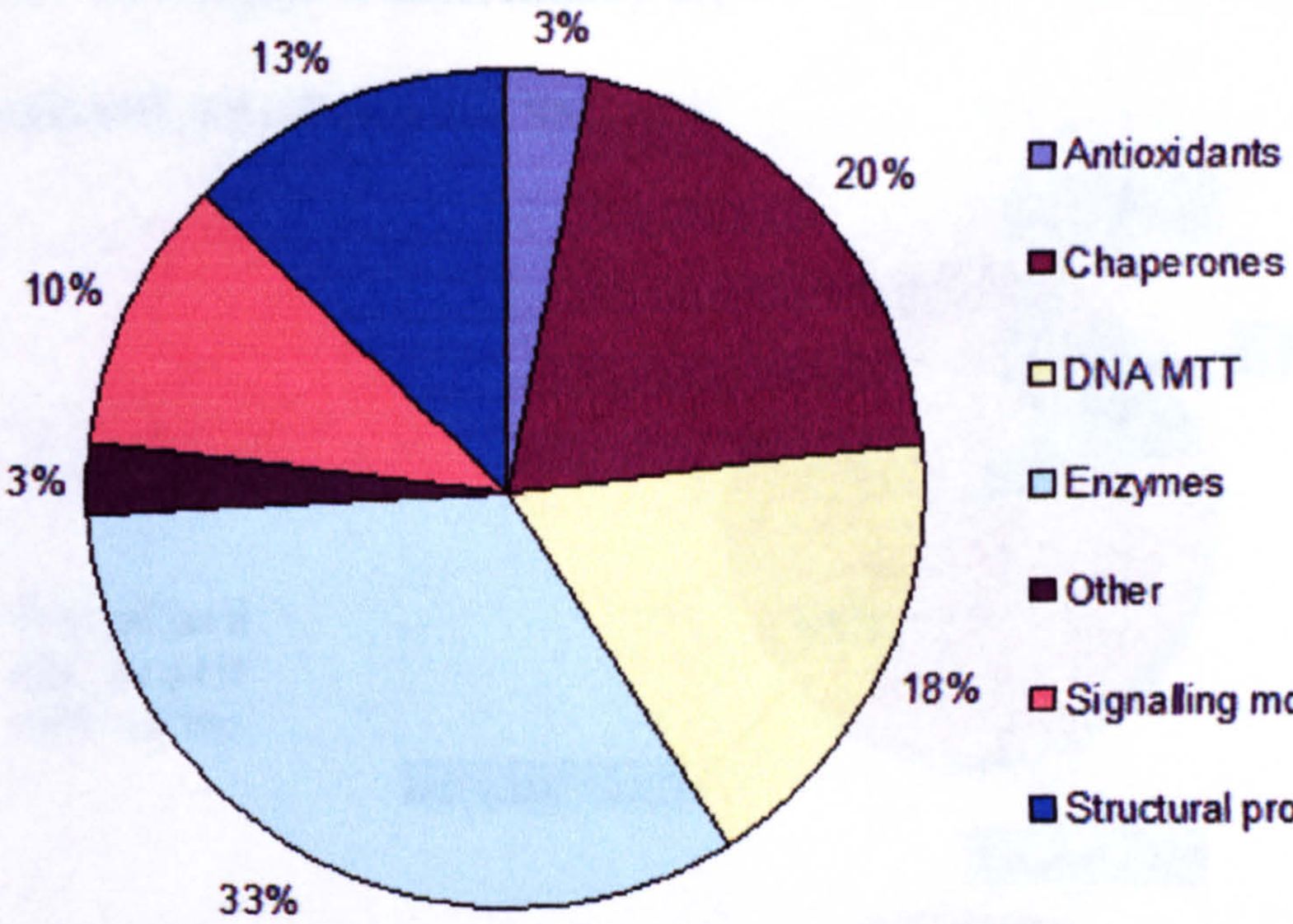

Figure 36. Proteins category pie chart showed that enzymes, chaperones and cell proliferation-related proteins are most abundant proteins species in Sca-1$^+$ cells.

A direct comparison of the protein profile of Sca-1$^+$ progenitor cells (n=4) with ES cells (n=4) and arterial SMCs (n=4) revealed that the percentage of differentially expressed spots (2 fold increased or decreased) was higher between arterial SMCs and Sca-1$^+$ progenitor cells indicating that the proteome of Sca-1$^+$ progenitor cells remained more similar to ES cells than arterial SMCs (Figure 37).

Figure 37. Percentage of differentially expressed spots in Sca-1$^+$ progenitor cell gels compared with ES cell gels and SMC gels

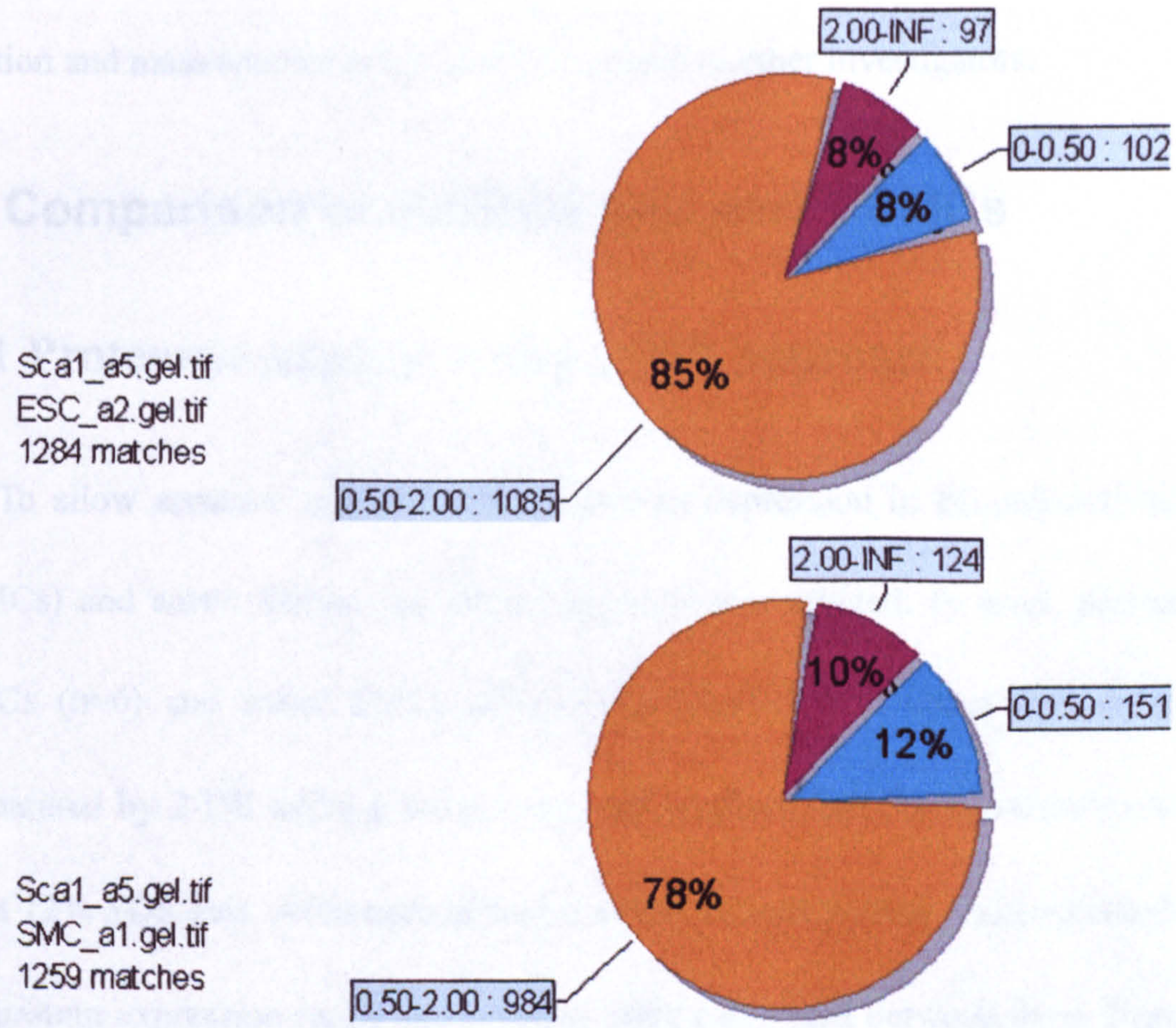

Figure 37. 2-DE gel images from Sca-1$^+$ progenitor cells (n=4), ES cells (n=4) and SMCs (n=4) were imported into the ProteomWeaver software. Average gels were created from 4 single gels per group. Pie charts show the percentage of protein spots with 2 fold increased and decreased protein expression between Sca-1$^+$ progenitor cells and ES cells (A) and between Sca-1$^+$ progenitor cells and SMCs (B).

3.3.2 Data presentation on the internet

I maintain a website at http://www.vascular-proteomics.com using Apache/ PHP/ MySQL, for our group presenting protocols, proteome maps, protein identifications, publications along with maps from mouse aortic SMCs (Mayr, Mayr et al. 2005) and other vascular cells (McGregor, Kempster et al. 2001; Dupont, Corseaux et al. 2005) published by other groups. The protein identifications were all saved in the MySQL database. After the users inquired the database through PHP language, the result was

displayed by Apache web server. The "SEARCH SPOTS" function allows the comparison of proteins across different maps and the detailed methods for 2-DE, tryptic digestion and mass spectrometry should be useful to other investigators.

3.4 Comparison of esSMCs and aortic SMCs

3.4.1 Proteomic analysis using DIGE approach

To allow accurate quantification of protein expression in ES cell-derived SMCs (esSMCs) and aortic SMCs, the DIGE approach was utilized. In brief, proteins from esSMCs (n=6) and aortic SMCs (n=2) were labelled with either Cy3 or Cy5 and co-separated by 2-DE using a broad range pH gradient (pH 3-10 nonlinear) and large format 12% SDS gels. After normalization to the internal pooled standard labelled with Cy2, protein expression ratios and p values were calculated between these 2 groups by DeCyder software. Totally there were 146 spots showed a significant ($p < 0.05$) 2 fold change. A representative image with labelled numbers was shown as Figure 38. Among these, 128 spots (88%) were successfully identified by MALDI-ToF MS or LC MS/MS and listed in Table 15 (see Appendix). Because ES cells were cultured in complete stem cell medium to keep an undifferentiated stage, they were not included in present comparison.

While cytoskeletal/myofilament proteins and calcium binding proteins were less abundant in esSMCs than in aortic SMCs, chaperones such as heat shock proteins were increased along with proteins regulating DNA maintenance, transcription and translation. Notably, upregulation of the cytosolic antioxidant peroxiredoxin 6 (spot 50)

coincided with a downregulation of mitochondrial manganese SOD (SOD-2, spot 77, 78) in esSMCs.

Figure 38. A representative DIGE image of esSMCs and aortic SMCs

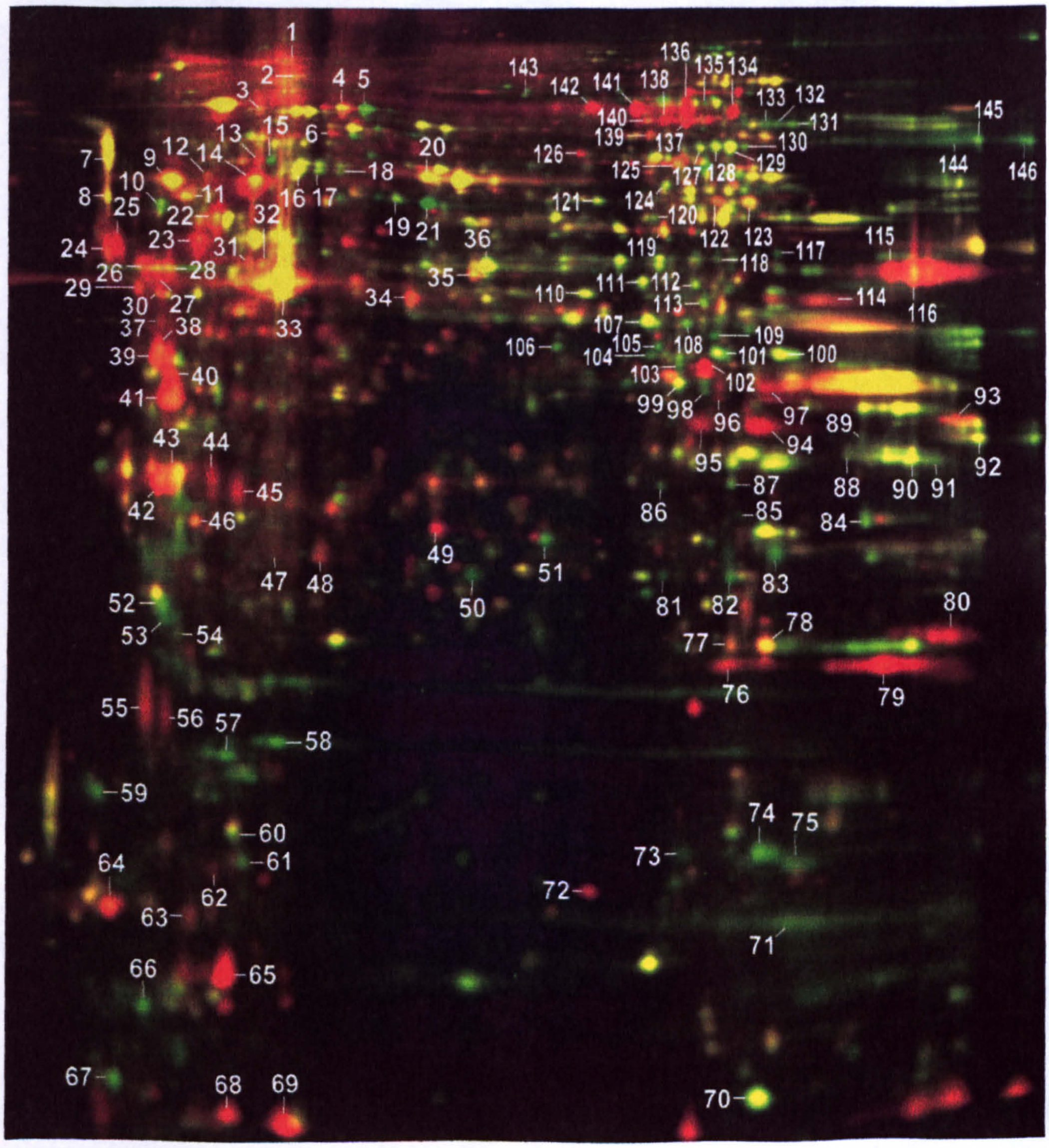

Figure 38. esSMCs (green, n=6) and aortic SMCs (red, n=2) were compared using the DIGE approach. In the representative gel, protein lysates of esSMCs and aortic SMCs were labelled with Cy3 and Cy5, respectively and co-separated in large format 2-DE gels. Images were acquired on a fluorescence scanner and analyzed by DeCyder software. Spots with 2 fold increase or decrease ($p < 0.05$) between esSMCs and aortic SMCs were numbered, picked and identified by mass spectrometry.

Figure 39. An illustration of DeCyder software

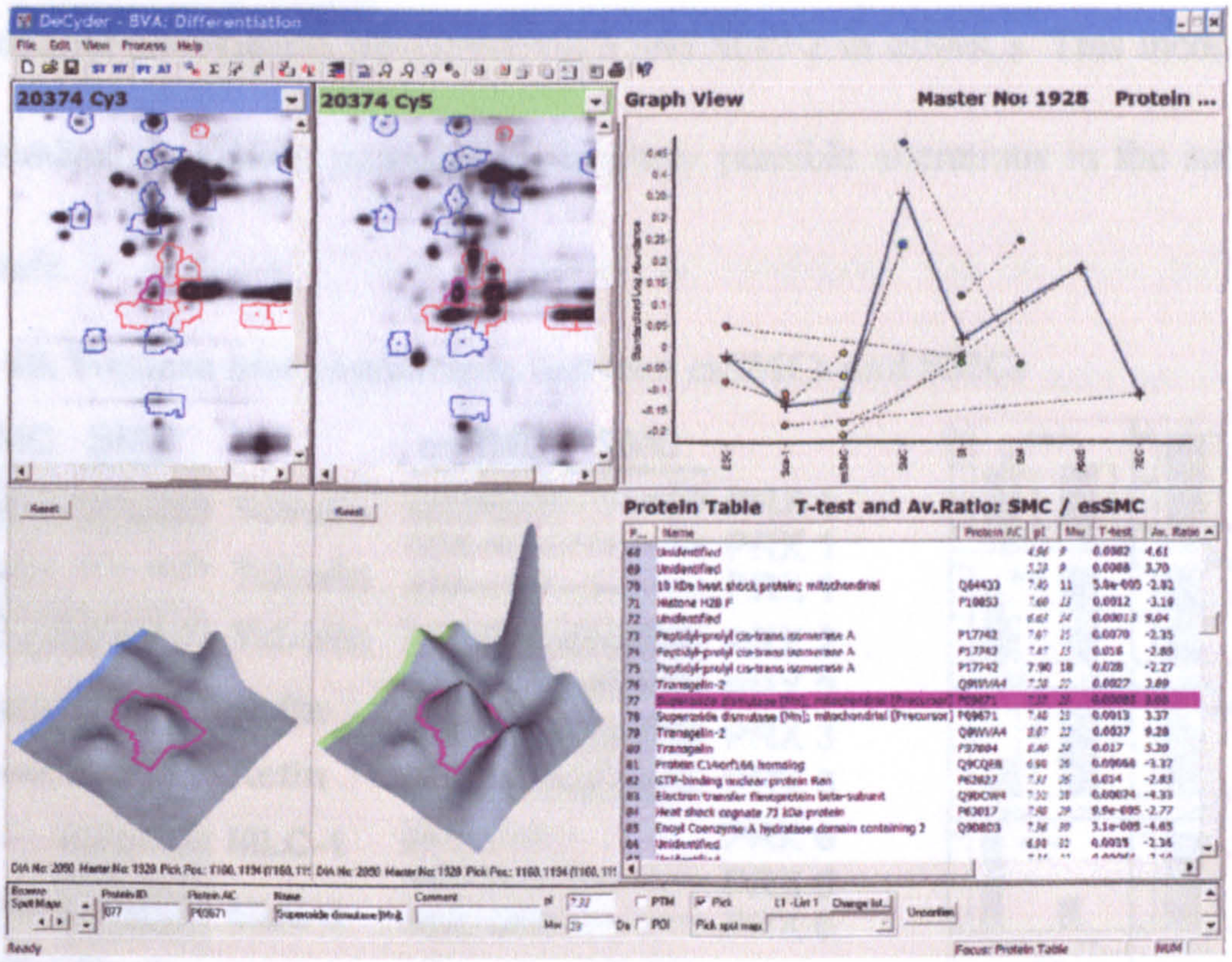

Figure 39. An illustration of the DeCyder software. Protein expression increases (red circle) and decreases (blue circle) in SMCs compared to esSMCs are shown in the top-left panel on selected gels. The intensity of the protein spot in each gel is shown as one spot in the top-right panel. There are 6 spots in esSMCs group (yellow) and 2 spots in SMCs group (blue). Y-axis is the standardized log abundance compared to the internal pool standard. The average abundance of each group is shown as a cross (+) and connected by the blue line. A 3-D comparison of selected spot is shown in the bottom-left panel. The selected spot (purple circle) is SOD-2 with a 3.06 fold increase in SMCs compare to esSMCs, p=0.00083, as shown in the bottom-right panel.

3.4.2 Confirmation of differentially expressed proteins

Some protein changes between esSMCs and aortic SMCs were verified by immunoblotting (Figure 40). For each protein, at least 2~3 Western blots were run with different cell lysates for comparison of protein expression between esSMCs and aortic SMCs. Cytoskeletal/myofilament proteins (actin, α-tubulin and myosin light chain) were less abundant in esSMCs than in aortic SMCs, while most chaperones were increased except crystallin α/β (HSP20). Notably, upregulation of the cytosolic

antioxidant peroxiredoxin 1, 2, 6 and SOD-1 were accompanied by downregulation of mitochondrial antioxidants peroxiredoxin 3 and SOD-2 in esSMCs. This inconsistency in antioxidant expression prompted us to study possible alterations in the subcellular redox state.

Figure 40. Western blot comparison between esSMCs and SMCs

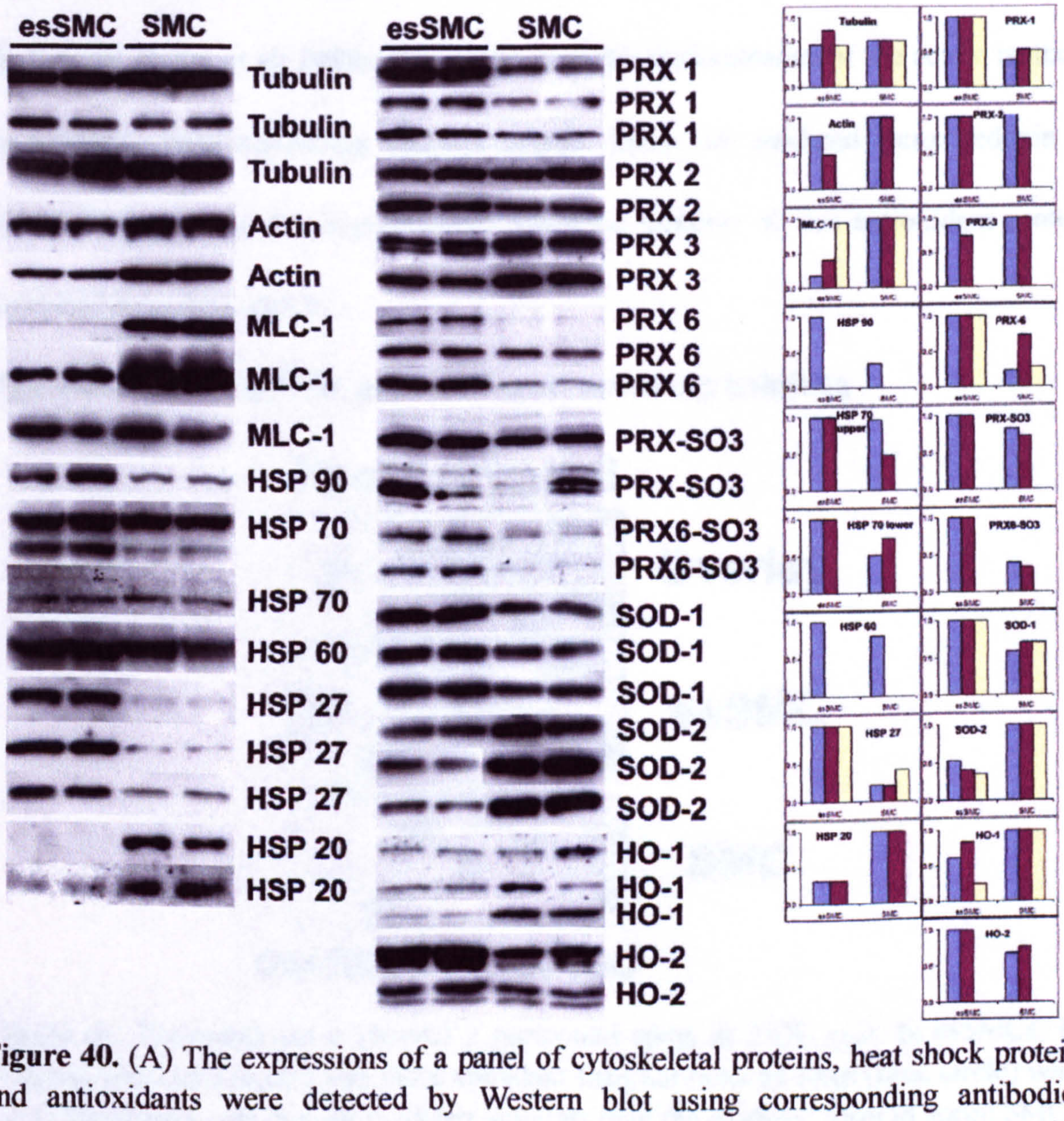

Figure 40. (A) The expressions of a panel of cytoskeletal proteins, heat shock proteins and antioxidants were detected by Western blot using corresponding antibodies. esSMCs showed decreased cytoskeletal proteins but increased heat shock proteins. Cytosolic antioxidants were increased in esSMCs but mitochondrial counterparts were decreased. (B) Bar graph showing clear differences of the protein expressions between these two cells. Relative average intensity (Y-axis) of each sample in each blot was calculated by normalizing with the average of the stronger sample bans of all blots. (**MLC**, myosin light chain; **HSP**, heat shock protein; **PRX**, peroxiredoxin; **PRX-SO3**, oxidized peroxiredoxin; **PRX6-SO3**, oxidized peroxiredoxin 6; **SOD**, superoxide dismutase; **HO**, heme oxygenase)

Besides revealing differences in protein expression, 2-DE gel also has the potential to display differences in posttranslational modifications. Peroxiredoxin 6 was encountered as doublet spots in 2-DE (Figure 41). The over-oxidation of peroxiredoxin 6 is likely to be irreversible under biological conditions and *de novo* synthesis is required to counteract the annihilation of the peroxiredoxin-based antioxidant defence (Rabilloud, Heller et al. 2002). Consistent with the predominance of the acidic isoform in esSMCs, immunoblotting showed higher levels of oxidized peroxiredoxin 6 (PRX6-SO3) (Figure 40), indicating an increased turnover of this antioxidant protein compared to mature SMCs.

Figure 41. Overlay of 2-DE gels showing peroxiredoxin 6 shifting

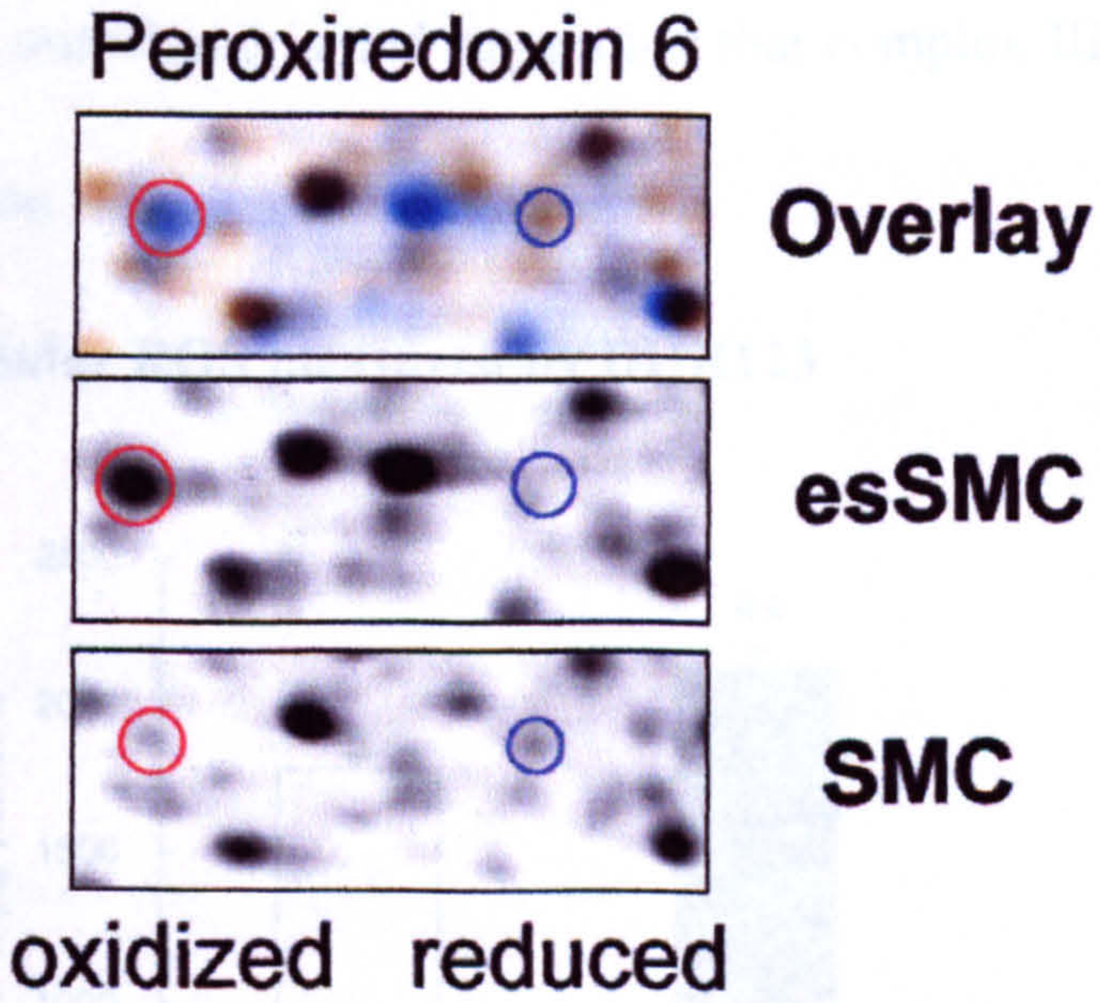

Figure 41. Peroxiredoxin 6 showed 2 horizontal spots in 2-DE gels. In esSMCs, the oxidized form (red circle) was more abundant than the reduced form (blue circle) while the reduced form was present in higher amounts than the oxidized form in aortic SMCs.

3.4.3 ROS production

We therefore quantified total ROS and mitochondrial superoxide production by DHR123 and MitoSOX staining, respectively. Consistent with the increased oxidation

of redox-sensitive proteins in esSMCs, the fluorescent signal intensity for DHR123 was higher in esSMCs compared to aortic SMCs (2133 ± 50 RFU/μg protein, n=3 vs. 1782 ± 64 RFU/μg protein, n=3, p=0.002) (Figure 42). Notably, the increase in total ROS production was accounted for by a rise in mitochondrial superoxide production as indicated by a corresponding increase in MitoSOX staining. To further clarify the site of ROS generation, we treated SMCs with rotenone and antimycin A, a mitochondrial complex I and III inhibitor, respectively. Antimycin A but not rotenone augmented mitochondrial superoxide and total ROS formations in esSMCs, but did not substantially alter the fluorescent signal of aortic SMCs (Figure 43), providing additional proof that the observed increase in oxidative stress in esSMCs is predominantly from mitochondria and suggesting that complex III acts as the principal site of ROS generation.

Figure 42. Total cellular ROS measured by DHR123

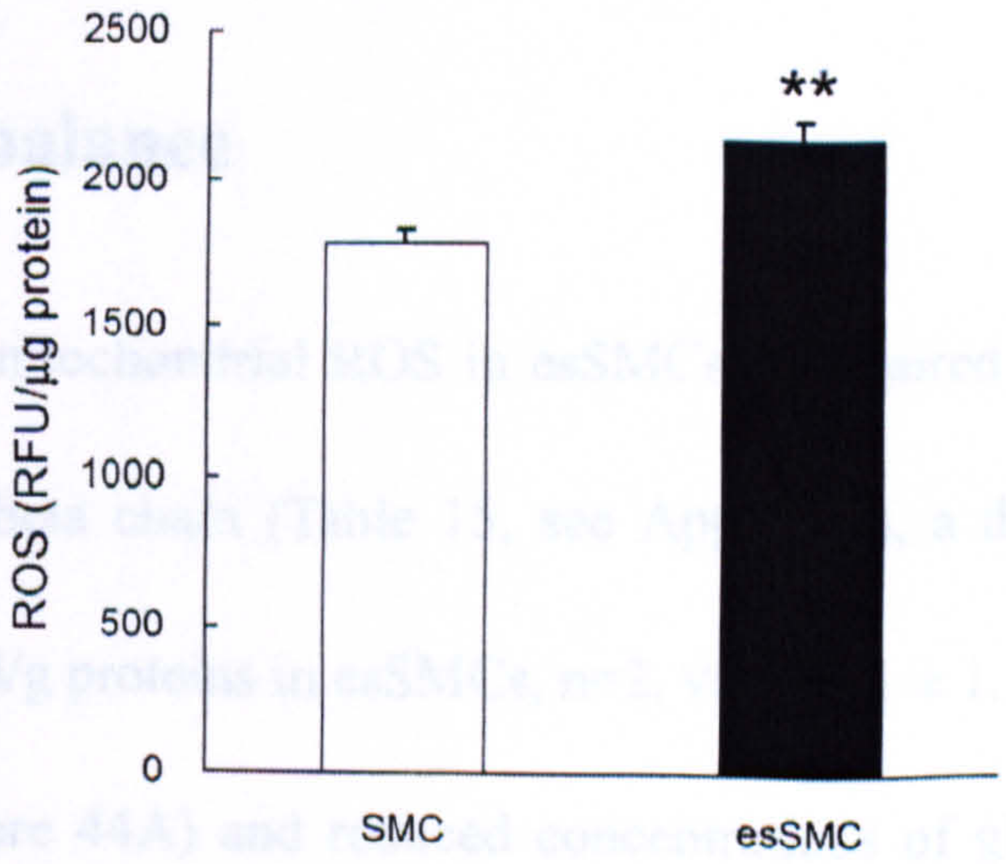

Figure 42. Aortic SMCs (n=3) and esSMCs (n=3) were incubated with DHR123 for 1 hour and harvested for fluorescence signal measurement and protein concentrations were determined. Normalized RFU indicates the total reactive oxygen species level in these cells. esSMCs showed significantly increased ROS than aortic SMCs. (The error bar indicates SE of each group, ** denotes p<0.01)

Figure 43. Total ROS and mitochondrial superoxide production

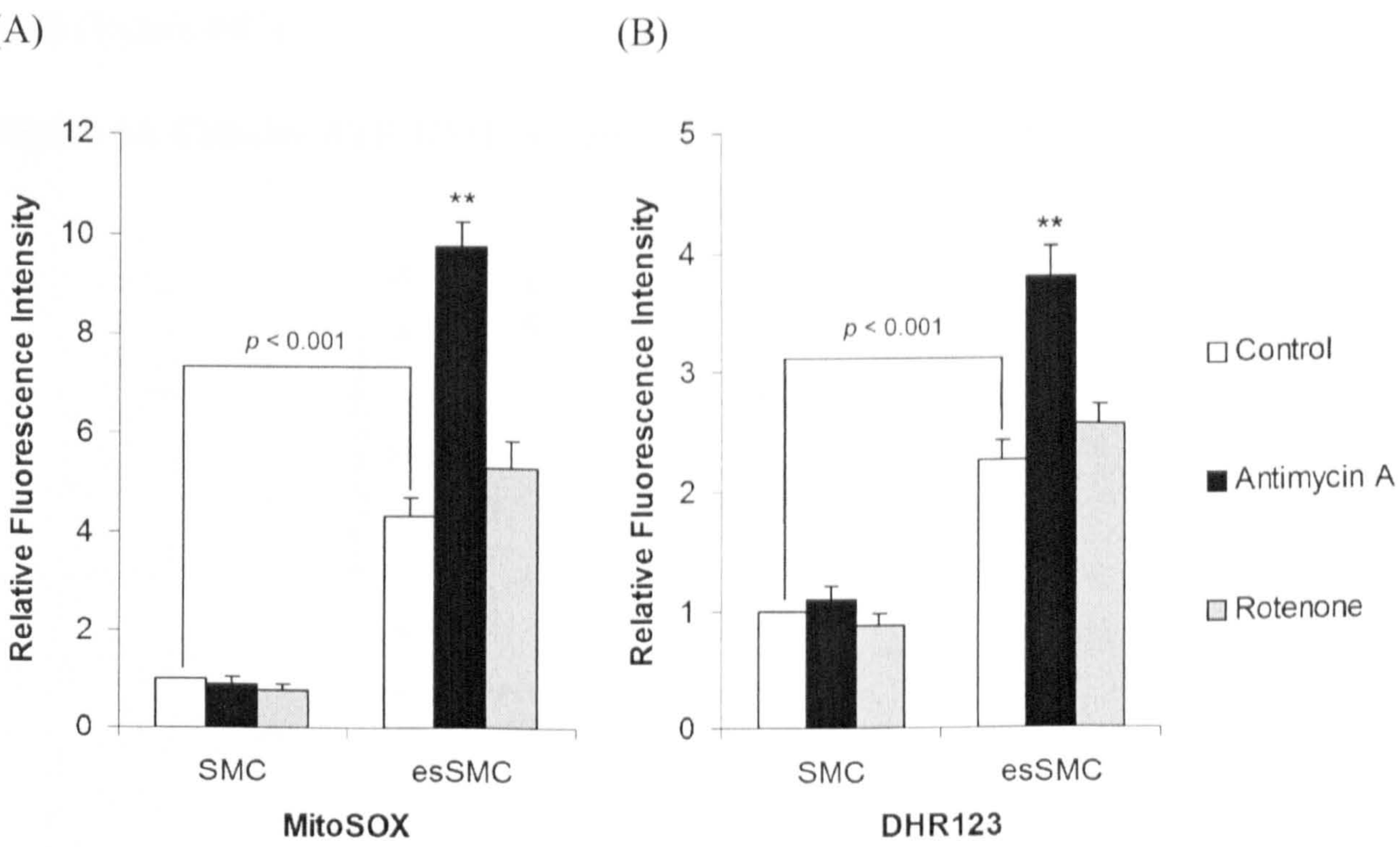

Figure 43. MitoSOX (A) and DHR123 (B) staining were used to assess total reactive oxygen species (ROS) and mitochondrial superoxide production in esSMCs (n=3) and aortic SMCs (n=3). esSMCs have a significant increase in mitochondrial superoxide production. Changes in oxidative stress were analyzed after treatment with rotenone and antimycin A, a complex I and III inhibitor, respectively. Note that the complex III inhibitor antimycin A resulted in a marked increase in mitochondrial superoxide production in esSMCs. (The error bar indicates SE of each group, ** $p<0.01$ compared to control)

3.4.4 Redox balance

The rise in mitochondrial ROS in esSMCs was paired with decreased expression of ATP synthase beta chain (Table 15, see Appendix), a drop in cellular ATP levels (19.52 ± 1.07μmol/g proteins in esSMCs, n=2, vs. 32.31 ± 1.10μmol/g proteins in aortic SMCs, n=2) (Figure 44A) and reduced concentrations of glutathione (GSH) (40.65 ± 0.52μmol/g protein in esSMCs, n=2, vs. 49.87 ± 1.34μmol/g protein in aortic SMCs, n=2) (Figure 44B). The reduction in cellular GSH, the major intracellular antioxidant, occurred despite a compensatory increase of glutathione reductase activity in esSMCs

(107.6 ± 2.8 IU/g protein in esSMCs, n=3, vs. 33.5 ± 1.1 IU/g protein in aortic SMCs, n=3) (Figure 44C).

Figure 44. Cellular ATP, GSH and glutathione reductase comparison

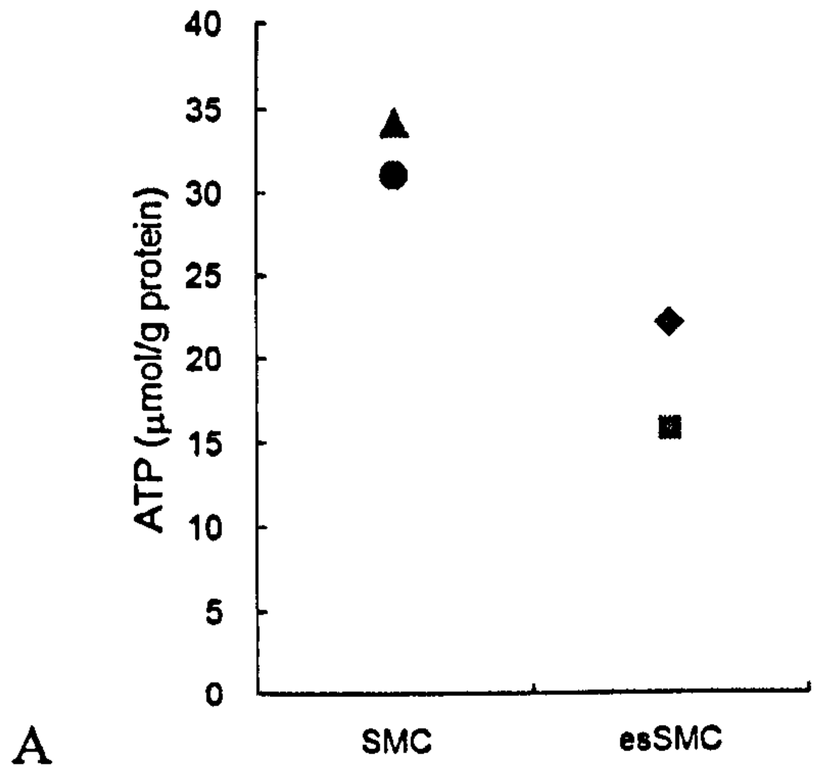

A

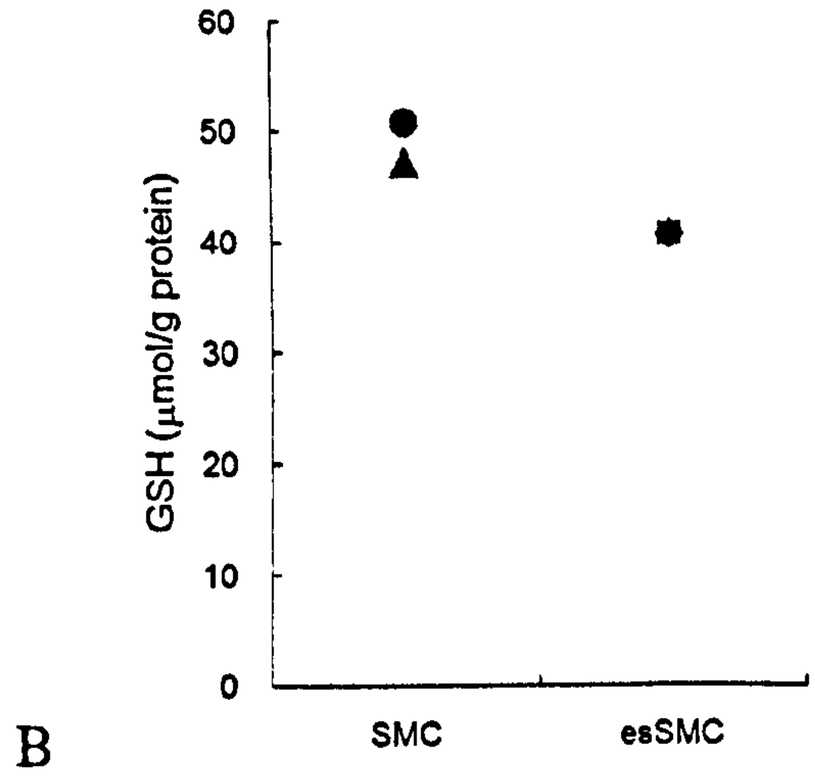

B

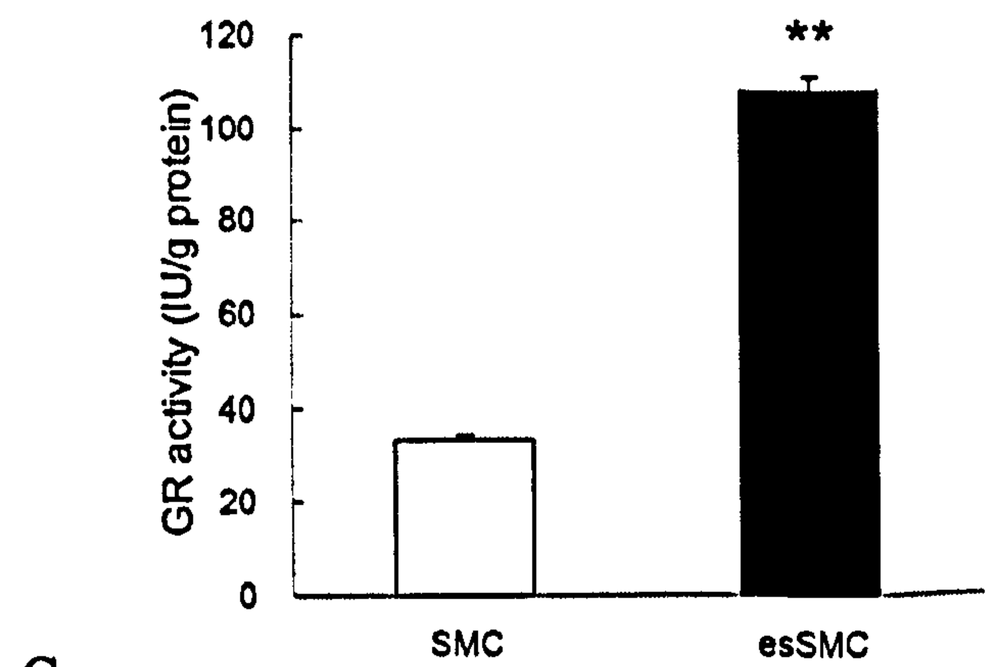

C

Figure 44. Cells were cultured in 6-well plates and harvested for measuring cellular ATP levels (n=2) (A), concentrations of reduced GSH (n=2) (B) and glutathione reductase activity (n=3) (C) in esSMCs and aortic SMCs. esSMCs showed lower ATP and reduced GSH levels but higher GSH reductase activity compared to aortic SMCs, indicating a higher ROS level in esSMCs. (The error bar indicates SE of each group, ** denotes $p<0.01$)

3.4.5 Cell viability

In normal culture conditions (with 50μM 2-ME), esSMCs grew faster than aortic SMCs. Cells were cultured in 6-well plates and change medium after 24 hours. At different time point, cells were scraped and lysed in 1mL 0.5M NaOH. Protein concentration was measured and plotted versus time (Figure 45). The slow down of the curve after 33 hours may be because shortage of nutritions in the medium.

Figure 45. Growth curve of esSMCs and aortic SMCs

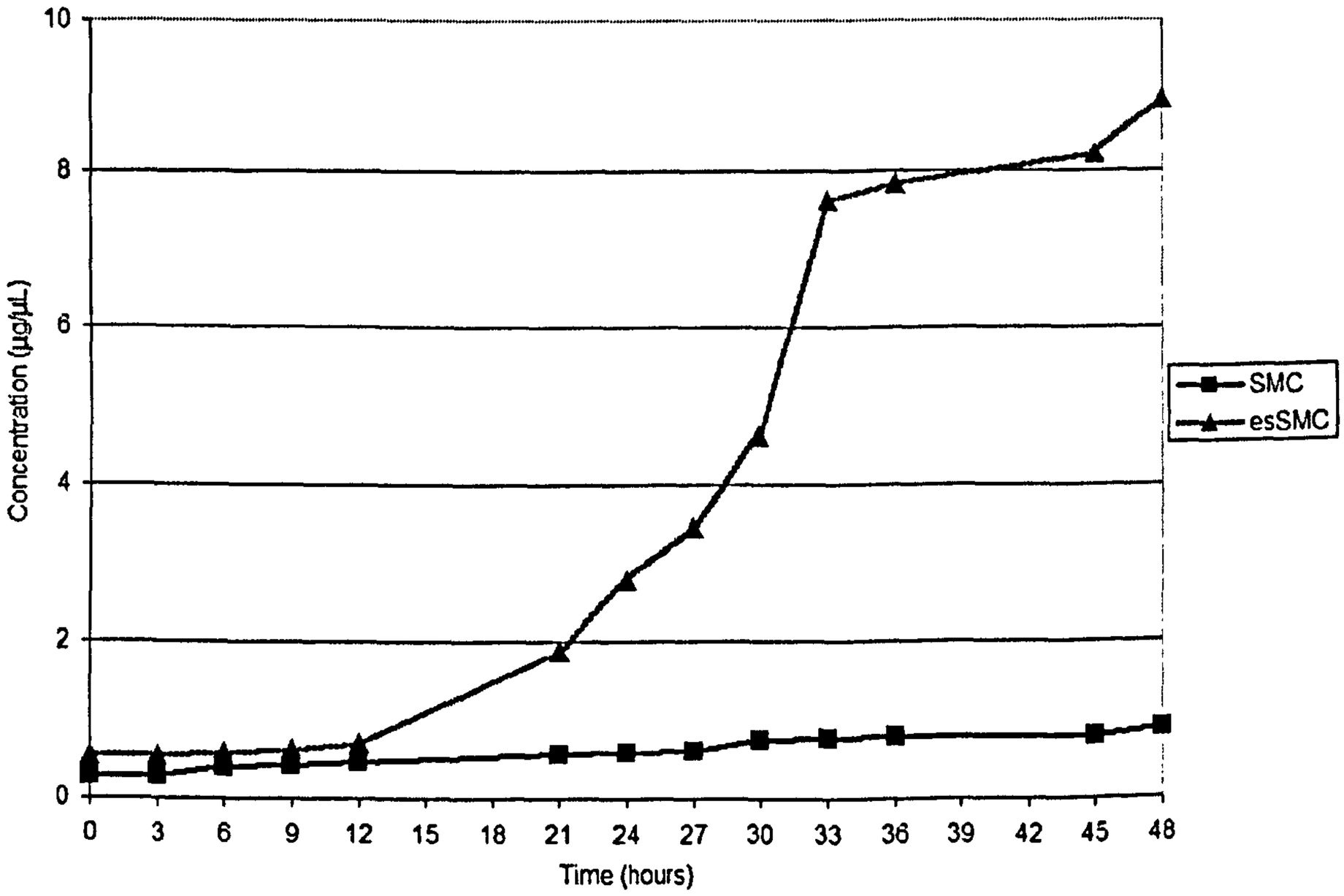

Figure 45. Cells were cultured in 6-well plates. Protein concentrations of cells from whole wells in different time points were measured and cell growth curve were made. esSMCs showed a much higher proliferation rate compared to aortic SMCs.

esSMCs were more susceptible to cell death upon treatment with both diethyl maleate (DEM) (Figure 46A), a sulphydryl-reactive agent that results in rapid depletion of GSH followed by a drop in ATP (Mayr, Siow et al. 2004), and carmustine (BCNU) (Figure 46B), a glutathione reductase inhibitor. In contrast, esSMCs viability improved on addition of 2-mercaptoethanol to the culture medium (Figure 46C), highlighting their

need for additional antioxidant protection.

DEM concentrations above 100μM are toxic. For the consist comparison with non-treated control, in this study DEM was directly added to DM containing 50μM of 2-ME, which leads to a lower effective concentration of DEM.

Figure 46. Cell viability after DEM, BCNU and 2-mercaptoethanol treatment

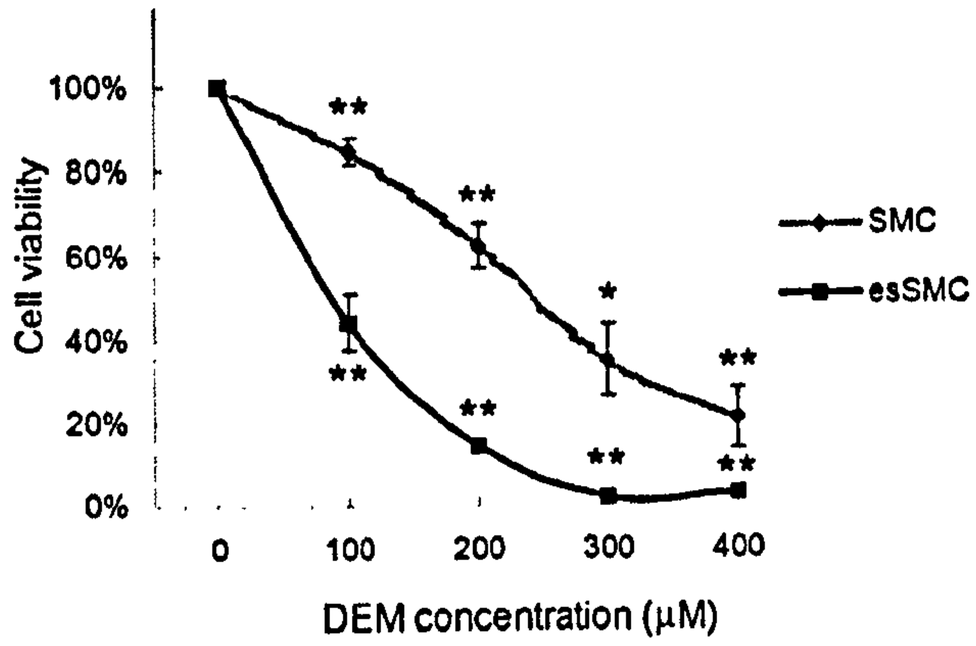

A

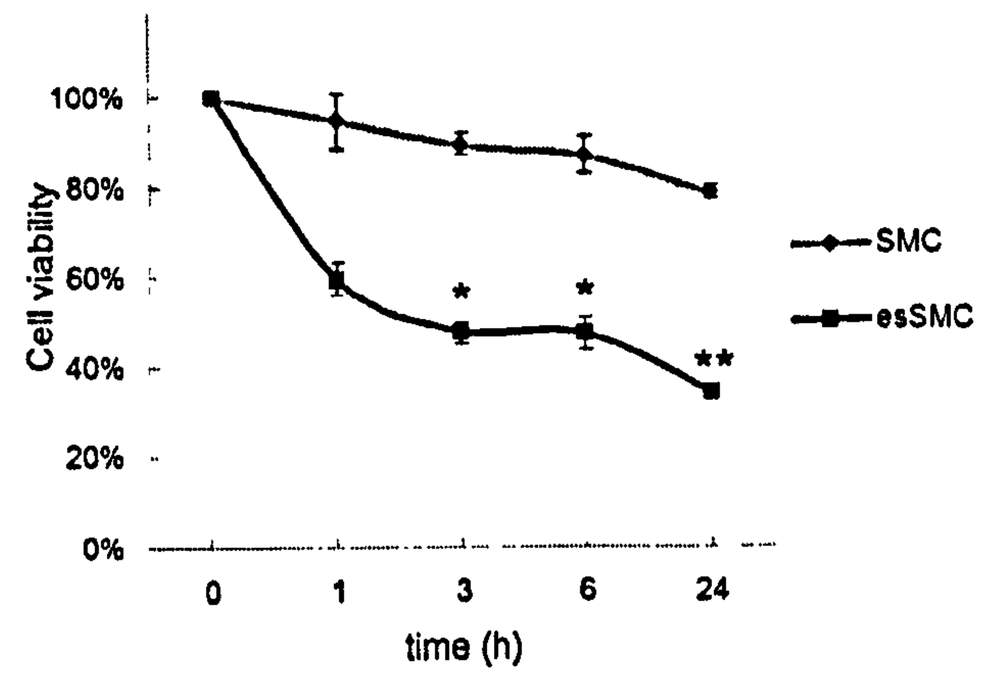

B

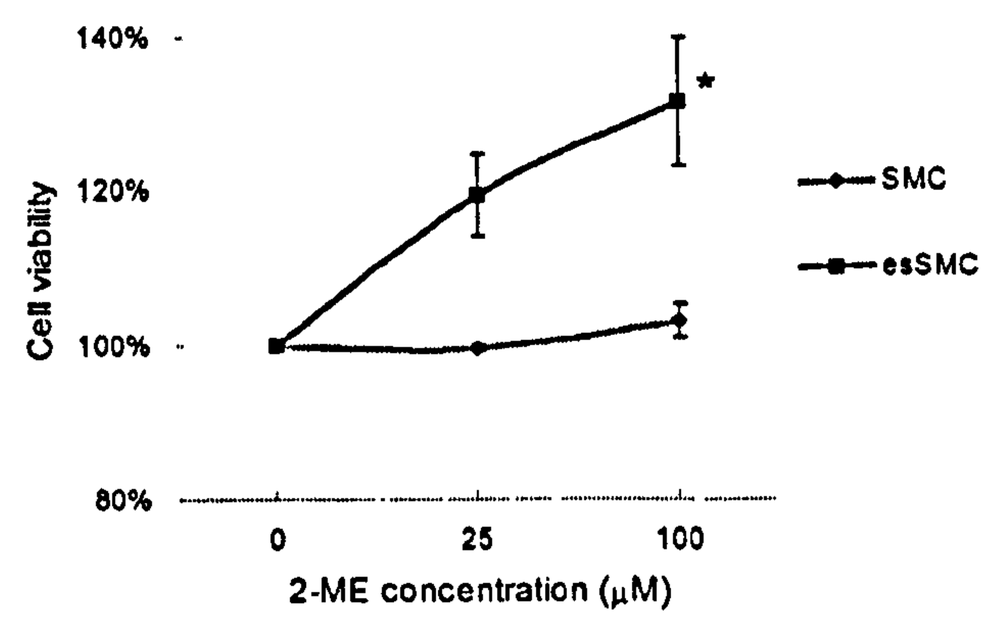

C

Figure 46. Cell viability after depletion of GSH by treatment with DEM (n=3) (A) or inhibition of glutathione reductase by BCNU (n=3) (B). Increase in esSMCs survival upon addition of 2-ME to the culture medium (n=4) (C). (The error bar indicates SE of each group, * $p<0.05$ compared to baseline, ** $p<0.01$)

3.4.6 Mitochondrial depolarization

JC-1 was used for detection of mitochondrial depolarization occurring in the early stage of apoptosis. The ratio of green (FL1) to red (FL2) fluorescence is dependent only on the membrane potential and not on other factors such as mitochondrial size, shape and density that may influence single-component fluorescent signals. The FL2/FL1 ratios of esSMCs and aortic SMCs were 2 and 10, respectively (Table 10, Figure 47). A lower ratio means lower membrane potential of mitochondria, indicating loss of mitochondrial potential in esSMCs. After adding 50μM of CCCP, the potential of mitochondrial membrane was completely lost and the ratios dropped to 0.1 for both cell lines.

Table 10. Fluorescence signal of JC-1 staining of esSMCs and aortic SMCs

Sample with 10μM JC-1	FL-1	FL-2	FL-2/FL-1
SMC control	90	900	10
esSMC control	700	1400	2
SMC + 50μM CCCP	300	30	0.1
esSMC + 50μM CCCP	100	10	0.1

Figure 47. JC-1 staining of esSMCs and aortic SMCs

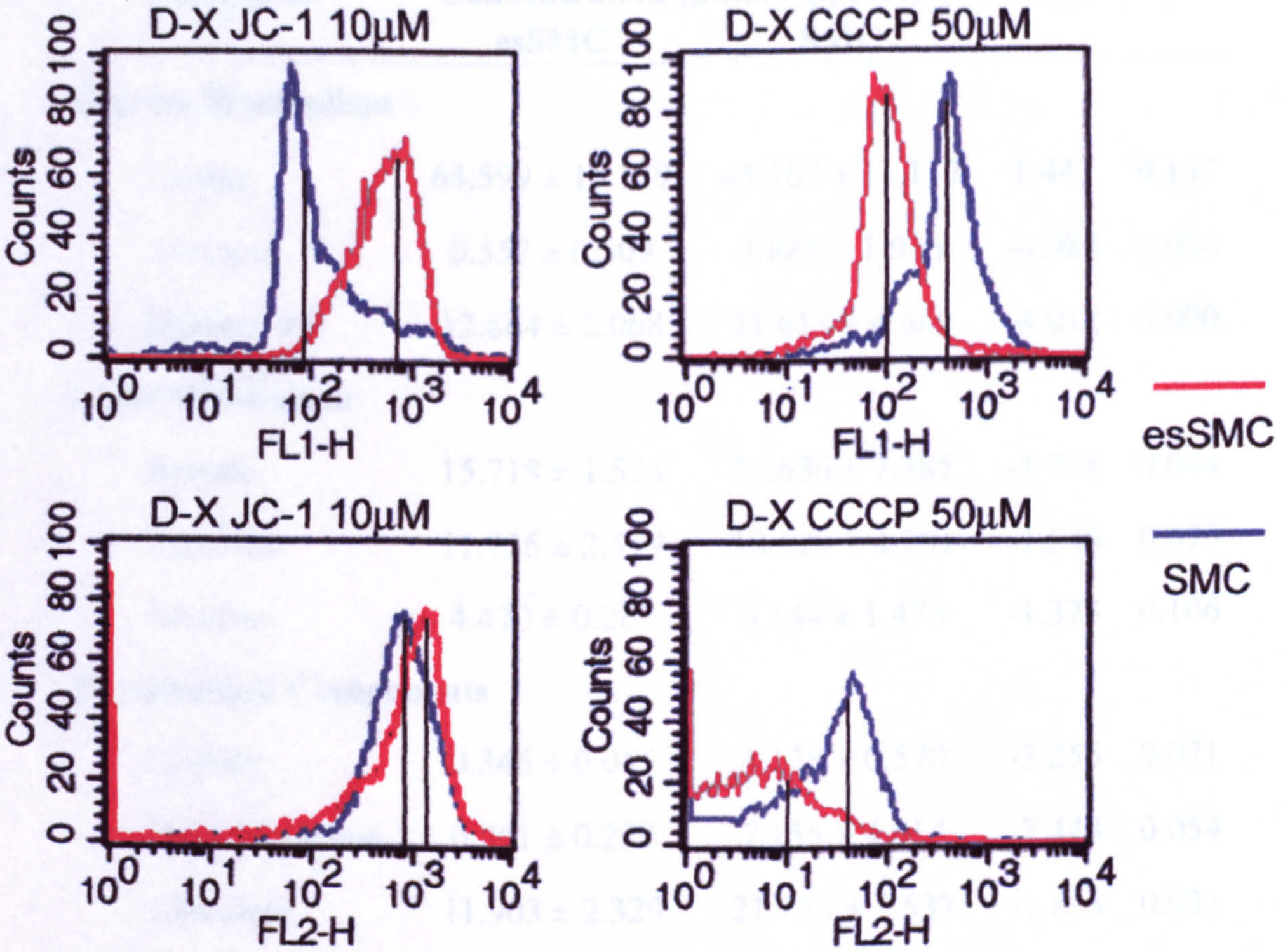

Figure 47. Cultured esSMCs and SMCs were dissociated in PBS and 10μM JC-1 or extra 50μM CCCP were added. After 30min of incubation in 37°C, the fluorescent signal of the cells was acquired by FACS. The cell count chart of each channel of esSMCs and aortic cells were generated and compared with each other. The average fluorescent signal readings were listed in Table 10 and FL1/FL2 ratio were calculated.

3.4.7 Metabolomic differences between esSMCs and SMCs

To clarify the metabolic effects of the differences shown at the protein level, esSMCs (n=3) and aortic SMCs (n=4) were harvested for NMR. Metabolites were measured by high-resolution NMR spectroscopy and protein concentrations were determined. The NMR analysis demonstrated several metabolites concentration changes between esSMCs and aortic SMCs. Those with ratio greater than 1.2 or less than -1.2 are listed in Table 11.

Table 11. Metabolites concentration changes between esSMCs and aortic SMCs

Metabolites	Concentration (μmol / g protein) esSMC	SMC	Ratio	*p*
Glucose Metabolism				
Lactate	64.599 ± 15.129	44.767 ± 11.157	1.443	0.137
Glucose	0.557 ± 0.509	3.888 ± 1.936	-6.984	0.036
Myoinositol	12.864 ± 2.068	51.613 ± 4.689	-4.012	0.000
Lipid Metabolism				
Acetate	15.718 ± 1.598	27.636 ± 7.385	-1.758	0.044
Carnitine	11.726 ± 2.519	18.129 ± 4.901	-1.546	0.079
Acetone	4.470 ± 0.287	6.144 ± 1.478	-1.375	0.106
Phospholipid Components				
Choline	0.346 ± 0.045	1.128 ± 0.570	-3.255	0.071
Phosphocholine	0.961 ± 0.228	7.155 ± 4.014	-7.443	0.054
Glycolate	11.903 ± 2.329	21.723 ± 5.537	-1.825	0.031
Amino Acids				
Glycine	21.933 ± 1.316	74.716 ± 16.046	-3.407	0.007
Aspartate	35.531 ± 3.658	15.557 ± 4.217	2.284	0.001
Glutamate	201.396 ± 8.205	95.992 ± 18.938	2.098	0.000
Glutamine	94.752 ± 6.606	75.738 ± 20.441	1.251	0.160
Taurine	47.022 ± 5.939	92.998 ± 35.210	-1.978	0.077
Energy Metabolism				
Adenosine pool	42.392 ± 1.761	35.317 ± 3.813	1.200	0.027
Phosphocreatine	21.738 ± 1.464	28.793 ± 6.523	-1.325	0.117
Succinate	6.611 ± 0.391	10.117 ± 1.999	-1.530	0.036
Fumarate	0.452 ± 0.011	0.312 ± 0.194	1.448	0.245
NAD+NADH	4.126 ± 0.520	2.659 ± 0.831	1.552	0.036

The most significant changes were observed for glucose, myoinositol, glycine, glutamate and aspartate. The low concentration of glucose may explain the low ATP

level in esSMCs. esSMCs appear to consume more glucose to meet their higher energetic demand. Glucose concentration is lower not only within esSMCs but also in the culture medium after 24 hours culture compare to the aortic SMC culture (Figure 48). Alternatively, their mitochondria may not generate ATP efficiently and they therefore need a higher rate of glycolysis.

Figure 48. Glucose concentration in the culture medium of esSMCs and aortic SMCs

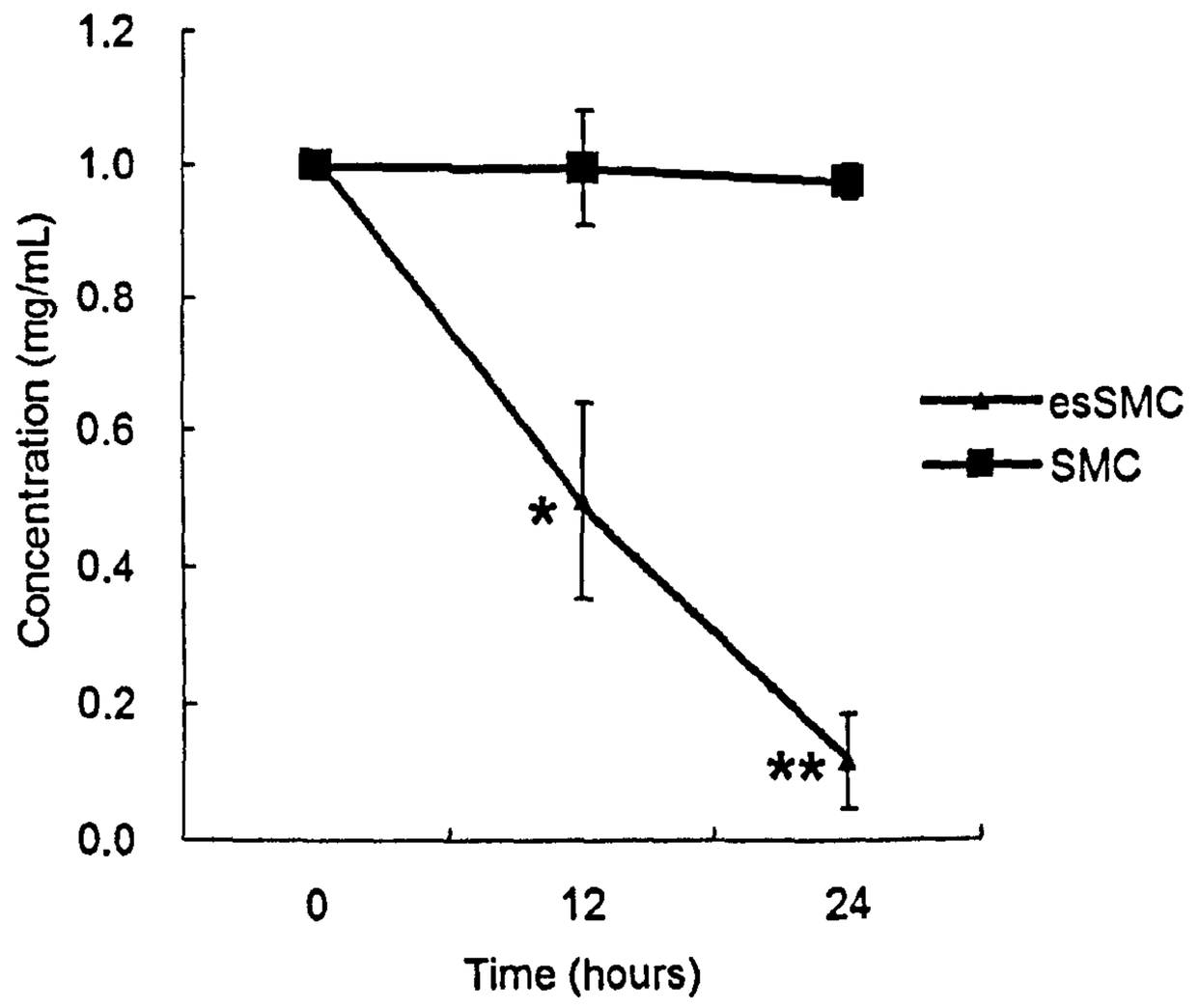

Figure 48. Culture medium samples were taken from the 6-well plates at different time points from esSMCs (n=3) and aortic SMCs (n=3) and glucose concentration were measured. The glucose concentration of esSMCs showed a very fast drop during the cell culture. (The error bar indicates SE of each group, * denotes $p<0.05$ compared to baseline, ** $p<0.01$)

In addition to ATP generation, mitochondria are also responsible for fatty acid oxidation. Notablely, metabolites involved in lipid metabolism and phospholipid components were all decreased in the esSMCs. Similarly, succinate, a supplementary carbon source in the citric cycle and in the electron transport chain complex II, showed a significant drop. Taken together, our proteomic and metabolomics data provide evidence for mitochondrial dysfunction in esSMCs.

4 DISCUSSION

4.1 Stem cells

4.1.1 The differentiation potential of stem cells

The remarkable differentiation potential of ES cells holds important research application including neoangiogenesis, stem cell-based therapies and tissue-engineering strategies, which may offer new clinical applications. ES cell differentiation is a complex process altering numerous proteins, not only at the transcriptional and translational level, but also by posttranslational modification.

Three criteria should be considered when using ES cell model for lineage-specific differentiation. First, protocols need to be established that promote the efficiency and reproducibility of the development of intereted cell type. If possible, selection strategies should be combined with optimal differentiation schemes to isolate highly enriched cell populations. Second, lineage development from ES cells should recapitulate the development program that establishes the lineage in the early embryo. Third, the mature cell populations that develop in these cultures must display appropriate functional properties both *in vitro* and *in vivo* (Keller 2005). The third one remains to be the major challenges in the field today.

The cellular heterogeneity is an intrinsic feature of the ES cell differentiation culture, which results in the pluripotent property of ES cells and makes the ES cell a considerable therapeutic potential source in the tissue engineering. However, the multiplicity is a major disadvantage of the ES cell differentiation culture when investigating cell type specific mechanism and teratomas can easily be formed when

injected *in vivo* (Martin 1981). In our studies, we used the positive selection (magnetic labelling cell sorting) of Sca-1$^+$ cells and stimulation with PDGF-BB to obtain highly purified esSMC population, which expressed similar SMC marker as mature aortic SMCs (Figure 25). During the differentiation from Sca-1$^+$ cells to esSMCs by PDGF-BB stimulation, the portion of SMC marker positive cells continuously increasing when treated with PDGF, from 50% at day 3 to 95% at passage 10. Additionally, esSMCs form vascular-like structures *in vivo* and no tumour-like tissue can be observed in the sections of cell grafts at 4 weeks (Xiao et al, unpublished data), indicating that esSMCs have angiogenesis activity and are safe for *in vivo* use. Another way to get highly purified SMCs is negative selection by puromycin on ES cell-derived SMCs with SM α-actin or SMMHC promoter controlled puromycin resistance gene (Sinha, Wamhoff et al. 2006). However, embryoid body differentiated up to day 28 still contained pluripotent cells. Thus, the highly efficient separation method is the critical requirement for the cell therapy and tissue engineering applications.

Many laboratories, including us, used serum as a growth supplement and/or as a source of inducing factors and successfully developed various cell lineage from ES cells. However, the use of serum has several serious drawbacks that induce batch-to-batch variability and the lack of identity of the inducing factors contained in it. It will be important to use serum-free conditions (such as serum replacement) and defined molecules for differentiation study. Several recent studies have eliminated serum and have begun to identify factors required for lineage-specific differentiation (Nakayama, Lee et al. 2000; Ying, Nichols et al. 2003; Kubo, Shinozaki et al. 2004; Park,

Afrikanova et al. 2004). As more protocols incorporate these approaches, both mouse and human ES cell mutilineage differentiation will become an easy routine technology in many labs.

4.1.2 Cell markers are not sufficient for differentiation

Undifferentiated stem cells and cells in different stage during the differentiation express different combinations of surface antigens. These antigens can be routinely utilized to detect the existence of stem cells, progenitor cells, or differentiated cells by Western immunoblotting, reverse transcription-PCR, immunofluorescence staining, immunohistochemistry staining, or to separate specific cells from heterogeneous cells by fluorescence activated cell sorting (FACS) and magnetic labelling cell sorting (MACS). The full list of human cell differentiation molecules is a helpful reference when we study the stem cell differentiation (http://www.hlda8.org/).

We used a panel of SMC markers which are widely accepted as sufficient to identify SMCs from heterogeneous cells, including SM α-actin and SMMHC, SM22, h-calponin. The SM α-actin and SMMHC expression within the developing embryoid body exhibited a high degree of SMC specificity/selectivity. *In vivo*, the SM α-actin promoter is expressed in all three muscle types during development but is restricted to smooth muscle by the time of birth (Mack and Owens 1999). The SMMHC promoter is more specific to SMCs and is only active in SMCs throughout embryogenesis and in a small subset of cardiomyocytes during very early development (Madsen, Regan et al. 1998; Regan, Manabe et al. 2000). Normally the purified cells comprise various

subpopulations of SMCs (such as vascular, gut or other organ specific SMC lineages) and these cells are best suited to study the common mechanism for all SMCs (Sinha, Wamhoff et al. 2006).

Although the esSMCs express a range of SMC markers, including two mature contractile SMC marker SM1 and SM2 (Xiao, Zeng et al. 2006), our proteomics comparison demonstrated that their ultimate phenotype and behaviour are profoundly different from mature vascular SMCs as revealed by the numerous differences between their proteome maps. Notably the esSMC 2-DE gel pattern is more like ES cells. Additionally, there are a lot of functional differences between these two cell types, especially their mitochondrial functions and their tolerance to oxidative stress. Similarly, ES cell-derived ECs also lack complete functional maturation in vitro (McCloskey, Smith et al. 2006). Mouse ES cell-derived ECs were compared with mouse aortic ECs. Although both cell types expressed EC markers (eNOS, Flk-1, Flt-1, VEcadherin, PECAM-1, CD34), ES cell-derived ECs showed a significantly lower levels of acetylated LDL uptake and von Willebrand factor and also their VEcadherin did not localize at the cell-cell junctions as in the mature counterpart. On the contrary, ES cell-derived ECs express much greater levels of the endothelial and hematopoietic stem cell marker CD34 and vasculogenic and angiogenic sprouting, indicating the immature stage of these differentiated cells.

These findings indicate the expression of cell markers may be indicative but not sufficient to characterize stem cell-derived cells or stages of cell differentiations. Thus, other approaches are needed to characterize ES cell-derived cells and mature

counterparts. Otherwise, functional differences between which would have gone unnoticed by only relying on a classification based on a panel of cell marker proteins. Since the ultimate phenotype of a cell is reflected in their instantaneous proteomic profile, the advent of novel proteomic approaches may offer an opportunity to obtain not only a better understanding of cell differentiation, but also to progress towards a molecular classification of stem-cell derived cells based on comparative analysis of protein expression patterns with other vascular cell types.

4.1.3 Mechanical stress and SMC maturation

Previous studies demonstrated that lack of hemodynamic forces triggers apoptosis in vascular ECs (Kaiser, Freyberg et al. 1997) and low intra-luminal pressure (10mmHg) resulted in decreased contents of smooth muscle marker proteins h-caldesmon and filamin (Birukov, Bardy et al. 1998), both of which hint that mechanical forces are essential stimuli for the maintenance of blood vessels. Similarly, the reason for the immature state of esSMCs may be the lack of mechanical stress. ES cells were cultured in static environment from the beginning without mechanical stress, while mature cells underwent stress from the very beginning and the hemodynamic forces last during the entile development of the vascular system. The different original environment may be responsible for the different function of these two cells. Although they were cultured under exactly same condition afterwards and showed some similarities, many of their physiological functions are different.

For tissue engineering, large numbers of proper functional and highly purified

cells will be needed to construct vessels. ES cells are easy to culture and have a high proliferation ability, which can be used to get enough cells in relatively short period. The purity of the ES cell-derived cells detected by FACS experiment is high enough to prevent the teratoma formation *in vivo* but the functions of these cells are very different from mature cells *in vitro* because of their immature stage.

For the use of esSMCs in tissue engineering, additional treatment besides chemical stimulation (PDGF-BB), e.g. mechanical stress, may be needed to induce differentiation to mature SMCs. With presence of cyclic stretch, total expression of smooth muscle specific myosin heavy chain (SM-1 and SM-2) and myosin light chain kinases increased in cultured vascular SMCs but non-muscle myosin-A decreased compared to static condition (Smith, Tokui et al. 1995; Reusch, Wagdy et al. 1996), which demonstrated the stimulatory effect of cyclic stretch on cytoskeleton protein expression. Using the same method, we can culture esSMCs in a tube and apply *ex vivo* mechanical stretch between the two ends and gradually increase to normal blood pressure. After the stimulation by cyclic stretch, these esSMCs might become more similar to mature SMCs in function.

4.1.4 Stem cell therapy

Because of the outstanding differentiation performance of mouse stem cells, the introduction of human stem cells has received the most attention in recent years as a novel source of cells for cell replacement therapy and tissue engineering strategies. Diseases caused by the loss or dysfunction of one or a limited number of cell types

could benefit from ES cell-based therapies, including Type I diabetes, Parkinson's disease, stroke, arthritis, multiple sclerosis, heart failure, blood diseases, certain type of liver disease and spinal cord lesions (Wert Gd and Mummery 2003). Transplantation of specific ES cell-derived cells into pre-clinical models of human diseases is already underway.

Although there is a promising future of the stem cell therapy, several important issues need to be addressed and settled before clinical practice. (a) The efficiency of establishing ES cell-derived cell lines has to be increased. Notably, apoptosis accompanying cell differentiation need to be resolved. If we discover the mechanisms and block the pathway of apoptosis during differentiation, we could increase the yield of purified progenitor/stem cells for implantation to injured tissue. (b) The compatibility of the donated embryos. Stem cell banks with a large numbers of ES cell lines would include a significant portion of the histocompatibility types in the population. Another trategy is to generate individualized ES cell lines through somatic cell nuclear transfer (SCNT), which would be genetically identical to the patient. (c) The purity of differentiated cell. Transplantation of undifferentiated ES cells can result in the development of teratomas (Thomson, Itskovitz-Eldor et al. 1998). With a combination of positive and negative selection, it should be possible to reproducibly generate grafts free of undifferentiated ES cells. (d) The number of cells to be transplanted. After the mechanisms controlling development of the desired lineage have been clarified, optimal conditions for the generation of the appropriate cell populations can be developed. (e) The delivery of the differentiated cells to the appropriate site, *i.e.* the homing of the

progenitor/stem cells. (f) The required stage of maturation depends to a large extent on the lineage under investigation. Relatively mature hepatocyte will be isolated and transplanted and end-stage of pancreatic β-cells is needed before transplantation, while hematopoietic transplantation requires the most immature cells, *i.e.* HSC. Optimization of the differentiation stage of ES cells at transplantation is critically required to meet the challenge for cell therapy in regeneration medicine (Yurugi-Kobayashi, Itoh et al. 2003).

Despite the potential benefit of using human ES cells in the treatment of disease, their use for research remains controversial and is currently high on the ethical and political agenda of many countries because they are derived from early human embryos. Although human ES cells can give rise to all somatic tissues, they cannot form extra-embryonic tissues which are necessary for complete embryo development, so that they cannot give rise to a complete new individual (Wert Gd and Mummery 2003). Messenchymal stem cells (MSCs) are highly attractive candidates for tissue engineering approaches in messenchymal tissue regeneration because they can easily be obtained and cultivated and are not ethically stigmatized. An ethical and practical limitation of SCNT is the requirement of enucleated oocytes. The development of oocytes from differentiated ES cells may provide one solution to this problem.

4.2 Proteomics

4.2.1 Gel-based or gel-free

Currently, there are basicly two different workflows for proteomics. One is the conventional 2-DE separation following protein identification by MS. Another is based

on gel-free "shotgun" approach, which injects the digested protein complex directly into MS without prior 2-DE.

Gel-based approach is very common due to the reasonable cost and is readily intergrated into other biochemical purification strategies. The high resolution can separate 2000 protein spots spontanously as shown in our proteome maps and all the Mr and pI information can be obtained. More importantly, some PTMs are also preserved, such as oxidation, phosphorylation and glycosylation. The drawback of gel-based approach is the time-consuming, labour intensive operation procedure, which demands qualified people to obtain reproducible results.

While non-gel based approach is much faster and less time consuming. Because the separation is performed at the peptide rather than protein level, most of the solubility problems associated with large size, low abundance and hydrophobic proteins are obviated (Peirce, Wait et al. 2004). This approach offers considerable advantages for study membrane proteins. The disadvantage of most shotgun strategies is that computationally intensive analysis of the entire dataset is always required, even when only a few proteins display changes in expression levels. Moreover, no information on the pI or Mr of the intact proteins is obtained, and all connectivity between parent proteins and their digestion products is lost, which hinders characterization of PTMs.

In this study, my subject is the proteome of ES cells and differentiated cells. The whole cell lysate is a very complex mixture of proteins. For quantification, mass spectrometry-based approaches are well suited to detect accurate differences in pairwise comparisons or few biological replicates. However, it remains a challenge to perform

comparisons across a large number of samples. Attempts are undertaken to perform label-free quantitation, but complex LC is required. Otherwise, quantitative differences in label-free LC-MS runs are influenced by co-eluting peptides as highly abundant ions suppress the ionization of less abundant ions. Undersampling of the mammalian proteome is another problem. For these reasons, the gel-based proteomic approach was used in this study although it is labour-intensive and requires more training. In addition, post-translational modifications such as the shift between the oxidized and reduced isoform of peroxiredoxin 6 would have gone unnoticed in a gel-free approach. However, this was a crucial observation and lead to all the functional studies into oxidative stress associated with the differentiation to esSMCs.

Gel- and non-gel based approaches provide closely related but distinct information about proteins, suggesting that they are complementary, or at least supplementary, methods, but not a replacement for gel-based proteomics (Monteoliva and Albar 2004). With the development of all related techniques during these years, advanced LC system can easily resolve mixtures of 1000 different proteins and also new fragmentation methods on mass spectrometers such as electron transfer dissociation (ETD) can be utilized to detect different PTMs. Thus, the shotgun approach also can be used for our future studies.

4.2.2 Silver staining or DIGE

Even within a same batch of 2-DE gels, silver stained gels still show a large variation because the dry stips and polyacrylamide gels are still not totally identical.

Gel-to-gel variation is the biggest problem for the reproducibility of our early studies. It is recommended that for a single biological replicate at least 9 different gels are required (3 different gels of three different samples of the same biological state) to overcome the gel-to-gel or intrinsic biological sample variations (Monteoliva and Albar 2004). It is very hard to use silver stained gels to study a large number samples and gel analysis is very time-consuming.

Compared to the traditional silver stained gels, 2-D DIGE eliminates gel-to-gel variation by running different samples in one gel. This greatly reduced the work. Silver staining only allows a comparison between two similar samples, *i.e.* the same cell line before and after treatement, because a similar spot number or density is required for the normalization between silver stained gels. It is less suitable for comparing totally different cell lines, *i.e.* esSMCs and aortic SMCs, as they might have a different number of overall spots. By using the same internal pooled standard across different gels along with high sensitivity and wider linear dynamic range of the fluorescent dyes, highly accurate quantatitive analysis can be performed even between very different samples. Despite the relatively expensive equipment and consumables, the DIGE approach is much more reliable than silver stained gels.

There were also some compatiblity issues when we transferred from silver stained system to DIGE comparison. DIGE lysis buffer contains Tris but not DTT. Tris can keep the DIGE lysis buffer in a stable pH of 8.5 for optimized labelling efficiency but introduced higher ion strength into the isoelectric focusing system. DTT will interfere with DIGE labelling and must be avoided in the lysis buffer before labelling. However,

the protein subunits or protein complex combined by double sulphate bond will not totally disaggregate in the lysis buffer without DTT. These component differences lead to potential differences in the spots pattern between 2-DE gels and DIGE gels.

Hydrophobic protein lysis from cellular compartment for 2-DE remains to be an unconquered problem in proteomics today and can presently only be accomplished in part with the help of specifically different isolation protocols (Klose 1999; Ramsby and Makowski 1999). Moreover, the precipitation step during cleanup procedure will cause protein loss because some of the precipitated proteins cannot be resolubilized back into the solutions at the final reconstitution step. Also the extended exposure to the low pH trichloroacetic acid solution may cause some protein degradation or modification, which may influence the protein pattern of 2-DE gels. However, the clean-up can remove most of the contaminants some of which may interfere with the isoelectric focusing and cause a loss of spots or even vertical empty gap across the gels. For these reasons, we use a sample clean-up and ran the 2-DE gels as a complementary map for the proteome map of the Sca-1^+ progenitor cells.

By using the internal calibration with the Mr/pI pairs of identified proteins, a grid map can be generated (Figure 29). Because the real observed Mr/pI of identified proteins may not exactly equal to the calculated one, a less bias method could be used. The best one is using external calibration, *i.e.* using Mr marker to calibrate Mr and using pH gradient shape of IPG strip from manufacturer for adjusting pI.

With more powerful computers, 2-DE gel analysis programs are also countinuously being developed and improved but image analysis remains a

time-consuming process. For DIGE experiments, DeCyder is the specially designed software for DIGE gels. It contains three modules, difference in-gel analysis (DIA), biological variation analysis (BVA) and extended data analysis (EDA). DIA module detects protein spots and directly compares the protein expression of the samples within one gel. BVA matches multiple images from different gels and calculates the relative ratio and statistical data of protein spots between multiple groups by normalizing and matching the internal pooled standard. The newly developed EDA module offers advanced statistical analysis in a simple-to-user format, uncovering patterns in expression data and relationships using multivariate analysis and sophisticated clustering methods. DeCyder provides statistical confidence and minimal user-to-user variation and reduces hands-on analysis time.

Direct comparison between esSMCs and aortic SMCs using the DIGE approach revealed reliable differences in protein expression (Table 15, see Appendix), which will give us further insights into the functional role of the identified proteins (Yin et al, 2006, Proteomics, in press). The DIGE experiment showed that the expressions of myofilaments and associated proteins (such as actin, lamin, myosin light chain, tropomyosin and vimentin), calcium-binding proteins (annexin, caldesmon 1, calreticulin, and transgelin), are lower in esSMCs, which indicates an early differentiation state of esSMCs. In contrast, proteins related to DNA maintenance, transcription and translation showed increased expression in esSMCs, e.g. heterogeneous nuclear ribonucleoprotein, translation initiation factor, elongation factor, which are consistent with the higher proliferation rate of esSMCs. Other differences in

signalling proteins may implicate certain receptors and signalling pathways in regulating stem cell differentiation.

HSPs are known to play an important role in chaperoning by transiently associating with nascent polypeptides to facilitate correct folding in the cytoplasm and nucleus. Notably, nearly all chaperones expressed at higher level in esSMCs than in aortic SMCs. This may due to the proliferation-related higher polypeptides synthesis rate in esSMCs. HSP 47 is known as molecular chaperon that specifically recognizes procollagen in the endoplasmic reticulum and is required for the maturation of type-IV collagen (Matsuoka, Kubota et al. 2004). The decreased expression level of HSP 47 (spot 115 and 116) in esSMCs may be due to the previous initiation of differentiation in collagen IV-coated flask, which did not demand high rate of collagen IV synthesis to form the basement membrane. Interestingly, stress-70 protein showed two pair of spots with the same Mr but different pI. The acidic form (spot 4 and 13) were both decreased while the alkali form (spot 5 and 15) were both increased in esSMCs compared to aortic SMCs. The pI shift may indicate phosphorylation or acetylation (Kim, Sprung et al. 2006). The two forms of stress-70 protein with or without PTMs must perform different functions in esSMCs and aortic SMCs, which should be clarified by further study.

The DIGE gel also showed SMCs specific marker, such as transgelin-2 (spot 76 and 79), transgelin (SM22, spot 80), calponin (spot 93), which were decreased in esSMCs. Increased oxidized peroxiredoxin 6 (spot 50) and decreased SOD-2 (spot 77 and 78) in esSMCs were also identified by DIGE gels, leading us to further investigate the redox status in esSMCs. Decreased ATP synthase B fragment (spot 22, 31, 32 and 63)

as well as increased VDAC (spot 88-91) suggested the mitochondrial dysfunction in esSMCs.

There are still some spots, which are relatively difficult to obtain reproducible results because of low protein concentrations, low quality of MS spectra, too small to get enough peptide peaks to be identified, or unavoidable keratin contamination of samples during manual spot picking and tryptic digestion.

4.2.3 Proteomics and differentiation

To understand complex biological systems such as cell differentiation, a more comprehensive approach is needed. Proteomics offers the possibility to simultaneously assess the expression of multiple proteins and will help to get a better understanding of stem/progenitor cells differentiation *in vitro* and *in vivo*.

There are several reports on stem cell and differentiation studies using proteomics technique. For example, proteome databases of murine R1 ES cells (Elliott, Crider et al. 2004) and human mesenchymal stem cells (hMSCs) (Feldmann, Bieback et al. 2005) were established by using 2-DE and MS. The hMSCs and differentiated osteoblast were compared and membrane proteins were identified by using the subcellular fractionation and LC/MS/MS techniques (Foster, Zeemann et al. 2005), including many low abundant signalling proteins and cell markers. A proteomic approach was also used to compare cytosolic proteins differentially expressed in HSCs ($CD34^+$ cells) and mature $CD15^+$ myeloid cells from human umbilical core blood (Tao, Wang et al. 2004). Although proteomics were applied to many stem cell studies, it has been hampered by the lack of

physiologically relevant cell models that can be expanded to generate enough of material required for proteomic studies.

Before we can analyze protein differences between different differentiation stage in detail, reliable and applicable reference protein maps of each stage during ES cell differentiation must be established. In addition to a protein map of mouse ES cells (Figure 28), we utilized the potential of proteomic techniques and provide a detailed map of proteins derived from Sca-1^+ progenitor cells (Figure 33 and 34) (Yin, Mayr et al. 2005), the early differentiation step from ES cell to SMCs. All these data are available in our website.

Vimentin is the most ubiquitous intermediate filament protein and the first to be expressed during cell differentiation. All primitive cell types including bone marrow and cord blood derived non-hematopoietic (mesenchymal, stromal) progenitor cells express vimentin, also in our Sca-1^+ progenitor cells. Therefore vimentin is a key protein to identify progenitor cells of mesodermal origin (Feldmann, Bieback et al. 2005). Vimentin is one of the most prominent phosphoproteins. A charge train of spots in 2-DE gels may imply a series of phosphorylated proteins with different number of phosphate residues. SMC specific markers like h-caldesmon, α-actin, transgelin, and tropomyosin are commonly detectable in SMC 2-DE gels but less expressed in ES cells or Sca-1^+ progenitor cells.

Beside the intracellular protein differences, the membrane proteins are also important for the full function of esSMCs. Recent studies showed that the integrin $\alpha_4\beta_1$ (VLA-4) promotes the homing of circulating bone marrow-derived progenitor cells to

the $\alpha_4\beta_1$ ligands, VCAM, and cellular fibronectin, which are expressed on actively remodelling neovasculature (Jin, Aiyer et al. 2006). The expression of the similar membrane proteins as the mature SMCs will enhances the mobility of the esSMCs and facilitates their homing to the injured area in the cell therapy.

As membrane proteins are normally very large hydrophobic proteins, new approaches are investigated by our lab to identify and quantify membrane proteins from SMCs (Sidibe, Yin et al. 2006, submitted), which combines cell surface labelling with Cy dye and biotinylation. After enrichment by the affinity capture with avidin and separation by 1D gradient SDS-PAGE, the Cy dye labelled proteins contained the majority of membrane, membrane-associated proteins and extracellular matrix proteins. Using this protocol, membrane proteins can be easier distinguished from co-purified intracellular contaminants.

4.2.4 Bioinformatics for proteomics

Currently increasing interest emerges in the validation of peptide identifications, the use of statistical methods to analyze results across multiple samples, the need to link mass spectrometric data to a multiplicity of genomic sequence entries, and the development of common standards for the dissemination of proteomic results. All these promote the development of proteomic bioinformatics.

As proteomics study will generate large amount of data, including gel images, protein spots position on the 2-DE gel, mass spectrometry raw data and spots identifications, many 2-DE gel database have been set up, including SMCs, HUVEC,

serum, mitochondria (http://www.expasy.org/ch2d/2d-index.html). Proteomic databases have been proven to be effective tools in basic and applied cell research (Resing 2002). The knowledge of the cellular proteome also provides a useful instrument for the assessment of differential protein expression changes under disease conditions, for the analysis of functional protein interactions and the clinical treatment protocols. For these reasons, we built our own website http://www.vascular-proteomics.com. Our gels show excellent resolution and represent a variety of proteins and different PTM. The identifications through all these proteome maps are highly consistent, which may be beneficial for other researchers. Future guidelines for publication of protein identifications (Carr, Aebersold et al. 2004; Wilkins, Appel et al. 2006) may require access to raw file of mass spectrometry, for which the website would provide an ideal platform.

4.3 Oxidative stress

One of the remarkable features of esSMCs was their high level of oxidative stress in esSMCs as indicated by the presence of oxidized antioxidants pointing towards a potential role for oxidative stress in stem cell differentiation.

4.3.1 Oxidative stress in stem cells differentiation

ROS are ideally suited as signalling molecules because they are rapidly generated, highly diffusible, and have a short half-life inducing signal transduction cascades of numerous pathways, which regulate biological effects such as differentiation toward

certain cell lineage (Sauer, Wartenberg et al. 2001; Poli, Leonarduzzi et al. 2004).

Compared with undifferentiated and dedifferentiated cells, differentiated cells generally exhibit higher rates of cyanide-resistant respiration, cyanide-insensitive SOD activity, peroxide concentration and lower levels of GSH (Sohal, Allen et al. 1986). Metabolic gradients in developing organisms are believed to influence development (Allen and Balin 1989) by resulting in differential oxygen supplies to tissues directing developmental events.

During embryoid body differentiation, embryoid bodies displayed significant endogenous production of ROS, accompanied by the expression of NADPH oxidase subunit $p67^{phox}$. 10~100nM of H_2O_2 significantly enhances cardiomyogenesis in embryoid bodies, whereas higher concentrations exceeding 1μM exhibits inhibitory effect. Continuous elevation of intracellular ROS is deleterious for cardiomyogenesis (Sauer and Wartenberg 2005).

PDGF is essential for the ES cells differentiation into SMCs. At the same time, PDGF is well known to increase ROS in a variety of cells (Kreuzer, Viedt et al. 2003; Weber, Taniyama et al. 2004) and involves Rac activation in its signal transduction cascade (Chiariello, Marinissen et al. 2001). Although PDGF-BB had been withdrawn for several passages at the beginning of the differentiation, the increased oxidative stress may not be overcome by the cell redox system. Antimycin A inhibition resulted in a great increase of mitochondrial superoxide generation in esSMCs (Figure 43), indicating that complex III is responsible for the marked ROS increase in esSMCs.

It has recently been shown that adult EPCs have increased antioxidant protection

(Dernbach, Urbich et al. 2004), that oxidative stress accelerates EPC senescence (Imanishi, Hano et al. 2005) and that glutathione peroxidase deficiency mice have dysfunctional EPCs with impaired ability to promote angiogenesis (Galasso, Schiekofer et al. 2006). Our data presented in this study provide solid evidence that esSMCs encounter increased oxidative stress due to a rise of mitochondrial-derived ROS and displayed higher levels of antioxidants, indicating that esSMCs share some similarities with adult progenitor cells.

The balance of the antioxidant and the ROS is very important for cell survival. It seems this balance is very fragile in esSMCs They are more susceptible to oxidative stress-induced cell death despite a compensatory increase in their endogenous antioxidant defence capacities and require exogenous antioxidant (2-mercaptoethanol) for survival. Thus, differences in protein expression relate to their altered cell function and maintaining the balance between ROS generation and antioxidative scavenging will be essential for the longevity of esSMCs and their potential use in tissue engineering.

4.3.2 Oxidative effects

In our study, peroxiredoxin 6 was mainly present as reduced isoform in aortic SMCs, but was predominantly oxidized in esSMCs (Figure 41), indicating a higher level of ROS in esSMCs, which is confirmed by the total ROS measurement with DHR123. In human blood vessels, the membrane-associated NAD(P)H oxidase is thought to be the principal source of superoxide and functionally related to cardiovascular risk factors (43,44). Besides its predominant role in the respiratory burst

oxidation of inflammatory cells, NADPH oxidase is also responsible for excess ROS production in vascular SMCs (45). But unlike mature SMCs, mitochondria appear to be the major source of excess ROS in esSMCs. The difference of mitochondria-derived superoxide was even more prominent between esSMCs and aortic SMCs (Figure 43), 4 fold increase at basal condition and 10 fold increase after treated with antimycin A, the mitochondrial complex III inhibitor, suggesting the mitochondrial complex III is contributing to a marked increase in mitochondria-derived free radicals.

In esSMCs, we observed lower levels of GSH than in aortic SMCs but higher GSH reductase activity. This may indicated that there is a higher consumption rate or a lower synthesis of GSH in esSMCs. Because of the drop in GSH, GCS activity needs to be measured. It has been reported that protein synthesis inhibitors shunt intracellular cysteine from protein synthesis to GSH synthesis (Ratan, Murphy et al. 1994), which increases the resistance to apoptosis. On the contrary, high protein synthesis activity also may cause cysteine shortage, leading to GSH depletion as observed in esSMCs.

4.3.3 Redox imbalance induces mitochondrial dysfunction

4.3.3.1 Mitochondria are more susceptible to oxidative stress

Because mitochondrial components are exposed to a relatively high flux of superoxide and H_2O_2, the oxidative damage is more significant in mitochondria.

The level of oxidized bases in mitochondrial DNA (mtDNA) is 10- to 20-fold higher than nuclear DNA without histone protection nor efficient DNA repair as their nuclear counterpart (Cadenas and Davies 2000). The hydroxyl radical ($HO^{\bullet}$) derived

from the respiratory chain can easily add onto the deoxyguanosine of DNA to form 8-hydroxydeoxyguanosine (8-OHdG) and induce gene mutations (Giulivi, Boveris et al. 1995).

$O_2^{\bullet-}$, H_2O_2 and $HO^{\bullet}$ exert quite different patterns of enzyme inactivation (Table 12). Overall, mitochondrial enzymes are all susceptible to inactivation by $HO^{\bullet}$ but rather resistant to the effects of H_2O_2 exposure (Zhang, Marcillat et al. 1990). This is consistent to our observation that esSMCs is less susceptible to relatively higher concentration of H_2O_2 treatment (data not shown).

Table 12. The different inhibition effects of oxidative stress to enzymes.

Enzymes	$HO^{\bullet}$	$HO^{\bullet} + O_2^{\bullet-}$	$O_2^{\bullet-}$	H_2O_2
NADH dehydrogenase	High	High	High	Partially
NADH oxidase	High	High	High	Partially
Succinate dehydrogenase	High	High	Mildly	-
Succinate oxidase	High	High	Poor	-
ATPase	High	High	High	-
Cytochrome oxidase	Resistant	Resistant	Resistant	Resistant
Cytochrome *c* oxidase	Resistant	Resistant	Resistant	Partially

Notably, esSMCs showed a depletion of mitochondrial ROS scavenging enzymes, but a coordinated up-regulation of cytosolic ROS scavenging enzymes. However, this coordinated rise in cytosolic antioxidative defence capacity was unable to compensate for the loss of mitochondrial antioxidants as esSMCs remained more susceptible to oxidative injury. While the increased cytosolic antioxidants may be an adaptation to

PDGF-induced ROS production, the sustained high level of mitochondrial ROS are likely to impair mitochondrial antioxidants and functions by mutating mtDNA or inhibiting the synthesis of antioxidants enzymes. More importantly, mitochondria-derived $O_2^{\bullet-}$ can be only eliminated by SOD-2. Prolonged mitochondrial dysfunction causes a drop in ATP level compromising survival.

4.3.3.2 SOD-2 is essential for maintaining normal cell function

The pathophysiology of mitochondrial diseases has been attributed to decreased ATP production and toxicity resulting from increased mitochondrial ROS generation. Under normal condition, 0.4%-4% of the oxygen consumed is converted to $O_2^{\bullet-}$ during the oxidative phosphorylation and reduced to H_2O_2 by SOD-2. Mice that genetically lack of SOD-2 die by day 10 after birth. Notably, SOD-2 was decreased only in esSMCs but is similar between ES cells and aortic SMCs (data not shown).

SOD-2 knockout mice have 30% less GSH when compared with wild-type mice and exhibit inhibition of electron transport chain complex I and II, inactivation of aconitase, development of a urine organic aciduria in conjunction with a partial defect in 3-hydroxy-3-methylglutaryl-CoA lyase, and accumulation of oxidative DNA damage (Williams, Van Remmen et al. 1998; Melov, Coskun et al. 1999). The SOD-2 deficient mice also showed 1.3 fold decrease of succinate in state 3 than wild type mice, which is consistent with our NMR data, indicating the dysfunction of the citric acid cycle might be a result of low SOD-2. SOD-2 deficiency mice showed no changes in cytosolic enzymes compare to wild-type mice. The increased cytosolic enzymes in esSMCs may

be passed on from the ES cells because Western blot show a similar expression of SOD-1 in ES cells and esSMCs (data not shown).

4.3.3.3 Citric acid cycle dysfunction causes GSH drop

The L-glutamate level is twice as high in esSMCs as in aortic SMCs; while the succinate concentration is 1.5 folds decreased in esSMCs. Succinate is the key intermediate in the citric acid cycle, which comes from the α-ketoglutarate and is oxidized into fumarate and generates $FADH_2$ at the same time. It is also involved in electron transport chain complex II to transfer electrons to ubiquinone. In the presence of low level of ROS, aconitase will be completely inactivated but α-ketoglutarate dehydrogenase is still functional. Glutamate becomes a key metabolite driving a segment of citric acid cycle with the final product being aspartate. When the ROS levels are increased, α-ketoglutarate dehydrogenase is also partially inhibited, resulting in an impaired respiratory capacity and decreased NADH production (Tretter and Adam-Vizi 2000). The high concentration of glutamate and aspartate and low levels of succinate in esSMCs indicated impaired citric acid cycle by increased ROS production in these cells. The glutathione synthesis using L-glutamate may be inhibited because the L-glutamate is diverted to drive the citric acid cycle. This may be another reason for the low GSH concentration in the esSMCs.

4.3.3.4 Electron transport chain dysfunction

We tried several inhibitors for ROS-generation enzymes, including apocynin,

oxypurinol, N^G-monomethyl L-arginine (L-NMMA), rotenone and antimycine A, which are the inhibitors for NAD(P)H oxidase, xanthine oxidase, iNOS/eNOS, electron transport chain complex I and III, respectively. The first 3 inhibitors did not show significant decrease of cell viability with treatment up to 400μM (data not shown). The rotenone and antimycin A lead to dramatic drop of cell viability at low concentration (5μM for rotenone, 10μg/mL for antimycin A) and cell death was higher in esSMCs compared to aortic SMCs, indicating that esSMCs are more susceptible to disruption of the mitochondrial electron transport chain.

The major net energy conversion catalyzed by the mitochondria is:

$$NADH + H^+ + \tfrac{1}{2}O_2 + ADP + Pi \rightarrow NAD^+ + ATP + 2H_2O$$

That means the ATP generation depends on the NADH concentration. The low level of ATP in esSMCs demands higher rate of oxidative phosphorylation. There are two source of the electron in the electron transport chain, from complex I and complex II. Both are largely activated and used up all the NADH as well as succinate (as shown in NMR data). From the cell proliferation experiment, we indirectly got the information that the reductant potential (NADH + succinate) is lower in esSMCs than in aortic SMCs. Low NADH level would result in less ATP production, compromising the supply of energy in esSMCs.

The complex I and II and aconitase defects are caused by the ROS-induced oxidation of iron-sulfur clusters, which release Fe^{2+}. This iron can participate in the Fenton reaction, generating hydroxyl radical ($HO^{\bullet}$) and leading to further oxidative damage. Fibroblasts from complex I-deficient patients have increased mitochondrial

derived ROS production when compared with control. In addition, their fibroblasts have impaired mitochondrial function, as reflected by depolarized mitochondrial membrane potential (Michelakis, Hampl et al. 2002), which are similar as our FACS results of JC-1 staining.

Complex III is one of the major sites of superoxide radical formation by one-electron transfer to molecular oxygen. Inhibition of mitochondrial complex III by antimycin A will block the pathway from ubisemiquinone to ubiquinone (Figure 17) (Chandel, Maltepe et al. 1998). The ubisemiquinone accumulates and keeps converting O_2 to $O_2^{\bullet-}$ so that superoxide levels increase. In SMCs, the superoxide can be converted to H_2O_2 by SOD-2 but the insufficiency of SOD-2 in esSMCs cannot antagonize all the superoxide and esSMCs show a higher fluorescent signal in the MitoSOX experiments. Complex III is the most important part of the electron transport chain because it connects the upstream complex I and complex II and the downstream complex IV and ensures the electron transport pathway. If complex IV is blocked, alternative electron acceptors (such as fumarate) could maintain a minimal electron transport chain activity (Hohl, Oestreich et al. 1987).

During the development, mitochondrial activity increases in cardiomyocytes. It may be the compensation of the increased energy demand or essential step of the maturation process. Addition of antimycin A (complex III inhibitor) completely blocked heart cell development, whereas neither TTFA (complex II inhibitor) nor KCN (complex IV inhibitor) blocks the differentiation, suggesting that specifically function of complex III of the electron transport chain rather than mitochondrial ATP production is

necessary for ES cells differentiation to cardiomyocytes (Spitkovsky, Sasse et al. 2004). The interference of the antimycin A with the heart cell differentiation indicates that some specific signalling pathways associated with mitochondrial complex III are important during the cardiomyocyte differentiation.

At the same time, the SM α-actin expression was detected in embryoid bodies with presence of antimycin A, indicating the SMC differentiation was not inhibited by this specific mechanism (Spitkovsky, Sasse et al. 2004). However, the concentration of antimycin A (50nM) is 20-fold lower than usually to exclude side effects as much as possible. Higher concentration of antimycin A led to an increase of mitochondrial-derived superoxide, demonstrating that mitochondrial complex III appears to be responsible for the marked increase in mitochondrial free radicals in esSMCs, which may impair the survival of the esSMCs. ROS derived from different intracellular sources (mitochondrial or cytosolic) may have different effects on downstream signalling cascades that are responsible for ES cell differentiation.

4.3.3.5 Energy metabolism

Oxidative metabolism serves as an important signal for adaptive responses to hypoxia. Prolonged hypoxia causes an inhibition of oxidative phosphorylation, leading to important adaptive increases in glucose transport (Mann, Yudilevich et al. 2003), especially GLUT1. ECs cultured under hypoxia conditions for 4 days exhibited increased rates of glucose transport and generated more lactic acid than normoxic cells. All these are coincident with our observation that the oxidative phosphorylation of

esSMCs was impaired, which generated more superoxide but less ATP, esSMCs consumed more glucose and the lactate was elevated in esSMCs (Table 11), and esSMCs deplenish all the glucose in medium after 24 hours (Figure 48), which relies on highly efficient glucose transport system. One explaination is esSMCs grow very fast, so that there may be not sufficient oxygen supply for their growth, i.e. they may face a hypoxia microenvironment. Another possibility is the esSMCs were depleted for energy, e.g. ATP production. Anaerobic glycolysis is the fastest way to generate ATP. At the same time, a large quantity of NADH is oxidized by reducing pyruvate to lactate. This reaction is carried out by lactate dehydrogenase (LDH).

The proton potential between inter membrane space and mitochondrial matrix are the determining factor for the ATP synthesis. If the electron transport chain cannot accumulate enough protons during the electron transport, there will be not enough energy for the mitochondria to generate enough ATP for cell metabolism. At the same time, the electron may be transfer directly to O_2 to form $O_2^{\bullet-}$ rather than to the next electron carrier in the electron transport chain. Thus, a low level of ATP synthesis rate is always coupled with higher superoxide in mitochondria. The constantly high level of superoxide will cause mitochondrial component damage and further lead to mitochondrial dysfunction.

Spontaneous contraction of the differentiated heart cells with embryoid bodies was not affected by inhibition of electron transport chain, suggesting that early heart cell function is sufficiently supported by anaerobic ATP production (Spitkovsky, Sasse et al. 2004). In contrast, alteration in mitochondrial redox status in esSMCs was associated

with cellular ATP level change.

4.3.4 Apoptosis

In the esSMCs, some cells generate relatively lower level of ROS and show a proliferation property while some other cells genereate more ROS exceeding their antioxidant ability resulting in apoptosis or necrosis.

Apoptosis is observed during the differentiation of ES cells into esSMCs. The results from our lab showed that esSMCs had a higher rate of both spontaneous and ROS-induced apoptosis and necrosis. FACS analysis of apoptosis using annexin V/Propidium iodide (PI) double-labelling indicated that more dead and apoptotic cells in esSMCs compared to aortic SMCs, when cultured in DM. The main population of dying cells underwent apoptosis in esSMCs after treatment with H_2O_2 or serum starvation. Furthermore, caspase-2 activity in esSMCs had approximately a two-fold increase compared to aortic SMCs. Cytochrome *c* and caspase-3 in esSMCs were markedly elevated compared to that in aortic SMCs (Figure 49). When inhibiting caspase-2 with Z-VDVAD-fmk, Sca-1^+ cells will direct toward differentiation direction instead of apoptosis (Xiao et al, unpublished data). These results indicate the apoptosis in esSMCs is mainly induced by the oxidative stress, which influenced the mitochondrial function and caused cytochrome *c* release. It could be interesting to further study the molecular mechanisms for regulating the balance between apoptosis and differentiation in stem cells.

Figure 49. Cytochrome *c* and caspase-3 expression in esSMCs and aortic SMCs

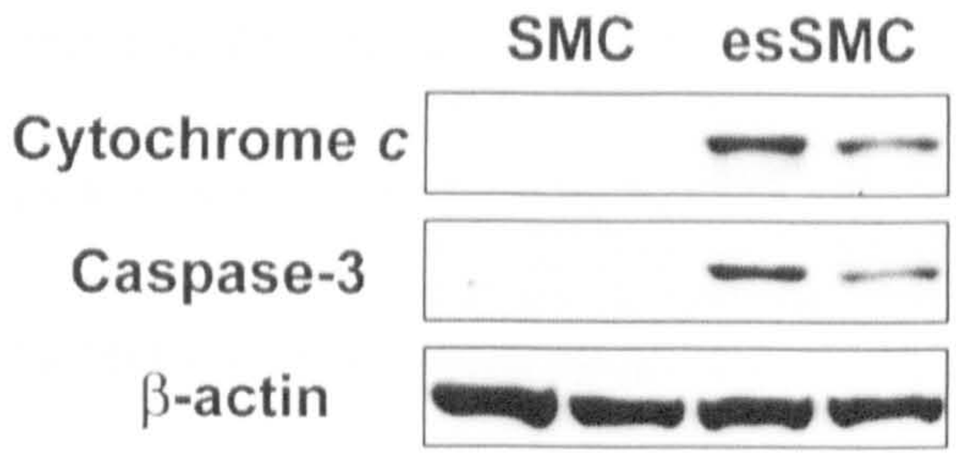

Figure 49. Western blots showed cytochrome *c* and caspase-3 were highly expressed in esSMCs (n=2) compared to aortic SMC (n=2), indicating higher apoptosis level in esSMCs.

Our studies would suggest that inhibiting pools of superoxide production, *i.e.* in mitochondria by improving cellular metabolism, or targeting specific cell types, *i.e.* stem cells to facilitate tissue repair, may be a better therapeutic strategy than global antioxidant interventions.

4.4 Conclusions and Potential Future Studies

We present the first proteomic comparison of murine aortic SMCs and esSMCs demonstrating that there is a requirement to define stem cell populations by proteomics for a systematic understanding of changes occurring during development. The high ROS level accompanied with the differentiation process is a challenge in front us and need more effort to resolve this problem so that obtain stable cells for cell therapy. We expect that our identification of differentially expressed proteins during stem cell differentiation may have profound implications in stem cell therapy and tissue engineering.

Since the ROS will impair the function of differentiated stem cells and induce apoptosis, we want to know whether this high ROS level is necessary for the stem cell

differentiation or just a hazardous by-product of PDGF stimulation. If we add antioxidants and induce cell differentiation, by comparison with cells differentiated without antioxidant, we will know whether the antioxidants inhibit cell differentiation or prevent the differentiated cells from apoptosis.

Moreover, mechanical stress can also induce stem cell differentiation. Some studies from our lab demonstrated that shear stress might induce mouse ES cells differentiation into ECs (Zeng, Xiao et al. 2006). Other kinds of stress may also be responsible for the SMC differentiation, i.e. by culturing ES cells on membrane and subjecting them to mechanical stretch. Furture studies will show where by combining chemical and mechanical stimulation, the differentiated esSMCs may acquire more similar behaviour as the aortic SMCs.

PUBLICATIONS

Journal articles

1. Mayr M, Mayr U, Chung Y-L, **Yin X**, Griffiths JR, Xu Q. Vascular proteomics: linking proteomic and metabolomic changes. ***Proteomics***. 2004 December; 4(12): 3751-3761.

2. Mayr M, Chung YL, Mayr U, **Yin X**, Ly L, Troy H, Fredericks S, Hu Y, Griffiths JR, Xu Q. Proteomic and Metabolomic Analyses of Atherosclerotic Vessels From Apolipoprotein E-Deficient Mice Reveal Alterations in Inflammation, Oxidative Stress, and Energy Metabolism. ***Arterioscler. Thromb. Vasc. Biol.*** 2005 October; 25(10): 2135-2142.

3. **Yin X**, Mayr M, Xiao Q, Mayr U, Tarelli E, Wait R, Wang W, Xu Q. Proteomic dataset of Sca-1^+ progenitor cells. ***Proteomics***. 2005 November; 5(17): 4533-4545.

4. Mayr U, Mayr M, **Yin X**, Begum S, Tarelli E, Wait R, Xu Q. Proteomic dataset of mouse aortic smooth muscle cells. ***Proteomics***. 2005 November; 5(17): 4546-4557.

5. **Yin X**, Mayr M, Xiao Q, Wang W, Xu Q. Proteomic Analysis Reveals Higher Demand for Antioxidant Protection in Embryonic Stem Cell-derived Smooth Muscle Cells. ***Proteomics***. 2006. (in press)

6. De Souza AI, Rossig L, **Yin X**, Mayr M, Dimmeler S, Xu Q. Proteomic Dataset of Human Endothelial Progenitor Cells. ***Proteomics***. 2006. (submitted)

7. Yusuf S, Mayr M, Mayr U, **Yin X**, Ly L, De Souza AI, Xu Q, Camm J. Proteomic and metabolomic analysis of the fibrillating heart. ***J. Am. Coll. Cardiol.*** 2006 (submitted)

8. Sidibe A, **Yin X**, Xu Q, Mayr M. Integrated Membrane Protein Analysis of Vascular Smooth Muscle Cells using a Novel Combination of Cy-dye/Biotin Labelling. ***Molecular & Cellular Proteomics***. 2006. (submitted)

9. Cuello F, Bardswell S, Haworth R, **Yin X**, Mayr M, Kentish J, Avkiran M. Cellular protein kinase D activity regulates cardiac troponin I phosphorylation and myofilament Ca^{2+} sensitivity in ventricular myocytes. ***Circulation research***. 2006 (submitted)

Meeting abstracts

1. **Yin X**, Mayr U, Mayr M, Xu Q. Comparative proteomic analysis of mouse stem cells and vascular smooth muscle cells. ***BAS meeting***. 2004 March; Oxford, UK. (poster)

2. **Yin X**, Xiao Q, Mayr M, Xu Q. Proteomic profiling of smooth muscle cells derived from embryonic stem cells. ***BAS meeting***. 2005 April; Oxford, UK. (poster)

3. **Yin X**, Xiao Q, Mayr U, Mayr M, Xu Q. Proteomic analysis reveals higher demand for antioxidant protection in embryonic stem cell-derived smooth muscle cells. ***BSCR meeting***. 2005 September; London, UK. (poster and oral presentation)

4. **Yin** X, Xiao Q, Mayr U, Mayr M, Xu Q. Proteomic analysis of stem cell-derived smooth muscle cells. ***3rd EMVBM***. 2005 September, Hamburg, Germany. (poster)

5. **Yin X**, Xiao Q, Mayr U, Mayr M, Xu Q. Proteomic Analysis Reveals Higher Demand for Antioxidant Protection in Stem Cell-Derived Smooth Muscle Cells. ***AHA Scientific Sessions***. 2005 November; Dallas, TX, USA. (poster)

6. **Yin X**, Xiao Q, Mayr U, Mayr M, Xu Q. Proteomics Analysis of Embryonic Stem Cell-derived Smooth Muscle Cells. ***XIVth International Vascular Biology Meeting***. 2006 June; Noordwijkerhout, The Netherlands. (poster)

Award

2005 Clinical Science Young Investigator Award on *British Society of Cardiovascular Research* meeting

APPENDIX

Recipes

Cell culture

Complete stem cell medium
DMEM (ATCC) containing 10ng/mL recombinant human leukaemia inhibitory factor (LIF, LIF1010, Chemicon), 10% fetal bovine serum (FBS, ATCC), 0.1mM 2-mercaptoethanol (M7522, Sigma), 2mM L-glutamine (Invitrogen), 100U/mL Penicillin (Invitrogen), and 100μg/mL streptomycin (Invitrogen)

Basic differentiation medium (DM)
Alpha-minimal essential medium (α-MEM, Invitrogen), supplemented with 10% fetal calf serum (FCS, Invitrogen), 50μM 2-mercaptoethanol (Sigma), 2mM L-glutamine (Invitrogen), 100U/mL Penicillin (Invitrogen), and 100μg/mL streptomycin (Invitrogen)

SMC primary culture medium
DMEM (Invitrogen) supplemented with 20% FCS (Invitrogen), 2mM L-glutamine (Invitrogen), 100U/mL penicillin (Invitrogen), and 100μg/mL streptomycin (Invitrogen)

2-DE

2-DE wash buffer
250mM sucrose, 10mM Tris, pH=7

2-DE lysis buffer
9.5M urea, 2% w/v CHAPS, 1% w/v DTT, and 0.8% w/v Pharmalyte (pH 3-10)

Rehydration solution
8M urea, 0.5% w/v CHAPS, 0.2% w/v DTT, 0.2% w/v Pharmalyte (pH 3-10), and trace Bromophenol blue

Equilibration buffer
6M urea containing 30% v/v glycerol, 2% w/v SDS and trace Bromphenol blue

DIGE

DIGE wash buffer
5mM Magnesium acetate, 10mM Tris, pH=8

DIGE lysis buffer
8M urea, 4% w/v CHAPS, 30mM TrisCl, pH=8.5

2× buffer
8M urea, 4% w/v CHAPS, 2% w/v DTT, 2% v/v Pharmalytes (pH 3-10)

Silver staining

Fixation solution
40% v/v methanol, 10% v/v acetic acid

Sensitizing solution
30% v/v methanol, 0.2% w/v sodium thiosulphate, 0.5M sodium acetate

Developing solution
2.5% w/v sodium carbonate, 0.0148% w/v formaldehyde

Stopping solution
1.46% w/v EDTA-Na_2•$2H_2O$

In-gel digestion

Extraction solution
5% v/v formic acid, 50% acetonitrile

Destaining solution
15mM potassium ferricyanide, 50mM sodium thiosulfate

Trypsin solution
10μg trypsin in 600μL of 2mM HCl / 10% ACN, then add 900μL 25mM ABC

MS

Matrix for MALDI-ToF MS
10mg α-cyano-4-hydroxy-cinnaminic acid in 300μl 0.1% v/v trifluoroacetic acid and 700 μl acetonitrile

Western blot

RIPA buffer
150mM NaCl, 65mM Tris Base, 1% v/v Nonidet P40, 0.25% w/v Deoxycholate Acid (Sodium Salt), 10mM EDTA, pH=7.4

RIPA lysis buffer
1mL RIPA buffer, 5μl sodium orthovanadate, 5μl NaF, 1μl leupeptin, 1μl pepstatin,

1μl aprotinin and 2.5μl PMSF

Laemmli buffer
250mM Tris, pH=6.8, 100mM DTT, 10% w/v SDS, 50% glycerol, trace Bromohpenol Blue

Transfer buffer
12mM Tris, 96mM Glycine, 20% v/v methanol

Others

Lysis buffer for GSH reductase activity measurement
containing 50mM Tris and 5mM EDTA (pH 7.5)

Reaction buffer for GSH concentration measurement
275μL of 80mM KH_2PO_4 (pH 8.0) containing 5mM EDTA

Reaction buffer for ATP concentration measurement
1:1:1 mixture of 80mM $MgSO_4 \cdot 7H_2O$ / 10mM KH_2PO_4 / 100mM Na_2AsO_4 (pH 7.4)

Lysis buffer for ROS measurement
0.1% CHAPS, 50mM K_2HPO_4 (pH 7.0), and 0.1 mM EDTA

Protein list of proteome maps

Table 13. Protein list of ES cells proteome map

ID	Protein Name	UniProt Entry Name	UniProt Accession No.	Calculated MM (kDa) / pI	Observed MM (kDa) / pI	Sequence coverage (%)	MASCOT Score
Antioxidants							
106	Peroxiredoxin-2	PRDX2_MOUSE	Q61171	21.647/5.20	21.4/5.1	58.08*	7**
108†	Peroxiredoxin-6	PRDX6_MOUSE	O08709	24.739/5.72	24.7/5.7	55	121
118	Superoxide dismutase [Cu-Zn]	SODC_MOUSE	P08228	15.811/6.03	17.4/5.6	38.96*	5**
120	Superoxide dismutase [Cu-Zn]	SODC_MOUSE	P08228	15.811/6.03	17.4/6.0	39	82
138	Superoxide dismutase [Mn], mitochondrial [Precursor]	SODM_MOUSE	P09671	24.603/8.80	22.2/7.8	40	95
139†	Peroxiredoxin-1	PRDX1_MOUSE	P35700	22.177/8.26	22.2/8.3	50	133
140	Peroxiredoxin-1	PRDX1_MOUSE	P35700	22.177/8.26	22.2/8.5	44	172
Cell Proliferation							
13	Heterogeneous nuclear ribonucleoprotein K	HNRPK_MOUSE	P61979	50.976/5.39	61.6/5.2	20	92
39	Heterogeneous nuclear ribonucleoprotein F	Q9Z2X1_MOUSE	Q9Z2X1	45.730/5.31	49.4/5.2	28	118
40	Eukaryotic translation initiation factor 3 subunit 5	IF35_MOUSE	Q9DCH4	38.000/5.33	48.4/5.3	19	91
44	Protein SET	SET_MOUSE	Q9EQU5	33.378/4.22	42.2/4.5	22	83
46	40S ribosomal protein SA	RSP4_MOUSE	P14206	32.588/4.74	40.4/4.9	30	70
59	Heterogeneous nuclear ribonucleoprotein H	HNRH1_MOUSE	O35737	49.068/5.89	52.6/5.7	44	164
60	Heterogeneous nuclear ribonucleoprotein H'	HNRH2_MOUSE	P70333	49.280/5.89	52.7/5.7	25	76
68	Nucleophosmin	NPM_MOUSE	Q61937	32.560/4.62	35.4/4.9	12.33*	3**
69	Nucleophosmin	NPM_MOUSE	Q61937	32.560/4.62	35.5/5.0	23	111
70	Nascent polypeptide-associated complex subunit alpha	NACA_MOUSE	Q60817	23.384/4.52	33.5/4.5	30	91

72	Proliferating cell nuclear antigen	PCNA_MOUSE	P17918	28.785/4.66	32.1/4.8	27	95
79	Elongation factor 1-beta	EF1B_MOUSE	O70251	24.562/4.53	30.7/4.7	29	87
86	Prohibitin	PHB_MOUSE	P67778	29.820/5.57	27.6/5.5	38	87
102	Prohibitin	PHB_MOUSE	P67778	29.820/5.57	22.8/5.3	28.31*	6**
105	Prohibitin	PHB_MOUSE	P67778	29.820/5.57	21.2/4.9	46.69*	14**
110	Eukaryotic translation initiation factor 5A-1	IF5A1_MOUSE	P63242	16.701/5.08	18.0/5.1	32	82
122	40S ribosomal protein S12	RS12_MOUSE	P63323	14.394/7.02	15.5/6.5	44	70
133	Zfp472 protein	Q8R5B3_MOUSE	Q8R5B3	59.250/8.73	19.5/7.3	22	70
135	mitochondrial ribosomal protein L15	Q9CRH4_MOUSE	Q9CRH4	34.897/10.29	21.9/5.9	24	69
141	Heterogeneous nuclear ribonucleoprotein H	HNRH1_MOUSE	O35737	49.068/5.89	22.8/6.3	21	84
151	High mobility group protein B2	HMGB2_MOUSE	P30681	24.031/7.05	24.7/7.8	12.92*	2**
174	Nucleolin	NUCL_MOUSE	P09405	76.592/4.69	33.8/6.3	15	93
179	Heterogeneous nuclear ribonucleoproteins A2/B1	ROA2_MOUSE	O88569	35.993/8.67	32.4/8.7	23	98
185	Mitotic checkpoint protein BUB3	BUB3_MOUSE	Q9WVA3	36.985/6.21	38.2/6.6	41.10*	12**
186	Poly(rC)-binding protein 1	PCBP1_MOUSE	P60335	37.498/6.66	37.7/6.7	22	72
189	Heterogeneous nuclear ribonucleoprotein A/B	ROAA_MOUSE	Q99020	30.831/7.69	36.7/7.8	32	119
193	Heterogeneous nuclear ribonucleoprotein A/B	ROAA_MOUSE	Q99020	30.831/7.69	39.7/6.0	42.11*	17**
197	Heterogeneous nuclear ribonucleoprotein A/B	ROAA_MOUSE	Q99020	30.831/7.69	39.5/6.4	33	100
200	TAR DNA-binding protein 43	TDBP_MOUSE	Q921F2	44.548/6.26	40.7/6.1	24	133
201	TAR DNA-binding protein 43	TDBP_MOUSE	Q921F2	44.548/6.26	42.5/6.1	22	93
205	Heterogeneous nuclear ribonucleoprotein D0	HNRPD_MOUSE	Q60668	38.354/7.61	42.5/7.8	25	95
208	Antigenic determinant of rec-A protein	Q8K339_MOUSE	Q8K339	44.722/9.14	41.0/8.9	17	64
211	Elongation factor Tu, mitochondrial [Precursor]	EFTU_MOUSE	Q8BFR5	49.508/7.23	43.9/6.4	28	134
212	Proliferation-associated protein 2G4	PA2G4_MOUSE	P50580	43.568/6.40	45.2/6.5	31	166
217	Elongation factor 1-alpha 1	EF1A1_MOUSE	P10126	50.114/9.10	50.5/9.3	21.64*	6**
220	Pre-mRNA-splicing factor 19	PR19_MOUSE	Q99KP6	55.239/6.14	55.3/6.2	23	134
222	RuvB-like 1	RUV1_MOUSE	P60122	50.214/6.02	53.1/6.2	29	135

242	Heterogeneous nuclear ribonucleoprotein L	HNRPL_MOUSE	Q8R081	60.123/6.65	63.2/6.6	19	107
243	Heterogeneous nuclear ribonucleoprotein L	HNRPL_MOUSE	Q8R081	60.123/6.65	63.4/6.7	17	132
244	Heterogeneous nuclear ribonucleoprotein L	HNRPL_MOUSE	Q8R081	60.123/6.65	63.3/6.9	16	118
246	Far upstream element-binding protein 1	FUBP1_MOUSE	Q91WJ8	68.540/7.73	71.1/7.4	16	102
247	Far upstream element-binding protein 1	FUBP1_MOUSE	Q91WJ8	68.540/7.73	70.7/6.9	10	83
253	KH-type splicing regulatory protein	Q3U0V1_MOUSE	Q3U0V1	76.810/6.90	76.9/6.6	20	96
255†	KH-type splicing regulatory protein	Q3U0V1_MOUSE	Q3U0V1	76.810/6.90	76.8/6.9	18	145
258	Elongation factor 2	EF2_MOUSE	P58252	95.183/6.42	86.9/6.7	13	112
Chaperones							
1†	Heat shock protein 4	Q99L75_MOUSE	Q99L75	94.081/5.13	94.1/5.1	24	155
2	Endoplasmin [Precursor]	ENPL_MOUSE	P08113	92.476/4.74	83.9/4.8	19	123
3†	78 kDa glucose-regulated protein [Precursor]	GRP78_MOUSE	P20029	72.422/5.07	72.4/5.1	34	237
4	78 kDa glucose-regulated protein [Precursor]	GRP78_MOUSE	P20029	72.422/5.07	72.3/5.1	16	92
8	Heat shock cognate 71 kDa protein	HSP7C_MOUSE	P63017	70.871/5.37	70.9/5.3	24	136
9†	Heat shock cognate 71 kDa protein	HSP7C_MOUSE	P63017	70.871/5.37	70.9/5.4	30	150
10	Stress-70 protein, mitochondrial [Precursor]	GRP75_MOUSE	P38647	73.528/5.91	71.3/5.4	14.43*	8**
11	Stress-70 protein, mitochondrial [Precursor]	GRP75_MOUSE	P38647	73.528/5.91	71.3/5.5	35	312
12	78 kDa glucose-regulated protein	GRP78_MOUSE	P20029	72.422/5.07	64.3/5.1	31.30*	17**
14	Stress-70 protein, mitochondrial [Precursor]	GRP75_MOUSE	P38647	73.528/5.91	59.7/5.1	13	104
15	Heat shock cognate 71 kDa protein	HSP7C_MOUSE	P63017	70.872/5.37	62.3/5.3	14.86*	7**
18	60 kDa heat shock protein, mitochondrial [Precursor]	CH60_MOUSE	P63038	60.955/5.91	59.6/5.4	22	94
19	60 kDa heat shock protein, mitochondrial [Precursor]	CH60_MOUSE	P63038	60.955/5.91	59.6/5.4	22	115
20	Stress-70 protein, mitochondrial [Precursor]	GRP75_MOUSE	P38647	73.528/5.91	63.5/5.5	16	107
21	Heat shock cognate 71 kDa protein	HSP7C_MOUSE	P63017	70.871/5.37	64.7/5.5	25	132
22	Stress-70 protein, mitochondrial [Precursor]	GRP75_MOUSE	P38647	73.528/5.91	65.1/5.5	15	72
23	Protein disulfide isomerase associated 3	Q99LF6_MOUSE	Q99LF6	56.678/5.88	58.8/5.6	17.62*	7**
24	T-complex protein 1 subunit epsilon	TCPE_MOUSE	P80316	59.624/5.72	60.2/5.6	14	90

25	Protein disulfide-isomerase A3 [Precursor]	PDIA3_MOUSE	P27773	56.621/5.99	58.4/5.7	32	135
26	T-complex protein 1 subunit alpha B	TCPA2_MOUSE	P11983	60.449/5.82	59.2/5.7	21	117
27	Calreticulin [Precursor]	CRTC_MOUSE	P14211	47.995/4.33	61.1/4.5	20	94
28	Protein disulfide-isomerase [Precursor]	PDIA1_MOUSE	P09103	57.144/4.79	58.1/4.9	27	203
29	Endoplasmin [Precursor]	ENPL_MOUSE	P08113	92.476/4.74	55.5/4.8	23.94*	17**
37	Protein disulfide-isomerase A6 [Precursor]	PDIA6_MOUSE	Q922R8	48.100/5.00	51.4/5.1	22	96
43	Calreticulin [Precursor]	CRTC_MOUSE	P14211	47.995/4.33	48.4/4.5	18.51*	4**
47	Heat shock cognate 71 kDa protein	HSP7C_MOUSE	P63017	70.871/5.37	40.7/5.1	18	64
54	Protein disulfide-isomerase [Precursor]	PDIA1_MOUSE	P09103	57.144/4.79	39.8/5.1	5.31*	2**
61	Heat shock cognate 71 kDa protein	HSP7C_MOUSE	P63017	70.871/5.37	50.7/5.8	19	118
63	60 kDa heat shock protein, mitochondrial [Precursor]	CH60_MOUSE	P63038	60.955/5.91	45.9/5.7	20	84
65	Heat shock cognate 71 kDa protein	HSP7C_MOUSE	P63017	70.871/5.37	41.6/5.8	16	104
73	60 kDa heat shock protein, mitochondrial [Precursor]	CH60_MOUSE	P63038	60.955/5.91	32.5/5.1	20	70
87	Protein disulfide isomerase associated 3	Q99LF6_MOUSE	Q99LF6	56.678/5.88	28.4/5.6	11	70
88	Protein disulfide-isomerase A3 [Precursor]	PDIA3_MOUSE	P27773	56.621/5.99	29.5/5.6	18.25*	9**
89	Protein disulfide-isomerase A3 [Precursor]	PDIA3_MOUSE	P27773	56.621/5.99	29.8/5.7	13	98
103	Translationally-controlled tumor protein	TCTP_MOUSE	P63028	19.462/4.76	22.2/4.9	33	83
119	Heat shock-related 70kD protein 2	HSP72_MOUSE	P17156	69.741/5.58	14.9/5.6	3.79*	2**
136	GrpE protein homolog 1, mitochondrial [Precursor]	GRPE1_MOUSE	Q99LP6	24.307/8.58	21.5/5.9	37	82
145	Heat-shock protein beta-1	HSPB1_MOUSE	P14602	23.014/6.12	25.0/6.0	47	169
153	Endoplasmic reticulum protein ERp29 [Precursor]	ERP29_MOUSE	P57759	28.823/5.90	26.9/6.0	26	91
156	Heat shock cognate 71 kDa protein	HSP7C_MOUSE	P63017	70.871/5.37	26.6/8.0	15	100
159	Heat shock cognate 71 kDa protein	HSP7C_MOUSE	P63017	70.871/5.37	27.9/8.6	19	139
165	Heat shock cognate 71 kDa protein	HSP7C_MOUSE	P63017	70.871/5.37	32.0/6.4	13.93*	8**
182	Heat shock cognate 71 kDa protein	HSP7C_MOUSE	P63017	70.871/5.37	35.8/6.3	15	77
195	Protein disulfide-isomerase A6 [Precursor]	PDIA6_MOUSE	Q922R8	48.100/5.00	39.4/6.2	15	69
216	47 kDa heat shock protein [Precursor]	HSP47_MOUSE	P19324	46.590/8.90	46.3/8.8	35.01*	8**

218	T-complex protein 1 subunit beta	TCPB_MOUSE	P80314	57.346/5.98	54.5/6.0	32	145
236	T-complex protein 1 subunit zeta	TCPZ_MOUSE	P80317	57.873/6.67	60.1/6.7	23	127
239	T-complex protein 1 subunit gamma	TCPG_MOUSE	P80318	60.630/6.28	64.0/6.3	25	150
240	Stress-induced-phosphoprotein 1	STI1_MOUSE	Q60864	62.582/6.40	61.5/6.4	34	182
Enzymes							
30	Histone-binding protein RBBP4	RBBP4_MOUSE	Q60972	47.524/4.79	55.0/4.8	22.77*	7**
34	Histone-binding protein RBBP7	RBBP7_MOUSE	Q60973	47.790/4.89	52.9/5.1	19	85
35	ATP synthase beta chain, mitochondrial [Precursor]	ATPB_MOUSE	P56480	56.300/5.19	52.6/5.1	49.34*	18**
36	ATP synthase beta chain, mitochondrial [Precursor]	ATPB_MOUSE	P56480	56.300/5.19	52.6/5.1	32	161
38	26S protease regulatory subunit 6B	PRS6B_MOUSE	P54775	47.281/5.18	49.8/5.1	27	120
42	Thioredoxin domain-containing protein 5 [Precursor]	TXND5_MOUSE	Q91W90	46.415/5.51	45.7/5.1	10.55*	3**
48	ATP synthase beta chain, mitochondrial [Precursor]	ATPB_MOUSE	P56480	56.300/5.19	44.7/5.1	35.73*	13**
64	Ornithine aminotransferase, mitochondrial [Precursor]	OAT_MOUSE	P29758	48.355/6.19	44.2/5.7	25	141
75	Inorganic pyrophosphatase	IPYR_MOUSE	Q9D819	32.667/5.37	32.7/5.3	25	86
76	Pyruvate dehydrogenase E1 component subunit beta, mitochondrial [Precursor]	ODPB_MOUSE	Q9D051	38.937/6.41	32.3/5.5	33	91
77	Pyruvate kinase isozyme M2	KPYM_MOUSE	P52480	57.756/7.42	32.8/5.5	4.33*	2**
83	tyrosine 3-monooxygenase/tryptophan 5-monooxygenase activation protein, epsilon polypeptide	Q8BPH1_MOUSE	Q8BPH1	29.189/4.63	29.4/4.7	36	114
92	Proteasome subunit alpha type 5	PSA5_MOUSE	Q9Z2U1	26.411/4.74	26.6/4.8	40	115
99	ATP synthase beta chain, mitochondrial [Precursor]	ATPB_MOUSE	P56480	56.300/5.19	23.9/5.1	15.69*	5**
104	Lactoylglutathione lyase	LGUL_MOUSE	Q9CPU0	20.678/5.25	22.1/5.1	28	113
109	UMP-CMP kinase	KCY_MOUSE	Q9DBP5	22.166/5.68	21.9/5.6	16.33*	3**
114	Mitochondrial import inner membrane translocase subunit Tim8 A	TIM8A_MOUSE	Q9WVA2	11.042/5.11	14.4/5.0	34.02*	3**
116	Cytochrome c oxidase polypeptide Va, mitochondrial [Precursor]	COX5A_MOUSE	P12787	16.030/6.08	14.5/5.1	17.93*	3**

121	Histidine triad nucleotide-binding protein 1	HINT1_MOUSE	P70349	13.646/6.39	15.2/6.3	23.81*	4**
125	Nucleoside diphosphate kinase A	NDKA_MOUSE	P15532	17.208/6.84	17.4/6.6	53	119
126	Peptidyl-prolyl cis-trans isomerase A	PPIA_MOUSE	P17742	17.840/7.88	17.8/6.6	30.49*	8**
127	Nucleoside diphosphate kinase B	NDKB_MOUSE	Q01768	17.363/6.97	18.3/7.3	69	135
128	Peptidyl-prolyl cis-trans isomerase A	PPIA_MOUSE	P17742	17.840/7.88	18.0/7.7	52	126
129	Peptidyl-prolyl cis-trans isomerase A	PPIA_MOUSE	P17742	17.840/7.88	17.8/8.0	53	133
134	Adenine phosphoribosyltransferase	APT_MOUSE	P08030	19.736/6.31	21.9/5.9	61	142
142	Proteasome subunit alpha type 2	PSA2_MOUSE	P49722	25.794/8.42	23.0/6.7	29	64
146	Proteasome subunit alpha type 6	PSA6_MOUSE	Q9QUM9	27.372/6.35	25.9/6.2	47	102
148	Alpha-enolase	ENOA_MOUSE	P17182	47.010/6.36	25.9/6.7	17.74*	6**
149	Triosephosphate isomerase	TPIS_MOUSE	P17751	26.581/7.09	25.0/6.7	45.78*	9**
150	Triosephosphate isomerase	TPIS_MOUSE	P17751	26.581/7.09	25.1/7.4	34	151
152	Proteasome subunit beta type 7 [Precursor]	PSB7_MOUSE	P70195	29.891/8.14	27.4/5.9	15	90
154	Phosphoglycerate mutase 1	PGAM1_MOUSE	Q9DBJ1	28.701/6.75	26.8/6.7	32	89
155	Adenylate kinase isoenzyme 2, mitochondrial	KAD2_MOUSE	Q9WTP6	25.474/7.16	27.0/7.6	46	84
157	Electron transfer flavoprotein subunit beta	ETFB_MOUSE	Q9DCW4	27.492/8.29	26.8/8.4	44	113
158	Proteasome subunit alpha type 7-like	PS7L_MOUSE	Q9CWH6	27.866/8.81	26.4/8.6	10.00*	2**
161†	Proteasome subunit alpha type 1	PSA1_MOUSE	Q9R1P4	29.547/6.00	29.5/6.0	22	79
163	26S proteasome non-ATPase regulatory subunit 14	PSDE_MOUSE	O35593	34.577/6.06	32.0/5.9	22	90
164	Uridine phosphorylase 1	UPP1_MOUSE	P52624	34.086/6.12	31.5/6.2	29	108
169	Electron transfer flavoprotein subunit alpha, mitochondrial [Precursor]	ETFA_MOUSE	Q99LC5	35.039/8.62	31.1/7.3	34	124
170	L-lactate dehydrogenase A chain	LDHA_MOUSE	P06151	36.367/7.76	32.2/7.8	32	128
175	Aldose reductase	ALDR_MOUSE	P45376	35.601/6.79	33.5/6.7	30	108
177	Glyceraldehyde-3-phosphate dehydrogenase	G3P_MOUSE	P16858	35.679/8.45	33.3/8.2	22	111
178	Glyceraldehyde-3-phosphate dehydrogenase	G3P_MOUSE	P16858	35.679/8.45	33.4/8.5	27	79
184	Alcohol dehydrogenase [NADP+]	AK1A1_MOUSE	Q9JII6	36.456/6.87	35.5/7.1	18	89

187	Alcohol dehydrogenase class 3	ADHX_MOUSE	P28474	39.502/7.59	37.9/6.8	24	86
188	40 kDa peptidyl-prolyl cis-trans isomerase	PPID_MOUSE	Q9CR16	40.611/7.06	37.8/7.4	26	104
190	Fructose-bisphosphate aldolase A	ALDOA_MOUSE	P05064	39.225/8.40	37.8/7.9	32	140
191	Fructose-bisphosphate aldolase A	ALDOA_MOUSE	P05064	39.225/8.40	37.6/8.1	31	133
192	Fructose-bisphosphate aldolase A	ALDOA_MOUSE	P05064	39.225/8.40	37.4/8.3	35	178
194	Alpha-enolase	ENOA_MOUSE	P17182	47.010/6.36	39.7/6.1	21	93
198	Aspartate aminotransferase, cytoplasmic	AATC_MOUSE	P05201	46.100/6.75	39.2/7.1	26	152
199	Aspartate aminotransferase, cytoplasmic	AATC_MOUSE	P05201	46.100/6.75	39.4/7.1	45	270
202	2-amino-3-ketobutyrate coenzyme A ligase, mitochondrial [Precursor]	KBL_MOUSE	O88986	44.931/6.92	41.1/6.7	20	79
203	Isocitrate dehydrogenase [NADP] cytoplasmic	IDHC_MOUSE	O88844	46.660/6.48	42.5/6.8	42.51*	16**
204	26S protease regulatory subunit S10B	PRS10_MOUSE	P62334	44.173/7.09	40.4/7.4	31	130
206	Medium-chain specific acyl-CoA dehydrogenase, mitochondrial [Precursor]	ACADM_MOUSE	P45952	46.481/8.60	40.6/7.8	18	90
207	Phosphoglycerate kinase 1	PGK1_MOUSE	P09411	44.405/7.52	41.3/8.1	17	75
209	Alpha-enolase	ENOA_MOUSE	P17182	47.010/6.36	47.5/6.0	30	110
210	Alpha-enolase	ENOA_MOUSE	P17182	47.010/6.36	47.8/6.2	29	126
213	26S protease regulatory subunit 8	PRS8_MOUSE	P62196	45.626/7.11	45.0/7.1	15	72
219	3-phosphoglycerate dehydrogenase	Q8C603_MOUSE	Q8C603	56.582/5.69	56.7/6.1	10	72
221	Uridine 5'-monophosphate synthase	PYR5_MOUSE	P13439	52.292/6.17	53.5/6.2	15	99
223	Aldehyde dehydrogenase, mitochondrial [Precursor]	ALDH2_MOUSE	P47738	56.538/7.53	52.0/6.3	22	145
226	Serine hydroxymethyltransferase, cytosolic	GLYC_MOUSE	P50431	52.585/6.47	51.3/6.5	21	115
227	Glutamate dehydrogenase 1, mitochondrial [Precursor]	DHE3_MOUSE	P26443	61.337/8.05	53.0/6.9	13	85
228	Serine hydroxymethyl transferase 2	Q99K87_MOUSE	Q99K87	55.761/8.72	53.1/8.1	34	237
229	ATP synthase alpha chain, mitochondrial [Precursor]	ATPA_MOUSE	Q03265	59.753/9.22	53.4/8.2	32	190
230	Dihydrolipoyl dehydrogenase, mitochondrial [Precursor]	DLDH_MOUSE	O08749	54.212/7.97	57.1/6.6	14	95
231	Leucine aminopeptidase 3	Q99P44_MOUSE	Q99P44	56.141/7.61	55.9/6.6	19	102

232	Cytosol aminopeptidase	AMPL_MOUSE	Q9CPY7	52.619/6.56	55.6/6.7	18	121
234	Inosine-5'-monophosphate dehydrogenase 2	IMDH2_MOUSE	P24547	55.815/6.84	55.1/6.9	22	90
235	Succinyl-CoA:3-ketoacid-coenzyme A transferase 1, mitochondrial [Precursor]	SCOT_MOUSE	Q9D0K2	55.989/8.73	55.7/7.4	15.48*	3**
237	Pyruvate kinase isozyme M2	KPYM_MOUSE	P52480	57.756/7.42	59.3/7.3	24	121
238	Pyruvate kinase isozyme M2	KPYM_MOUSE	P52480	57.756/7.42	59.1/7.7	35	130
241	Bifunctional purine biosynthesis protein PURH	PUR9_MOUSE	Q9CWJ9	64.157/6.30	62.5/6.5	23	115
245	Transketolase	TKT_MOUSE	P40142	67.630/7.23	65.0/7.6	26	198
248	Phosphoenolpyruvate carboxykinase [GTP], mitochondrial [Precursor]	PPCKM_MOUSE	Q8BH04	70.528/6.92	65.7/6.4	17	119
250	Glycerol-3-phosphate dehydrogenase, mitochondrial [Precursor]	GPDM_MOUSE	Q64521	80.900/6.17	69.4/5.9	14	69
254	ATP-dependent RNA helicase DDX3X	DDX3X_MOUSE	Q62167	72.970/6.73	73.5/6.7	27	192
256	Aconitate hydratase, mitochondrial [Precursor]	ACON_MOUSE	Q99KI0	85.464/8.08	77.2/7.8	23	137
257	ATP-dependent metalloprotease YME1L1	YMEL1_MOUSE	O88967	80.028/9.01	73.5/8.5	11	71
259	Trifunctional purine biosynthetic protein adenosine-3	PUR2_MOUSE	Q64737	107.395/6.25	92.4/6.4	11	95
Others							
49	Methylosome protein 50	MEP50_MOUSE	Q99J09	36.943/5.09	42.5/5.1	9.36*	2**
57	Suppressor of G2 allele of SKP1 homolog	SUGT1_MOUSE	Q9CX34	38.028/5.32	37.2/5.2	29	114
90	HIRA-interacting protein 5	HIRP5_MOUSE	Q9QZ23	22.140/4.23	25.9/4.5	26.13*	4**
107	Phosphatidylethanolamine-binding protein 1	PEBP1_MOUSE	P70296	20.699/5.19	21.4/5.1	22	71
147	Protein C14orf166 homolog	CN166_MOUSE	Q9CQE8	28.152/6.40	25.0/6.4	52.87*	15**
160	Protein C14orf166 homolog	CN166_MOUSE	Q9CQE8	28.152/6.40	28.3/6.2	21.72*	4**
168	similar to 3' of D-CONTAINING PROTEIN [Fragment]	Q8BZS8_MOUSE	Q8BZS8	31.265/8.22	31.8/7.4	33	75
183	LIM and SH3 domain protein 1	LASP1_MOUSE	Q61792	29.994/6.61	34.8/6.5	27	81
Signalling molecules							
62	Rab GDP dissociation inhibitor beta	GDIB_MOUSE	Q61598	50.537/5.93	47.9/5.8	20	97

67	Hyaluronan mediated motility receptor	HMMR_MOUSE	Q00547	91.800/5.47	36.5/5.1	13	68
84	Tumor necrosis factor receptor superfamily member 5 [Precursor]	TNR5_MOUSE	P27512	32.111/6.30	28.9/5.0	26	72
96	Ran-specific GTPase-activating protein	RANG_MOUSE	P34022	23.596/5.15	26.4/5.1	26	80
100	Rho GDP-dissociation inhibitor 1	GDIR_MOUSE	Q99PT1	23.276/5.12	24.4/5.1	36	155
115	SH3 domain-binding glutamic acid-rich-like protein	SH3L1_MOUSE	Q9JJU8	12.811/4.87	14.6/5.0	11.40*	1**
143	GTP-binding nuclear protein Ran	RAN_MOUSE	P62827	24.292/7.20	22.4/7.0	53	164
144	GTP-binding nuclear protein Ran	RAN_MOUSE	P62827	24.292/7.20	22.6/7.4	16.67*	6**
171†	guanine nucleotide binding protein, beta 2, related sequence 1	Q9CSQ0_MOUSE	Q9CSQ0	30.961/7.72	31.0/7.7	62	203
181	TNF receptor-associated factor 5	TRAF5_MOUSE	P70191	61.145/7.71	35.4/6.1	16	63
233	Hypothetical protein D10Wsu52e	Q99LF4_MOUSE	Q99LF4	55.249/6.77	56.5/6.9	24	128
Structural proteins							
6	Lamin-B1	LMNB1_MOUSE	P14733	66.654/5.11	66.5/5.1	28	142
7†	Lamin-B1	LMNB1_MOUSE	P14733	66.654/5.11	66.7/5.1	33	191
17	Lamin-B1	LMNB1_MOUSE	P14733	66.654/5.11	58.8/5.4	18.20*	9**
31	Tubulin beta-5 chain	TBB5_MOUSE	P99024	49.671/4.78	54.6/5.1	27	110
32	Vimentin	VIME_MOUSE	P20152	53.556/5.06	56.9/5.1	26	104
41	Vimentin	VIME_MOUSE	P20152	53.556/5.06	46.1/5.1	2.15*	1**
50	Actin, cytoplasmic 1	ACTB_MOUSE	P60710	41.737/5.29	42.0/5.1	27	120
51†	Actin, cytoplasmic 1	ACTB_MOUSE	P60710	41.737/5.29	41.7/5.3	29	123
52	Actin, cytoplasmic 2	ACTG_MOUSE	P63260	41.793/5.31	41.9/5.3	25	101
53	Actin, cytoplasmic 1	ACTB_MOUSE	P60710	41.737/5.29	41.7/5.4	4.20*	1**
55	Actin, cytoplasmic 1	ACTB_MOUSE	P60710	41.737/5.29	40.1/5.1	18	85
80	Tropomyosin 3, gamma	Q8K0Z5_MOUSE	Q8K0Z5	33.149/4.73	30.9/4.8	14.11*	3**
81	Actin, cytoplasmic 1	ACTB_MOUSE	P60710	41.737/5.29	30.9/5.3	9.04*	3**
82	Actin, cytoplasmic 1	ACTB_MOUSE	P60710	41.737/5.29	31.0/5.3	13.83*	4**

85	Actin, cytoplasmic 2	ACTG_MOUSE	P63260	41.793/5.31	28.1/5.4	16	68
97	Actin, cytoplasmic 1	ACTB_MOUSE	P60710	41.737/5.29	25.8/5.4	20	110
98	Tubulin beta-3 chain	TBB3_MOUSE	Q9ERD7	50.419/4.82	23.9/4.8	9.78*	3**
112†	Myosin light polypeptide 6	MYL6_MOUSE	Q60605	16.799/4.56	16.8/4.5	47	106
124†	Profilin-1	PROF1_MOUSE	P62962	14.826/8.50	14.8/8.5	68	143
131†	Cofilin-1	COF1_MOUSE	P18760	18.428/8.26	18.4/8.2	46	128
132	Cofilin-1	COF1_MOUSE	P18760	18.428/8.26	18.4/8.5	30	73
137	Transgelin 2	Q91VU2_MOUSE	Q91VU2	22.395/8.40	21.2/8.4	63	113
172	Voltage-dependent anion-selective channel protein 1	VDAC1_MOUSE	Q60932	32.351/8.55	30.9/8.7	30	111
176	Annexin A2	ANXA2_MOUSE	P07356	38.545/7.53	33.5/8.0	20.71*	6**
180	Apolipoprotein A-IV [Precursor]	APOA4_MOUSE	P06728	45.029/5.41	36.9/6.0	24	71
224	Fascin	FSCN1_MOUSE	Q61553	54.274/6.21	53.1/6.4	46.04*	23**
225	Septin-11	SEP11_MOUSE	Q8C1B7	49.563/6.26	51.7/6.5	42	113
251	Ezrin	EZRI_MOUSE	P26040	69.276/5.83	74.9/5.8	21	124
252	Mitochondrial inner membrane protein	IMMT_MOUSE	Q8CAQ8	83.900/6.18	77.2/5.8	13	88
Unidentified							
5	Unidentified	-	-	-	65.5/4.8	-	-
16	Unidentified	-	-	-	58.0/5.3	-	-
33	Unidentified	-	-	-	54.1/5.4	-	-
45	Unidentified	-	-	-	44.7/4.7	-	-
56	Unidentified	-	-	-	38.5/5.1	-	-
58	Unidentified	-	-	-	46.0/5.6	-	-
66	Unidentified	-	-	-	37.1/5.7	-	-
71	Unidentified	-	-	-	33.4/5.1	-	-
74	Unidentified	-	-	-	32.0/5.1	-	-
78	Unidentified	-	-	-	30.9/4.5	-	-
91	Unidentified	-	-	-	26.5/4.7	-	-

93	Unidentified	-	-	-	27.2/5.0	-	-
94	Unidentified	-	-	-	27.6/5.1	-	-
95	Unidentified	-	-	-	25.9/5.0	-	-
101	Unidentified	-	-	-	22.8/5.2	-	-
111	Unidentified	-	-	-	17.1/5.0	-	-
113	Unidentified	-	-	-	14.3/4.8	-	-
117	Unidentified	-	-	-	18.3/5.6	-	-
123	Unidentified	-	-	-	12.7/7.5	-	-
130	Unidentified	-	-	-	17.3/8.5	-	-
162	Unidentified	-	-	-	30.4/6.3	-	-
166	Unidentified	-	-	-	31.9/6.6	-	-
167	Unidentified	-	-	-	31.1/6.9	-	-
173	Unidentified	-	-	-	31.8/9.3	-	-
196	Unidentified	-	-	-	39.1/6.3	-	-
214	Unidentified	-	-	-	45.9/8.1	-	-
215	Unidentified	-	-	-	48.4/8.6	-	-
249	Unidentified	-	-	-	71.6/6.4	-	-

† Reference spots for generating the Mr/pI grid picture (Figure 29).

* Data aquired by MS/MS; others by MALDI-ToF MS.

** Number of matched peptides in MS/MS identifications.

Table 14. Protein list of Sca-1$^+$ progenitor cells proteome map

ID	Protein Name	UniProt Entry Name	UniProt Accession No.	Calculated MM (kDa) / pI	Observed MM (kDa) / pI	Sequence coverage (%)	MASCOT Score
Antioxidants							
33	Protein disulfide-isomerase A6 [Precursor]	PDIA6_MOUSE	Q922R8	48.100/5.00	51.4/5.1	22	96
41	Thioredoxin domain containing protein 5 [Precursor]	TXND5_MOUSE	Q91W90	46.415/5.51	45.7/5.1	10.55 a)	3 b)
116	Superoxide dismutase [Cu-Zn]	SODC_MOUSE	P08228	15.811/6.03	17.4/5.6	38.96 a)	5 b)
119	Superoxide dismutase [Cu-Zn]	SODC_MOUSE	P08228	15.811/6.03	17.4/6.0	39	82
142	Superoxide dismutase [Mn], mitochondrial [Precursor]	SODM_MOUSE	P09671	24.603/8.8	22.2/7.8	40	95
143	Peroxiredoxin 1	PRDX1_MOUSE	P35700	22.177/8.26	22.2/8.3	50	133
144	Peroxiredoxin 1	PRDX1_MOUSE	P35700	22.177/8.26	22.2/8.5	44	172
151	Peroxiredoxin 6	PRDX6_MOUSE	O08709	24.739/5.72	24.9/5.7	55	121
Chaperones							
1	Heat shock protein 4	Q99L75_MOUSE	Q99L75	94.081/5.13	94.0/5.1	24	155
3	Endoplasmin [Precursor]	ENPL_MOUSE	P08113	92.476/4.74	83.9/4.8	19	123
4	78 kDa glucose-regulated protein [Precursor]	GRP78_MOUSE	P20029	72.422/5.07	72.4/5.1	34	237
5	78 kDa glucose-regulated protein [Precursor]	GRP78_MOUSE	P20029	72.422/5.07	72.3/5.1	16	92
8	Heat shock cognate 71 kDa protein	HSP7C_MOUSE	P63017	70.871/5.37	70.9/5.3	24	136
9	Heat shock cognate 71 kDa protein	HSP7C_MOUSE	P63017	70.871/5.37	70.8/5.4	30	150
10	Stress-70 protein, mitochondrial [Precursor]	GRP75_MOUSE	P38647	73.528/5.91	71.3/5.4	14.43 a)	8 b)
11	Stress-70 protein, mitochondrial [Precursor]	GRP75_MOUSE	P38647	73.528/5.91	71.3/5.5	35	312
13	Stress-70 protein, mitochondrial [Precursor]	GRP75_MOUSE	P38647	73.528/5.91	65.1/5.5	15	72
14	Heat shock cognate 71 kDa protein	HSP7C_MOUSE	P63017	70.871/5.37	64.7/5.5	25	132
15	Stress-70 protein, mitochondrial [Precursor]	GRP75_MOUSE	P38647	73.528/5.91	63.5/5.5	16	107

17	60 kDa heat shock protein, mitochondrial [Precursor]	CH60_MOUSE	P63038	60.955/5.91	59.6/5.4	22	115
18	60 kDa heat shock protein, mitochondrial [Precursor]	CH60_MOUSE	P63038	60.955/5.91	59.6/5.4	22	94
21	78 kDa glucose-regulated protein [Precursor]	GRP78_MOUSE	P20029	72.422/5.07	64.3/5.1	31.30 a)	17 b)
23	Stress-70 protein, mitochondrial [Precursor]	GRP75_MOUSE	P38647	73.528/5.91	59.7/5.1	13	104
25	Protein disulfide isomerase [Precursor]	PDIA1_MOUSE	P09103	57.144/4.79	58.1/4.9	27	203
26	Endoplasmin [Precursor]	ENPL_MOUSE	P08113	92.476/4.74	55.5/4.8	23.94 a)	17 b)
28	Calreticulin [Precursor]	CRTC_MOUSE	P14211	47.995/4.33	61.1/4.5	20	94
43	Calreticulin [Precursor]	CRTC_MOUSE	P14211	47.995/4.33	48.4/4.4	18.51 a)	4 b)
46	Heat shock cognate 71 kDa protein	HSP7C_MOUSE	P63017	70.871/5.37	40.7/5.1	18	64
53	Protein disulfide isomerase [Precursor]	PDIA1_MOUSE	P09103	57.144/4.79	39.8/5.1	5.31 a)	2 b)
62	60 kDa heat shock protein, mitochondrial [Precursor]	CH60_MOUSE	P63038	60.955/5.91	32.5/5.1	20	70
117	Heat shock-related 70kD protein 2	HSP72_MOUSE	P17156	69.741/5.58	14.9/5.6	3.79 a)	2 b)
140	GrpE protein homolog 1, mitochondrial [Precursor]	GRPE1_MOUSE	Q99LP6	24.307/8.58	21.5/5.9	37	82
153	Heat-shock protein beta-1	HSPB1_MOUSE	P14602	23.014/6.12	25.0/6.0	47	169
161	Endoplasmic reticulum protein ERp29 [Precursor]	ERP29_MOUSE	P57759	28.823/5.90	26.9/6.0	26	91
164	Heat shock cognate 71 kDa protein	HSP7C_MOUSE	P63017	70.871/5.37	27.4/8.0	15	100
167	Heat shock cognate 71 kDa protein	HSP7C_MOUSE	P63017	70.871/5.37	27.9/8.6	19	139
168	Protein disulfide isomerase associated 3	Q99LF6_MOUSE	Q99LF6	56.678/5.88	28.4/5.6	11	70
169	Protein disulfide isomerase A3 precursor	PDIA3_MOUSE	P27773	56.621/5.99	29.5/5.6	18.25 a)	9 b)
170	Protein disulfide-isomerase A3 [Precursor]	PDIA3_MOUSE	P27773	56.621/5.99	29.8/5.7	13	98
185	Heat shock cognate 71 kDa protein	HSP7C_MOUSE	P63017	70.871/5.37	31.7/6.4	13.93 a)	8 b)
200	Heat shock cognate 71 kDa protein	HSP7C_MOUSE	P63017	70.871/5.37	35.8/6.3	15	77
210	DnaJ homolog subfamily B member 11 [Precursor]	DNJBB_MOUSE	Q99KV1	40.555/5.92	39.7/6.0	23.18 a)	9 b)
230	47 kDa heat shock protein [Precursor]	HSP47_MOUSE	P19324	46.590/8.90	46.3/8.8	35.01 a)	8 b)
234	T complex protein-10 (Tcp-10b) mRNA. [Fragment]	O35706_MOUSE	O35706	45.306/5.60	47.8/5.7	13	65
236	Heat shock cognate 71 kDa protein	HSP7C_MOUSE	P63017	70.871/5.37	41.6/5.8	16	104
237	60 kDa heat shock protein, mitochondrial [Precursor]	CH60_MOUSE	P63038	60.955/5.91	45.9/5.7	20	84

239	Heat shock cognate 71 kDa protein	HSP7C_MOUSE	P63017	70.871/5.37	50.7/5.8	19	118
244	Protein disulfide isomerase associated 3	Q99LF6_MOUSE	Q99LF6	56.678/5.88	58.8/5.6	17.62 a)	7 b)
245	T-complex protein 1, epsilon subunit	TCPE_MOUSE	P80316	59.624/5.72	60.2/5.6	14	90
246	Protein disulfide-isomerase A3 [Precursor]	PDIA3_MOUSE	P27773	56.621/5.99	58.4/5.7	32	135
247	T-complex protein 1, alpha subunit B	TCPA2_MOUSE	P11983	60.449/5.82	59.2/5.7	21	117
249	T-complex protein 1, beta subunit	TCPB_MOUSE	P80314	57.346/5.98	54.5/6.0	32	145
263	T-complex protein 1, gamma subunit	TCPG_MOUSE	P80318	60.630/6.28	64.0/6.3	25	150
265	Stress-induced-phosphoprotein 1	STIP1_MOUSE	Q60864	62.582/6.40	61.5/6.4	34	182
270	T-complex protein 1, zeta subunit	TCPZ_MOUSE	P80317	57.873/6.67	60.1/6.7	23	127
288	Heat shock protein 75 kDa, mitochondrial [Precursor]	TRAP1_MOUSE	Q9CQN1	80.209/6.25	71.0/5.7	17	135
DNA maintenance, transcription and translation							
16	Heterogeneous nuclear ribonucleoprotein K	HNRPK_MOUSE	P61979	50.976/5.39	62.2/5.4	25	121
22	Heterogeneous nuclear ribonucleoprotein K	HNRPK_MOUSE	P61979	50.976/5.39	61.6/5.2	20	92
27	Chromatin assembly factor 1 subunit C	RBBP4_MOUSE	Q60972	51.770/4.95	55.0/4.8	22.77 a)	7 b)
30	Histone acetyltransferase type B subunit 2	RBBP7_MOUSE	Q60973	47.790/4.89	52.9/5.1	19	85
36	Heterogeneous nuclear ribonucleoprotein F	Q9Z2X1_MOUSE	Q9Z2X1	45.730/5.31	49.4/5.2	28	118
37	Eukaryotic translation initiation factor 3 subunit 5	IF35_MOUSE	Q9DCH4	38.000/5.33	48.4/5.3	19	91
44	SET protein	SET_MOUSE	Q9EQU5	33.378/4.22	42.2/4.5	22	83
45	40S ribosomal protein SA	RSSA_MOUSE	P14206	32.588/4.74	40.4/4.9	30	70
57	Nucleophosmin	NPM_MOUSE	Q61937	32.560/4.62	35.5/5.0	23	111
58	Nucleophosmin	NPM_MOUSE	Q61937	32.560/4.62	35.4/4.9	12.33 a)	3 b)
59	Nascent polypeptide-associated complex alpha subunit	NACA_MOUSE	Q60817	23.384/4.52	33.5/4.4	30	91
60	Proliferating cell nuclear antigen	PCNA_MOUSE	P17918	28.785/4.66	32.1/4.8	27	95
65	Ribosome biogenesis regulatory protein homolog	RRS1_MOUSE	Q9CYH6	41.552/10.77	32.1/5.2	30	62
71	Elongation factor 1-beta	EF1B_MOUSE	O70251	24.562/4.53	30.7/4.7	29	87
85	Prohibitin	PHB_MOUSE	P67778	29.820/5.57	27.6/5.5	38	87
93	Prohibitin	PHB_MOUSE	P67778	29.820/5.57	22.8/5.3	28.31 a)	6 b)

94	Translationally controlled tumor protein	TCTP_MOUSE	P63028	19.462/4.76	22.2/4.9	33	83
98	Prohibitin	PHB_MOUSE	P67778	29.820/5.57	21.2/4.9	46.69 a)	14 b)
106	Eukaryotic translation initiation factor 5A	IF5A_MOUSE	P63242	16.701/5.08	18.0/5.1	32	82
121	40S ribosomal protein S12	RS12_MOUSE	P63323	14.394/7.02	15.5/6.5	44	70
135	Zfp472 protein	Q8R5B3_MOUSE	Q8R5B3	59.250/8.73	19.5/7.3	22	70
139	mitochondrial ribosomal protein L15, full insert sequence. [Fragment]	Q9CRH4_MOUSE	Q9CRH4	34.897/10.29	21.9/5.9	24	69
147	Heterogeneous nuclear ribonucleoprotein H	HNRH1_MOUSE	O35737	49.068/5.89	22.8/6.3	21	84
188	Heterogeneous nuclear ribonucleoproteins A2/B1	ROA2_MOUSE	O88569	35.993/8.67	32.4/8.7	23	98
189	Nucleolin	NUCL_MOUSE	P09405	76.592/4.69	33.8/6.3	15	93
202	Heterogeneous nuclear ribonucleoprotein A/B	ROAA_MOUSE	Q99020	30.831/7.69	36.7/7.8	32	119
208	Poly(rC)-binding protein 1	PCBP1_MOUSE	P60335	37.498/6.66	37.7/6.7	22	72
209	Mitotic checkpoint protein BUB3	BUB3_MOUSE	Q9WVA3	36.985/6.21	38.2/6.6	41.10 a)	12 b)
214	Heterogeneous nuclear ribonucleoprotein A/B	ROAA_MOUSE	Q99020	30.831/7.69	39.5/6.4	33	100
217	TAR DNA-binding protein-43	TADBP_MOUSE	Q921F2	44.548/6.26	40.7/6.1	24	133
218	TAR DNA-binding protein-43	TADBP_MOUSE	Q921F2	44.548/6.26	42.5/6.1	22	93
224	Heterogeneous nuclear ribonucleoprotein D0	HNRPD_MOUSE	Q60668	38.354/7.61	42.5/7.8	25	95
231	Antigenic determinant of rec-A protein	Q8K339_MOUSE	Q8K339	44.722/9.14	41.0/8.9	17	64
240	Heterogeneous nuclear ribonucleoprotein H	HNRH2_MOUSE	P70333	49.280/5.89	52.7/5.7	25	76
241	Heterogeneous nuclear ribonucleoprotein H	HNRH1_MOUSE	O35737	49.068/5.89	52.6/5.7	44	164
251	PRP19/PSO4 homolog	PRP19_MOUSE	Q99KP6	55.239/6.14	55.3/6.2	23	134
253	RuvB-like 1	RUVB1_MOUSE	P60122	50.214/6.02	53.1/6.2	29	135
259	Elongation factor Tu, mitochondrial [Precursor]	EFTU_MOUSE	Q8BFR5	49.876/7.23	43.9/6.4	28	134
260	Proliferation-associated protein 2G4	PA2G4_MOUSE	P50580	43.699/6.41	45.2/6.5	31	166
267	Heterogeneous nuclear ribonucleoprotein L	HNRPL_MOUSE	Q8R081	60.123/6.65	63.2/6.6	19	107
268	Heterogeneous nuclear ribonucleoprotein L	HNRPL_MOUSE	Q8R081	60.123/6.65	63.4/6.7	17	132
269	Heterogeneous nuclear ribonucleoprotein L	HNRPL_MOUSE	Q8R081	60.123/6.65	63.3/6.9	16	118

299	Elongation factor 2	EF2_MOUSE	P58252	95.183/6.42	86.9/6.7	13	112
Enzymes							
31	ATP synthase beta chain, mitochondrial [Precursor]	ATPB_MOUSE	P56480	56.300/5.19	52.6/5.1	49.34 a)	18 b)
32	ATP synthase beta chain, mitochondrial [Precursor]	ATPB_MOUSE	P56480	56.300/5.19	52.6/5.1	32	161
35	26S protease regulatory subunit 6B	PRS6B_MOUSE	P54775	47.281/5.18	49.8/5.1	27	120
39	Ubiquinol-cytochrome C reductase complex core protein I, mitochondrial [Precursor]	UQCR1_MOUSE	Q9CZ13	52.769/5.75	47.6/5.4	22.92 a)	8 b)
47	ATP synthase beta chain, mitochondrial [Precursor]	ATPB_MOUSE	P56480	56.300/5.19	44.7/5.1	35.73 a)	13 b)
66	Inorganic pyrophosphatase	IPYR_MOUSE	Q9D819	32.667/5.37	32.7/5.3	25	86
68	Pyruvate dehydrogenase E1 component beta subunit, mitochondrial [Precursor]	ODPB_MOUSE	Q9D051	38.937/6.41	32.3/5.5	33	91
69	Pyruvate kinase, isozyme M2	KPYM_MOUSE	P52480	57.756/7.42	32.8/5.5	4.33 a)	2 b)
75	tyrosine 3-monooxygenase/tryptophan 5-monooxygenase activation protein, epsilon polypeptide, full insert sequence	Q8BPH1_MOUSE	Q8BPH1	29.189/4.63	29.4/4.7	36	114
79	Proteasome subunit alpha type 5	PSA5_MOUSE	Q9Z2U1	26.411/4.74	26.6/4.8	40	115
89	Proteasome subunit alpha type 5	PSA5_MOUSE	Q9Z2U1	26.411/4.74	24.3/4.8	15.77 a)	3 b)
90	ATP synthase beta chain, mitochondrial [Precursor]	ATPB_MOUSE	P56480	56.300/5.19	23.9/5.1	15.69 a)	5 b)
97	Lactoylglutathione lyase	LGUL_MOUSE	Q9CPU0	20.678/5.25	22.1/5.1	28	113
112	Mitochondrial import inner membrane translocase subunit TIM8 A	TIM8A_MOUSE	Q9WVA2	11.042/5.11	14.4/5.0	34.02 a)	3 b)
114	Cytochrome c oxidase polypeptide Va, mitochondrial [Precursor]	COX5A_MOUSE	P12787	16.030/6.08	14.5/5.1	17.93 a)	3 b)
125	Nucleoside diphosphate kinase A	NDKA_MOUSE	P15532	17.208/6.84	17.4/6.6	53	119
127	Peptidyl-prolyl cis-trans isomerase A	PPIA_MOUSE	P17742	17.840/7.88	17.8/6.6	30.49 a)	8 b)
129	Nucleoside diphosphate kinase B	NDKB_MOUSE	Q01768	17.363/6.97	18.3/7.3	69	135
130	Peptidyl-prolyl cis-trans isomerase A	PPIA_MOUSE	P17742	17.840/7.88	18.0/7.7	52	126
131	Peptidyl-prolyl cis-trans isomerase A	PPIA_MOUSE	P17742	17.840/7.88	17.8/8.0	53	133
137	UMP-CMP kinase	KCY_MOUSE	Q9DBP5	22.166/5.68	21.9/5.6	16.33 a)	3 b)
138	Adenine phosphoribosyltransferase	APT_MOUSE	P08030	19.736/6.31	21.9/5.9	61	142

148	Proteasome subunit alpha type 2	PSA2_MOUSE	P49722	25.794/8.42	23.0/6.7	29	64
154	Proteasome subunit alpha type 6	PSA6_MOUSE	Q9QUM9	27.372/6.35	25.9/6.2	47	102
156	Alpha enolase	ENOA_MOUSE	P17182	47.010/6.36	25.5/6.7	17.74 a)	6 b)
157	Triosephosphate isomerase	TPIS_MOUSE	P17751	26.581/7.09	25.0/6.7	45.78 a)	9 b)
158	Triosephosphate isomerase	TPIS_MOUSE	P17751	26.581/7.09	25.1/7.4	34	151
160	Proteasome subunit beta type 7 [Precursor]	PSB7_MOUSE	P70195	29.891/8.14	27.4/5.9	15	90
162	Phosphoglycerate mutase 1	PGAM1_MOUSE	Q9DBJ1	28.701/6.75	26.8/6.7	32	89
163	Adenylate kinase isoenzyme 2, mitochondrial	KAD2_MOUSE	Q9WTP6	25.474/7.16	27.0/7.6	46	84
165	Electron transfer flavoprotein beta-subunit	ETFB_MOUSE	Q9DCW4	27.310/8.56	26.8/8.4	44	113
166	Similar to kynurenine aminotransferase III	-	gi | 51761828 c)	45.037/9.87	26.4/8.6	28	113
171	Proteasome subunit alpha type 1	PSA1_MOUSE	Q9R1P4	29.547/6.00	29.8/6.0	22	79.
178	Electron transfer flavoprotein alpha-subunit, mitochondrial [Precursor]	ETFA_MOUSE	Q99LC5	35.039/8.62	31.1/7.3	34	124
183	26S proteasome non-ATPase regulatory subunit 14	PSDE_MOUSE	O35593	34.577/6.06	32.0/5.9	22	90
184	Uridine phosphorylase 1	UPP1_MOUSE	P52624	34.086/6.12	31.5/6.2	29	108
187	L-lactate dehydrogenase A chain	LDHA_MOUSE	P06151	36.367/7.76	32.2/7.8	32	128
192	Aldose reductase	ALDR_MOUSE	P45376	35.601/6.79	33.5/6.7	30	108
195	Glyceraldehyde 3-phosphate dehydrogenase	G3P_MOUSE	P16858	35.679/8.45	33.3/8.2	22	111
196	Glyceraldehyde 3-phosphate dehydrogenase	G3P_MOUSE	P16858	35.679/8.45	33.4/8.5	27	79
201	Alcohol dehydrogenase [NADP+]	AK1A1_MOUSE	Q9JII6	36.456/6.87	35.5/7.1	18	89
203	Fructose-bisphosphate aldolase A	ALDOA_MOUSE	P05064	39.225/8.40	37.8/7.9	32	140
204	Fructose-bisphosphate aldolase A	ALDOA_MOUSE	P05064	39.225/8.40	37.6/8.1	31	133
205	Fructose-bisphosphate aldolase A	ALDOA_MOUSE	P05064	39.225/8.40	37.4/8.3	35	178
206	40 kDa peptidyl-prolyl cis-trans isomerase	PPID_MOUSE	Q9CR16	40.611/7.06	37.8/7.4	26	104
207	Alcohol dehydrogenase class III	ADHX_MOUSE	P28474	39.502/7.59	37.9/6.8	24	86
211	Alpha enolase	ENOA_MOUSE	P17182	47.010/6.36	39.7/6.1	21	93
215	Aspartate aminotransferase, cytoplasmic	AATC_MOUSE	P05201	46.100/6.75	39.4/7.1	26	152

216	Aspartate aminotransferase, cytoplasmic	AATC_MOUSE	P05201	46.100/6.75	39.2/7.1	45	270
220	2-amino-3-ketobutyrate coenzyme A ligase, mitochondrial [Precursor]	KBL_MOUSE	O88986	44.931/6.92	41.1/6.7	20	79
221	Isocitrate dehydrogenase [NADP] cytoplasmic	IDHC_MOUSE	O88844	46.661/6.48	42.5/6.8	42.51 a)	16 b)
222	26S protease regulatory subunit 8	PRS8_MOUSE	P62196	45.626/7.11	45.0/7.1	15	72
223	26S protease regulatory subunit S10B	PRS10_MOUSE	P62334	44.173/7.09	40.4/7.4	31	130
226	Acyl-CoA dehydrogenase, medium-chain specific, mitochondrial [Precursor]	ACADM_MOUSE	P45952	46.481/8.60	40.6/7.8	18	90
227	Phosphoglycerate kinase 1	PGK1_MOUSE	P09411	44.405/7.52	41.3/8.1	17	75
235	Ornithine aminotransferase, mitochondrial [Precursor]	OAT_MOUSE	P29758	48.355/6.19	44.2/5.7	25	141
242	Alpha enolase	ENOA_MOUSE	P17182	47.010/6.36	47.5/6.0	30	110
250	3-phosphoglycerate dehydrogenase, full insert sequence	Q8C603_MOUSE	Q8C603	56.582/5.69	56.7/6.1	10	72
252	Uridine 5-monophosphate synthase	PYR5_MOUSE	P13439	52.292/6.17	53.5/6.2	15	99
254	Aldehyde dehydrogenase, mitochondrial [Precursor]	ALDH2_MOUSE	P47738	56.538/7.53	52.0/6.3	22	145
257	Serine hydroxymethyltransferase, cytosolic	GLYC_MOUSE	P50431	52.585/6.47	51.3/6.5	21	115
258	Alpha enolase	ENOA_MOUSE	P17182	47.010/6.36	47.8/6.2	29	126
264	Phosphoenolpyruvate carboxykinase, mitochondrial precursor [GTP]	PPCKM_MOUSE	Q8BH04	70.528/6.92	65.7/6.4	17	119
266	Bifunctional purine biosynthesis protein PURH	PUR9_MOUSE	Q9CWJ9	64.157/6.30	62.5/6.5	23	115
271	Dihydrolipoyl dehydrogenase, mitochondrial [Precursor]	DLDH_MOUSE	O08749	54.212/7.97	57.1/6.6	14	95
272	Leucine aminopeptidase 3	Q99P44_MOUSE	Q99P44	56.141/7.61	55.9/6.6	19	102
273	Cytosol aminopeptidase	AMPL_MOUSE	Q9CPY7	52.619/6.56	55.6/6.7	18	121
275	Inosine-5-monophosphate dehydrogenase 2	IMDH2_MOUSE	P24547	55.815/6.84	55.1/6.9	22	90
276	Glutamate dehydrogenase 1, mitochondrial [Precursor]	DHE3_MOUSE	P26443	61.337/8.05	53.0/6.9	13	85
278	Succinyl-CoA:3-ketoacid-coenzyme A transferase 1, mitochondrial [Precursor]	SCOT_MOUSE	Q9D0K2	55.989/8.73	55.7/7.4	15.48 a)	3 b)
279	Pyruvate kinase, isozyme M2	KPYM_MOUSE	P52480	57.756/7.42	59.3/7.3	24	121

280	Pyruvate kinase, isozyme M2	KPYM_MOUSE	P52480	57.756/7.42	59.1/7.7	35	130
281	Serine hydroxymethyl transferase 2	Q99K87_MOUSE	Q99K87	55.761/8.72	53.1/8.1	34	237
282	ATP synthase alpha chain, mitochondrial [Precursor]	ATPA_MOUSE	Q03265	59.753/9.22	53.4/8.2	32	190
285	Transketolase	TKT_MOUSE	P40142	67.630/7.23	65.0/7.6	26	198
289	Glycerol-3-phosphate dehydrogenase, mitochondrial [Precursor]	GPDM_MOUSE	Q64521	80.900/6.17	69.4/5.9	14	69
295	Aconitate hydratase, mitochondrial [Precursor]	ACON_MOUSE	Q99KI0	85.464/8.08	77.2/7.8	23	137
296	ATP-dependent metalloprotease YME1L1	YMEL1_MOUSE	O88967	80.028/9.01	73.5/8.5	11	71
298	Trifunctional purine biosynthetic protein adenosine-3	PUR2_MOUSE	Q64737	107.395/6.25	92.4/6.4	11	95
Others							
40	Similar to RIKEN cDNA 4921537P18	-	gi | 51706188 c)	39.257/6.19	45.6/5.3	28	66
155	Protein C14orf166 homolog	CN166_MOUSE	Q9CQE8	28.152/6.40	25.0/6.4	52.87 a)	15 b)
172	Protein C14orf166 homolog	CN166_MOUSE	Q9CQE8	28.152/6.40	28.3/6.2	21.72 a)	4 b)
186	similar to 3 of D-CONTAINING PROTEIN [Fragment]	Q8BZS8_MOUSE	Q8BZS8	31.265/8.22	31.8/7.4	33	75
190	LIM and SH3 domain protein 1	LASP1_MOUSE	Q61792	29.994/6.61	34.8/6.5	27	81
233	Serine protease inhibitor A3F	SPA3F_MOUSE	Q80X76	52.756/4.93	46.0/5.6	6	56
274	Hypothetical protein D10Wsu52e (P55)	Q99LF4_MOUSE	Q99LF4	55.249/6.77	56.5/6.9	24	128
Signalling molecules							
2	Caspase-8 [Precursor]	CASP8_MOUSE	O89110	55.357/5.12	94.1/5.3	15	68
12	Rho-associated protein kinase 2	ROCK2_MOUSE	P70336	160.586/5.73	68.4/5.6	10	72
55	Suppressor of G2 allele of SKP1 homolog	SUGT1_MOUSE	Q9CX34	38.159/5.32	37.2/5.2	29	114
56	Hyaluronan mediated motility receptor	HMMR_MOUSE	Q00547	91.800/5.47	36.5/5.1	13	68
76	Tumor necrosis factor receptor superfamily member 5 [Precursor]	TNR5_MOUSE	P27512	32.111/6.30	28.9/5.0	26	72
77	HIRA-interacting protein 5	HIRP5_MOUSE	Q9QZ23	22.140/4.23	25.9/4.4	26.13 a)	4 b)
87	Ran-specific GTPase-activating protein	RANG_MOUSE	P34022	23.596/5.15	26.4/5.1	26	80
91	Rho GDP-dissociation inhibitor 1	GDIR_MOUSE	Q99PT1	23.407/5.12	23.4/5.1	36	155
100	Phosphatidylethanolamine-binding protein	PEBP_MOUSE	P70296	20.699/5.19	21.4/5.1	22	71
103	S-phase kinase-associated protein 1A	SKP1_MOUSE	Q9WTX5	18.541/4.4	19.2/4.5	23.31 a)	3 b)

120	Histidine triad nucleotide-binding protein 1	HINT1_MOUSE	P70349	13.646/6.39	15.2/6.3	23.81 a)	4 b)
149	GTP-binding nuclear protein Ran	RAN_MOUSE	P62827	24.423/7.01	22.4/7.0	53	164
150	GTP-binding nuclear protein Ran	RAN_MOUSE	P62827	24.423/7.01	22.6/7.4	23.61 a)	6 b)
159	High mobility group protein 2	HMG2_MOUSE	P30681	24.031/7.05	24.7/7.8	12.92 a)	2 b)
175	Guanine nucleotide-binding protein beta subunit 2-like 1	GBLP_MOUSE	P68040	35.077/7.60	30.7/7.0	33	128
179	GUANINE NUCLEOTIDE-BINDING PROTEIN BETA SUBUNIT-LIKE PROTEIN 12.3, full insert sequence. [Fragment]	Q9CSQ0_MOUSE	Q9CSQ0	30.961/7.72	30.9/7.7	62	203
191	Transmembrane GTPase MFN1	MFN1_MOUSE	Q811U4	83.740/6.08	34.6/6.6	15	78
199	TNF receptor associated factor 5	TRAF5_MOUSE	P70191	61.145/7.71	35.4/6.1	16	63
238	Rab GDP dissociation inhibitor beta-2	GDIC_MOUSE	Q61598	50.537/5.93	47.9/5.8	20	97
283	Far upstream element binding protein 1	FUBP1_MOUSE	Q91WJ8	68.540/7.73	70.7/6.9	10	83
284	Far upstream element binding protein 1	FUBP1_MOUSE	Q91WJ8	68.540/7.73	71.1/7.4	16	102
287	Mitogen-activated protein kinase 11	MK11_MOUSE	Q9WUI1	41.357/5.45	64.9/8.3	28	81
292	Far upstream element binding protein 1	FUBP1_MOUSE	Q91WJ8	74.226/6.38	76.9/6.6	20	96
293	DEAD-box protein 3, X-chromosomal	DDX3X_MOUSE	Q62167	72.970/6.73	73.5/6.7	27	192
294	Far upstream element binding protein 1	FUBP1_MOUSE	Q91WJ8	74.226/6.38	76.7/6.9	18	145
Structural proteins							
6	Lamin B1	LAM1_MOUSE	P14733	66.654/5.11	66.5/5.1	28	142
7	Lamin B1	LAM1_MOUSE	P14733	66.654/5.11	66.7/5.1	33	191
19	Lamin B1	LAM1_MOUSE	P14733	66.654/5.11	58.8/5.4	18.20 a)	9 b)
24	Vimentin	VIME_MOUSE	P20152	53.556/5.06	56.9/5.1	26	104
29	Tubulin beta-5 chain	TBB5_MOUSE	P05218	49.671/4.78	54.6/5.1	27	110
42	Vimentin	VIME_MOUSE	P20152	53.556/5.06	46.1/5.1	2.15 a)	1 b)
48	Vimentin	VIME_MOUSE	P20152	53.556/5.06	42.5/5.1	4.95 a)	2 b)
49	Actin, cytoplasmic 1	ACTB_MOUSE	P60710	41.737/5.29	42.0/5.1	27	120
50	Actin, cytoplasmic 2	ACTG_MOUSE	P63260	41.793/5.31	41.6/5.2	29	124
51	Actin, cytoplasmic 1	ACTB_MOUSE	P60710	41.737/5.29	41.9/5.3	25	100

52	Actin, cytoplasmic 1	ACTB_MOUSE	P60710	41.676/5.37	41.7/5.4	4.2 a)	1 b)
54	Actin, cytoplasmic 1	ACTB_MOUSE	P60710	41.737/5.29	40.1/5.1	18	85
64	Tropomyosin beta chain	TPM2_MOUSE	P58774	32.837/4.66	31.7/5.2	15	67
67	Tubulin beta-5 chain	TBB5_MOUSE	P05218	49.671/4.78	32.8/5.4	20	105
72	Tropomyosin 3, gamma	Q8K0Z5_MOUSE	Q8K0Z5	33.149/4.73	30.9/4.8	14.11 a)	3 b)
73	Actin, cytoplasmic 1	ACTB_MOUSE	P60710	41.816/5.30	31.0/5.3	13.83 a)	4 b)
74	Actin, cytoplasmic 1	ACTB_MOUSE	P60710	41.816/5.30	30.9/5.3	9.04 a)	3 b)
84	Actin, cytoplasmic 2	ACTG_MOUSE	P63260	41.793/5.31	28.1/5.4	16	68
88	Actin, cytoplasmic 1	ACTB_MOUSE	P60710	41.737/5.29	25.8/5.4	20	110
108	Myosin light polypeptide 6	MYL6_MOUSE	Q60605	16.799/4.56	17.1/4.5	47	106
124	Profilin I	PROF1_MOUSE	P62962	14.826/8.50	14.9/8.5	68	143
132	Cofilin, non-muscle isoform	COF1_MOUSE	P18760	18.428/8.26	18.5/8.2	46	128
133	Cofilin, non-muscle isoform	COF1_MOUSE	P18760	18.428/8.26	18.5/8.5	30	73
136	Transgelin 2	Q91VU2_MOUSE	Q91VU2	22.395/8.4	21.2/8.4	63	113
181	Voltage-dependent anion-selective channel protein 1	VDAC1_MOUSE	Q60932	32.351/8.55	30.9/8.7	30	111
194	Annexin A2	ANXA2_MOUSE	P07356	38.545/7.53	33.5/8.0	20.71 a)	6 b)
198	Apolipoprotein A-IV [Precursor]	APOA4_MOUSE	P06728	45.029/5.41	36.9/6.0	24	71
255	Fascin	FSCN1_MOUSE	Q61553	54.274/6.21	53.1/6.4	46.04 a)	23 b)
256	Septin 11	SEP11_MOUSE	Q8C1B7	49.695/6.24	51.7/6.5	42	113
290	Mitochondrial inner membrane protein	IMMT_MOUSE	Q8CAQ8	83.900/6.18	77.2/5.8	13	88
291	Ezrin	EZRI_MOUSE	P26040	69.276/5.83	74.9/5.8	21	124
Unidentified							
20	Unidentified	-	-	-	58.0/5.3	-	-
34	Unidentified	-	-	-	54.1/5.4	-	-
38	Unidentified	-	-	-	49.1/5.4	-	-
61	Unidentified	-	-	-	33.4/5.1	-	-
63	Unidentified	-	-	-	32.0/5.1	-	-

70	Unidentified	-	-	-	30.9/4.5	-	-
78	Unidentified	-	-	-	26.5/4.7	-	-
80	Unidentified	-	-	-	27.8/4.9	-	-
81	Unidentified	-	-	-	27.2/5.0	-	-
82	Unidentified	-	-	-	27.6/5.1	-	-
83	Unidentified	-	-	-	27.8/5.1	-	-
86	Unidentified	-	-	-	25.9/5.0	-	-
92	Unidentified	-	-	-	22.8/5.2	-	-
95	Unidentified	-	-	-	22.0/4.9	-	-
96	Unidentified	-	-	-	22.2/5.1	-	-
99	Unidentified	-	-	-	21.4/5.1	-	-
101	Unidentified	-	-	-	21.8/5.5	-	-
102	Unidentified	-	-	-	20.3/5.4	-	-
104	Unidentified	-	-	-	18.9/4.5	-	-
105	Unidentified	-	-	-	18.0/4.3	-	-
107	Unidentified	-	-	-	17.7/5.1	-	-
109	Unidentified	-	-	-	17.1/5.0	-	-
110	Unidentified	-	-	-	15.4/4.3	-	-
111	Unidentified	-	-	-	14.3/4.8	-	-
113	Unidentified	-	-	-	14.6/5.0	-	-
115	Unidentified	-	-	-	18.3/5.6	-	-
118	Unidentified	-	-	-	16.9/5.7	-	-
122	Unidentified	-	-	-	12.7/7.5	-	-
123	Unidentified	-	-	-	13.5/8.1	-	-
126	Unidentified	-	-	-	17.2/7.7	-	-
128	Unidentified	-	-	-	17.5/6.7	-	-
134	Unidentified	-	-	-	18.6/6.0	-	-

141	Unidentified	-	-	-	22.3/6.9	-	-
145	Unidentified	-	-	-	22.5/5.8	-	-
146	Unidentified	-	-	-	22.4/6.1	-	-
152	Unidentified	-	-	-	25.2/5.9	-	-
173	Unidentified	-	-	-	30.4/6.3	-	-
174	Unidentified	-	-	-	31.1/6.9	-	-
176	Unidentified	-	-	-	29.5/7.0	-	-
177	Unidentified	-	-	-	28.8/7.0	-	-
180	Unidentified	-	-	-	31.2/8.4	-	-
182	Unidentified	-	-	-	32.6/5.9	-	-
193	Unidentified	-	-	-	34.0/7.5	-	-
197	Unidentified	-	-	-	37.1/5.7	-	-
212	Unidentified	-	-	-	39.4/6.2	-	-
213	Unidentified	-	-	-	39.1/6.3	-	-
219	Unidentified	-	-	-	43.3/6.6	-	-
225	Unidentified	-	-	-	41.3/7.7	-	-
228	Unidentified	-	-	-	45.9/8.1	-	-
229	Unidentified	-	-	-	48.4/8.6	-	-
232	Unidentified	-	-	-	50.5/9.0	-	-
243	Unidentified	-	-	-	46.0/6.0	-	-
248	Unidentified	-	-	-	56.8/5.9	-	-
261	Unidentified	-	-	-	71.6/6.4	-	-
262	Unidentified	-	-	-	65.8/6.3	-	-
277	Unidentified	-	-	-	54.1/7.2	-	-
286	Unidentified	-	-	-	68.8/7.9	-	-
297	Unidentified	-	-	-	87.3/6.1	-	-

300	Unidentified		-	-	-	88.4/6.9	-	-		

a) Coverage by tandem MS.

b) Number of peptides identified by tandem MS.

c) Entry number from NCBI database.

Table 15. Protein differences between esSMC and aortic SMCs

No	Protein Name	UniProt Entry Name	UniProt Accession No.	Calculated MM (kDa) / pI	Observed MM (kDa) / pI	Sequence coverage %	No of Pep.	Prob.	Ratio b)	*p*
DNA Maintenance, Transcription, Translation										
10	Chromatin assembly factor 1 subunit C	RBBP4_MOUSE	Q60972	51.6/4.95	52/4.5	22.77	7	2.7E-09	2.87	0.001
92	ELAV-like protein 1	ELAV1_MOUSE	P70372	36.1/9.23	34/9.3	25.76	8	5.1E-05	2.53	0.013
111	Elongation factor Tu, mitochondrial [Precursor]	EFTU_MOUSE	Q8BFR5	49.5/7.23	47/6.9	19.47	9	5.1E-08	2.03	0.000
60	Eukaryotic translation initiation factor 5A-1	IF5A1_MOUSE	P63242	16.7/5.08	16/5.1	32	78 a)	2.3E-04	2.24	0.043
83	Eukaryotic translation initiation factor 4H	IF4H_MOUSE	Q9WUK2	27.2/6.91	28/7.5	13.71	2	1.3E-04	4.33	0.001
92	Heterogeneous nuclear ribonucleoprotein A1	ROA1_MOUSE	P49312	34.1/9.27	34/9.3	32.19	11	4.1E-09	2.53	0.013
100	Heterogeneous nuclear ribonucleoprotein A/B	ROAA_MOUSE	Q99020	30.8/7.69	41/7.6	32	97 a)	3.3E-06	2.21	0.011
101	Heterogeneous nuclear ribonucleoprotein A/B	ROAA_MOUSE	Q99020	30.8/7.69	41/7.3	25.62	7	1.1E-06	2.79	0.008
107	Heterogeneous nuclear ribonucleoprotein A/B	ROAA_MOUSE	Q99020	30.8/7.69	44/6.9	31	98 a)	2.6E-06	2.41	0.000

99	Heterogeneous nuclear ribonucleoprotein D-like	Q9Z130_MOUSE	Q9Z130	33.6/6.85	34/6.9	24.25	7	5.4E-10	2.20	0.002
112	Heterogeneous nuclear ribonucleoprotein D0	HNRPD_MOUSE	Q60668	38.4/7.61	47/7.1	11.26	4	1.5E-06	2.03	0.002
120	Heterogeneous nuclear ribonucleoprotein H	HNRH1_MOUSE	O35737	49.1/5.89	53/7.0	6.02	2	3.1E-04	3.10	0.000
6	Heterogeneous nuclear ribonucleoprotein K	HNRPK_MOUSE	P61979	51.0/5.39	61/5.4	25	116 a)	3.8E-08	-2.73	0.000
127	Heterogeneous nuclear ribonucleoprotein L	HNRPL_MOUSE	Q8R081	60.1/6.65	61/7.2	19	98 a)	2.4E-06	2.46	0.001
128	Heterogeneous nuclear ribonucleoprotein L	HNRPL_MOUSE	Q8R081	60.1/6.65	61/7.2	17	117 a)	3.0E-08	3.20	0.000
129	Heterogeneous nuclear ribonucleoprotein L	HNRPL_MOUSE	Q8R081	60.1/6.65	61/7.3	16	106 a)	3.8E-07	3.38	0.000
130	Heterogeneous nuclear ribonucleoprotein L	HNRPL_MOUSE	Q8R081	60.1/6.65	61/7.4	4.32	2	2.8E-05	2.73	0.000
131	Heterogeneous nuclear ribonucleoprotein L	HNRPL_MOUSE	Q8R081	60.1/6.65	63/7.6	9.00	4	6.4E-07	2.80	0.001
132	Heterogeneous nuclear ribonucleoprotein L	HNRPL_MOUSE	Q8R081	60.1/6.65	63/7.6	18.18	7	1.7E-07	3.83	0.000
133	Heterogeneous nuclear ribonucleoprotein L	HNRPL_MOUSE	Q8R081	60.1/6.65	63/7.4	12.78	6	2.2E-08	2.04	0.015
71	Histone H2B F	H2B1_MOUSE	P10853	13.8/10.32	13/7.6	7.94	1	1.1E-03	3.19	0.001
121	Pre-mRNA splicing factor 19	PRP19_MOUSE	Q99KP6	55.2/6.14	55/6.1	23	116 a)	3.8E-08	2.66	0.002
144	Probable ATP-dependent RNA helicase DDX5	DDX5_MOUSE	Q61656	69.3/9.06	61/8.4	19.21	10	8.9E-08	3.98	0.000
145	Probable ATP-dependent RNA helicase DDX5	DDX5_MOUSE	Q61656	69.3/9.06	61/8.6	22.14	12	5.1E-09	2.94	0.000
146	Probable ATP-dependent RNA helicase DDX5	DDX5_MOUSE	Q61656	69.3/9.06	60/9.4	13.35	7	2.1E-07	2.92	0.000
59	Nucleophosmin	NPM_MOUSE	Q61937	32.6/4.62	17/4.3	7.19	1	2.3E-03	2.78	0.026
66	Nucleophosmin	NPM_MOUSE	Q61937	32.6/4.62	11/4.5	7.19	1	9.4E-06	3.95	0.012
124	Nucleoporin p54	NUP54_MOUSE	Q8BTS4	55.7/6.53	57/7.0	25.09	10	4.6E-07	2.37	0.001
105	Replication factor C (Activator 1) 4	Q99J62_MOUSE	Q99J62	39.9/6.29	42/7.0	28.29	10	7.7E-08	3.30	0.001
110	TAR DNA-binding protein 43	TADBP_MOUSE	Q921F2	44.5/6.26	46/6.6	23.92	7	3.5E-06	2.46	0.001
Chaperones										
70	10 kDa heat shock protein, mitochondrial	CH10_MOUSE	Q64433	10.8/8.18	11/7.5	35.29	3	2.2E-07	2.82	0.000
49	47 kDa heat shock protein [Precursor]	HSP47_MOUSE	P19324	46.6/8.90	29/5.89	3.60	1	3.3E-06	-7.22	0.001
115	47 kDa heat shock protein [Precursor]	HSP47_MOUSE	P19324	46.6/8.90	48/8.1	18.71	6	1.8E-10	-12.24	0.000
116	47 kDa heat shock protein [Precursor]	HSP47_MOUSE	P19324	46.6/8.90	47/8.2	29.98	11	2.5E-09	-11.14	0.001

16	60 kDa heat shock protein, mitochondrial [Precursor]	CH60_MOUSE	P63038	61.0/5.91	58/5.2	13.26	6	6.7E-08	2.13	0.001
17	60 kDa heat shock protein, mitochondrial [Precursor]	CH60_MOUSE	P63038	61.0/5.91	57/5.3	20.58	8	7.2E-08	2.46	0.000
18	60 kDa heat shock protein, mitochondrial [Precursor]	CH60_MOUSE	P63038	61.0/5.91	57/5.4	5.75	3	1.3E-04	2.66	0.002
19	60 kDa heat shock protein, mitochondrial [Precursor]	CH60_MOUSE	P63038	61.0/5.91	54/5.7	10.11	4	1.0E-06	2.69	0.000
36	60 kDa heat shock protein, mitochondrial [Precursor]	CH60_MOUSE	P63038	61.0/5.91	48/6.2	20	97 a)	3.2E-06	2.41	0.000
54	60 kDa heat shock protein, mitochondrial [Precursor]	CH60_MOUSE	P63038	61.0/5.91	23/4.6	5.06	2	8.7E-04	2.79	0.002
103	60 kDa heat shock protein, mitochondrial [Precursor]	CH60_MOUSE	P63038	61.0/5.91	40/7.1	18.49	9	1.6E-06	3.13	0.000
37	78 kDa glucose-regulated protein [Precursor]	GRP78_MOUSE	P20029	72.4/5.07	42/4.5	12.07	7	1.2E-04	-2.98	0.001
118	DnaJ homolog subfamily A member 1	DNJA1_MOUSE	P63037	44.9/6.65	49/7.2	3.27	1	7.2E-06	2.71	0.002
51	Endoplasmic reticulum protein ERp29 [Precursor]	ERP29_MOUSE	P57759	28.8/5.90	29/5.9	26	80 a)	1.5E-04	3.11	0.000
1	Heat shock 70 kDa protein 4	HSP74_MOUSE	Q61316	94.1/5.15	94/5.1	24	150 a)	1.5E-11	-2.39	0.000
84	Heat shock cognate 71 kDa protein	HSP7C_MOUSE	P63017	70.9/5.37	29/8.0	19	125 a)	4.8E-09	2.77	0.000
73	Peptidyl-prolyl cis-trans isomerase A	PPIA_MOUSE	P17742	17.8/7.88	15/7.1	26.23	6	6.2E-06	2.35	0.007
74	Peptidyl-prolyl cis-trans isomerase A	PPIA_MOUSE	P17742	17.8/7.88	15/7.5	52	111 a)	1.2E-07	2.89	0.018
75	Peptidyl-prolyl cis-trans isomerase A	PPIA_MOUSE	P17742	17.8/7.88	18/7.9	53	140 a)	1.5E-10	2.27	0.028
4	Stress-70 protein, mitochondrial [Precursor]	GRP75_MOUSE	P38647	73.5/5.91	63/5.4	14.43	8	1.0E-09	-3.29	0.000
5	Stress-70 protein, mitochondrial [Precursor]	GRP75_MOUSE	P38647	73.5/5.91	63/5.5	34	255 a)	4.8E-22	6.30	0.000
13	Stress-70 protein, mitochondrial [Precursor]	GRP75_MOUSE	P38647	73.5/5.91	58/5.0	11.49	6	6.0E-06	-2.06	0.016
15	Stress-70 protein, mitochondrial [Precursor]	GRP75_MOUSE	P38647	73.5/5.91	58/5.1	12.53	6	7.4E-06	5.81	0.000
Cytoskeleton										
44	Actin, cytoplasmic 1	ACTB_MOUSE	P60710	41.7/5.29	31/4.8	4.26	1	2.6E-05	-3.57	0.000
47	Actin, cytoplasmic 1	ACTB_MOUSE	P60710	41.7/5.29	28/5.1	4.27	1	2.6E-05	-2.02	0.005
48	Actin, cytoplasmic 1	ACTB_MOUSE	P60710	41.7/5.29	28/5.3	19	94 a)	6.0E-06	-2.35	0.003
62	Actin, cytoplasmic 1	ACTB_MOUSE	P60710	41.7/5.29	15/4.9	4.80	1	6.7E-03	-2.29	0.004
33	Actin, cytoplasmic 2	ACTG_MOUSE	P63260	41.8/5.31	42/5.3	10.13	4	1.6E-09	-2.84	0.001
137	Lamin-A/C	LMNA_MOUSE	P48678	74.2/6.54	63/7.1	35.01	20	7.4E-09	-18.35	0.000

138	Lamin-A/C	LMNA_MOUSE	P48678	74.2/6.54	74/6.5	32.93	19	2.5E-07	-9.82	0.000
140	Lamin-A/C	LMNA_MOUSE	P48678	74.2/6.54	63/6.9	26.01	14	1.2E-06	-3.03	0.000
64	Myosin light polypeptide 6	MYL6_MOUSE	Q60605	16.8/4.56	14/4.6	42.38	6	2.3E-05	-6.05	0.000
55	Myosin regulatory light chain 2, smooth muscle isoform	MLRN_MOUSE	Q9CQ19	19.7/4.80	20/4.8	6.40	1	8.4E-03	-4.02	0.000
41	Tropomyosin 1 alpha chain	TPM1_MOUSE	P58771	32.7/4.69	36/4.6	20.07	7	9.8E-09	-14.76	0.000
42	Tropomyosin alpha-4 chain	TPM4_MOUSE	Q6IRU2	28.3/4.65	31/4.5	12.10	2	8.4E-05	-10.76	0.000
43	Tropomyosin alpha-3 chain	TPM3_MOUSE	P21107	32.9/4.68	31/4.6	7.39	2	1.4E-07	-3.50	0.027
39	Tropomyosin beta chain	TPM2_MOUSE	P58774	32.8/4.66	33/4.7	13.38	6	3.5E-11	-10.20	0.002
9	Vimentin	VIME_MOUSE	P20152	53.6/5.06	55/4.5	47	187 a)	3.2E-15	-2.55	0.000
12	Vimentin	VIME_MOUSE	P20152	53.6/5.06	56/4.8	18.25	6	3.8E-11	-2.59	0.001
14	Vimentin	VIME_MOUSE	P20152	53.6/5.06	54/5.1	53.43	26	4.9E-12	-21.78	0.000
23	Vimentin	VIME_MOUSE	P20152	53.6/5.06	49/4.7	20.65	8	2.5E-11	-17.08	0.000
24	Vimentin	VIME_MOUSE	P20152	53.6/5.06	48/4.2	11.16	3	4.3E-11	-4.49	0.000
27	Vimentin	VIME_MOUSE	P20152	53.6/5.06	46/4.5	51.29	22	5.3E-07	-6.13	0.002
28	Vimentin	VIME_MOUSE	P20152	53.6/5.06	47/4.6	12.26	4	3.6E-07	-8.31	0.000
30	Vimentin	VIME_MOUSE	P20152	53.6/5.06	44/4.5	10.32	3	1.5E-07	-3.17	0.000
Cytoskeleton Regulators										
102	Annexin A1	ANXA1_MOUSE	P10107	38.6/7.15	40/7.2	35.65	9	5.9E-14	-11.93	0.000
96	Annexin A2	ANXA2_MOUSE	P07356	38.5/7.53	37/7.3	13.61	3	3.9E-08	-2.76	0.009
97	Annexin A2	ANXA2_MOUSE	P07356	38.5/7.53	38/7.5	36.98	8	3.1E-11	-3.41	0.005
143	Ezrin	EZRI_MOUSE	P26040	69.3/5.83	65/6.4	9.04	4	1.7E-08	2.53	0.005
119	Septin-11	SEP11_MOUSE	Q8C1B7	49.6/6.26	50/6.3	33.64	13	4.7E-08	-2.02	0.001
80	Transgelin	TAGL_MOUSE	P37804	22.4/8.86	24/8.4	14.50	2	1.6E-04	-5.20	0.017
76	Transgelin-2	TAGL2_MOUSE	Q9WVA4	23.5/6.83	22/7.3	22.64	4	8.9E-07	-3.89	0.003
79	Transgelin-2	TAGL2_MOUSE	Q9WVA4	23.5/6.83	22/8.1	31.13	6	2.4E-10	-9.28	0.004

Calcium binding proteins										
135	Caldesmon 1	Q8VCQ8_MOUSE	Q8VCQ8	60.5/6.98	65/7.2	4.52	2	1.5E-04	2.88	0.029
136	Caldesmon 1	Q8VCQ8_MOUSE	Q8VCQ8	60.5/6.98	64/7.1	11.87	7	1.5E-04	-40.51	0.000
141	Caldesmon 1	Q8VCQ8_MOUSE	Q8VCQ8	60.5/6.98	64/6.9	2.26	1	8.8E-03	-45.90	0.000
7	Calreticulin [Precursor]	CALR_MOUSE	P14211	48.0/4.33	57/4.2	20	119 a)	1.9E-08	-2.03	0.018
8	Calreticulin [Precursor]	CALR_MOUSE	P14211	48.0/4.33	53/4.3	15.38	3	5.2E-10	-2.14	0.009
25	Calumenin [Precursor]	CALU_MOUSE	O35887	37.1/4.49	48/4.3	21.59	4	4.4E-07	-5.97	0.000
26	Reticulocalbin-1 [Precursor]	RCN1_MOUSE	Q05186	38.1/4.70	47/4.4	14.46	4	8.3E-07	-3.86	0.002
29	Reticulocalbin-1 [Precursor]	RCN1_MOUSE	Q05186	38.1/4.70	45/4.4	3.69	1	2.5E-05	-3.81	0.002
26	Reticulocalbin-3 [Precursor]	RCN3_MOUSE	Q8BH97	38.0/4.74	47/4.4	18.28	6	1.1E-09	-3.86	0.002
52	Translationally controlled tumor protein	TCTP_MOUSE	P63028	19.5/4.76	25/4.5	33	73 a)	7.3E-04	2.83	0.001
Electron transport and oxidative phosphorylation										
22	ATP synthase beta chain, mitochondrial [Precursor]	ATPB_MOUSE	P56480	56.3/5.19	51/4.8	32	161 a)	1.2E-12	-5.74	0.000
31	ATP synthase beta chain, mitochondrial [Precursor]	ATPB_MOUSE	P56480	56.3/5.19	47/5.0	8.13	3	4.2E-07	-4.08	0.002
32	ATP synthase beta chain, mitochondrial [Precursor]	ATPB_MOUSE	P56480	56.3/5.19	48/5.1	5.49	2	1.6E-05	-3.10	0.007
63	ATP synthase beta chain, mitochondrial [Precursor]	ATPB_MOUSE	P56480	56.3/5.19	14/4.7	3.59	1	5.1E-04	-2.27	0.001
88	Voltage-dependent anion-selective channel protein 1	VDAC1_MOUSE	Q60932	32.4/8.55	33/7.9	39.87	8	2.2E-08	2.04	0.000
89	Voltage-dependent anion-selective channel protein 1	VDAC1_MOUSE	Q60932	32.4/8.55	34/8.0	26.35	6	5.4E-08	2.08	0.000
90	Voltage-dependent anion-selective channel protein 1	VDAC1_MOUSE	Q60932	32.4/8.55	33/8.2	60.14	14	6.6E-09	2.10	0.000
91	Voltage-dependent anion-selective channel protein 1	VDAC1_MOUSE	Q60932	32.4/8.55	33/8.3	7.77	2	1.0E-03	2.15	0.000
Glycolysis										
94	Glyceraldehyde-3-phosphate dehydrogenase	G3P_MOUSE	P16858	35.7/8.45	35/7.4	31.33	6	1.8E-19	-5.37	0.016
95	Glyceraldehyde-3-phosphate dehydrogenase	G3P_MOUSE	P16858	35.7/8.45	35/7.1	59.16	15	6.2E-08	-5.72	0.005
139	Phosphoenolpyruvate carboxykinase, mitochondrial	PPCKM_MOUSE	Q8BH04	70.5/6.92	62/6.9	32.05	16	1.8E-11	-2.46	0.000

	precursor [GTP]									
114	Phosphoglycerate kinase 1	PGK1_MOUSE	P09411	44.4/7.52	45/7.8	13	67 a)	3.2E-03	-3.10	0.004
Ketolysis										
122	Succinyl-CoA:3-ketoacid-coenzyme A transferase 1, mitochondrial [Precursor]	SCOT_MOUSE	Q9D0K2	56.0/8.73	55/7.2	5.65	1	8.2E-04	-2.19	0.001
123	Succinyl-CoA:3-ketoacid-coenzyme A transferase 1, mitochondrial [Precursor]	SCOT_MOUSE	Q9D0K2	56.0/8.73	55/7.4	30.96	9	1.3E-08	-2.17	0.006
Lipid metabolism										
109	Acyl-CoA dehydrogenase, short-chain specific, mitochondrial [Precursor]	ACADS_MOUSE	Q07417	44.9/8.96	42/7.2	39.31	12	1.3E-08	3.95	0.000
85	Enoyl Coenzyme A hydratase domain containing 2	Q9DBD3_MOUSE	Q9DBD3	26.2/7.68	30/7.4	18.70	3	1.2E-04	4.65	0.000
Antioxidants										
50	Peroxiredoxin 6 (oxidized form)	PRDX6_MOUSE	O08709	24.7/5.72	25/5.7	55	119 a)	1.9E-08	2.89	0.001
11	Protein disulfide-isomerase [Precursor]	PDIA1_MOUSE	P09103	57.1/4.79	54/4.7	35.95	13	2.8E-06	-2.77	0.000
46	Protein disulfide-isomerase [Precursor]	PDIA1_MOUSE	P09103	57.1/4.79	29/4.7	12.57	5	1.1E-06	-2.34	0.001
20	Protein disulfide-isomerase A3 [Precursor]	PDIA3_MOUSE	P27773	56.6/5.99	57/5.9	10.32	5	2.4E-06	-2.23	0.000
77	Superoxide dismutase [Mn], mitochondrial [Precursor]	SODM_MOUSE	P09671	24.6/8.80	23/7.3	12.61	2	6.3E-06	-3.08	0.001
78	Superoxide dismutase [Mn], mitochondrial [Precursor]	SODM_MOUSE	P09671	24.6/8.80	23/7.5	31.99	5	1.1E-08	-3.37	0.001
Signalling proteins										
34	Cathepsin D [Precursor]	CATD_MOUSE	P18242	45.0/6.71	45/5.8	8.78	2	2.3E-04	-3.67	0.000
82	GTP-binding nuclear protein Ran	RAN_MOUSE	P62827	24.4/7.01	26/7.3	16.20	3	2.4E-06	2.83	0.014

108	Mitotic checkpoint protein BUB3	BUB3_MOUSE	Q9WVA3	37.0/6.21	43/7.1	18.71	5	3.3E-07	2.89	0.000
Mixture										
38	Protein disulfide-isomerase [Precursor]	PDIA1_MOUSE	P09103	57.1/4.79	40/4.5	11.79	5	6.0E-05	-5.84	0.000
38	Tropomyosin beta chain	TPM2_MOUSE	P58774	32.8/4.66	40/4.5	18.66	5	2.4E-06	-5.84	0.000
61	Actin, cytoplasmic 1	ACTB_MOUSE	P60710	41.7/5.29	15/5.0	7.20	2	3.1E-03	2.60	0.007
61	ATP synthase beta chain, mitochondrial [Precursor]	ATPB_MOUSE	P56480	56.3/5.19	15/5.0	4.73	2	6.8E-06	2.60	0.007
93	Calponin-1	CNN1_MOUSE	Q08091	33.4/9.05	36/8.5	13.80	3	1.2E-06	-2.01	0.024
93	Heterogeneous nuclear ribonucleoprotein A1	ROA1_MOUSE	P49312	34.1/9.27	36/8.5	30.95	8	1.0E-08	-2.01	0.024
106	Mitochondrial 28S ribosomal protein S22	RT22_MOUSE	Q9CXW2	41.2/8.63	42/6.5	21.44	7	1.8E-07	2.84	0.000
106	Stomatin-like protein 2	STML2_MOUSE	Q99JB2	38.4/8.95	42/6.5	38.25	10	1.0E-07	2.84	0.000
113	2-amino-3-ketobutyrate coenzyme A ligase, mitochondrial [Precursor]	KBL_MOUSE	O88986	44.9/6.92	45/7.2	13.22	4	8.4E-04	2.00	0.009
113	Alpha-2-macroglobulin receptor-associated protein [Precursor]	AMRP_MOUSE	P55302	42.2/7.35	45/7.2	19.44	7	1.2E-03	2.00	0.009
125	Lamin-A/C	LMNA_MOUSE	P48678	74.2/6.54	59/7.1	29.76	18	2.2E-08	-3.82	0.000
125	T-complex protein 1 subunit zeta	TCPZ_MOUSE	P80317	57.9/6.67	59/7.1	21.65	7	4.6E-07	-3.82	0.000
Others										
98	Aldose reductase	ALDR_MOUSE	P45376	35.6/6.79	38/7.2	29	129 a)	1.9E-09	2.31	0.002
126	Dihydropyrimidinase related protein-2	DPYL2_MOUSE	O08553	62.2/5.95	60/6.6	10.66	4	1.0E-02	-3.36	0.011
65	Galectin-1	LEG1_MOUSE	P16045	14.7/5.32	12/4.9	33.58	4	1.4E-06	-15.76	0.000
35	Ornithine aminotransferase, mitochondrial [Precursor]	OAT_MOUSE	P29758	48.4/6.19	48/6.1	25	125 a)	4.8E-09	-2.45	0.005
81	Protein C14orf166 homolog	CN166_MOUSE	Q9CQE8	28.2/6.40	26/7.0	10.66	2	1.1E-06	3.37	0.001
134	Serotransferrin [Precursor]	TRFE_MOUSE	Q921I1	76.7/6.94	64/7.3	6.31	3	1.1E-05	-16.84	0.000

Unidentified										
2	Unidentified	-	-	-/-	67/5.2	-	-	-	-2.03	0.007
3	Unidentified	-	-	-/-	63/5.0	-	-	-	-2.19	0.000
21	Unidentified	-	-	-/-	54/5.9	-	-	-	8.33	0.023
40	Unidentified	-	-	-/-	38/4.6	-	-	-	-8.27	0.009
45	Unidentified	-	-	-/-	31/4.9	-	-	-	-6.34	0.000
53	Unidentified	-	-	-/-	24/4.6	-	-	-	5.20	0.001
56	Unidentified	-	-	-/-	20/4.6	-	-	-	-20.22	0.002
57	Unidentified	-	-	-/-	19/4.9	-	-	-	6.08	0.006
58	Unidentified	-	-	-/-	19/5.2	-	-	-	4.87	0.005
67	Unidentified	-	-	-/-	10/4.4	-	-	-	4.67	0.009
68	Unidentified	-	-	-/-	9/5.0	-	-	-	-4.61	0.008
69	Unidentified	-	-	-/-	9/5.2	-	-	-	-3.70	0.009
72	Unidentified	-	-	-/-	14/6.6	-	-	-	-9.04	0.000
86	Unidentified	-	-	-/-	32/7.0	-	-	-	2.36	0.004
87	Unidentified	-	-	-/-	32/7.3	-	-	-	2.10	0.001
104	Unidentified	-	-	-/-	41/6.9	-	-	-	2.57	0.034
117	Unidentified	-	-	-/-	50/7.6	-	-	-	3.32	0.001
142	Unidentified	-	-	-/-	64/6.7	-	-	-	-12.50	0.000

a) Score of identifications from MALDI-ToF MS

b) Protein expression ratio of esSMCs versus aortic SMCs.

REFERENCES

Abe, K., H. Niwa, et al. (1996). "Endoderm-specific gene expression in embryonic stem cells differentiated to embryoid bodies." Exp Cell Res **229**(1): 27-34.

Aicher, A., C. Heeschen, et al. (2003). "Essential role of endothelial nitric oxide synthase for mobilization of stem and progenitor cells." Nat Med **9**(11): 1370-6.

Alexander, R. W. and V. J. Dzau (2000). "Vascular biology: the past 50 years." Circulation **102**(20 Suppl 4): IV112-6.

Allen, R. G. and A. K. Balin (1989). "Oxidative influence on development and differentiation: an overview of a free radical theory of development." Free Radic Biol Med **6**(6): 631-61.

Alvarez, R. J., S. J. Gips, et al. (1997). "17beta-estradiol inhibits apoptosis of endothelial cells." Biochem Biophys Res Commun **237**(2): 372-81.

Amit, M., M. K. Carpenter, et al. (2000). "Clonally derived human embryonic stem cell lines maintain pluripotency and proliferative potential for prolonged periods of culture." Dev Biol **227**(2): 271-8.

Anderson, D. J., F. H. Gage, et al. (2001). "Can stem cells cross lineage boundaries?" Nat Med **7**(4): 393-5.

Ando, J., A. Ohtsuka, et al. (1993). "Wall shear stress rather than shear rate regulates cytoplasmic Ca++ responses to flow in vascular endothelial cells." Biochem Biophys Res Commun **190**(3): 716-23.

Asahara, T., T. Murohara, et al. (1997). "Isolation of putative progenitor endothelial cells for angiogenesis." Science **275**(5302): 964-7.

Assmus, B., V. Schachinger, et al. (2002). "Transplantation of Progenitor Cells and Regeneration Enhancement in Acute Myocardial Infarction (TOPCARE-AMI)." Circulation **106**(24): 3009-17.

Aw, T. Y. (1999). "Molecular and cellular responses to oxidative stress and changes in oxidation-reduction imbalance in the intestine." Am J Clin Nutr **70**(4): 557-65.

Badorff, C., R. P. Brandes, et al. (2003). "Transdifferentiation of blood-derived human adult endothelial progenitor cells into functionally active cardiomyocytes." Circulation **107**(7): 1024-32.

Bain, G., D. Kitchens, et al. (1995). "Embryonic stem cells express neuronal properties in vitro." Dev Biol **168**(2): 342-57.

Banach, K., M. D. Halbach, et al. (2003). "Development of electrical activity in cardiac myocyte aggregates derived from mouse embryonic stem cells." Am J Physiol Heart Circ Physiol **284**(6): H2114-23.

Banks, R. E., M. J. Dunn, et al. (2000). "Proteomics: new perspectives, new biomedical opportunities." Lancet **356**(9243): 1749-56.

Barbee, K. A., P. F. Davies, et al. (1994). "Shear stress-induced reorganization of the surface topography of living endothelial cells imaged by atomic force microscopy." Circ Res **74**(1): 163-71.

Barberi, T., P. Klivenyi, et al. (2003). "Neural subtype specification of fertilization and nuclear transfer embryonic stem cells and application in parkinsonian mice." Nat Biotechnol **21**(10): 1200-7.

Barja, G. (1999). "Mitochondrial oxygen radical generation and leak: sites of production in states 4 and 3, organ specificity, and relation to aging and longevity." J Bioenerg Biomembr **31**(4): 347-66.

Barja, G. (2002). "Rate of generation of oxidative stress-related damage and animal longevity." Free Radic Biol Med **33**(9): 1167-72.

Bautch, V. L., W. L. Stanford, et al. (1996). "Blood island formation in attached cultures of murine

embryonic stem cells." Dev Dyn 205(1): 1-12.

Becker, K. and R. H. Schirmer (1995). "1,3-Bis(2-chloroethyl)-1-nitrosourea as thiol-carbamoylating agent in biological systems." Methods Enzymol 251: 173-88.

Beckman, K. B. and B. N. Ames (1998). "The free radical theory of aging matures." Physiol Rev 78(2): 547-81.

Bernal-Mizrachi, C., A. C. Gates, et al. (2005). "Vascular respiratory uncoupling increases blood pressure and atherosclerosis." Nature 435(7041): 502-6.

Berthiaume, F. and J. A. Frangos (1992). "Flow-induced prostacyclin production is mediated by a pertussis toxin-sensitive G protein." FEBS Lett 308(3): 277-9.

Birukov, K. G., N. Bardy, et al. (1998). "Intraluminal pressure is essential for the maintenance of smooth muscle caldesmon and filamin content in aortic organ culture." Arterioscler Thromb Vasc Biol 18(6): 922-7.

Bjornson, C. R., R. L. Rietze, et al. (1999). "Turning brain into blood: a hematopoietic fate adopted by adult neural stem cells in vivo." Science 283(5401): 534-7.

Boheler, K. R., J. Czyz, et al. (2002). "Differentiation of pluripotent embryonic stem cells into cardiomyocytes." Circ Res 91(3): 189-201.

Bourassa, M. G., L. Campeau, et al. (1982). "Changes in grafts and coronary arteries after saphenous vein aortocoronary bypass surgery: results at repeat angiography." Circulation 65(7 Pt 2): 90-7.

Bradford, M. M. (1976). "A rapid and sensitive method for the quantitation of microgram quantities of protein utilizing the principle of protein-dye binding." Anal Biochem 72: 248-54.

Bradley, A., M. Evans, et al. (1984). "Formation of germ-line chimaeras from embryo-derived teratocarcinoma cell lines." Nature 309(5965): 255-6.

Brazelton, T. R., F. M. Rossi, et al. (2000). "From marrow to brain: expression of neuronal phenotypes in adult mice." Science 290(5497): 1775-9.

Bruneel, A., V. Labas, et al. (2005). "Proteomics of human umbilical vein endothelial cells applied to etoposide-induced apoptosis." Proteomics 5(15): 3876-84.

Bruneel, A., V. Labas, et al. (2003). "Proteomic study of human umbilical vein endothelial cells in culture." Proteomics 3(5): 714-23.

Brunini, T. M., A. C. Mendes-Ribeiro, et al. (2006). "Platelet nitric oxide synthesis in uremia and malnutrition: A role for l-arginine supplementation in vascular protection?" Cardiovasc Res.

Brunini, T. M., N. B. Roberts, et al. (2002). "Activation of L-arginine transport in peripheral blood mononuclear cells in chronic renal failure." Pflugers Arch 445(1): 147-51.

Brunini, T. M., M. M. Yaqoob, et al. (2003). "Increased nitric oxide synthesis in uraemic platelets is dependent on L-arginine transport via system y(+)L." Pflugers Arch 445(5): 547-50.

Brustle, O., K. N. Jones, et al. (1999). "Embryonic stem cell-derived glial precursors: a source of myelinating transplants." Science 285(5428): 754-6.

Burkert, U., T. von Ruden, et al. (1991). "Early fetal hematopoietic development from in vitro differentiated embryonic stem cells." New Biol 3(7): 698-708.

Buttery, L. D., S. Bourne, et al. (2001). "Differentiation of osteoblasts and in vitro bone formation from murine embryonic stem cells." Tissue Eng 7(1): 89-99.

Cadenas, E. and K. J. Davies (2000). "Mitochondrial free radical generation, oxidative stress, and aging." Free Radic Biol Med 29(3-4): 222-30.

Cai, H. and D. G. Harrison (2000). "Endothelial dysfunction in cardiovascular diseases: the role of oxidant stress." Circ Res 87(10): 840-4.

Campbell, J. H. and G. R. Campbell (1994). "The role of smooth muscle cells in atherosclerosis." Curr Opin Lipidol 5(5): 323-30.

Carr, S., R. Aebersold, et al. (2004). "The need for guidelines in publication of peptide and protein identification data: Working Group on Publication Guidelines for Peptide and Protein Identification Data." Mol Cell Proteomics 3(6): 531-3.

Carroll, K., K. Ray, et al. (2000). "Two-dimensional electrophoresis reveals differential protein expression in high- and low-secreting variants of the rat basophilic leukaemia cell line." Electrophoresis 21(12): 2476-86.

Cerdan, C., A. Rouleau, et al. (2004). "VEGF-A165 augments erythropoietic development from human embryonic stem cells." Blood 103(7): 2504-12.

Chadwick, K., L. Wang, et al. (2003). "Cytokines and BMP-4 promote hematopoietic differentiation of human embryonic stem cells." Blood 102(3): 906-15.

Chandel, N. S., E. Maltepe, et al. (1998). "Mitochondrial reactive oxygen species trigger hypoxia-induced transcription." Proc Natl Acad Sci U S A 95(20): 11715-20.

Chandra, J., A. Samali, et al. (2000). "Triggering and modulation of apoptosis by oxidative stress." Free Radic Biol Med 29(3-4): 323-33.

Chen, S. and R. J. Lechleider (2004). "Transforming growth factor-beta-induced differentiation of smooth muscle from a neural crest stem cell line." Circ Res 94(9): 1195-202.

Chiariello, M., M. J. Marinissen, et al. (2001). "Regulation of c-myc expression by PDGF through Rho GTPases." Nat Cell Biol 3(6): 580-6.

Choi, K., M. Kennedy, et al. (1998). "A common precursor for hematopoietic and endothelial cells." Development 125(4): 725-32.

Clark, A. T., M. S. Bodnar, et al. (2004). "Spontaneous differentiation of germ cells from human embryonic stem cells in vitro." Hum Mol Genet 13(7): 727-39.

Clarke, D. L., C. B. Johansson, et al. (2000). "Generalized potential of adult neural stem cells." Science 288(5471): 1660-3.

Conway, E. M., D. Collen, et al. (2001). "Molecular mechanisms of blood vessel growth." Cardiovasc Res 49(3): 507-21.

Corthals, G., Gygi,SP, Aebesold,R, Patterson,SD (2000). "Identification of proteins by mass spectrometry." Proteome Research: Two-Dimensional Gel Electrophoresis and Identification Methods.: 197-227.

Cossarizza, A., M. Baccarani-Contri, et al. (1993). "A new method for the cytofluorimetric analysis of mitochondrial membrane potential using the J-aggregate forming lipophilic cation 5,5',6,6'-tetrachloro-1,1',3,3'-tetraethylbenzimidazolcarbocyanine iodide (JC-1)." Biochem Biophys Res Commun 197(1): 40-5.

Cotgreave, I. A. and R. G. Gerdes (1998). "Recent trends in glutathione biochemistry--glutathione-protein interactions: a molecular link between oxidative stress and cell proliferation?" Biochem Biophys Res Commun 242(1): 1-9.

Cremona, O., M. Muda, et al. (1995). "Differential protein expression in aortic smooth muscle cells cultured from newborn and aged rats." Exp Cell Res 217(2): 280-7.

Cuzzocrea, S., D. P. Riley, et al. (2001). "Antioxidant therapy: a new pharmacological approach in shock, inflammation, and ischemia/reperfusion injury." Pharmacol Rev 53(1): 135-59.

Cybulsky, M. I. and M. A. Gimbrone, Jr. (1991). "Endothelial expression of a mononuclear leukocyte adhesion molecule during atherogenesis." Science 251(4995): 788-91.

Daheron, L., S. L. Opitz, et al. (2004). "LIF/STAT3 signaling fails to maintain self-renewal of human embryonic stem cells." Stem Cells 22(5): 770-8.

Dani, C., A. G. Smith, et al. (1997). "Differentiation of embryonic stem cells into adipocytes in vitro." J Cell Sci 110 (Pt 11): 1279-85.

Davies, K. J. (1999). "The broad spectrum of responses to oxidants in proliferating cells: a new paradigm for oxidative stress." IUBMB Life 48(1): 41-7.

Davies, M. J. (2005). "The oxidative environment and protein damage." Biochim Biophys Acta 1703(2): 93-109.

Davies, P. F. (1995). "Flow-mediated endothelial mechanotransduction." Physiol Rev 75(3): 519-60.

Davies, P. F., K. A. Barbee, et al. (1997). "Spatial relationships in early signaling events of flow-mediated endothelial mechanotransduction." Annu Rev Physiol 59: 527-49.

Davies, P. F., D. C. Polacek, et al. (1999). "A spatial approach to transcriptional profiling: mechanotransduction and the focal origin of atherosclerosis." Trends Biotechnol 17(9): 347-51.

De Flora, S., A. Izzotti, et al. (1997). "Molecular epidemiology of atherosclerosis." Faseb J 11(12): 1021-31.

De Vecchi, E., L. Lubatti, et al. (1998). "Protection from renal ischemia-reperfusion injury by the 2-methylaminochroman U83836E." Kidney Int 54(3): 857-63.

Dernbach, E., C. Urbich, et al. (2004). "Antioxidative stress-associated genes in circulating progenitor cells: evidence for enhanced resistance against oxidative stress." Blood 104(12): 3591-7.

Dewey, C. F., Jr., S. R. Bussolari, et al. (1981). "The dynamic response of vascular endothelial cells to fluid shear stress." J Biomech Eng 103(3): 177-85.

Dietrich, H., Y. Hu, et al. (2000). "Rapid development of vein graft atheroma in ApoE-deficient mice." Am J Pathol 157(2): 659-69.

Dimmeler, S., B. Assmus, et al. (1998). "Fluid shear stress stimulates phosphorylation of Akt in human endothelial cells: involvement in suppression of apoptosis." Circ Res 83(3): 334-41.

Dimmeler, S., I. Fleming, et al. (1999). "Activation of nitric oxide synthase in endothelial cells by Akt-dependent phosphorylation." Nature 399(6736): 601-5.

Doetschman, T. C., H. Eistetter, et al. (1985). "The in vitro development of blastocyst-derived embryonic stem cell lines: formation of visceral yolk sac, blood islands and myocardium." J Embryol Exp Morphol 87: 27-45.

Drab, M., H. Haller, et al. (1997). "From totipotent embryonic stem cells to spontaneously contracting smooth muscle cells: a retinoic acid and db-cAMP in vitro differentiation model." Faseb J 11(11): 905-15.

D'Souza, S. L., A. G. Elefanty, et al. (2005). "SCL/Tal-1 is essential for hematopoietic commitment of the hemangioblast but not for its development." Blood 105(10): 3862-70.

Dunn, M. J. (1997). "Two-dimensional polyacrylamide gel electrophoresis for the separation of proteins for chemical characterization." Methods Mol Biol 64: 25-36.

Dunn, M. J. (2000). "Studying heart disease using the proteomic approach." Drug Discov Today 5(2): 76-84.

Dupont, A., D. Corseaux, et al. (2005). "The proteome and secretome of human arterial smooth muscle cells." Proteomics 5(2): 585-96.

Duran, M. C., S. Mas, et al. (2003). "Proteomic analysis of human vessels: application to atherosclerotic plaques." Proteomics 3(6): 973-8.

Dzau, V. J., G. H. Gibbons, et al. (1993). "Vascular biology and medicine in the 1990s: scope, concepts,

potentials, and perspectives." Circulation 87(3): 705-19.
Elliott, S. T., D. G. Crider, et al. (2004). "Two-dimensional gel electrophoresis database of murine R1 embryonic stem cells." Proteomics 4(12): 3813-32.
Ema, M., P. Faloon, et al. (2003). "Combinatorial effects of Flk1 and Tal1 on vascular and hematopoietic development in the mouse." Genes Dev 17(3): 380-93.
Evans, M. J. and M. H. Kaufman (1981). "Establishment in culture of pluripotential cells from mouse embryos." Nature 292(5819): 154-6.
Faloon, P., E. Arentson, et al. (2000). "Basic fibroblast growth factor positively regulates hematopoietic development." Development 127(9): 1931-41.
Faux, M. C. and J. D. Scott (1996). "More on target with protein phosphorylation: conferring specificity by location." Trends Biochem Sci 21(8): 312-5.
Fehling, H. J., G. Lacaud, et al. (2003). "Tracking mesoderm induction and its specification to the hemangioblast during embryonic stem cell differentiation." Development 130(17): 4217-27.
Feldmann, R. E., Jr., K. Bieback, et al. (2005). "Stem cell proteomes: a profile of human mesenchymal stem cells derived from umbilical cord blood." Electrophoresis 26(14): 2749-58.
Feraud, O. and D. Vittet (2003). "Murine embryonic stem cell in vitro differentiation: applications to the study of vascular development." Histol Histopathol 18(1): 191-9.
Ferrari, G., G. Cusella-De Angelis, et al. (1998). "Muscle regeneration by bone marrow-derived myogenic progenitors." Science 279(5356): 1528-30.
Fey, S. J. and P. M. Larsen (2001). "2D or not 2D. Two-dimensional gel electrophoresis." Curr Opin Chem Biol 5(1): 26-33.
Filomeni, G., G. Rotilio, et al. (2005). "Disulfide relays and phosphorylative cascades: partners in redox-mediated signaling pathways." Cell Death Differ.
Foster, L. J., P. A. Zeemann, et al. (2005). "Differential expression profiling of membrane proteins by quantitative proteomics in a human mesenchymal stem cell line undergoing osteoblast differentiation." Stem Cells 23(9): 1367-77.
Frid, M. G., E. C. Dempsey, et al. (1997). "Smooth muscle cell heterogeneity in pulmonary and systemic vessels. Importance in vascular disease." Arterioscler Thromb Vasc Biol 17(7): 1203-9.
Frid, M. G., E. P. Moiseeva, et al. (1994). "Multiple phenotypically distinct smooth muscle cell populations exist in the adult and developing bovine pulmonary arterial media in vivo." Circ Res 75(4): 669-81.
Furchgott, R. F. and J. V. Zawadzki (1980). "The obligatory role of endothelial cells in the relaxation of arterial smooth muscle by acetylcholine." Nature 288(5789): 373-6.
Galasso, G., S. Schiekofer, et al. (2006). "Impaired angiogenesis in glutathione peroxidase-1-deficient mice is associated with endothelial progenitor cell dysfunction." Circ Res 98(2): 254-61.
Galli, R., U. Borello, et al. (2000). "Skeletal myogenic potential of human and mouse neural stem cells." Nat Neurosci 3(10): 986-91.
Gepstein, L. (2002). "Derivation and potential applications of human embryonic stem cells." Circ Res 91(10): 866-76.
Gibbons, G. H. and V. J. Dzau (1994). "The emerging concept of vascular remodeling." N Engl J Med 330(20): 1431-8.
Girotti, A. W. (1998). "Lipid hydroperoxide generation, turnover, and effector action in biological systems." J Lipid Res 39(8): 1529-42.
Giulivi, C., A. Boveris, et al. (1995). "Hydroxyl radical generation during mitochondrial electron transfer

and the formation of 8-hydroxydesoxyguanosine in mitochondrial DNA." Arch Biochem Biophys 316(2): 909-16.

Griendling, K. K. and G. A. FitzGerald (2003). "Oxidative stress and cardiovascular injury: Part I: basic mechanisms and in vivo monitoring of ROS." Circulation 108(16): 1912-6.

Griendling, K. K. and G. A. FitzGerald (2003). "Oxidative stress and cardiovascular injury: Part II: animal and human studies." Circulation 108(17): 2034-40.

Griendling, K. K., C. A. Minieri, et al. (1994). "Angiotensin II stimulates NADH and NADPH oxidase activity in cultured vascular smooth muscle cells." Circ Res 74(6): 1141-8.

Griendling, K. K., D. Sorescu, et al. (2000). "NAD(P)H oxidase: role in cardiovascular biology and disease." Circ Res 86(5): 494-501.

Griffith, O. W. (1999). "Biologic and pharmacologic regulation of mammalian glutathione synthesis." Free Radic Biol Med 27(9-10): 922-35.

Gudi, S., J. P. Nolan, et al. (1998). "Modulation of GTPase activity of G proteins by fluid shear stress and phospholipid composition." Proc Natl Acad Sci U S A 95(5): 2515-9.

Gudi, S. R., C. B. Clark, et al. (1996). "Fluid flow rapidly activates G proteins in human endothelial cells. Involvement of G proteins in mechanochemical signal transduction." Circ Res 79(4): 834-9.

Guevara, N. V., H. S. Kim, et al. (1999). "The absence of p53 accelerates atherosclerosis by increasing cell proliferation in vivo." Nat Med 5(3): 335-9.

Gussoni, E., Y. Soneoka, et al. (1999). "Dystrophin expression in the mdx mouse restored by stem cell transplantation." Nature 401(6751): 390-4.

Gygi, S. P., B. Rist, et al. (1999). "Quantitative analysis of complex protein mixtures using isotope-coded affinity tags." Nat Biotechnol 17(10): 994-9.

Haar, J. L. and G. A. Ackerman (1971). "A phase and electron microscopic study of vasculogenesis and erythropoiesis in the yolk sac of the mouse." Anat Rec 170(2): 199-223.

Hallmann, R., D. N. Mayer, et al. (1995). "Novel mouse endothelial cell surface marker is suppressed during differentiation of the blood brain barrier." Dev Dyn 202(4): 325-32.

Han, C. I., G. R. Campbell, et al. (2001). "Circulating bone marrow cells can contribute to neointimal formation." J Vasc Res 38(2): 113-9.

Hart, G. W. (1992). "Glycosylation." Curr Opin Cell Biol 4(6): 1017-23.

Hazell, L. J. and R. Stocker (1997). "Alpha-tocopherol does not inhibit hypochlorite-induced oxidation of apolipoprotein B-100 of low-density lipoprotein." FEBS Lett 414(3): 541-4.

He, J. Q., Y. Ma, et al. (2003). "Human embryonic stem cells develop into multiple types of cardiac myocytes: action potential characterization." Circ Res 93(1): 32-9.

Heil, M. and W. Schaper (2004). "Influence of mechanical, cellular, and molecular factors on collateral artery growth (arteriogenesis)." Circ Res 95(5): 449-58.

Hellstrom, M., M. Kalen, et al. (1999). "Role of PDGF-B and PDGFR-beta in recruitment of vascular smooth muscle cells and pericytes during embryonic blood vessel formation in the mouse." Development 126(14): 3047-55.

Hescheler, J., B. K. Fleischmann, et al. (1997). "Embryonic stem cells: a model to study structural and functional properties in cardiomyogenesis." Cardiovasc Res 36(2): 149-62.

Hidaka, K., J. K. Lee, et al. (2003). "Chamber-specific differentiation of Nkx2.5-positive cardiac precursor cells from murine embryonic stem cells." Faseb J 17(6): 740-2.

Hill, J. M., G. Zalos, et al. (2003). "Circulating endothelial progenitor cells, vascular function, and cardiovascular risk." N Engl J Med 348(7): 593-600.

Hillebrands, J. L., F. A. Klatter, et al. (2001). "Origin of neointimal endothelium and alpha-actin-positive smooth muscle cells in transplant arteriosclerosis." J Clin Invest 107(11): 1411-22.

Hirashima, M., H. Kataoka, et al. (1999). "Maturation of embryonic stem cells into endothelial cells in an in vitro model of vasculogenesis." Blood 93(4): 1253-63.

Hirschi, K. K., S. A. Rohovsky, et al. (1998). "PDGF, TGF-beta, and heterotypic cell-cell interactions mediate endothelial cell-induced recruitment of 10T1/2 cells and their differentiation to a smooth muscle fate." J Cell Biol 141(3): 805-14.

Hissin, P. J. and R. Hilf (1976). "A fluorometric method for determination of oxidized and reduced glutathione in tissues." Anal Biochem 74(1): 214-26.

Hobbs, A. J. and L. J. Ignarro (1996). "Nitric oxide-cyclic GMP signal transduction system." Methods Enzymol 269: 134-48.

Hohl, C., R. Oestreich, et al. (1987). "Evidence for succinate production by reduction of fumarate during hypoxia in isolated adult rat heart cells." Arch Biochem Biophys 259(2): 527-35.

Holycross, B. J., M. J. Peach, et al. (1993). "Angiotensin II stimulates increased protein synthesis, not increased DNA synthesis, in intact rat aortic segments, in vitro." J Vasc Res 30(2): 80-6.

Hristov, M., W. Erl, et al. (2003). "Endothelial progenitor cells: mobilization, differentiation, and homing." Arterioscler Thromb Vasc Biol 23(7): 1185-9.

Hu, Q., R. J. Noll, et al. (2005). "The Orbitrap: a new mass spectrometer." J Mass Spectrom 40(4): 430-43.

Hu, Y., F. Davison, et al. (2002). "Smooth muscle cells in transplant atherosclerotic lesions are originated from recipients, but not bone marrow progenitor cells." Circulation 106(14): 1834-9.

Hu, Y., F. Davison, et al. (2003). "Endothelial replacement and angiogenesis in arteriosclerotic lesions of allografts are contributed by circulating progenitor cells." Circulation 108(25): 3122-7.

Hu, Y., M. Mayr, et al. (2002). "Both donor and recipient origins of smooth muscle cells in vein graft atherosclerotic lesions." Circ Res 91(7): e13-20.

Hu, Y., Z. Zhang, et al. (2004). "Abundant progenitor cells in the adventitia contribute to atherosclerosis of vein grafts in ApoE-deficient mice." J Clin Invest 113(9): 1258-65.

Hu, Y., Y. Zou, et al. (1999). "Inhibition of neointima hyperplasia of mouse vein grafts by locally applied suramin." Circulation 100(8): 861-8.

Huber, L. A., K. Pfaller, et al. (2003). "Organelle proteomics: implications for subcellular fractionation in proteomics." Circ Res 92(9): 962-8.

Hubner, K., G. Fuhrmann, et al. (2003). "Derivation of oocytes from mouse embryonic stem cells." Science 300(5623): 1251-6.

Humphery-Smith, I., S. J. Cordwell, et al. (1997). "Proteome research: complementarity and limitations with respect to the RNA and DNA worlds." Electrophoresis 18(8): 1217-42.

Imanishi, T., T. Hano, et al. (2005). "Angiotensin II accelerates endothelial progenitor cell senescence through induction of oxidative stress." J Hypertens 23(1): 97-104.

Inoue, M., E. F. Sato, et al. (2003). "Mitochondrial generation of reactive oxygen species and its role in aerobic life." Curr Med Chem 10(23): 2495-505.

Inui, K., R. O. Oreffo, et al. (1997). "Effects of beta mercaptoethanol on the proliferation and differentiation of human osteoprogenitor cells." Cell Biol Int 21(7): 419-25.

Itskovitz-Eldor, J., M. Schuldiner, et al. (2000). "Differentiation of human embryonic stem cells into embryoid bodies compromising the three embryonic germ layers." Mol Med 6(2): 88-95.

Iwashina, M., M. Shichiri, et al. (1998). "Transfection of inducible nitric oxide synthase gene causes

apoptosis in vascular smooth muscle cells." Circulation 98(12): 1212-8.

Izzotti, A., S. De Flora, et al. (1995). "Cancer biomarkers in human atherosclerotic lesions: detection of DNA adducts." Cancer Epidemiol Biomarkers Prev 4(2): 105-10.

Jackson, K. A., S. M. Majka, et al. (2001). "Regeneration of ischemic cardiac muscle and vascular endothelium by adult stem cells." J Clin Invest 107(11): 1395-402.

Jackson, K. A., T. Mi, et al. (1999). "Hematopoietic potential of stem cells isolated from murine skeletal muscle." Proc Natl Acad Sci U S A 96(25): 14482-6.

Jahn, M., J. W. Baynes, et al. (1999). "The reaction of hyaluronic acid and its monomers, glucuronic acid and N-acetylglucosamine, with reactive oxygen species." Carbohydr Res 321(3-4): 228-34.

Jenner, A. M., J. E. Ruiz, et al. (2002). "Vitamin C protects against hypochlorous Acid-induced glutathione depletion and DNA base and protein damage in human vascular smooth muscle cells." Arterioscler Thromb Vasc Biol 22(4): 574-80.

Jin, H., A. Aiyer, et al. (2006). "A homing mechanism for bone marrow-derived progenitor cell recruitment to the neovasculature." J Clin Invest 116(3): 652-62.

Kaiser, D., M. A. Freyberg, et al. (1997). "Lack of hemodynamic forces triggers apoptosis in vascular endothelial cells." Biochem Biophys Res Commun 231(3): 586-90.

Kannan, R. Y., H. J. Salacinski, et al. (2005). "Current status of prosthetic bypass grafts: a review." J Biomed Mater Res B Appl Biomater 74(1): 570-81.

Kaufman, D. S., E. T. Hanson, et al. (2001). "Hematopoietic colony-forming cells derived from human embryonic stem cells." Proc Natl Acad Sci U S A 98(19): 10716-21.

Kehat, I., L. Khimovich, et al. (2004). "Electromechanical integration of cardiomyocytes derived from human embryonic stem cells." Nat Biotechnol 22(10): 1282-9.

Keller, G. (2005). "Embryonic stem cell differentiation: emergence of a new era in biology and medicine." Genes Dev 19(10): 1129-55.

Keller, G., M. Kennedy, et al. (1993). "Hematopoietic commitment during embryonic stem cell differentiation in culture." Mol Cell Biol 13(1): 473-86.

Keller, G. M. (1995). "In vitro differentiation of embryonic stem cells." Curr Opin Cell Biol 7(6): 862-9.

Kennedy, M., M. Firpo, et al. (1997). "A common precursor for primitive erythropoiesis and definitive haematopoiesis." Nature 386(6624): 488-93.

Kiechl, S. and J. Willeit (1999). "The natural course of atherosclerosis. Part I: incidence and progression." Arterioscler Thromb Vasc Biol 19(6): 1484-90.

Kim, S. C., R. Sprung, et al. (2006). "Substrate and functional diversity of lysine acetylation revealed by a proteomics survey." Mol Cell 23(4): 607-18.

Klaunig, J. E. and L. M. Kamendulis (2004). "The role of oxidative stress in carcinogenesis." Annu Rev Pharmacol Toxicol 44: 239-67.

Klose, J. (1975). "Protein mapping by combined isoelectric focusing and electrophoresis of mouse tissues. A novel approach to testing for induced point mutations in mammals." Humangenetik 26(3): 231-43.

Klose, J. (1999). "Fractionated extraction of total tissue proteins from mouse and human for 2-D electrophoresis." Methods Mol Biol 112: 67-85.

Klug, M. G., M. H. Soonpaa, et al. (1996). "Genetically selected cardiomyocytes from differentiating embronic stem cells form stable intracardiac grafts." J Clin Invest 98(1): 216-24.

Kockx, M. M., B. A. Cambier, et al. (1994). "Foam cell replication and smooth muscle cell apoptosis in human saphenous vein grafts." Histopathology 25(4): 365-71.

Kolossov, E., B. K. Fleischmann, et al. (1998). "Functional characteristics of ES cell-derived cardiac precursor cells identified by tissue-specific expression of the green fluorescent protein." J Cell Biol 143(7): 2045-56.

Kramer, J., C. Hegert, et al. (2000). "Embryonic stem cell-derived chondrogenic differentiation in vitro: activation by BMP-2 and BMP-4." Mech Dev 92(2): 193-205.

Kreuzer, J., C. Viedt, et al. (2003). "Platelet-derived growth factor activates production of reactive oxygen species by NAD(P)H oxidase in smooth muscle cells through Gi1,2." Faseb J 17(1): 38-40.

Kubo, A., K. Shinozaki, et al. (2004). "Development of definitive endoderm from embryonic stem cells in culture." Development 131(7): 1651-62.

Lagasse, E., H. Connors, et al. (2000). "Purified hematopoietic stem cells can differentiate into hepatocytes in vivo." Nat Med 6(11): 1229-34.

Lan, Q., K. O. Mercurius, et al. (1994). "Stimulation of transcription factors NF kappa B and AP1 in endothelial cells subjected to shear stress." Biochem Biophys Res Commun 201(2): 950-6.

Lawson, K. A., N. R. Dunn, et al. (1999). "Bmp4 is required for the generation of primordial germ cells in the mouse embryo." Genes Dev 13(4): 424-36.

Lehoux, S. and A. Tedgui (1998). "Signal transduction of mechanical stresses in the vascular wall." Hypertension 32(2): 338-45.

Levenberg, S., J. S. Golub, et al. (2002). "Endothelial cells derived from human embryonic stem cells." Proc Natl Acad Sci U S A 99(7): 4391-6.

Li, C., Y. Hu, et al. (1999). "Cyclic strain stress-induced mitogen-activated protein kinase (MAPK) phosphatase 1 expression in vascular smooth muscle cells is regulated by Ras/Rac-MAPK pathways." J Biol Chem 274(36): 25273-80.

Li, C., Y. Hu, et al. (2000). "Ras/Rac-Dependent activation of p38 mitogen-activated protein kinases in smooth muscle cells stimulated by cyclic strain stress." Arterioscler Thromb Vasc Biol 20(3): E1-9.

Li, J., X. Han, et al. (2001). "Vascular smooth muscle cells of recipient origin mediate intimal expansion after aortic allotransplantation in mice." Am J Pathol 158(6): 1943-7.

Liao, D. F., Z. G. Jin, et al. (2000). "Purification and identification of secreted oxidative stress-induced factors from vascular smooth muscle cells." J Biol Chem 275(1): 189-96.

Libby, P. and D. I. Simon (2001). "Inflammation and thrombosis: the clot thickens." Circulation 103(13): 1718-20.

Lopez, M. F. and S. Melov (2002). "Applied proteomics: mitochondrial proteins and effect on function." Circ Res 90(4): 380-9.

Loscalzo, J. (2003). "Proteomics in cardiovascular biology and medicine." Circulation 108(4): 380-3.

Mack, C. P. and G. K. Owens (1999). "Regulation of smooth muscle alpha-actin expression in vivo is dependent on CArG elements within the 5' and first intron promoter regions." Circ Res 84(7): 852-61.

Madsen, C. S., C. P. Regan, et al. (1998). "Smooth muscle-specific expression of the smooth muscle myosin heavy chain gene in transgenic mice requires 5'-flanking and first intronic DNA sequence." Circ Res 82(8): 908-17.

Mahoney, W. M. and S. M. Schwartz (2005). "Defining smooth muscle cells and smooth muscle injury." J Clin Invest 115(2): 221-4.

Maines, M. D. (1997). "The heme oxygenase system: a regulator of second messenger gases." Annu Rev Pharmacol Toxicol 37: 517-54.

Maltsev, V. A., J. Rohwedel, et al. (1993). "Embryonic stem cells differentiate in vitro into cardiomyocytes representing sinusnodal, atrial and ventricular cell types." Mech Dev 44(1): 41-50.

Manevich, Y., T. Sweitzer, et al. (2002). "1-Cys peroxiredoxin overexpression protects cells against phospholipid peroxidation-mediated membrane damage." Proc Natl Acad Sci U S A 99(18): 11599-604.

Mann, G. E., D. L. Yudilevich, et al. (2003). "Regulation of amino acid and glucose transporters in endothelial and smooth muscle cells." Physiol Rev 83(1): 183-252.

Mann, M., R. C. Hendrickson, et al. (2001). "Analysis of proteins and proteomes by mass spectrometry." Annu Rev Biochem 70: 437-73.

Marchetti, S., C. Gimond, et al. (2002). "Endothelial cells genetically selected from differentiating mouse embryonic stem cells incorporate at sites of neovascularization in vivo." J Cell Sci 115(Pt 10): 2075-85.

Mariano, F., B. Bussolati, et al. (2003). "Platelet-activating factor synthesis by neutrophils, monocytes, and endothelial cells is modulated by nitric oxide production." Shock 19(4): 339-44.

Martin, G. R. (1981). "Isolation of a pluripotent cell line from early mouse embryos cultured in medium conditioned by teratocarcinoma stem cells." Proc Natl Acad Sci U S A 78(12): 7634-8.

Matsuoka, Y., H. Kubota, et al. (2004). "Insufficient folding of type IV collagen and formation of abnormal basement membrane-like structure in embryoid bodies derived from Hsp47-null embryonic stem cells." Mol Biol Cell 15(10): 4467-75.

Matsuura, K., T. Nagai, et al. (2004). "Adult cardiac Sca-1-positive cells differentiate into beating cardiomyocytes." J Biol Chem 279(12): 11384-91.

Mayr, M., Y. L. Chung, et al. (2005). "Proteomic and metabolomic analyses of atherosclerotic vessels from apolipoprotein E-deficient mice reveal alterations in inflammation, oxidative stress, and energy metabolism." Arterioscler Thromb Vasc Biol 25(10): 2135-42.

Mayr, M., Y. Hu, et al. (2002). "Mechanical stress-induced DNA damage and rac-p38MAPK signal pathways mediate p53-dependent apoptosis in vascular smooth muscle cells." Faseb J 16(11): 1423-5.

Mayr, M., C. Li, et al. (2000). "Biomechanical stress-induced apoptosis in vein grafts involves p38 mitogen-activated protein kinases." Faseb J 14(2): 261-70.

Mayr, M., R. Siow, et al. (2004). "Proteomic and metabolomic analysis of vascular smooth muscle cells: role of PKCdelta." Circ Res 94(10): e87-96.

Mayr, U., M. Mayr, et al. (2002). "Loss of p53 accelerates neointimal lesions of vein bypass grafts in mice." Circ Res 90(2): 197-204.

Mayr, U., M. Mayr, et al. (2005). "Proteomic dataset of mouse aortic smooth muscle cells." Proteomics 5(17): 4546-4557.

McCloskey, K. E., D. A. Smith, et al. (2006). "Embryonic stem cell-derived endothelial cells may lack complete functional maturation in vitro." J Vasc Res 43(5): 411-21.

McGregor, E. and M. J. Dunn (2003). "Proteomics of heart disease." Hum Mol Genet 12 Spec No 2: R135-44.

McGregor, E., L. Kempster, et al. (2004). "F-actin capping (CapZ) and other contractile saphenous vein smooth muscle proteins are altered by hemodynamic stress: a proteonomic approach." Mol Cell Proteomics 3(2): 115-24.

McGregor, E., L. Kempster, et al. (2001). "Identification and mapping of human saphenous vein medial

smooth muscle proteins by two-dimensional polyacrylamide gel electrophoresis." Proteomics 1(11): 1405-14.

Mehta, J. L., L. Y. Chen, et al. (1995). "Identification of constitutive and inducible forms of nitric oxide synthase in human platelets." J Lab Clin Med **125**(3): 370-7.

Melov, S., P. Coskun, et al. (1999). "Mitochondrial disease in superoxide dismutase 2 mutant mice." Proc Natl Acad Sci U S A 96(3): 846-51.

Mezey, E., K. J. Chandross, et al. (2000). "Turning blood into brain: cells bearing neuronal antigens generated in vivo from bone marrow." Science **290**(5497): 1779-82.

Michelakis, E. D., V. Hampl, et al. (2002). "Diversity in mitochondrial function explains differences in vascular oxygen sensing." Circ Res **90**(12): 1307-15.

Miller, F. J., Jr., D. D. Gutterman, et al. (1998). "Superoxide production in vascular smooth muscle contributes to oxidative stress and impaired relaxation in atherosclerosis." Circ Res **82**(12): 1298-305.

Mockett, R. J., R. S. Sohal, et al. (1999). "Overexpression of glutathione reductase extends survival in transgenic Drosophila melanogaster under hyperoxia but not normoxia." Faseb J **13**(13): 1733-42.

Molloy, M. P. (2000). "Two-dimensional electrophoresis of membrane proteins using immobilized pH gradients." Anal Biochem **280**(1): 1-10.

Moncada, S., M. W. Radomski, et al. (1988). "Endothelium-derived relaxing factor. Identification as nitric oxide and role in the control of vascular tone and platelet function." Biochem Pharmacol **37**(13): 2495-501.

Monteoliva, L. and J. P. Albar (2004). "Differential proteomics: an overview of gel and non-gel based approaches." Brief Funct Genomic Proteomic **3**(3): 220-39.

Muller, M., B. K. Fleischmann, et al. (2000). "Selection of ventricular-like cardiomyocytes from ES cells in vitro." Faseb J **14**(15): 2540-8.

Murry, C. E., M. H. Soonpaa, et al. (2004). "Haematopoietic stem cells do not transdifferentiate into cardiac myocytes in myocardial infarcts." Nature **428**(6983): 664-8.

Nakabeppu, Y., K. Sakumi, et al. (2006). "Mutagenesis and carcinogenesis caused by the oxidation of nucleic acids." Biol Chem **387**(4): 373-9.

Nakajima, Y., V. Mironov, et al. (1997). "Expression of smooth muscle alpha-actin in mesenchymal cells during formation of avian endocardial cushion tissue: a role for transforming growth factor beta3." Dev Dyn **209**(3): 296-309.

Nakano, T., H. Kodama, et al. (1994). "Generation of lymphohematopoietic cells from embryonic stem cells in culture." Science **265**(5175): 1098-101.

Nakayama, N., J. Lee, et al. (2000). "Vascular endothelial growth factor synergistically enhances bone morphogenetic protein-4-dependent lymphohematopoietic cell generation from embryonic stem cells in vitro." Blood **95**(7): 2275-83.

Neumann, D., M. Zierke, et al. (1998). "Withdrawal of 2-mercaptoethanol induces apoptosis in a B-cell line via Fas upregulation." J Cell Physiol **177**(1): 68-75.

Nir, S. G., R. David, et al. (2003). "Human embryonic stem cells for cardiovascular repair." Cardiovasc Res **58**(2): 313-23.

Nishikawa, S. I., S. Nishikawa, et al. (1998). "Progressive lineage analysis by cell sorting and culture identifies FLK1+VE-cadherin+ cells at a diverging point of endothelial and hemopoietic lineages." Development **125**(9): 1747-57.

O'Farrell, P. H. (1975). "High resolution two-dimensional electrophoresis of proteins." J Biol Chem **250**(10): 4007-21.

Okabe, S., K. Forsberg-Nilsson, et al. (1996). "Development of neuronal precursor cells and functional postmitotic neurons from embryonic stem cells in vitro." Mech Dev **59**(1): 89-102.

Olesen, S. P., D. E. Clapham, et al. (1988). "Haemodynamic shear stress activates a K+ current in vascular endothelial cells." Nature **331**(6152): 168-70.

Ong, S. E., B. Blagoev, et al. (2002). "Stable isotope labeling by amino acids in cell culture, SILAC, as a simple and accurate approach to expression proteomics." Mol Cell Proteomics **1**(5): 376-86.

Orlic, D., J. Kajstura, et al. (2001). "Bone marrow cells regenerate infarcted myocardium." Nature **410**(6829): 701-5.

Park, C., I. Afrikanova, et al. (2004). "A hierarchical order of factors in the generation of FLK1- and SCL-expressing hematopoietic and endothelial progenitors from embryonic stem cells." Development **131**(11): 2749-62.

Patton, W. F. (2000). "A thousand points of light: the application of fluorescence detection technologies to two-dimensional gel electrophoresis and proteomics." Electrophoresis **21**(6): 1123-44.

Patton, W. F., H. Erdjument-Bromage, et al. (1995). "Components of the protein synthesis and folding machinery are induced in vascular smooth muscle cells by hypertrophic and hyperplastic agents. Identification by comparative protein phenotyping and microsequencing." J Biol Chem **270**(36): 21404-10.

Patton, W. F., M. G. Pluskal, et al. (1990). "Development of a dedicated two-dimensional gel electrophoresis system that provides optimal pattern reproducibility and polypeptide resolution." Biotechniques **8**(5): 518-27.

Peirce, M. J., R. Wait, et al. (2004). "Expression profiling of lymphocyte plasma membrane proteins." Mol Cell Proteomics **3**(1): 56-65.

Perez-Campo, R., M. Lopez-Torres, et al. (1998). "The rate of free radical production as a determinant of the rate of aging: evidence from the comparative approach." J Comp Physiol [B] **168**(3): 149-58.

Perkins, D. N., D. J. Pappin, et al. (1999). "Probability-based protein identification by searching sequence databases using mass spectrometry data." Electrophoresis **20**(18): 3551-67.

Petersen, B. E., W. C. Bowen, et al. (1999). "Bone marrow as a potential source of hepatic oval cells." Science **284**(5417): 1168-70.

Pittenger, M. F., A. M. Mackay, et al. (1999). "Multilineage potential of adult human mesenchymal stem cells." Science **284**(5411): 143-7.

Podmore, I. D., H. R. Griffiths, et al. (1998). "Vitamin C exhibits pro-oxidant properties." Nature **392**(6676): 559.

Poli, G., G. Leonarduzzi, et al. (2004). "Oxidative stress and cell signalling." Curr Med Chem **11**(9): 1163-82.

Poliard, A., A. Nifuji, et al. (1995). "Controlled conversion of an immortalized mesodermal progenitor cell towards osteogenic, chondrogenic, or adipogenic pathways." J Cell Biol **130**(6): 1461-72.

Quaini, F., K. Urbanek, et al. (2002). "Chimerism of the transplanted heart." N Engl J Med **346**(1): 5-15.

Rabilloud, T. (1999). "Solubilization of proteins in 2-D electrophoresis. An outline." Methods Mol Biol **112**: 9-19.

Rabilloud, T., M. Heller, et al. (2002). "Proteomics analysis of cellular response to oxidative stress. Evidence for in vivo overoxidation of peroxiredoxins at their active site." J Biol Chem **277**(22): 19396-401.

Rafii, S. (2000). "Circulating endothelial precursors: mystery, reality, and promise." J Clin Invest **105**(1): 17-9.

Ramsby, M. L. and G. S. Makowski (1999). "Differential detergent fractionation of eukaryotic cells. Analysis by two-dimensional gel electrophoresis." Methods Mol Biol **112**: 53-66.

Ratan, R. R., T. H. Murphy, et al. (1994). "Macromolecular synthesis inhibitors prevent oxidative stress-induced apoptosis in embryonic cortical neurons by shunting cysteine from protein synthesis to glutathione." J Neurosci **14**(7): 4385-92.

Rauscher, F. M., P. J. Goldschmidt-Clermont, et al. (2003). "Aging, progenitor cell exhaustion, and atherosclerosis." Circulation **108**(4): 457-63.

Regan, C. P., I. Manabe, et al. (2000). "Development of a smooth muscle-targeted cre recombinase mouse reveals novel insights regarding smooth muscle myosin heavy chain promoter regulation." Circ Res **87**(5): 363-9.

Remuzzi, A., C. F. Dewey, Jr., et al. (1984). "Orientation of endothelial cells in shear fields in vitro." Biorheology **21**(4): 617-30.

Resing, K. A. (2002). "Analysis of signaling pathways using functional proteomics." Ann N Y Acad Sci **971**: 608-14.

Resnick, N. and M. A. Gimbrone, Jr. (1995). "Hemodynamic forces are complex regulators of endothelial gene expression." Faseb J **9**(10): 874-82.

Reubinoff, B. E., M. F. Pera, et al. (2000). "Embryonic stem cell lines from human blastocysts: somatic differentiation in vitro." Nat Biotechnol **18**(4): 399-404.

Reusch, P., H. Wagdy, et al. (1996). "Mechanical strain increases smooth muscle and decreases nonmuscle myosin expression in rat vascular smooth muscle cells." Circ Res **79**(5): 1046-53.

Righetti, P. G. (1990). "Recent developments in electrophoretic methods." J Chromatogr **516**(1): 3-22.

Risau, W., H. Sariola, et al. (1988). "Vasculogenesis and angiogenesis in embryonic-stem-cell-derived embryoid bodies." Development **102**(3): 471-8.

Roepstorff, P. (1997). "Mass spectrometry in protein studies from genome to function." Curr Opin Biotechnol **8**(1): 6-13.

Rohwedel, J., V. Maltsev, et al. (1994). "Muscle cell differentiation of embryonic stem cells reflects myogenesis in vivo: developmentally regulated expression of myogenic determination genes and functional expression of ionic currents." Dev Biol **164**(1): 87-101.

Ross, R. (1993). "The pathogenesis of atherosclerosis: a perspective for the 1990s." Nature **362**(6423): 801-9.

Ross, R. (1999). "Atherosclerosis--an inflammatory disease." N Engl J Med **340**(2): 115-26.

Ross, R., J. Glomset, et al. (1977). "Response to injury and atherogenesis." Am J Pathol **86**(3): 675-84.

Saiura, A., M. Sata, et al. (2001). "Circulating smooth muscle progenitor cells contribute to atherosclerosis." Nat Med **7**(4): 382-3.

Sales, K. M., H. J. Salacinski, et al. (2005). "Advancing vascular tissue engineering: the role of stem cell technology." Trends Biotechnol **23**(9): 461-7.

Salvioli, S., A. Ardizzoni, et al. (1997). "JC-1, but not DiOC6(3) or rhodamine 123, is a reliable fluorescent probe to assess delta psi changes in intact cells: implications for studies on mitochondrial functionality during apoptosis." FEBS Lett **411**(1): 77-82.

Sanchez-Ramos, J., S. Song, et al. (2000). "Adult bone marrow stromal cells differentiate into neural cells in vitro." Exp Neurol **164**(2): 247-56.

Sata, M. (2003). "Circulating vascular progenitor cells contribute to vascular repair, remodeling, and

lesion formation." Trends Cardiovasc Med 13(6): 249-53.

Sata, M., A. Saiura, et al. (2002). "Hematopoietic stem cells differentiate into vascular cells that participate in the pathogenesis of atherosclerosis." Nat Med 8(4): 403-9.

Sauer, H. and M. Wartenberg (2005). "Reactive oxygen species as signaling molecules in cardiovascular differentiation of embryonic stem cells and tumor-induced angiogenesis." Antioxid Redox Signal 7(11-12): 1423-34.

Sauer, H., M. Wartenberg, et al. (2001). "Reactive oxygen species as intracellular messengers during cell growth and differentiation." Cell Physiol Biochem 11(4): 173-86.

Schmitt, R. M., E. Bruyns, et al. (1991). "Hematopoietic development of embryonic stem cells in vitro: cytokine and receptor gene expression." Genes Dev 5(5): 728-40.

Schwartz, S. M. (1999). "The intima : A new soil." Circ Res 85(10): 877-9.

Shen, J., F. W. Luscinskas, et al. (1992). "Fluid shear stress modulates cytosolic free calcium in vascular endothelial cells." Am J Physiol 262(2 Pt 1): C384-90.

Shevchenko, A., M. Wilm, et al. (1996). "Mass spectrometric sequencing of proteins silver-stained polyacrylamide gels." Anal Chem 68(5): 850-8.

Shimizu, K., S. Sugiyama, et al. (2001). "Host bone-marrow cells are a source of donor intimal smooth-muscle-like cells in murine aortic transplant arteriopathy." Nat Med 7(6): 738-41.

Shirota, T., H. He, et al. (2003). "Human endothelial progenitor cell-seeded hybrid graft: proliferative and antithrombogenic potentials in vitro and fabrication processing." Tissue Eng 9(1): 127-36.

Sies, H. (1991). "Oxidative stress: from basic research to clinical application." Am J Med 91(3C): 31S-38S.

Sies, H. and E. Cadenas (1985). "Oxidative stress: damage to intact cells and organs." Philos Trans R Soc Lond B Biol Sci 311(1152): 617-31.

Simper, D., P. G. Stalboerger, et al. (2002). "Smooth muscle progenitor cells in human blood." Circulation 106(10): 1199-204.

Sinha, S., B. R. Wamhoff, et al. (2006). "Assessment of Contractility of Purified Smooth Muscle Cells Derived from Embryonic Stem Cells." Stem Cells.

Siow, R. C., H. Sato, et al. (1999). "Heme oxygenase-carbon monoxide signalling pathway in atherosclerosis: anti-atherogenic actions of bilirubin and carbon monoxide?" Cardiovasc Res 41(2): 385-94.

Smith, A. G. (2001). "Embryo-derived stem cells: of mice and men." Annu Rev Cell Dev Biol 17: 435-62.

Smith, A. G., J. K. Heath, et al. (1988). "Inhibition of pluripotential embryonic stem cell differentiation by purified polypeptides." Nature 336(6200): 688-90.

Smith, P. G., T. Tokui, et al. (1995). "Mechanical strain increases contractile enzyme activity in cultured airway smooth muscle cells." Am J Physiol 268(6 Pt 1): L999-1005.

Sohal, R. S., R. G. Allen, et al. (1986). "Oxygen free radicals play a role in cellular differentiation: an hypothesis." J Free Radic Biol Med 2(3): 175-81.

Song, J., J. Stastny, et al. (1985). "Effect of aging on human aortic protein composition. II. Two-dimensional polyacrylamide gel electrophoretic analysis." Exp Mol Pathol 43(3): 297-304.

Soria, B., E. Roche, et al. (2000). "Insulin-secreting cells derived from embryonic stem cells normalize glycemia in streptozotocin-induced diabetic mice." Diabetes 49(2): 157-62.

Spitkovsky, D., P. Sasse, et al. (2004). "Activity of complex III of the mitochondrial electron transport chain is essential for early heart muscle cell differentiation." Faseb J 18(11): 1300-2.

Stary, H. C. (1989). "Evolution and progression of atherosclerotic lesions in coronary arteries of children

and young adults." Arteriosclerosis 9(1 Suppl): I19-32.

Stastny, J., E. Fosslien, et al. (1986). "Human aortic intima protein composition during initial stages of atherogenesis." Atherosclerosis 60(2): 131-9.

Stastny, J. J. and E. Fosslien (1992). "Quantitative alteration of some aortic intima proteins in fatty streaks and fibro-fatty lesions." Exp Mol Pathol 57(3): 205-14.

Steinberg, D., S. Parthasarathy, et al. (1989). "Beyond cholesterol. Modifications of low-density lipoprotein that increase its atherogenicity." N Engl J Med 320(14): 915-24.

Stone, J. R. and M. A. Marletta (1994). "Soluble guanylate cyclase from bovine lung: activation with nitric oxide and carbon monoxide and spectral characterization of the ferrous and ferric states." Biochemistry 33(18): 5636-40.

Strong, J. P. (1995). "Natural history and risk factors for early human atherogenesis. Pathobiological Determinants of Atherosclerosis in Youth (PDAY) Research Group." Clin Chem 41(1): 134-8.

Strong, J. P., G. T. Malcom, et al. (1992). "Early lesions of atherosclerosis in childhood and youth: natural history and risk factors." J Am Coll Nutr 11 Suppl: 51S-54S.

Strong, J. P., M. C. Oalmann, et al. (1984). "Coronary heart disease in young black and white males in New Orleans: Community Pathology Study." Am Heart J 108(3 Pt 2): 747-59.

Syka, J. E., J. J. Coon, et al. (2004). "Peptide and protein sequence analysis by electron transfer dissociation mass spectrometry." Proc Natl Acad Sci U S A 101(26): 9528-33.

Szmitko, P. E., P. W. Fedak, et al. (2003). "Endothelial progenitor cells: new hope for a broken heart." Circulation 107(24): 3093-100.

Tao, W., M. Wang, et al. (2004). "Comparative proteomic analysis of human CD34+ stem/progenitor cells and mature CD15+ myeloid cells." Stem Cells 22(6): 1003-14.

Taurin, S., V. Seyrantepe, et al. (2002). "Proteome analysis and functional expression identify mortalin as an antiapoptotic gene induced by elevation of [Na+]i/[K+]i ratio in cultured vascular smooth muscle cells." Circ Res 91(10): 915-22.

Thomson, J. A., J. Itskovitz-Eldor, et al. (1998). "Embryonic stem cell lines derived from human blastocysts." Science 282(5391): 1145-7.

Tiwari, A., H. J. Salacinski, et al. (2001). "Tissue engineering of vascular bypass grafts: role of endothelial cell extraction." Eur J Vasc Endovasc Surg 21(3): 193-201.

Touyz, R. M. (2004). "Reactive oxygen species, vascular oxidative stress, and redox signaling in hypertension: what is the clinical significance?" Hypertension 44(3): 248-52.

Tretter, L. and V. Adam-Vizi (2000). "Inhibition of Krebs cycle enzymes by hydrogen peroxide: A key role of [alpha]-ketoglutarate dehydrogenase in limiting NADH production under oxidative stress." J Neurosci 20(24): 8972-9.

Trocino, R. A., S. Akazawa, et al. (1995). "Significance of glutathione depletion and oxidative stress in early embryogenesis in glucose-induced rat embryo culture." Diabetes 44(8): 992-8.

Tseng, H., T. E. Peterson, et al. (1995). "Fluid shear stress stimulates mitogen-activated protein kinase in endothelial cells." Circ Res 77(5): 869-78.

Tuan, R. S., G. Boland, et al. (2003). "Adult mesenchymal stem cells and cell-based tissue engineering." Arthritis Res Ther 5(1): 32-45.

Unlu, M., M. E. Morgan, et al. (1997). "Difference gel electrophoresis: a single gel method for detecting changes in protein extracts." Electrophoresis 18(11): 2071-7.

Vasa, M., S. Fichtlscherer, et al. (2001). "Increase in circulating endothelial progenitor cells by statin therapy in patients with stable coronary artery disease." Circulation 103(24): 2885-90.

Vittet, D., M. H. Prandini, et al. (1996). "Embryonic stem cells differentiate in vitro to endothelial cells through successive maturation steps." Blood 88(9): 3424-31.

Wagner, E., S. Luche, et al. (2002). "A method for detection of overoxidation of cysteines: peroxiredoxins are oxidized in vivo at the active-site cysteine during oxidative stress." Biochem J 366(Pt 3): 777-85.

Wang, L., L. Li, et al. (2004). "Endothelial and hematopoietic cell fate of human embryonic stem cells originates from primitive endothelium with hemangioblastic properties." Immunity 21(1): 31-41.

Weber, C. A., C. A. Duncan, et al. (1990). "Depletion of tissue glutathione with diethyl maleate enhances hyperbaric oxygen toxicity." Am J Physiol 258(6 Pt 1): L308-12.

Weber, D. S., Y. Taniyama, et al. (2004). "Phosphoinositide-dependent kinase 1 and p21-activated protein kinase mediate reactive oxygen species-dependent regulation of platelet-derived growth factor-induced smooth muscle cell migration." Circ Res 94(9): 1219-26.

Weindruch, R. and R. S. Sohal (1997). "Seminars in medicine of the Beth Israel Deaconess Medical Center. Caloric intake and aging." N Engl J Med 337(14): 986-94.

Wert Gd, G. and C. Mummery (2003). "Human embryonic stem cells: research, ethics and policy." Hum Reprod 18(4): 672-82.

White, C. W., R. F. Mimmack, et al. (1986). "Accumulation of lung tissue oxidized glutathione (GSSG) as a marker of oxidant induced lung injury." Chest 89(3 Suppl): 111S-113S.

Wiersma, J. A., M. Bos, et al. (1994). "High strength poly(meth)acrylamide copolymer hydrogels." Polymer Bulletin 33: 615-622.

Wilkins, M. R., R. D. Appel, et al. (2006). "Guidelines for the next 10 years of proteomics." Proteomics 6(1): 4-8.

Wilkins, M. R., C. Pasquali, et al. (1996). "From proteins to proteomes: large scale protein identification by two-dimensional electrophoresis and amino acid analysis." Biotechnology (N Y) 14(1): 61-5.

Wilkins, M. R., J. C. Sanchez, et al. (1996). "Progress with proteome projects: why all proteins expressed by a genome should be identified and how to do it." Biotechnol Genet Eng Rev 13: 19-50.

Williams, M. D., H. Van Remmen, et al. (1998). "Increased oxidative damage is correlated to altered mitochondrial function in heterozygous manganese superoxide dismutase knockout mice." J Biol Chem 273(43): 28510-5.

Williams, R. L., D. J. Hilton, et al. (1988). "Myeloid leukaemia inhibitory factor maintains the developmental potential of embryonic stem cells." Nature 336(6200): 684-7.

Wilm, M., A. Shevchenko, et al. (1996). "Femtomole sequencing of proteins from polyacrylamide gels by nano-electrospray mass spectrometry." Nature 379(6564): 466-9.

Wissler, R. W. (1992). "Theories and new horizons in the pathogenesis of atherosclerosis and the mechanisms of clinical effects." Arch Pathol Lab Med 116(12): 1281-91.

Wood, Z. A., E. Schroder, et al. (2003). "Structure, mechanism and regulation of peroxiredoxins." Trends Biochem Sci 28(1): 32-40.

Xiao, Q., L. Zeng, et al. (2006). "Stem Cell-derived Sca-1+ Progenitors Differentiate into Smooth Muscle Cells, which is Mediated by Collagen IV-Integrin {alpha}1/{beta}1/{alpha}v and PDGF Receptor Pathways." Am J Physiol Cell Physiol.

Xu, C., M. S. Inokuma, et al. (2001). "Feeder-free growth of undifferentiated human embryonic stem cells." Nat Biotechnol 19(10): 971-4.

Xu, Q. (2000). "Biomechanical-stress-induced signaling and gene expression in the development of arteriosclerosis." Trends Cardiovasc Med 10(1): 35-41.

Xu, Q. (2006). "The impact of progenitor cells in atherosclerosis." Nat Clin Pract Cardiovasc Med **3**(2): 94-101.

Xu, Q., Z. Zhang, et al. (2003). "Circulating progenitor cells regenerate endothelium of vein graft atherosclerosis, which is diminished in ApoE-deficient mice." Circ Res **93**(8): e76-86.

Yamane, T., S. Hayashi, et al. (1999). "Derivation of melanocytes from embryonic stem cells in culture." Dev Dyn **216**(4-5): 450-8.

Yamashita, J., H. Itoh, et al. (2000). "Flk1-positive cells derived from embryonic stem cells serve as vascular progenitors." Nature **408**(6808): 92-6.

Yan, J. X., R. Wait, et al. (2000). "A modified silver staining protocol for visualization of proteins compatible with matrix-assisted laser desorption/ionization and electrospray ionization-mass spectrometry." Electrophoresis **21**(17): 3666-72.

Yang, Y., J. Y. Min, et al. (2002). "VEGF enhances functional improvement of postinfarcted hearts by transplantation of ESC-differentiated cells." J Appl Physiol **93**(3): 1140-51.

Yates, J. R., 3rd, J. K. Eng, et al. (1995). "Method to correlate tandem mass spectra of modified peptides to amino acid sequences in the protein database." Anal Chem **67**(8): 1426-36.

Yeh, E. T., S. Zhang, et al. (2003). "Transdifferentiation of human peripheral blood CD34+-enriched cell population into cardiomyocytes, endothelial cells, and smooth muscle cells in vivo." Circulation **108**(17): 2070-3.

Yin, X., M. Mayr, et al. (2005). "Proteomic dataset of Sca-1(+) progenitor cells." Proteomics **5**(17): 4533-45.

Ying, Q. L., J. Nichols, et al. (2003). "BMP induction of Id proteins suppresses differentiation and sustains embryonic stem cell self-renewal in collaboration with STAT3." Cell **115**(3): 281-92.

Yurugi-Kobayashi, T., H. Itoh, et al. (2003). "Effective contribution of transplanted vascular progenitor cells derived from embryonic stem cells to adult neovascularization in proper differentiation stage." Blood **101**(7): 2675-8.

Zandstra, P. W., C. Bauwens, et al. (2003). "Scalable production of embryonic stem cell-derived cardiomyocytes." Tissue Eng **9**(4): 767-78.

Zeng, L., Q. Xiao, et al. (2006). "HDAC3 is crucial in shear- and VEGF-induced stem cell differentiation toward endothelial cells." J Cell Biol **174**(7): 1059-69.

Zhang, S. H., R. L. Reddick, et al. (1992). "Spontaneous hypercholesterolemia and arterial lesions in mice lacking apolipoprotein E." Science **258**(5081): 468-71.

Zhang, Y., O. Marcillat, et al. (1990). "The oxidative inactivation of mitochondrial electron transport chain components and ATPase." J Biol Chem **265**(27): 16330-6.

Zhou, Q., G. R. Hellermann, et al. (1995). "Nitric oxide release from resting human platelets." Thromb Res **77**(1): 87-96.

Zou, Y., Y. Hu, et al. (1998). "Signal transduction in arteriosclerosis: mechanical stress-activated MAP kinases in vascular smooth muscle cells (review)." Int J Mol Med **1**(5): 827-34.

zur Nieden, N. I., G. Kempka, et al. (2003). "In vitro differentiation of embryonic stem cells into mineralized osteoblasts." Differentiation **71**(1): 18-27.

I'm the happiest man in the world now!

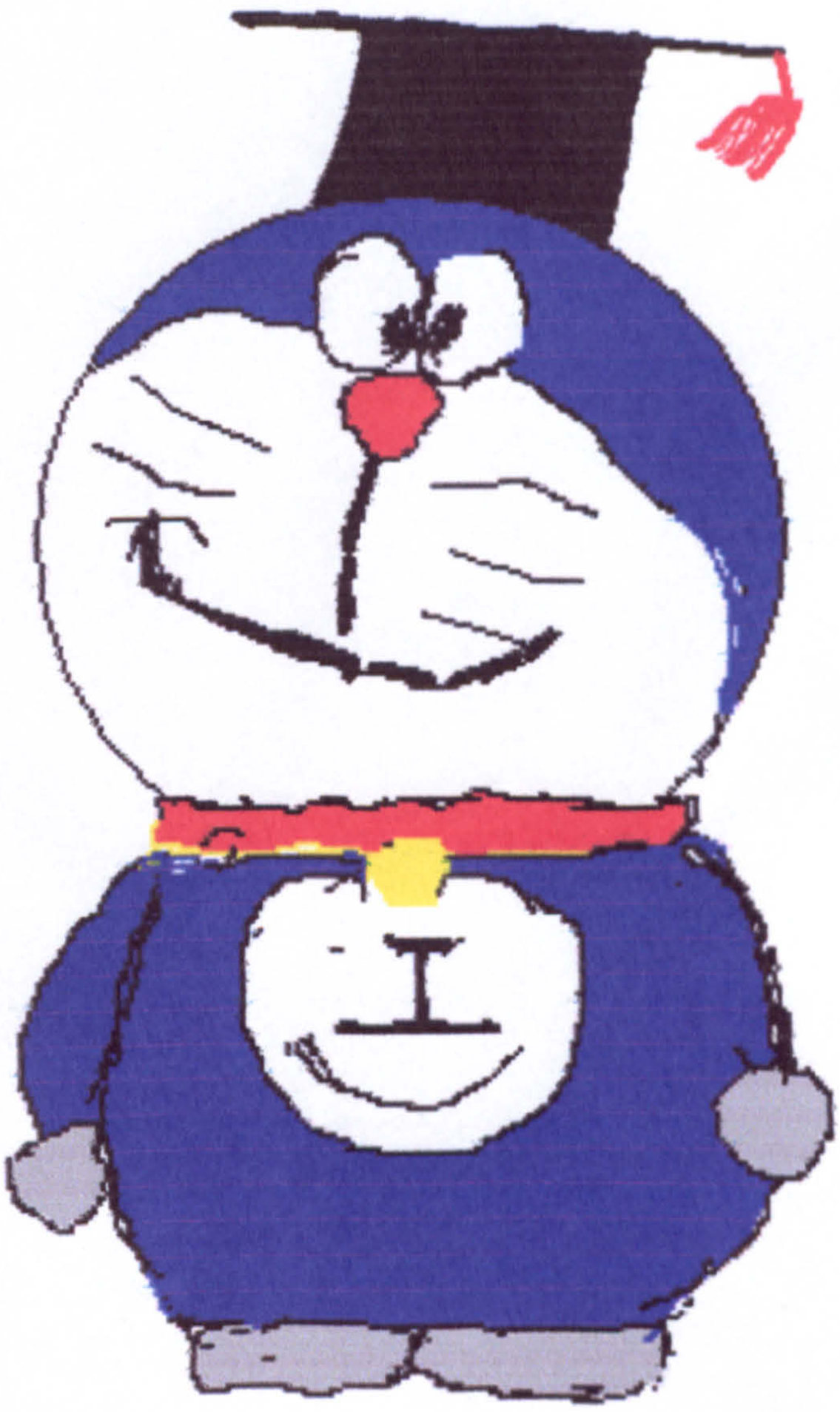

Masterpiece of Qiuru Xing